THE UNIVERSITY
of EDINBURGH

Molecular studies of Tobacco Rattle Virus (TRV) infection in Potato

Ghulam Mustafa Sahi

Doctor of Philosophy

Institute of Molecular Plant Sciences
School of Biological Sciences
The University of Edinburgh
and
Cell and Molecular Sciences Group
The James Hutton Institute (JHI)

2015

Contents

3. Systemic Infection of TRV isolates

4. Utilizing Diploid Potatoes for VIGS

5. Molecular Studies of Spraing Disease of Potato

Declaration

I hereby declare that the work presented here in this thesis is my own and includes nothing that is the outcome of work done in collaboration, except where specifically stated here, or in the text. The work has not been submitted in any form for any degree, diploma or any other qualification at this university or any other university.

Ghulam Mustafa Sahi

Acknowledgements

I am indebted to my supervisors Prof. Gary J. Loake (The University of Edinburgh) and Dr. Stuart A. MacFarlane (The James Hutton Institute) for providing the opportunity to undertake this Ph.D study. Special thanks must go to Dr. MacFarlane for his continued kind encouragement, guidance, constructive criticism, and patience. I am also obliged to Drs. Andrew Love and Tracey Valentine for fruitful discussions.

I would like to thank Wendy McGavin, Graham Cowan, and Hazel McLellan, for their technical guidance and inputs in the studies. I am also thankful to Gavin Ramsay and Ralph Wilson for providing the potato germplasm. Provision of spraing-affected tubers by Louise Sullivan, Finlay Dale (JHI) and Christophe Lacomme (the Science and Advice for Scottish Agriculture, SASA) is also duly acknowledged. My sincere thanks go to Pete E. Hedley and Jenny Morris for their technical assistance in the gene expression and microarray analyses. I am grateful to Alison Roberts, Kath Wright, Laurence Ducreux, and Wayne Morris for extending their support in various research issues.

Special appreciations to my office mates Aqeel Al-Abedy and Adnan Al-Lahuf, for their valuable discussions and help. The company of Yuwen Lu, Jian Yang, Chulang Yu, Xiaodan Wang, Yong Yang, Zongtao Sun, Junmin Li, Xuming Wang, Jie Zhou, Vladimir Guschin, Mireia Sancho Such, and Maiju Laurila for their friendly and enjoyable working relation is also appreciated. I also wish to thank Alison Dolan, Samantha Charman, and Sarah Robertson for making me feel at home.

I am highly indebted to my mother and sisters for their prayers, encouragement and support to achieve my ambitions. Thanks are also due to my late uncle Chaudhary Muhammad Akbar Maan for putting me on the track to education. Very special thanks to my wife and kids for their understanding and patience in missing my company. Special acknowledgments are owed to Merit Scholarship Programme (MSP), Islamic Development Bank (IDB), Jeddah, Kingdom of Saudi Arabia; University of Agriculture, Faisalabad (UAF), Pakistan; and Economic Affairs Division (EAD), Government of Pakistan, for providing a scholarship for me to pursue these studies.

Dedication

To my mother and late father, Chaudhary Muhammad Yaqoob Sahi, for educating me, their continuous support, endless love, inspiration, and desire to see me glittering in the galaxy of scientists who serve humanity

Publications arising from this work

1. Molecular and biochemical examination of spraing disease in potato tuber in response to Tobacco rattle virus infection (DOI: 10.1094/MPMI-08-16-0169-R)

2. Diploid potatoes: a useful resource for investigating TRV-induced gene silencing (Manuscript in drafting stage)

Abstract

Tobacco rattle virus (TRV) is a bipartite plant virus that infects potato tubers to produce the spraing or corky ring spot (CRS) disease of potato. TRV is primarily a soil-borne pathogen that is vectored by trichodorid nematodes. Spraing is characterized by the production of brown arcs and flecks in the tuber flesh or circular rings on its external surface. Spraing has been described as a hypersensitive response (HR). However, the genetic and biochemical nature of spraing had not been previously investigated experimentally.

I have conducted studies to reveal the gene expression and the biochemical basis for spraing formation. Microarray analysis of RNA extracted from tuber-tissue showing spraing symptoms, revealed up-regulation of several defence related genes. Quantitative RT-PCR (qRT-PCR) of some of the differentially-expressed potato defence related genes was done for verification of the microarray data. Biochemical tests for cell death response reactions and staining for HR-related compounds or production of reactive oxygen species (ROS) also revealed the operation of HR-related processes in the spraing-affected tuber. Uneven distribution of the TRV RNA-1 in a spraing-symptomatic tuber also supports the notion that it's a virus-induced HR-response.

RNA-2 of TRV besides coding for the CP also carries the non-structural genes, 2b and 2c genes that are responsible for the nematode transmission of TRV. Fifteen different TRV recombinant isolates were prepared and the influence of the RNA-2 specific genes, encoded by a range of TRV-isolates, in causing infection among different cultivars of potato was also evaluated.

Investigations were conducted to identify TRV-susceptible genotypes in which virus could move systemically and accumulate to a sufficient level to be useful for TRV-infection and VIGS-related studies for functional analysis of potato genes.

List of Figures

List of Figures (continued…….l)

List of Figures (continued…….ll)

List of Tables

Abbreviations

µg	Microgram
µl	Microliter
µM	Micromolar
A°	Absorbance
aa	Amino acid
AFU	Arbitrary fluorescence unit
AGO protein	Argonaute protein
AL isolate	*Alstroemeria aurae* (Peruvian-lily) isolate
AMV	*Alfalfa mosaic virus*
ATP	Adenosine tri-phosphate
Avr	Avirulence gene
BCIP	5-Bromo-4-chloro-3-indolyl phosphate
BLAST	Basic local alignment search tool
bp	Base pair
BPMV	*Bean pod mottle Comovirus*
BSA	Bovine serum albumin
BSMV	*Barley stripe mosaic virus*
ByKT (Bav) isolate	Southern Germany (Bavaria) isolate
ByKT (LS) isolate	Northern Central Germany (Lower Saxony) isolate
CaLCuV	*Cabbage leaf curl virus*
CaMV	*Cauliflower mosaic virus*
CB	Cell Biology
CD	Cell-death
cDNA	Complementary DNA
CIP	Centro Internacional De La Pappa (International Potato Centre)
cm	Centimetre
CMS	Cell and Molecular Sciences Group, JHI
CMV	*Cucumber mosaic virus*
CP	Coat protein
CPC	Commonwealth potato collection
cRNA	Complementary RNA

Abbreviations (continued…….l)

CRP	Cysteine-rich protein
CRS	Corky ringspot
C_T S.Ds	C_T standard deviations
C_T	Cyclic threshold
CymRSV	*Cymbidium ringspot virus*
CyP	Cyclophilin
DAB	3, 3′-Diaminobenzidine
Deb57	De¸bnica 57 isolate (Northern Poland)
DNA	Deoxyribonucleic acid
dNTP	Deoxyribonucleotides
dpi	Days post inoculation, infection, infiltration
ds	Double stranded
DTT	Dithiothreitol
E. coli	*Escherichia coli*
EDTA	Ethylenediaminetetraacetic acid
Ef-1α	Elongation factor-1 alpha
EFF %	Amplification efficiency
ELISA	Enzyme linked immunosorbent assay
ER	Extreme resistance or immunity
FAO	Food and Agriculture Organization
fs mutant	frameshift mutant
g	Gram
GBSS	*Granule bound starch synthase*
GFP	Green fluorescent protein
GM	Genetically modified
GO	Gene ontology
gRNA	genomic RNA
GST	*Glutathione-S-transferase*
H_2O_2	Hydrogen peroxide
Hc-Pro	Helper component protein
Ho isolate	Hosta isolate
HPLC	High Performance Liquid Chromatography

Abbreviations (continued…….II)

HR	Hypersensitive response
I6 isolate	Italian-6 isolate (Northern Italy)
IPTG	Isopropyl β-D-1-thiogalactopyranoside
JHI	James Hutton Institute
KCPfs	coat-protein frameshift mutant of Pp-K20 isolate
KD	Knockdown
KDa	Kilo-Dalton
KO	Knockout
LB	Luria-Bertani broth
LBAIX	LB medium supplemented with ampicillin, IPTG, and X-gal
LiCl	Lithium chloride
LRR	Leucine-rich repeat
M	Molar
MES	2-(N-morpholino) ethanesulfonic acid
mg	milligram
MI-1 isolate	Michigan-1 isolate
miRNA	MicroRNA
ml	millilitre
Mlo57 isolate	Młochow 57 isolate (Central Poland)
mM	milliMolar
mm^3	Cubic millimetre
MOPS	3-(N-morpholino) propanesulfonic acid
MP	Movement protein
mRNA	Messenger RNA
MS	Murashige and Skoog medium
M-type	Multiplying type or particle producing type
MW	Molecular weight
NADPH	Nicotinamide adenine dinucleotide phosphate
Nb.	*Nicotiana benthamiana*
NBS	Nucleotide binding site
NBT	Nitro blue tetrazolium chloride

Abbreviations (continued…….lll)

NCR	Non-coding region
NEB	New England BioLabs® Inc
NIAB	National Institute of Agriculture and Botany
NTC	Non template control / negative control
NM-type	Non-multiplying type
nts.	Nucleotides
O^{-2}	Superoxide
OD600	Optical density at 600nm
ON isolate	Onion isolate
ORF	Open reading frame
ORY isolate	Oregon yellow isolate (North America)
PAGE	Polyacrylamide gel electrophoresis
PAR-1c	Pathogen-related protein-1c
PaY4 strain	*Paratrichodorus anemones* York-4 strain
PBS	Phosphate-buffered saline
PCD	Programmed cell death
PCR	Polymerase chain reaction
PD	Pentland Dell
PDS	*Phytoene desaturase*
PEBV	*Pea early browning virus*
PepRSV	*Pepper ringspot virus*
PER	*Peroxidase*
PGSC	Potato Genome Sequencing Consortium
PLRV	*Potato leaf roll virus*
PMTV	*Potato mop top virus*
POCI array	Potato Oligo Chip Initiative array Potato Centre
PpK20 strain	*Paratrichodorus pachydermus* Kinshaldy-20 strain
PpO85 strain	*Paratrichodorus pachydermus* Overloon-85 strain
PR protein	Pathogen related protein
PRN isolate	Potato ring necrosis isolate
PTA-ELISA	Plate Trapped Antigen- ELISA
PTGS	Post transcriptional gene-silencing

Abbreviations (continued…….IV)

p-value	Probability value
PVX	*Potato virus X*
PVY	*Potato virus Y*
QC	Quality check
qRT-PCR	Quantitative real-time PCR
QTL	Quantitative trait loci
R gene	*Resistance* gene
R^2	Regression co-efficient
RBO	*Respiratory Burst Oxidase*
RdRP	RNA-dependent RNA Polymerase
RIN	Relative Integrity Number
RISC	RNA induced silencing complex
RNA	Ribonucleic acid
RNAi	RNA interference
ROI	Reactive oxygen intermediates
ROS	Reactive oxygen species
RQ	Relative quantity
rRNA	Ribosomal RNA
RT-PCR	Reverse transcriptase PCR
SAR	Systemic acquired resistance
SASA	Science and Advice for Scottish Agriculture
SCRI	Scottish Crop Research Institute
SDS	Sodium dodecyl sulphate
SE	Standard error
SEL	Size exclusion limit
SF	Spraing-free
sgRNA	subgenomic RNA
SHM isolate	Hessen isolate (Southern central Germany)
siRNA	short interfering RNA
Slu24	Słupsk 24 isolate (Northern Poland)
SP isolate	Spinach isolate
SP	*Suberization anionic peroxidase*

Abbreviations (continued…….V)

SP5 isolate	Swaffham P5 isolate (England,UK)
SPS	Sanitary and Phytosanitary
sqRT-PCR	Semiquantitative RT-PCR
sRNA	Small RNA
ss	Single-stranded
SS2	*Starch Synthase 2*
SSC	Saline sodium citrate buffer
ssRNA	single-stranded RNA
St.	*Solanum tuberosum*
SYM strain	Spinach yellow mottle strain
TAIR	The *Arabidopsis* information resource
TBE	Tris –borate-EDTA buffer
TBS	Tris -buffered saline
TCM isolate	Tulip isolate of TRV
T-DNA	Transfer DNA
TEV	*Tobacco etch virus*
TGB	Triple gene block
TGMV	*Tomato golden mosaic virus*
TGS	Transcriptional gene silencing
Tm	Melting temperature
TMV	*Tobacco mosaic virus*
TpA56 isolate	*Trichodorus primitivus (*Croxton Farm, Fulmodestone, UK)
TpO1 isolate	*Trichodorus primitivus* Oxfordshire-1 isolate
TRV	*Tobacco rattle virus*
UGA	Opal termination codon
UTR	Untranslated region
UV	Ultra violet light
VIGS	Virus-induced gene silencing
VPg	Viral protein genome-linked
vRNA	Viral RNA
vRNPC	Viral ribonucleo-protein complex

Abbreviations (continued…….VI)

wt.	Wild type
WTO	World Trade Organization
X-gal	5-bromo-4-chloro-3-indolyl-β-D-galactopyranoside (also abbreviated BCIG)
ZEP	*Zeaxanthin epoxidase*
β ME	2-Mercaptoethanol
$\Delta\Delta C_T$	Comparative C_T quantitation method

1. Introduction

1.1. Potato and its viruses

The cultivated potato (*Solanum tuberosum* L.) is a temperate climate crop that has been cultivated for more than twenty centuries. Initially potato was cultivated in the Andes mountains of Peru and Bolivia (South-America) and later, at around five centuries ago, the Spanish traders introduced it to Europe from where it began to be cultivated world-wide (Hawkes, 1991a; Askew, 2001). Across the world potato is grown in more than one hundred countries and consumed by more than a billion people. Among the top ten global crops it ranks fifth in production, following sugar cane, maize, rice and wheat, with an overall crop production of more than three-hundred and sixty four million metric tonnes (FAO Stats, 2014). In terms of human consumption, potato is globally ranked third among the important food crops, following rice and wheat, and is an important source of dietary carbohydrates as well as providing more proteins from a comparable acreage than rice or wheat (Rowe, 1993; Stevenson, *et al*., 2001; Askew, 2001). Potatoes contain practically no fats (Storey, 2007). Compared to maize, boiled potatoes provide a higher amount of protein and double the quantity of calcium (CIP, 2014). Besides being known as a rich source of carbohydrates, potato is also equipped with some nutritive and medicinal values, an aspect that has been overlooked in the past. Consumption of potato can help to supplement the dietary requirements of our body for essential vitamins (like vitamin C (ascorbate) and vitamin B1/ thiamine) and mineral nutrients (like iron and zinc). Inadequate-intake of these essential nutrients can result in diseases like beriberi (vitamin B1 deficiency), anaemia, dyspnoea and gastrointestinal bleeding (Fe deficiency), and mental illness (Zn deficiency). Potato also contains valuable protective compounds e.g, carotenoids such as zeaxanthin and xanthophyll (lutein) that help maintain the eyesight and protect the body against

heart diseases and cancer-related disorders. The antioxidative polyphenolic compounds e.g, chlorogenic acid and anthocyanin, shield the body against hypertension and malignant disorders such as diabetes and cardiovascular diseases. Whereas, the glycolalkaloids can have a role in anti-cancer defence in the human body (Camire *et al*., 2009; Stewart and McDougall, 2012; Lister, 2013). However, the glycoalkaloids (chiefly chaconine and solanine) are also poisonous, and found in almost all potato tissues. They are of uneven distribution within the tuber and are usually found in lower amounts in the tuber-flesh. Glycoalkaloids are more predominant in the tuber periderm (skin), greener portion of the tuber, and the tissue surrounding the tuber eyes (Storey, 2007; FAO, 2008). Potatoes possess the greatest satiety index (SI) among all the botanical-origin food products (Haase, 2008). Currently, more than fifty percent of the overall global production of potato is being contributed by the developing countries. Potato singly comprises nearly fifty percent of the universal tuber and root crop production which also includes yams, sweet potato, cassava and taro (Shewry, 2003; FAO Stats, 2014; CIP, 2014).

The genus *Solanum* of the family Solanaceae (also known as the nightshade family) includes different herbaceous and shrub plants comprising about a thousand species, of which there are nearly two-hundred tuber producing wild potato species, including some of the cultivated potato species (Hawkes, 1991b). All these species vary in their genetical, morphological and ecological diversity (Jones, 1981).

The genome of potato is composed of a set of 12 chromosomes with the ploidy in wild species ranging from diploid to hexaploid (2n to 6n) but for the cultivated species, developed through various genetical and evolutionary processes, it does not exceed pentaploidy (Hawkes, 1991b). Among cultivated potatoes, *S. tuberosum* is the most abundant with a range of germplasm diversity (Jones, 1981). Most of the cultivated species are grown in the Andes mountains of South America (Hijmans and Spooner, 2001).

The wild relatives of potato comprising the diploid potatoes are a good resource for exploring natural genetic diversity to identify useful traits for deployment in potato breeding programmes. Wild potatoes are narrowly distributed and are mostly restricted to their historic natural reservoirs. Peru, where at least ninety-three wild potato species have been domesticated, has the richest natural genetic collection of wild potatoes (Hijmans and Spooner, 2001). Exploiting wild species for desirable traits like yield and disease resistance is an important feature of potato breeding to improve modern commercial cultivars.

Potato, being a vegetatively propagated crop has greater exposure to infections and the spread of plant pathogens and their resulting diseases. The harboured pathogens can easily be carried over from one season to the next. Among the various potato diseases, viral diseases, due to the non-availability of any effective direct chemical control method, pose a continuous threat to the crop, causing reduction in both quality and yield (Ruiz de Galerreta *et al*., 1998). The first available record of potato viral disease refers to the ‘‘degeneration’’ or ‘‘run out’’ disease of potato seed-stock that has been known since the 18^{th} century (Salaman, 1921; Rich, 1983; Rowe, 1993). Potato stock that showed reduction in the quantity and quality of the produce were known as being ‘‘run out’’ among the potato growers (Goss, 1925). This degeneration syndrome of potato was chiefly associated with a complex of potato diseases such as potato leaf roll and potato mosaic that later with the advent of plant virology were discovered to be plant viral infections.

Potato is naturally infected by nearly forty plant viruses that vary in their prevalence and distribution (Palukaitis, 2012). Potato viruses, based on their infectivity, can be categorized into two types; the specific potato viruses, which chiefly infect the potato plant, and the common potato viruses that infect a large number of both solanaceous and non-solanaceous plants and are globally prevalent. The various viruses adopt different strategies for their spread and survival, so that Potato virus Y (PVY), Potato mop top virus (PMTV) and Tobacco rattle virus (TRV) are transmitted by different

vector organisms, whereas, Potato virus X (PVX) is mechanically disseminated to other plants through physical contact. Of the vector-transmitted potato viruses, at least six are known to be spread by soil-dwelling vectors and include the economically important TRV and PMTV, both of which induce a tuber infection known as spraing. Transmission of potato viruses through true seed is not a significant cause of disease spread, although infected tubers are important for spreading virus diseases (Jones, 1981; Palukaitis, 2012).

TRV infection can be diagnosed and differentiated from PMTV (a *Pomovirus*) infections either by molecular tests such as nucleic acid hybridization or reverse transcriptase polymerase chain reaction (RT-PCR) or by using a biological assay involving inoculation to indicator plants. For example, PMTV infection on the leaves of *Nicotiana tabacum* c.v Xanthi, produces a very distinct systemic line pattern and inoculation to *Chenopodium amaranticolor* results in a non-systemic infection producing concentric necrotic-lesions that sometimes may result in a single spreading lesion extending over half of the leaf lamina. TRV infection on C. *amaranticolor* plants is mostly non-systemic, depending upon the virus isolate, producing small, necrotic lesions. The soil-borne potato diseases have been reviewed by Fiers *et al*. (2012). The main potato viruses have been described by Brunt (2001) and those transmitted by soil-borne vectors have been discussed by Weingartner (2001).

1.2. Tobraviruses

The name Tobravirus was first suggested by Harrison *et al*., (1971) for a group of plant viruses causing a range of diseases. The *Tobravirus* genus of plant viruses includes three species namely TRV, Pea early-browning virus (PEBV) and Pepper ringspot virus (PepRSV). TRV is the type species of the *Tobravirus* genus. The tobraviruses have a genome consisting of two RNA molecules (bipartite genome), encapsidated separately in rod-shaped particles of characteristic length (Lister, 1966; 1968; MacFarlane, 1999; 2010). These viruses are transmitted between plants by

root-feeding, ectoparasitic nematodes of the genera *Trichodorus* and *Paratrichodorus*, which are referred to as trichodorid or stubby-root nematodes (Harrison and Robinson, 1986; MacFarlane, 2010). The earliest record of diseases incited by tobraviruses refers to the soil-borne *Mauche disease* of tobacco, reported from Germany by Behrens in 1899 and later shown to be caused by TRV (Cadman and Harrison, 1959; Harrison and Robinson, 1978; Robinson and Harrison, 1989).

Among the tobraviruses, PepRSV (formerly known as TRV CAM strain and belonging to TRV Serotype III; Robinson and Harrison, 1985a) differs from TRV in its antigenic properties and has been reported only from South-America (Brazil) where it, in addition to infecting the perennial thistle plant and globe artichoke, also infects the solanaceous plants pepper and tomato. Biologically, TRV infection can be differentiated from PEBV infection by inoculation to field pea (*Pisum sativum* subsp. arvense) and broad bean (*Vicia faba*) plants, as TRV produces pinpoint confined lesions and is incapable of producing systemic infection in both of these plants, whereas, PEBV produces systemic symptoms in these plants (Robinson *et al*., 1987; Robinson and Harrison, 1989; Ploeg *et al*., 1992b).

1.3. Tobacco rattle virus, economic, and pathological significance

TRV, firstly characterized by Quanjer (1943), consists of two rod-shaped particles. The larger (L) particle (containing RNA-1) is of about 185 nm in length and the smaller (S) particle (containing RNA-2) is of about 50 to 115 nm length that varies depending on the particular TRV isolate (Harrison and Woods, 1966; Robinson and Harrison, 1989). Earlier studies identified two types of TRV infections that were described as the ‘‘multiplying type or particle producing type’’ (M-Type) and the ‘‘non-multiplying type’’ (NM-Type) infection (Lister, 1966; Harrison and Robinson, 1978). An isolate from an M-type infection has both viral RNAs, forms particles, is mechanically or nematode transmissible and antigenically detectable. Isolates from the NM-type infections, consisting only of the non-encapsidated RNA-1, are not

easily mechanically transmissible (Lister, 1966, 1968; Cadman, 1959; MacFarlane, 1999). NM-type infections cannot be detected by methods based on antigenic properties (as the virus is incapable of producing nucleoprotein particles) due to the lack of RNA-2 and are non-transmissible by nematodes (Nicolaisen *et al*., 1999). Nevertheless, RNA-1 by itself can multiply and spread in infected plants producing a systemic infection (Hamilton *et al*., 1987; MacFarlane, 1999). NM-type infections or isolates are common in potato and they can be isolated from plants if extracted using phenol (Harrison and Robinson, 1982; MacFarlane, 2010). M-type isolates and infections are more stable than the NM-types whereas, the latter are said to be more severe in pathogenicity than M-type infections (Lister, 1966; Robinson and Harrison, 1989).

The TRV particle is stable at different pH concentrations and also in various inorganic and organic solutions. TRV is soil-borne and transmitted between cultivated and weed plants by trichodorid nematodes, in a very precise association (van Hoof, 1968; Hamilton *et al*., 1987; Hernandez *et al*., 1995; Sudarshana and Berger, 1998; MacFarlane *et al*., 1999). TRV is also seed-transmissible in some plant species (Gasper *et al*., 1984; Sudarshana and Berger, 1998; Visser *et al.*, 1999). The trichodorid nematodes are most commonly found in sandy soils, being most abundant in the top-most soil layers, where after successful TRV acquisition they may remain viruliferous for several years (Taylor and Brown, 1997).

TRV is global in its distribution and it infects numerous hosts including both cultivated and wild plant species (Brunt *et al.*, 1996; Dale, 2009). Its infection produces economically important diseases that are known by different names, in plants of the Solanaceae family, especially potato and tobacco, and also in plants of the Chenopodiaceae family such as spinach and sugarbeet. Besides these crop plants, many ornamental plants including most notably gladiolus (sword-lily), hyacinth and aster are also infected by TRV (Harrison and Robinson, 1986; Robinson and Harrison, 1989; Heinze *et al.*, 2000). Infection of potato by TRV is an economically

important disease worldwide and soil-borne vector-transmitted viruses can reduce crop yields by more than one quarter (Hide and Lapwood, 1992). These viruses (TRV and PMTV) can produce diseases (such as spraing) that can be a serious concern for the potato industry in the following years (Santala *et al.*, 2010).

1.4. TRV infection in potato

TRV infection in potato is categorised into two main diseases based on the symptoms that are produced. If the disease symptoms appear on the foliage of the potato plant it is named ‘‘stem mottle disease’’ and if they are expressed in the tubers then it is termed ‘‘spraing disease’’ (Cadman, 1959; van Hoof, 1964a). Stem mottle disease is a result of secondary infection from TRV-infected tubers and its progression into the developing potato plant, whereas, spraing disease is a consequence of primary tuber-infection arising from virus inoculation by TRV-bearing trichodorid nematodes. TRV infection of seed potatoes is of paramount concern for the seed-production industry as it results in progeny tubers that are reduced in size and number with a consequent ultimate reduction in the quantity of produce (Cadman, 1959; Weingartner, 2001). Moreover, often these infected tubers are not marketable due to their inferior quality and the stringent quality standards required for potatoes destined for use by the processing industry (Hooker, 1980; Mojtahedi *et al*., 2000; Brown *et al*., 2009). Consignments containing as little as 2% of spraing-affected tubers are rejected by the supermarkets (Dale, 2009). Sometimes, the severity of infection and/or high incidence of TRV may result in rejection of the whole potato crop (Brown and Skyes, 1973). Stem mottle disease is of relatively greater significance to the seed-production industry and spraing disease is of more concern for the potato-processing industry (Stevenson *et al*., 2001).

In this era of the World Trade Organization (WTO) and the associated Sanitary and Phytosanitary (SPS) measures, consumers are more concerned about the disease-status and quality of the potatoes, demanding more stringent standards in

international merchandise and necessitating governments to be more alert to plant and public health issues.

1.4.1. Stem mottle disease

The stem mottle disease is characterized by the production of chevron-shaped chlorotic or necrotic spots on the foliage of a few, but not on all, undersized haulms that sprout from a virus-infected tuber. These diseased leaves may be smaller in size, mottled, rippled, distorted with the development of yellow lines and have interveinal chlorosis (Banttari *et al.,* 1993). Occasionally the symptoms in more severely affected plants may advance to the stem causing its necrosis. Tubers produced from such affected plants are deformed with arcs of dead tissue and dark-coloured flecks in the tuber-flesh. Progression of the disease to the progeny tubers occurs in an inconsistent manner (Cadman, 1959; Cadman and Harrison, 1959). Stem mottle symptoms are more obvious at temperatures less than 20°C and become masked at elevated temperatures (Stevenson *et al*., 2001).

Cadman (1959) in his stem mottle disease-associated experiments conducted in the U.K, observed that the TRV isolated from the diseased potato haulms (above ground potato stems) was mostly of the NM- type and when he attempted to recover the TRV from spraing-affected tubers, it every time proved to be of the NM-type. He further suggested that TRV-infected tubers were better for virus isolation, when freshly harvested rather than after their storage. Moreover, surprisingly, he recovered NM-type infections from potato plants that had been leaf-inoculated with a M-type isolate. Later, the tobravirus infectivity studies performed by Lister (1966, 1968) showed that lesion-formation and viral multiplication in the infected plants was associated with the NM-type viral preparations. Whereas, the coat-protein formation and production of virus-particles was associated with the M-type viral-inoculum (i.e., comprising both RNA1 and RNA2).

Potato plants affected with stem mottle disease in the U.K have been found to be associated with NM-type isolates (Weingartner, 2001).

1.4.2. Spraing disease

The potato tuber is a vital underground photosynthate storage organ that provides nutrients to young plants that emerge as sprouts which develop into new, tuber-bearing plants. In some cultivars, TRV infection produces distinct symptoms in the tuber that are known as ‘‘corky ringspot (CRS)’’ or ‘‘spraing’’. The name CRS is commonly used in the North-American states whereas the term spraing is prevalent in the European countries. The disease is characterized by the production of distinct symptoms of brown arcs and spots of dark-coloured corky tissue in the tuber-flesh (Fig.1.1) that may also appear externally as annular, coarse flecks on the tuber skin (Fig.1.2). In case of primary infection, these symptoms are suggested to locate near the feeding sites of the trichodorid vector nematodes, in the outer layers of infected tissue and later to advance and spread into the deeper tuber-flesh. It is hypothesized that if the disease initiates at the maturing stage of the tubers then the symptoms are absent from the inner tuber-flesh or are restricted to the outer-most layers of the tubers (Weingartner, 2001).

Lihnell (1958) reported that freshly infected tubers obtained from nematode infested soil, developed localised diseased tissue near the outer layers of the infected tubers. Whereas, the progeny tubers harvested from the TRV-infected plants were lacking the infected tissue in the peripheral tuber layers. This suggested direct infection of the tubers by the trichodorid nematodes in the infested-soil (Cadman, 1959). Spraing had been mostly found associated with the sowing of potatoes in light textured soils. van Hoof (1964a) observed a link between spraing development following tuber feeding of TRV-carrying nematodes rather than their feeding on the potato roots, and thus suggested that spraing development was related to TRV infection at a particular age-linked growth stage of the tubers.

Figure 1.1. Internal symptoms of a spraing-affected tuber. Pronounced arcs and flecks of brownish, cork-like tissue in the tuber flesh are evident.

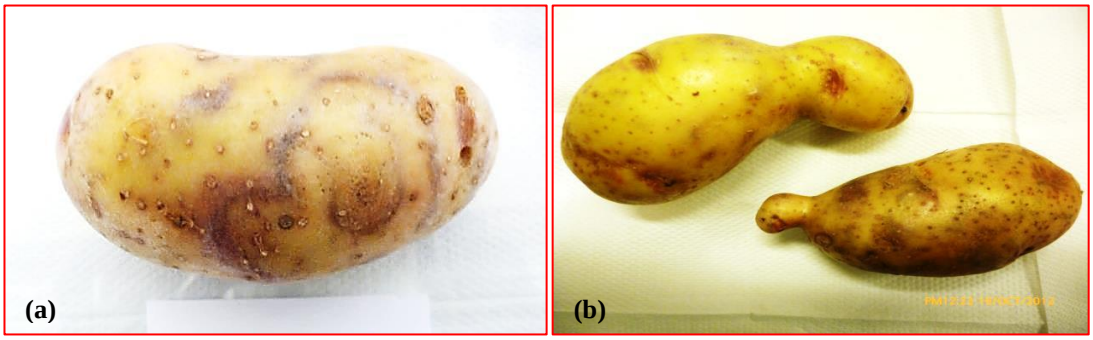

Figure 1.2. External symptoms of spraing-affected tubers. (a) Brownish and necrotic arcs of spraing are obvious on the tuber-periderm. **(b)** Misshapen-tubers with knobby-growth due to TRV-infection.

Further, the possibility of intercellular movement of TRV from infected roots to the developing tubers was rejected. Similar observations were recorded by Engsbro (1973), who proposed a relationship between higher trichodorid population build-up in the top soil layers during the rainy season, giving them greater opportunity for direct feeding on the tubers, and the subsequent greater occurrence of spraing. Direct feeding of trichodorid nematodes on potato roots rather than tubers, happening due to the prevalence of prolonged dry-spells during potato growing season, tends not to result in disease development. Sowing of seed potatoes at various soil depths has not proved to influence spraing induction and prevalence as production of progeny tubers, irrespective of the sowing depth, takes place at almost the same depth. The disease development remains constant during storage of infected tubers, suggesting no effect of storage period on spraing.

Repeated vegetative propagation of spraing-affected potatoes results in the reduction of observable spraing symptoms in the progeny tubers. TRV translocation from spraing-affected tubers to the sprouts and the subsequent progeny tubers, inducing a secondary spraing is inconsistent, with most tubers being spraing-free but perhaps not virus-free. (Engsbro, 1973; Harrison and Robinson, 1981, 1982, 1986; Xenophontos *et al.*, 1998).

Depending upon the potato cultivar and the infecting TRV isolate, the intensity and spread of spraing is greater if TRV infection occurs at an initial tuber development stage, causing spreading of necrosis into the whole tuber (Fig.1.1) with the production of brownish and necrotic arcs of spraing on the tuber-periderm, occasional development of cracks, knobby-growths and deformation of the tubers (Fig.1.2. a, b).

As with the usual association (in the U.K) of stem mottle-affected plants with NM-type TRV isolates, spraing symptoms have also been mostly found allied to NM-type TRV isolates (Harrison *et al.*, 1983; Weingartner, 2001). Robinson (2004) also found the induction of spraing in a potato cultivar Bintje was due to the involvement of an

NM-type variant of a TRV isolate (PpO85). Previously, Bintje was thought to be resistant to TRV-infection.

With the introduction of modern molecular detection methods, Xenophontos *et al.*, (1998) unexpectedly detected TRV in some asymptomatic potato tubers and proposed such tubers as a possible source of TRV spread to some sites not known to have TRV-bearing vector nematodes. Moreover, they also confirmed (using a serological detection test) the presence of M-type TRV in the foliage and roots of some potato plants. Likewise, Robinson and Dale (1994) also reported upward systemic movement of M-type TRV, from asymptomatic infected tubers of potato cv. Wilja, to the foliage and then later to the newly produced tubers.

Tuber symptoms produced by PMTV have also been referred to as spraing and are similar in physical appearance to those induced by TRV. However, TRV-induced spraing is generally composed of corky-tissue whereas PMTV-induced spraing is lacking in this character. PMTV-produced spraing has symptoms mostly obvious on the external surface of affected-tubers, whereas, TRV generally produces internal symptoms of spraing and the appearance of external symptoms is rare with this virus. Moreover, the soil-texture and field history of spraing-affected tubers can also give clues to guess the causative agent, as the TRV-vector nematodes thrive in sandy soils but the PMTV vector proliferates in clay-type soils. Due to its sensitivity to PMTV and resistance to TRV, potato cv. Saturna can serve as a biological assay plant to differentiate the causative agent of spraing (Sokmen *et al.*, 1998; Dale, 2009). Authentic diagnosis is through laboratory-based tests that include ELISA (for PMTV, as there is not much serological diversity among the few known strains) and RT-PCR (for TRV, due to the prevalence of many serologically diverse strains).

Ryden *et al.* (1994) showed that asymptomatic TRV-infected tubers of known spraing-sensitive cultivars, stored for a month at ambient conditions, after inspection were found to remain symptomless. Whereas, such infected tubers developed spraing when they were diced and then stored at the same ambient conditions for a month.

The development of spraing was thus suggested to be associated with changed physico-chemical processes, such as sucrose content, and better aeration of the infected tubers. Spraing symptoms can be sometimes confused with the brownish discolouration of ‘‘internal rust spot’’ that is due to calcium deficiency in the affected soil (Collier *et al.*, 1978). Potato viruses such as PVY-N and Alfalfa mosaic virus (AMV) can also produce tuber discolouration resembling spraing. Reliable diagnosis requires the use of molecular diagnostic tests like RT-PCR and ELISA.

1.5. Genomic structure and organization of TRV

The genome of TRV is composed of two messenger (+ve) sense, single-stranded (ss) ribonucleic acids (RNAs), called RNA-1 and RNA-2. These are contained separately in two rigid rod-shaped L and S particles, respectively, with variable genomic sizes being found among different isolates. Both genomic RNAs (Fig. 1.3) have conserved sequences (of less than 100 nucleotides) at their 5′ and 3′ termini and the 5′ end of both RNA segments is capped with a 7-Methyl Guanosine structure, whereas, the 3′ end has a tRNA-like structure (Pelham, 1979; Harrison and Robinson, 1986; Hamilton *et al.*, 1987).

1.5.1. TRV RNA-1

The larger RNA, called RNA-1, is about 6.8 kb in size. The RNA1 from different TRV isolates is highly conserved, being more than 90% identical in nucleotide sequence (Koenig *et al.*, 2011; 2012). RNA-1 has four open reading frames (ORFs) of which the largest, the helicase gene, is at the 5′ proximal position with an opal translation termination codon at its distal end (Fig. 1.3.a). This first ORF encodes a 134 kDa protein with predicted methyl transferase and nucleotide-binding and helicase activities. Immediately downstream of the helicase gene, in the same reading frame, is the polymerase gene that is expressed by read-through translation of the opal (UGA) termination codon of the helicase gene creating a 194 kDa protein with

predicted RNA-dependent RNA Polymerase (RdRp) activity (Hamilton *et al*., 1987). These two ORFs, consisting of both helicase and polymerase genes comprise the replicase gene that embraces about 75% of the total RNA-1 genome and is involved in RNA replication (MacFarlane, 1999; Crosslin *et al*., 2003). The next ORF, downstream of the polymerase gene, is the ‘‘P1a’’ gene, translated as a 29 kDa protein (also known as the 1a protein). It is a 30K superfamily-like movement protein (MP) that is involved in the inter-cellular movement of TRV. At the 3′ proximal position in RNA-1 is the ORF for the ‘‘P1b’’ gene, translated as a 16 kDa cysteine-rich protein (also known as CRP or 1b protein), that functions in TRV pathogenicity as an antagonist of gene silencing and is possibly also, as was demonstrated for PEBV, involved in seed transmission (Wang *et al*., 1997; Liu *et al*., 2002; Ghazala *et al*., 2008; Martin-Hernández and Baulcombe, 2008) of TRV. An additional ORF is also found within the P1b gene that could, in theory, be translated as a 13kDa protein of unknown function (MacFarlane, 1999). The replicase gene acting as a mRNA is translated directly from the RNA-1 without the need of any subgenomic RNA (sgRNA) for its expression. In contrast, the 1a and 1b genes are not expressed directly from RNA-1 but are translated through two subgenomic RNAs designated ‘‘sgRNA1a’’ and ‘‘sgRNA1b’’ of 1.5 kb and 0.7kb size, respectively, of which the former is encapsidated and the latter non-encapsidated (Pelham, 1979; Robinson *et al*., 1983, 1987; Boccara *et al*., 1986; MacFarlane, 1999; Mandahar, 2006). RNA-1 alone is infectious, as its replication and movement within plants is independent of the presence of RNA-2 but it does need RNA-2 to be encapsidated (particle formation) and for nematode transmission (Hamilton, *et al*., 1987; Hernandez *et al*., 1995; MacFarlane and Brown, 1995; MacFarlane *et al*., 1999; Visser and Bol, 1999; Vassillakos *et al*., 2001).

At the amino acid level, the replicase protein is the most conserved (>95% identical), and is followed by the MP protein with >93% identity among all the TRV RNA-1 isolates. Whereas, the CRP or 1b protein is the least conserved (Robinson, 2004; Crosslin *et al*., 2010, Yin *et al.*, 2014b), with up to 15% difference.

1.5.2. TRV RNA-2

The smaller genomic RNA, known as RNA-2, ranges in size (depending on virus isolate) from 1.9 to nearly 4.0 kb (Cornelissen *et al*., 1986; Vassillakos *et al.*, 2001). This genome segment of TRV, in contrast to RNA-1, is highly variable among different isolates for its size, nucleotide sequence and organization of the encoded genes (Robinson *et al*., 1983; Bergh *et al.*, 1985; Cornelissen *et al*., 1986; Angenent *et al*., 1986; Goulden *et al*., 1990; Sudarshana and Berger, 1998). This makes it difficult to completely describe the genomic structure of a typical TRV isolate. RNA-2 often codes for three or four ORFs (Fig. 1.3.b). Both extremities of RNA-2 possess a non-coding region (NCR) with varying sequence length. The 3′ NCR is highly conserved among all the tobraviruses although the length of the conserved sequence may vary among TRV isolates. The 5′ NCR ranges from 381-709 nucleotides and differs noticeably in sequence identity among different isolates. The 5′ NCR plays a vital role in the multiplication of RNA-2 (Bergh *et al.*, 1985; Angenent *et al*., 1989). Besides always coding for the coat protein (CP) gene, located usually near the 5′ end (Bergh *et al.*, 1985; Goulden *et al.*, 1990), RNA-2 may also carry one or more non-structural protein-encoding genes (2b and 2c genes). These genes are located mostly downstream of the CP (also known as the 2a) gene. In some instances, as with the TRV-PSG strain and PepRSV, the RNA-2 encodes only one gene, namely the CP gene (Bergh *et al*., 1985; Cornelissen *et al*., 1986). Exceptionally, in the case of TRV-SYM, the CP gene is downstream of three novel ORFs and located in almost the centre of the RNA-2 genome (Ashfaq *et al.*, 2011). Likewise, the CP gene of the recently sequenced Mlo7 isolate is also located in the centre of the RNA-2 genome, alongwith an ORF for a hypothetical protein located upstream of the CP gene (Yin *et al.*, 2014a). The C-terminus of the tobravirus CP possesses a peptide sequence, extending from the virus particle, which is thought to be involved in the virus-nematode interaction (Mayo *et al.*, 1994). The 2b gene encodes the 2b protein which is responsible for nematode transmission of TRV. So far, the function of the 2c gene

of any TRV isolate is not known, although, the 2c gene of PEBV (TpA56 isolate) has been shown to be involved in nematode transmission of that virus (Ploeg *et al.*, 1993a, b; MacFarlane *et al*., 1996; Hernandez *et al*., 1995; 1997; MacFarlane, 2003). During studies to determine the complete RNA-2 nucleotide sequence of a nematode-transmissible TRV isolate (PpK20) and to observe the influence of RNA-2 encoded genes on the replication of TRV in *N. tabacum* plants, Hernandez *et al.* (1995) developed a full-length infectious-clone of this RNA. Mutagenesis studies of the 2b and 2c genes carried on this infectious clone proved that the 2b gene was involved in nematode transmission (Hernandez, *et al*., 1997). MacFarlane *et al*. (1996) produced mutations in the four coding genes of the PEBV RNA-2 (TpA56 isolate) and proved that deletion of the 15 amino acids from the C-terminus of the CP cistron resulted in the failure of nematode transmission of the virus. Besides, the CP, three other proteins (9K, 2b and 2c) were also found to affect the nematode transmission of PEBV. Although the presence of ORF 2b and 2c varies among different TRV isolates, MacFarlane (2010) has emphasised the essential role of the 2b protein in nematode transmission and possibly its involvement in the vector specificity of TRV. Also, Valentine *et al.* (2004) reported a role for the 2b protein in the movement of TRV to non-inoculated leaves and roots of *N. benthamiana* and *Arabidopsis thaliana* plants, suggesting its possible involvement as an antagonist of the plant defence system. RNA-2 isolates lacking ORFs 2b and 2c such as TRV-PSG, TRV-PLB, TRV-R and TRV-TCM (lacking the 2c gene only) may evolve naturally either following recurring mechanical inoculation of the virus or through repeated vegetative propagation of infected tubers (MacFarlane, 1999; Heinze *et al*., 2000). Contrary to RNA-1, RNA-2 lacks mRNA activity and produces all its proteins only through the expression of subgenomic (sg) RNAs. The CP gene is expressed from an encapsidated ‘‘sgRNA2a’’, whereas, the translational mechanism of the non-structural proteins that differ in sequence homologies and sizes among different TRV isolates has not been demonstrated experimentally (MacFarlane, 1999).

A salient character of TRV genomes is RNA recombination, where sequences from the 3′ end of RNA-2 are replaced by the 3′ sequences from RNA-1 (MacFarlane, 1997). The TRV-TCM strain (isolated from Tulip in Netherlands and with antigenic resemblance to the Dutch serotype of PEBV, Cornelissen *et al*., 1986) possesses the 2a gene, coding for the CP of 29.1 kDa, and also carries an additional RNA-1 derived 16 kDa gene (Angenent *et al*., 1986) at its 3′end. Thus, in this instance the TCM strain has two copies of the 16K gene, at the 3′ termini of both RNA-1 and RNA-2 (Hamilton *et al*., 1987). Likewise, RNA-2 from TRV-PSG, TRV-PLB and TRV-R isolates also carries some sequences of the RNA-1 16K gene at their 3′ termini, due to a genetic recombination of the RNA-1 and RNA-2 genomic segments. This natural genetic recombination between the two TRV genomic RNAs is common. Yin *et al.* (2014b) have described two natural recombinant Polish isolates of TRV i.e.; Slu24 and Deb57, that carry a truncated part of the 16K gene acquired from RNA1 of the related (Slu24) or unrelated (SYM or PpK20) isolates, respectively. Mechanistically it is proposed that the TRV RNA-2 genomes may base pair with an unrelated RNA-1 genome during replication, leading to deletion of a significant part of the RNA-2 (Koenig *et al*., 2012). Additionally, two TRV strains, TRV-PpK20 and TRV-R, possess an extra ORF located between the CP and 2b genes coding for putative 6.51 kDa and 8 kDa proteins, respectively. Any function of these extra ORFs is not known yet, however, MacFarlane *et al.* (1999) identified a 9K ORF of PEBV-SP5 (RNA-2) located between the CP and 2b genes and suggested its participation in nematode transmission.

Recently, Koenig *et al*. (2011) reported a new strain of TRV (AL-strain), comprising one TRV RNA-1 (AL TRV RNA-1) accompanied by seven dissimilar RNA-2 genomes (AL TRV RNA-2, all differing in their sizes and RNA-1-related 3′ termini). These TRV genomes were isolated and identified by synthesizing cDNA directly from a naturally infected Peruvian-lily plant (*Alstroemeria aurae).* AL TRV RNA-1 was more than 90% identical in its nucleotide sequence with the published complete RNA-1 sequences of five other TRV strains (PpK20, ORY, SYM, PpO85 and MI).

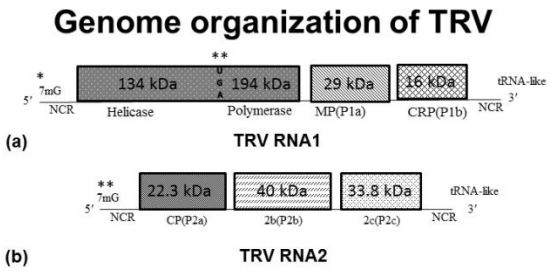

Figure 1.3. Genome arrangement and structure of TRV (PpK20). (*=7mG=7-Methyl Guanosine structure; NCR=Non Coding Region, **=UGA= Opal stop codon) **(a)** The RNA-1 segment of TRV is responsible for the replication, movement and pathogenicity of the virus as it is composed of four important genes encoding helicase (134kDa), polymerase (194kDa), both jointly known as the replicase, movement protein (MP, 29kDa) and the cysteine rich protein (CRP,16kDa). **(b)** The RNA-2 segment of TRV (PpK20 isolate) is required for encapsidation and transmission of the virus as it encodes the coat protein (CP) and the 2b (nematode transmission protein) and 2c (unknown function) proteins.

Genome organization of various TRV RNA-2 isolates

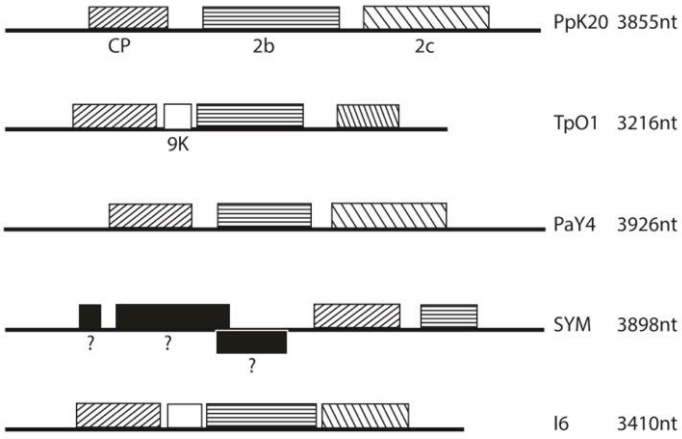

Figure 1.4. Genome organization of RNA-2 of isolates used to make recombinant viruses. Isolate name and RNA-2 size are shown at right of figure. Gene name appear under the genome diagrams. Boxes denote relative size and position of genes, and boxes with the same fill pattern denote conserved genes. Expression of SYM 5′ genes denoted by ? has not been demonstrated experimentally.

Whereas, for the seven identified AL TRV RNA-2 genomes (TC3′ AL-a, -b, -c, -d; TC3′ PE-a,-b and TC3′ PE-c), the nucleotide sequences of their 5′ NCR, CP gene and 2b gene (in some molecules) were more than 99.7% identical with the RNA-2 of the tulip isolate (TRV TCM strain). The CP sequence of all these seven RNA-2 genomes was found to be nearly 100% identical with the CP of TRV TCM strain. Interestingly, all seven AL RNA-2 molecules had a common 3′ termini, but of different lengths, which is derived from the 3′ terminus of TRV RNA-1. Three of these RNA-2 molecules (TC3′ PE-a-c) had a 3′ terminal part most similar to a British strain of PEBV (SP5), whereas, the other four (TC3′ AL-a-d) had a 3′ terminal part most similar to the AL RNA-1.

The presence or absence of novel ORFs, the cistrons for the 2b and 2c proteins and the different sizes of the 3′ terminal RNA-2 sequences derived from RNA-1, account for the differences in the particle lengths and genome sizes of the various RNA-2s of different TRV isolates (Hernandez *et al*., 1995). TRV RNA-2 by itself, in contrast to RNA-1, is non-infectious, as it is devoid of the replication and movement functions which are supplied by RNA-1.

1.6. Specific examples of TRV isolates and strains

Many isolates of TRV have been described and an ever increasing number have been sequenced (particularly RNA-2). Among all the known TRV isolates, the Potato Ring Necrosis (PRN) isolate, collected from a potato field in Scotland, is the oldest and is the type strain of TRV (Cadman and Harrison, 1959; Robinson and Harrison, 1989).

More than 28 complete or partial TRV RNA-1 nucleotide sequences have been deposited in the GenBank nucleotide sequence database. Most of these (>19) are potato isolates (e.g; ORY, PpK20, PpO85 and MI-1 etc.,), and a few of them are isolates from other crops such as the Spinach isolate (SYM), the Peruvian-Lily

isolate (AL) and the Hosta isolate (Ho). The three RNA-1 isolates used in the current study are briefly discussed here:-

1. *TRV-SYM RNA-1* (Spinach Yellow Mottle strain; Hamilton *et al*., 1987; accession number D00155). SYM was isolated from infected spinach (*Spinacia oleracea*) plants collected from a field in South of England (Robinson and Harrison, 1985a). The RNA-1 genome of the SYM strain was the first to be fully sequenced and consists of 6,791 nucleotides (nts).

2. *TRV-PpK20 RNA-1* (Kinshaldy-20 strain transmitted by *Paratrichodorus pachydermus*; Ratcliff *et al*., 2001; accession number AF314165). PpK20 was initially isolated from the roots of a *Petunia hybrida* bait-plant, after transmission by a single viruliferous *P. pachydermus* nematode, collected in soil at a potato farm in Kinshaldy, Scotland (Ploeg *et al*., 1992b). The RNA-1 sequence is composed of 6,791 nts.

3. *TRV-PpO85 RNA-1* (Overloon-85 strain transmitted by *P. pachydermus*; Robinson, 2004; accession number AJ586803). The potato cultivar Bintje was earlier considered to be resistant to TRV infection but over a period of time it was reported to develop spraing at certain specific localities in the U.K, Belgium, Sweden and Netherlands, suggesting the possibility of some variation in TRV populations at these places. Robinson (2004), to investigate the possible reason of Bintje resistance-breaking, acquired TRV isolates from individual *P. pachydermus* nematodes, collected from a potato-field at Overloon, Netherlands. RNA-1 of TRV isolate PpO85 was shown to be responsible for TRV resistance-breaking in potato cv. Bintje and differs from other TRV RNA-1 sequences by less than 5.5 %, with the most variation occurring in the 1b gene. The full-length RNA-1 sequence comprises 6,617 nts, and is smaller than the full-length RNA-1 sequences of the other two TRV (i.e.; SYM and PpK20) isolates under study.

More than forty RNA-2 molecules from various TRV isolates have been fully sequenced, to date, and only those involved in the current studies are briefly discussed here. A schematic illustration for general comparison of their genome organizations is presented in Fig. 1.4.

1. *TRV-PpK20 RNA-2* (Kinshaldy-20 strain transmitted by *P. pachydermus*; Hernandez, *et al*., 1995; accession number Z36974). The PpK20 isolate was originally isolated from a *P. pachydermus*-infested soil sample, collected from a potato-field at Kinshaldy in Scotland. This RNA-2 has a sequence of 3,855 nts consisting of three ORFs along with 5′ and 3′ NCRs of 556 nts and 401 nts, respectively. The first ORF covering 615 nts, encodes the CP (of 22.3kDa), the second ORF of 1065 nts encodes the 2b protein (of 40kDa; Visser and Bol, 1999, previously reported to be 29.4kDa protein) and the last ORF consisting of 869 nts encodes the 2c protein (of 32.8kDa). An additional ORF of 212 nts for a putative c.6.5kDa protein had also been suggested to exist between the 2b and 2c genes, by Hernandez, *et al*., 1995, but not experimentally studied. Each of the RNA-2 genes is separated with non-coding sequences of variable lengths. TRV-PpK20 is transmissible by the trichodorid nematode *P. pachydermus.*

2. *TRV-I6 RNA-2* (Italian isolate transmitted by *Trichodorus viruliferous*; Robinson, 1994; accession number S72875.1). The I6 isolate alongwith six other TRV Italian isolates (I1-5, and I7) was originally isolated, by van Hoof *et al* (1966), from one of 29 tested soil samples. All these soil samples were collected from various locations in northern Italy. The soil sample of the I6 isolate was taken from a wheat field at Mesola (Po estuary), in northern Italy. Two of the tested isolates (I2 and I5), on direct mechanical inoculation to the developing tubers of potato variety ‘‘Eersteling’’, induced spraing. Whereas, I6 failed to produce any spraing symptoms. The I6 isolate of TRV had not been fully sequenced in the past and only the nucleotide sequences of its RNA-2 termini published by Robinson (1994) were available. Serologically, I6 was found to be more closely related to PEBV serotypes. Further characterization and assessment

of all these seven TRV isolates was not done. As part of this Ph.D study the genetic sequence of this isolate has been completely determined to be of 3,410 nts. I6 RNA2 has four ORFs, the first ORF of 627nts for the CP, followed by the 240nts of the 9K gene, the 768nts of the 2b (29kDa 2b protein) gene and the 627nts of the 2c (23kDa 2c protein) gene. I6 RNA-2 is very similar in its genetic configuration to the RNA-2 of TRV TpO1 and the RNA-2 of PEBV TpA56. The 5′ NCR and 3′ NCR are of 551nts and 487nts, respectively. The I6 RNA-2 is highly similar in nucleic acid sequence and serological properties to the RNA-2 of PEBV-SP5 and TpA56 strains (MacFarlane *et al*., 1999; van Hoof *et al*., 1966; Robinson *et al*., 1987). However, the replication of I6 RNA-2 is mediated by the TRV RNA-1 encoded replicase proteins. Whereas, the replication of PEBV RNA-2 cannot be achieved by the TRV encoded replicase.

3. *TRV-PaY4 RNA-2* (PaY4 strain transmitted by *P. anemones*; Vassilakos *et al.*, 2001*;* accession number AJ250488). This English strain was isolated from a trichodorid nematode, *P. anemones,* collected from York (Ploeg *et al.*, 1992b). RNA-2 of this isolate, consisting of 3,926 nts, is the largest known TRV RNA-2 segment that has been sequenced so far. It is composed of three ORFs, a CP ORF of 633nts, 2b ORF of 717 nts and a 2c ORF of 861 nts, yielding proteins of about 22.5kDa, 27kDa and 32kDa, respectively. The CP of PaY4 is very closely similar in its peptide sequence to the CP of TRV-SP (spinach isolate, Germany), followed by TRV-ON (onion isolate, Germany) and TRV-TCM (tulip isolate, Netherlands). The 3′ terminal sequence of RNA-2, of about 266 nts, includes the RNA-1 encoded 16K gene. Although PaY4 is a recombinant strain it retains the transmission genes and is nematode-transmissible. It is the first known tobravirus to be flexible in its nematode transmissibility and thus rather than being strictly transmitted by only one nematode species (*P. anemones*), it can also be transmitted by *P. pachydermus*.

4. *TRV-TpO1 RNA-2* (TpO1 strain transmitted by *T. primitivus*; MacFarlane *et al*., 1999; accession number AJ009833). The TpO1 isolate was acquired from a viruliferous *T. primitivus* nematode, extracted from a soil sample, collected from Oxfordshire in England (Ploeg *et al*., 1992b). TpO1 RNA-2 comprises 3,216 nts with four ORFs, and 5′ and 3′ NCRs of 474 nts and 413 nts, respectively. The first ORF covers 591 nts, encoding the CP (21.51kDa), and the second ORF extends to 246 nts encoding a 9K (9 kDa) protein. The third ORF of 774 nts encodes the 2b protein (29kDa) and the last ORF consisting of 468 nts encodes the 2c (18kDa) protein. The RNA-2 of TRV TpO-1 and PEBV TpA56 RNA-2 are very similar in their genetic arrangement. Both these viruses have the same molecular size of the corresponding 9K and 2b proteins but they differ in the molecular size of the 2c proteins. The role of this 2c protein in TRV transmission is not proved. The tobravirus isolates TRV TpO-1 and PEBV TpA56, are both transmitted by *T. primitivus* nematodes.

5. *TRV-SYM RNA-2* (SYM strain; Ashfaq *et al*., 2011; accession number FR854197.1). The RNA-2 of SYM is an exceptional case due to the unusual structural arrangement of the TRV RNA-2 genes. It consist of 3,898 nts comprising five ORFs. The SYM CP (24kDa) is encoded by the fourth ORF (645 nts) and is preceded by three other novel ORFs. This CP gene is therefore located in the centre of RNA-2 and is followed by an ORF of 408 nts encoding a C-terminally- truncated 2b protein of about 16kDa. The SYM strain is unique from the other strains in causing systemic infection in *C. amaranticolor* plants (Ploeg *et al*., 1992b).

All the five TRV RNA-2 isolates described above belong to different serological groups (serotypes). So that PpK20, TpO1 and SYM have PRN, RQ and SYM serotypes, respectively (Ploeg *et al*., 1992b). The antigenic property of the PaY4 isolate is not known (Vassilakos, *et al*., 2001) as all the 9 isolates (PaY1-PaY9) from

the soil samples collected in York, poorly reacted with 8 diverse TRV-specific antisera when tested by Ploeg *et al*., 1992b.

A phylogenetic analysis of partial or full-length nucleotide sequences of various TRV RNA-1 isolates, by using the MEGA6-package (default function. Tamura *et al*., 2013), is presented in Fig. 1.5.a. The dendrogram shows that RNA-1 of PpK20 and SYM isolates clusters with ByKt (Bav), ORY, and SHM isolates. Whereas, the RNA-1 of PpO85 isolate is more closely related to the partially sequenced PSG isolate. The dendrogram of the helicase, replicase and movement proteins is presented in (b), (c) and (d), respectively. The replicases of SYM, PpK20 and PpO85 cluster closely together, but the MP and 16K of PpO85 (Fig. 1.6.a.) are less related to those of PpK20 and SYM isolates.

Phylogenetic analysis of partial or full-length nucleotide sequences of various TRV RNA-2 isolates, presented in Fig. 1.7.a., shows that the RNA-2 of I6 isolate is most closely related to the RNA-2 of PEBV strain (SP5); that was used as out-group in the analysis. Both these isolates formed a common clade with a bootstrap value of 99. Similarly, the phylogenetic analysis of the coat-proteins, 2b-proteins, 2c-proteins and the 9K-proteins of various TRV RNA-2 isolates is presented in Fig. 1.7.b., c, d and Fig. 1.6.b., respectively. In all these dendrograms the I6 RNA-2 encoded proteins formed a common group with those of PEBV-SP5 strain (bootstrap values of 96-100%).

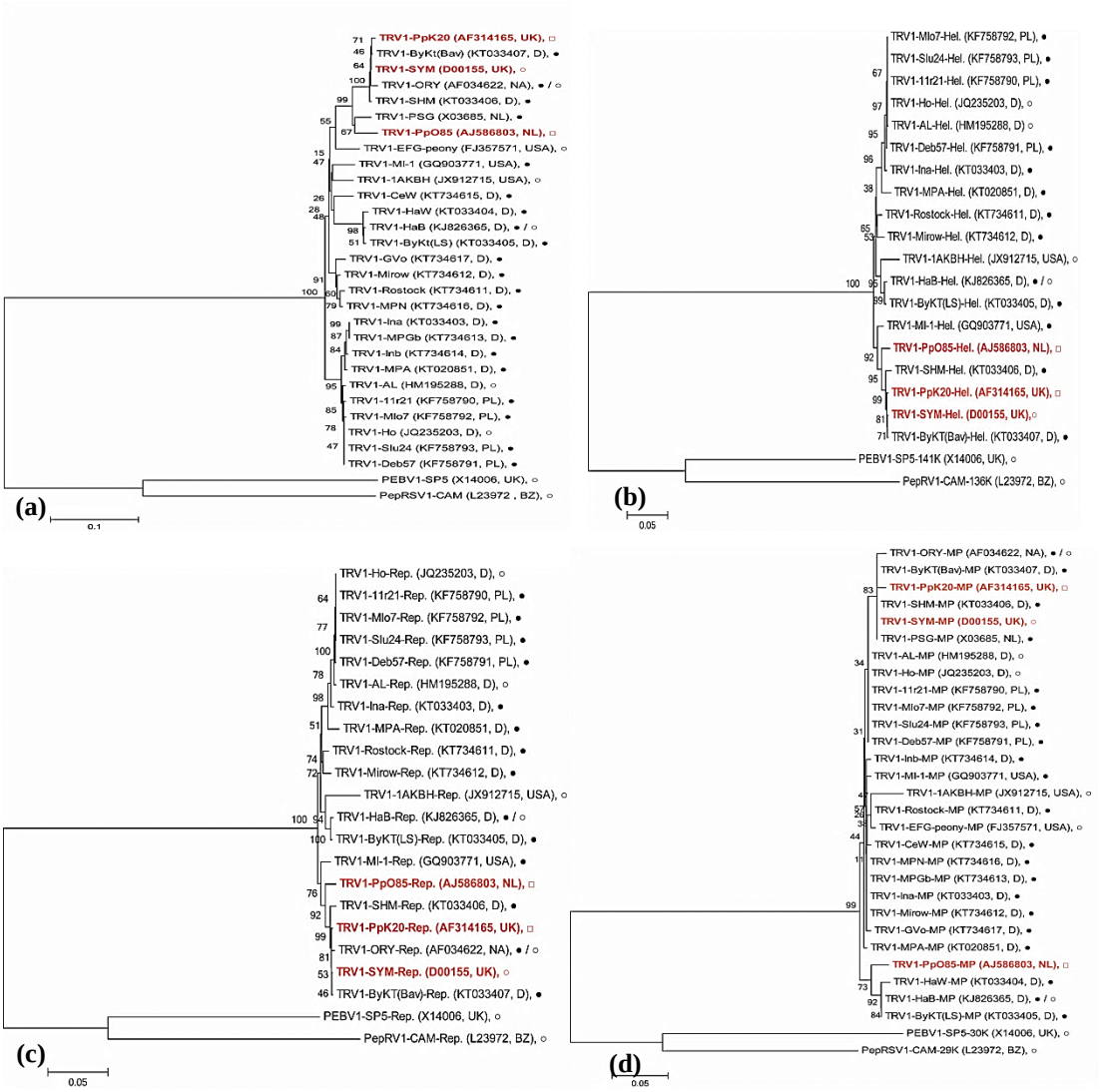

Figure 1.5. Phylogenetic analysis of the nucleic acid and protein sequences of various TRV RNA-1 isolates. Dendrogram of various TRV **(a)** RNA-1 nucleotide sequences. **(b)** Helicase proteins. **(c)** Replicase proteins **(d)** and Movement proteins. The dendrograms were constructed by the neighbour-joining method and the support of tree-nodes was assessed by using 1000 bootstrap-replications. The NCBI accession number and country of TRV isolation is given in parenthesis. United Kingdom, Germany, Netherlands, Poland, Brazil, Portugal, Italy, South Korea, North-America and United States of America are abbreviated as UK, D, NL, PL, BZ, PT, IT, SK, NA and USA, respectively. Host plant or isolation source of TRV from potato crop, other-crops and nematodes is specified by a filled-circle (•), an open-circle (◦), and open-square (□), repectively. The scale-bar measures phylogenetic-distance (nucleotide or amino-acid substitution / site) and the isolates in current study are in bold and red text.

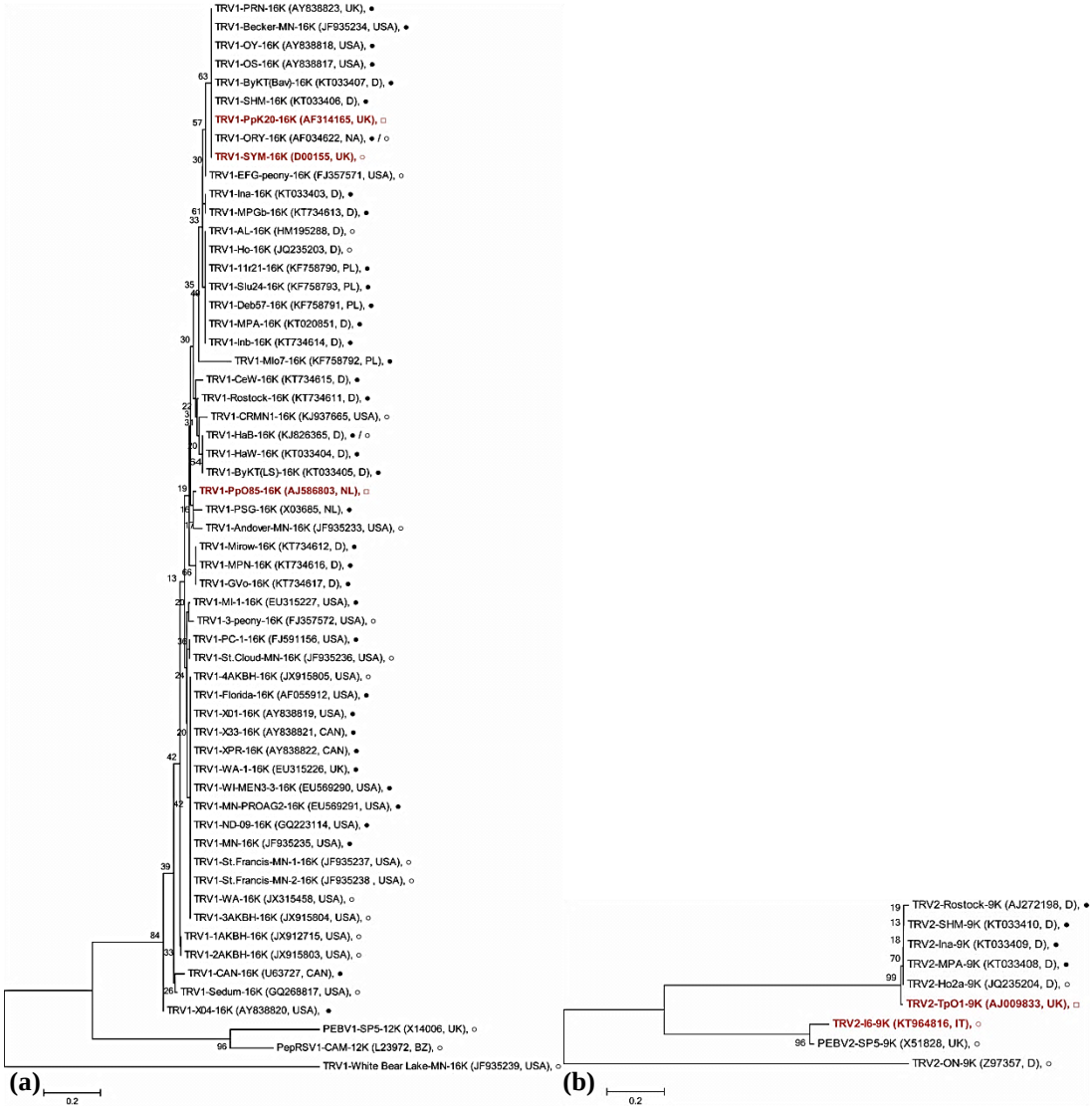

Figure 1.6. Phylogenetic analysis of the 16K and 9K proteins of various TRV isolates. Dendrogram of various TRV **(a)** 16K and **(b)** 9K amino-sequences. The dendrograms were constructed by the neighbour-joining method and the support of tree-nodes was assessed by using 1000 bootstrap-replications. The NCBI accession number and country of TRV isolation is given in parenthesis. United Kingdom, Germany, Netherlands, Poland, Brazil, Portugal, Italy, South Korea, North-America, Canada and United States of America are abbreviated as UK, D, NL, PL, BZ, PT, IT, SK, NA, CAN and USA, respectively. Host plant or isolation source of TRV from potato crop, other-crops and nematodes is specified by a filled-circle (•), an open-circle (◦), and open-square (□), respectively. The scale-bar measures phylogenetic-distance (nucleotide or amino-acid substitution / site) and the isolates in current study are in bold and red text.

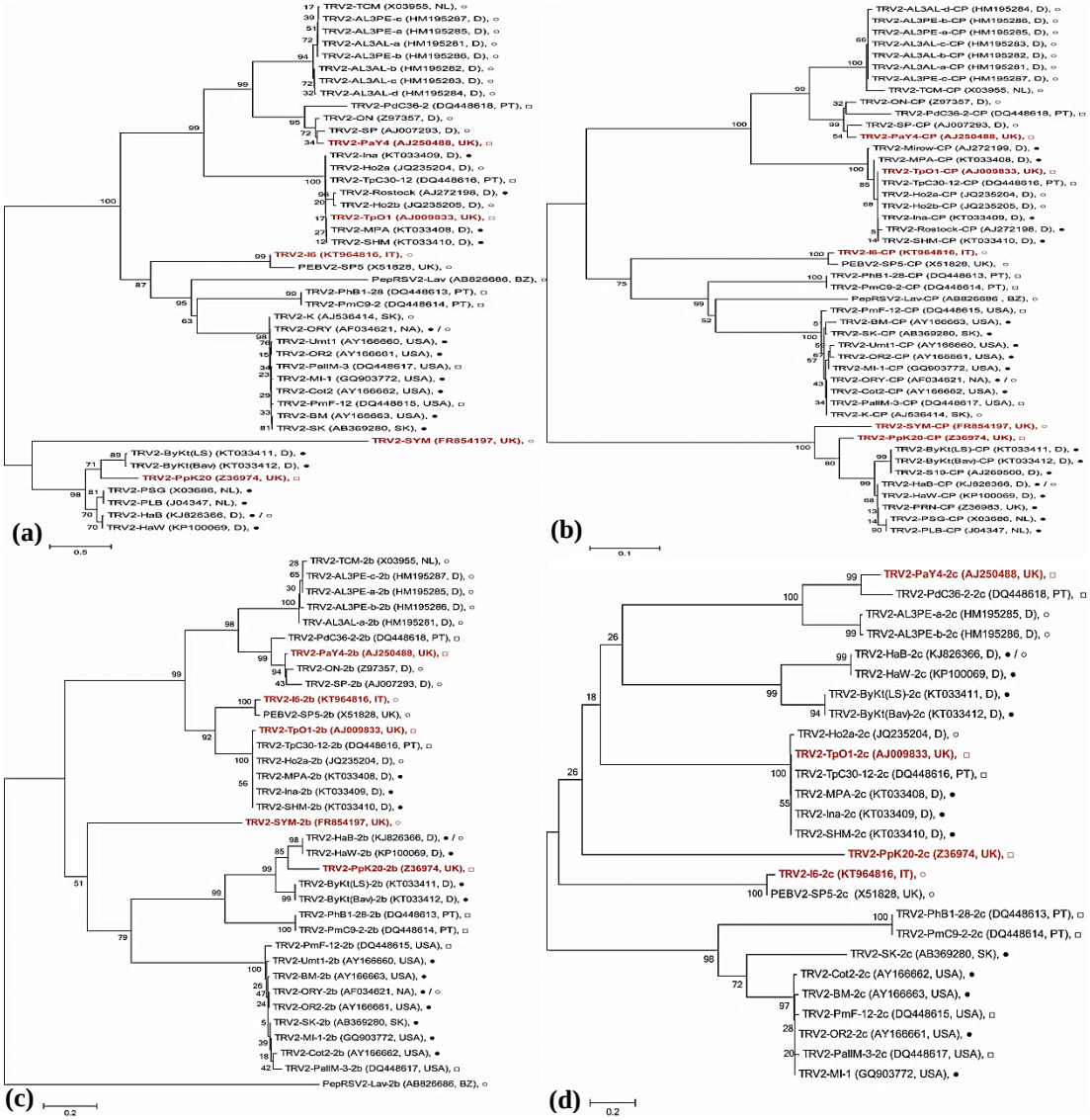

Figure 1.7. Phylogenetic analysis of the nucleic acid and protein sequences of various TRV RNA-2 isolates. Dendrogram of various TRV **(a)** RNA-2 nucleotide sequences. **(b)** CPs **(c)** 2b proteins **(d)** and 2c proteins. The dendrograms were constructed by the neighbour-joining method and the support of tree-nodes was assessed by using 1000 bootstrap-replications. The NCBI accession number and country of TRV isolation is given in parenthesis. United Kingdom, Germany, Netherlands, Poland, Brazil, Portugal, Italy, South Korea, North-America and United States of America are abbreviated as UK, D, NL, PL, BZ, PT, IT, SK, NA and USA, respectively. Host plant or isolation source of TRV from potato crop, other-crops and nematodes is specified by a filled-circle (•), an open circle (◦), and open-square (□), respectively. The scale-bar measures phylogenetic-distance (nucleotide or amino-acid substitution / site) and the isolates in current study are in bold and red text.

1.7. TRV pseudorecombinant isolates

A pseudorecombinant isolate is an experimentally derived virus that consists of RNA-1 from one isolate and RNA-2 of another, different isolate but of the same virus species (Sänger, 1968; Lister and Bracker, 1969). Pseudorecombinants formed by combining the RNA-1 and -2 from two different tobravirus species (e.g., TRV and PEBV) are not viable (Frost *et al*., 1967; Lister, 1968). However, some TRV isolates such as I6, N5 and TCM exist in which RNA-2 carries PEBV-derived genes but retains 5′ and 3′ sequences from TRV (Goulden, *et al.*, 1991; Robinson, 1994). These naturally occurring recombinant isolates are infectious. The experimental reconstitution of TRV isolates and the making of pseudorecombinants has been employed as an effective strategy to reveal the mechanistic details of TRV infection in various host plants.

Ploeg *et al.* (1993b) produced pseudorecombinant isolates, by mixing the genomes of TRV isolates PpK20 and PLB, which differ in their ability to be nematode-transmitted. The PpK20 isolate is nematode transmissible and PLB is non-transmissible. This pseudorecombinant study proved the involvement of PpK20 RNA-2 in the nematode transmission process and suggested the possible involvement of the CP in this virus-vector interaction. MacFarlane and Brown (1995) further supported this finding in the nematode transmission studies of PEBV-TPA56 (transmissible) and SP5 (non-transmissible) isolates, suggesting the possibility of an active role of the 2b protein in the virus-vector transmission process. Hernandez *et al.* (1995, 1997) in mutagenesis studies of the RNA-2 infectious clone of TRV PpK20 further demonstrated the involvement of the 2b protein in vector transmission. They suggested its possible interaction with the CP for binding TRV particles inside the nematode vector and also showed that 2b and 2c proteins are not required for RNA-2 multiplication.

Potato c.v Bintje had been known for many years as a TRV-resistant and spraing-free variety. During the last few years reports emerged that Bintje crops were developing spraing symptoms at certain specific localities, especially at Overloon in the Netherlands. Robinson (2004) collected from field nematodes Bintje-resistance-breaking TRV isolates for sequencing and pseudorecombinant studies. He made five pseudorecombinant isolates, derived from the two TRV isolates PpK20, and PpO85 (able to infect Bintje). Each pseudorecombinant isolate was inoculated using nematodes to one spraing-reactant (Pentland Dell, TRV susceptible) and five TRV resistant (including Bintje) potato varieties. All the pseudorecombinant isolates containing PpK20 RNA-1 failed to induce spraing in any of the five TRV-resistant potato varieties and produced spraing only in Pentland Dell. Exceptionally, a pseudorecombinant isolate carrying Pp085 RNA-1, succeeded in producing spraing in both the previously TRV-resistant and spraing-producing potato varieties. This work showed that RNA-1 of TRV isolate PpO85 gave resistance-breaking properties to the virus.

1.8. Spraing and resistance to TRV

Management of plant viruses by developing varieties resistant to viral infection is the most effective, economical, durable and environment-friendly approach. Resistance of plants to viruses has broadly been classified into non-host and host-resistance. Immunity (complete resistance, no infection) among all the genotypes of a specific host-virus combination has been described as non-host resistance (Palukaitis and Carr, 2008). It is the most stable and long-lasting type of resistance. The wild tobacco species, *N. benthamiana*, is used as a permissive host for many viruses but for Bean pod mottle Comovirus (BPMV) it exhibits non-host resistance (Lin, 2013). Non-host resistance against viruses is a less-explored area, due to the complexity of the mechanism, although, in recent years some progress has been made to discover the underlying mechanism acting against pathogens such as fungi and bacteria. For example, the cellular structure and production of a variety of secondary metabolites

by the host cell, such as production of saponins by oats, can cause non-host resistance to *Gaeumannomyces graminis* var. *tritici* (Mysore and Ryu, 2004). Host resistance, involving a specific interaction between virus and plant and mediated by one of more than two hundred plant-encoded resistance (R) genes (Kang *et al*., 2005), has further been categorized into extreme resistance (ER), hypersensitive response (HR) and systemic acquired resistance (SAR). The ER and HR are also known as ‘‘innate resistance’’. In the case of ER, very little or no virus infection takes place in the challenged plant. Virus in this situation is either non-detectable or can be detected only by very sensitive techniques. Potato plants exhibiting ER either mostly remain completely asymptomatic or produce extremely localised necrosis in the form of very tiny (pin point) lesions in a few potato genotypes (Valkonen *et al*., 1996). Mostly, in the case of ER, virus does not replicate or in rare cases can replicate in only a restricted area thereby inciting induced resistance that halts further replication of the virus. The coat protein of PVX can incite broad-spectrum resistance when viral RNA is inoculated into protoplasts of the potato cultivar Cara (Köhm, 1993). The ER genes are dominant over the HR genes. Extreme resistance can be wide-ranging, and can give resistance to many strains or viruses and is thus preferred by breeders for introgression into potato breeding lines (Barker and Dale, 2006). Plants have many different R genes, each protecting against a particular virus (Soosaar *et al*., 2005). The Rx1 gene (on chromosome twelve) and Rx2 gene (on chromosome five) give ER for PVX in *S. tuberosum* subsp. *andigenum* and *S. acaule*, respectively. Likewise, the Ry_{adg} (*S. andigenum*) and Ry_{sto} (*S. stoloniferum*) genes, both mapped to a similar region on chromosome eleven, provide ER for the potyvirus PVY (Gebhardt and Valkonen, 2001). Recently, four new Rx genes (Rx3-Rx6) have been documented from diverse potato species. These genes also mediate ER to PVX and have significant sequence similarity with the earlier known Rx1 and Rx2 genes of potato (Vleeshouwers *et al*., 2011).

HR, also known as apoptosis or Programmed Cell Death (PCD), is mostly an outcome of incompatible host-pathogen interplay. It commonly results in the

production of local, necrotic or chlorotic spots on the inoculated leaves, to restrict the further spread and movement of the pathogen. In the case of more severe infection in potato, spreading necrosis may be produced. The N-gene of *Nicotiana glutinosa* is a HR gene that provides resistance against Tobacco mosaic virus (TMV) infection. (Bawden, 1936, Valkonen, *et al*., 1996; Wright, *et al.*, 2000). The Nx_{phu} gene (on chromosome nine) and Na_{adj} gene (on chromosome eleven) mediate the HR in *S. phureja* and. *tuberosum* subsp. *andigenum*, against PVX and PVA, respectively (Gebhardt and Valkonen, 2001). HR is mostly linked with localised cell death that halts further spread of the invading virus. However, for the occurrence of HR, cell death of tissue is not an absolute requirement as it is an ancillary process connected to HR (Palukaitis and Carr, 2008). The movement protein of TRV (MP, 29K) PpK20 isolate has been found to be as elicitor of ER and HR-like responses in tetraploid potato cvs. Saturna, and Bintje, respectively and of ‘‘spreading necrosis’’ or susceptibility responses in cv. Russet Burbank (Ghazala and Varrelmann, 2007). Likewise, grafting of PVA-infected implants onto Shepody (a tetraploid cultivar) produces a novel HR response that is characterized by development of very tiny lesions on the foliage of the inoculated plant. These lesions are later succeeded by the formation of yellowish symptoms, identical to mosaic, and production of necrosis in the tuber tissue. This HR response in Shepody seems to be mediated by two separate dominant genes (Singh, *et al.*, 2000). The HR is associated with production of short-lived reactive oxygen species (ROS), commonly known as the ‘‘oxidative burst’’, that produces the reactive oxygen intermediates (ROI) consisting of superoxide (O^{-2}) and hydrogen peroxide (H_2O_2) that are involved in the host defence mechanism (Wojtaszek, 1997; Grant and Loake, 2000). ROS are produced integrally during routine plant metabolism to maintain cellular and physiological activities. However, their production increases significantly during stressful conditions such as during pathogen attack or other adverse environmental conditions. This abnormal ROS production has detrimental effects on the cellular and histological activities of an organism. These harmful events may include lipid degradation, protein denaturation,

nucleic acid disintegration, inactivation of enzymes, induction of PCD and death of affected cells. H_2O_2 is also utilized in the cell as a substrate for lignin and suberin biogenesis which are involved in the formation of cork-like tissues to block further spread of the pathogen. Abnormal H_2O_2 production, above a certain threshold level, can also cause death of the affected tissue (Tenhaken *et al.*, 1995; May *et al.*, 1996; Grant and Loake, 2000; Sharma *et al.*, 2012). The oxidative burst has been reviewed elsewhere by Lamb and Dixon (1997) and by Gadjev *et al.*, (2008). HR can also further activate other defence-related responses such as local and systemic acquired resistance (SAR), either close to or far from the site of infection (Graham and Graham, 1999). SAR is frequently associated with the activation of genes encoding a variety of proteins that are together called pathogenesis-related proteins (PRs) such as PR-1, PR-2 (1, 3-β-glucanases) and PR-3 chitinases (Kombrink and Schmelzer, 2001). These PR proteins are commonly involved in the defence mechanism of the host plant and are universal in their occurrence (Kemp *et al.*, 1999). PR-proteins have been broadly grouped into 15 different families, of which the most extensively investigated proteins are 1, 3-β-glucanases and chitinases, that are involved in degradation of the chitins found in fungi (Scherer *et al.*, 2005; Wang *et al.*, 2005). TMV-infected tobacco plants also produce glucanases as well as glycosyl hydrolase active chitinases that are involved in virus-induced resistance to guard the plant from subsequent fungal and bacterial infections (Bol and Linthorst, 1990). The developments in research into PR-proteins, over more than a decade, have been reviewed by Edreva (2005) and Sels *et al.* (2008).

The failure of viruses to move to the non-inoculated leaves of the plant could also be due to resistance imposed by the host on virus movement (Palukaitis and Carr, 2008) affecting either intercellular movement or systemic transport via the phloem (Blackburn and Barker, 2001).

Potato cultivars vary in their sources of resistance to TRV infection and so far no single, dominant R-gene against TRV has been reported (Ghazala and Varrelmann,

2007; MacFarlane, 2010). Cadman (1959) observed variation in potato varietal responses to TRV infection, and spraing production was proposed as a resistance-related hypersensitive response (Engsbro, 1973). At the National Institute of Agricultural Botany (NIAB), Cambridge, U.K, screening of potato cultivars for TRV resistance is done by scoring tubers for spraing symptoms. The field harvested tubers are subjected to visual inspection for recording the incidence and intensity of spraing symptoms. The disease assessment, to corroborate the level of resistance found in tested cultivars, is done based on a scale ranging in values from 1 to 9. The value of 1 is assigned to potatoes that are severely affected with spraing and the value of 9 is assigned to tubers that are asymptomatic for spraing production (Xenophontos *et al.*, 1998). Similarly, Dale and Solomon (1988) at the Scottish Crop Research Institute, SCRI (currently the James Hutton Institute, JHI) used viruliferous nematode-infested soil to infect glass-house grown tubers with TRV. Based on susceptibility to TRV infection and spraing production, these infected tubers were assessed using the NIAB TRV disease rating scale and commercial potato cultivars were divided into three categories (Robinson and Dale, 1994; Dale and Neilson, 2006). The number given in parenthesis against the cultivar represents the NIAB TRV disease (resistance) rating.

1. *Fully resistant (TRV-resistant):-*

   This group of potatoes, including the cultivars Bintje (7), Arran Pilot (9), Record (8), and Saturna (7), is completely resistant (immune) to TRV isolates, except for the PpO85 resistance-breaking isolate which is responsible for spraing induction in the cultivar Bintje. These cultivars do not exhibit any spraing symptoms and TRV is also not detectable in these cultivars even when using sensitive virus detection techniques such as ELISA or RT-PCR. Generally, these cultivars have a NIAB TRV-disease rating of 7-9.

2. *Spraing reactant (TRV-sensitive):-*

   Potato cultivars Pentland Dell (1), Maris Bard (2) and Russet Burbank (2) that exhibit an intermediate response between complete resistance and complete

susceptibility, are included in this category and they react to TRV infection by producing spraing in their tubers. So these are TRV sensitive cultivars, and both spraing and virus are present in such cultivars. Generally, they have NIAB TRV-disease rating of 1-3.

3. *Tolerant (TRV-susceptible) :-*

   These potatoes include the cultivars Rocket (5), Nadine (6), Shepody (6), Saxon (7), Wilja (5) and King Edward (6) that are susceptible to TRV infection without the production of any noticeable symptoms except for the reduction in number and size of the tubers. The infected tubers, sometimes, may exhibit brownish coloured spots (flecks) that are few in number but there is no characteristic spraing production. TRV in these tubers is detectable by ELISA and RT-PCR. Generally, they have a NIAB TRV-disease rating of 5-7.

1.9. RNA silencing and Virus Induced Gene Silencing (VIGS)

Plant diseases can incite huge crop losses. Conventional methods of combating these diseases and causative pathogens, involve the cross-protection (immunization) technique and harnessing of the natural resistance found in the plants through conventional breeding programmes. As discussed in the previous section, plants carry many R genes that recognize specific pathogens and trigger defensive reactions to limit or, in some cases, completely inhibit pathogen invasion. Sequencing of the potato genome has revealed more than 750 R genes, although which pathogen each of them targets is not yet known (Jupe *et al.*, 2013).

Recently, an additional host-encoded pathogen defence mechanism, known as RNA silencing, has been identified. RNA silencing is also known as quelling (fungi), RNA interference (RNAi, in animals) and co-suppression or post transcriptional gene silencing (PTGS, in plants). It operates through the sequence specific degradation of the target mRNA in eukaryotic organisms, with the known exceptions of

Saccahromyces cerevisiae (Baker's yeast), and some species of Trypanosomes (eukaryotic protozoan parasites).

RNA silencing is broadly categorized into two classes i)- transcriptional gene silencing (TGS) that impedes RNA production in the nucleus by methylation in the promoter region of the gene ii)- post-transcriptional gene silencing (PTGS) that causes sequence homology-based RNA degradation in the cytoplasm. PTGS is generally known as RNA silencing (Anandalakshmi *et al*., 1998; Mlotshwa *et al*., 2002).

The RNA silencing pathway responds to the presence of double-stranded (ds) RNA in the host cell. Subsequently, the dsRNA is cleaved by the Dicer enzyme (ribonuclease, RNase III) to form small RNAs of 21 to 24 nucleotides. These small RNAs are broadly classified as short interfering RNAs (siRNAs) and microRNAs (miRNAs). More types of these small RNAs are continually being discovered. The small dsRNAs, formed by the Dicer activity, consist of two strands with a phosphate group at the 5′end and a hydroxyl group at the 3′end, leaving an overhang of 2 bases at the 3′ termini. One of these strands (anti-sense strand) that mediates the silencing is referred to as ''the guide'', whereas, the second strand (sense strand) known as ''the passenger'' is eventually degraded. The guide strand finally integrates into the RNA induced silencing complex (RISC), containing the Argonaute protein (AGO) alongwith some other associated proteins. Here, the guide strand base pairs with the corresponding mRNA (the target) that is then cleaved by the ''slicer'' enzyme activity of the AGO (Ghildiyal and Zamore, 2009). miRNAs (also referred to in the past as small temporal RNAs, stRNAs) are of 21-22 nucleotides in size. Unlike siRNAs, miRNas are imperfectly matched to their target mRNA and down-regulate the translation of their targeted mRNA either by cleavage or stalling of translation. Most sequenced miRNAs are without any known target. Some miRNas have more than one target mRNA. (Mlotshwa *et al*., 2002; Zhixin and Qi, 2008; Axtel, M.J., 2008). Endogenous RNA silencing, besides safeguarding the genome from

transposon elements and controlling plant gene expression, also plays a defensive role against viral infection (Baulcombe, 2004).

Current plant molecular biology research aims to seek global systematic insight to define the gene (s), biological function of the proteins encoded by the genes and their interactions in various biochemical pathways of an organism. Analysis of gene function could either be carried out by following a forward genetics (from phenotype to genotype) or a reverse genetics (from genotype to phenotype) approach. The various conventional approaches used for functional gene analysis in plants such as the creation of stable transgenic plants or transposon tagging require the development of genetically modified (GM) plants (Ramachandran and Sundaresan, 2001). The establishment of GM plants involves plant transformation protocols that are complex and not suitable for some plant species.

An alternative and fast technique for functional genomics study involves the directed stimulation of the RNA silencing mechanism to reduce or completely prevent the expression of the host genes under study. This can be achieved either by the production of antisense RNA transcripts in the plant system (asRNA technology), by excessive transgene expression (overexpression, co-suppression), by the coexpression of both sense and antisense transcripts as transgenes (inverted repeat transgenes) or by the introduction of a viral vector engineered to target a particular host gene (virus induced gene silencing, VIGS) to cause degradation of the specific host mRNA (Benedito *et al.*, 2004).

VIGS is designed to stimulate the anti-viral response in a manner that results in sequence-specific degradation of a selected host plant mRNA. This is achieved by inclusion of a complementary plant gene (target) fragment engineered into the viral vector. VIGS is preferred among other RNA silencing techniques due to its procedural simplicity, rapidity, dispensation of the necessity for stable plant transformation and the ability to cause silencing of the members of a multi-gene family. Other advantages of VIGS are that it does not cause any structural change in

the targeted gene and is also suitable for plant species that are not amenable for plant transformation (Benedito *et al.*, 2004). Lacomme *et al.*, 2003 showed that co-expression of both sense and anti-sense RNA transcripts in plants resulted in an efficient induction of VIGS when the virus-vector was engineered with 40-60nts inverted repeat sequences of the targeted gene. The mRNA pool of the targeted endogenous PDS gene in *N.benthamiana* and barley plants was reduced by 87% and 90%, respectively, when these plants were challenged with the corresponding TMV-based and BSMV-based vectors engineered with 60nts inverted repeats of the PDS gene. Likewise, a considerable suppression of GFP expression was achieved when transgenic GFP-expressing *N. benthamiana* plants were inoculated with a TMV-based vector engineered with 40nts inverted repeats of the GFP gene. Also, RNA transcripts enriched in secondary structure are proficient inducers (Purkayastha and Dasgupta, 2009). The viral vector is an inducer of VIGS as well as at the same time being a target of the host defense response (Vaucheret, *et al.*, 2001; Burgyan, 2006). For the VIGS to become operative, a productive infection of the host plant by the viral vector is required. Once the viral vector is successful in establishing itself in the host, then at the local site of infection it generates a silencing signal directed at the mRNA transcript (host endogenous gene) that is homologous to the gene sequence engineered into the viral vector. Once the local silencing signal is established it is disseminated systemically in the host plant. Viruses have evolved special proteins called ‘‘silencing suppressors’’ e.g., the Hc-Pro of the potyvirus TEV (Anandalakshmi *et al.*, 1998; Kasschau and Carrington, 1998), p19 of the tombusvirus CymRSV (Lakatos, *et al.*, 2004), 2b of the cucumovirus CMV (Brigneti *et al.*, 1998; Zhang *et al.*, 2006), P6 of CaMV (Love *et al.*, 2007), and the 16K of TRV (Ghazala *et al.*, 2008). These silencing suppressors are effective against the antiviral defence of the host plant and promote pathogenicity of the virus. If the virus vector encodes a vigorous silencing suppressor it will result in high virus accumulation (higher viral-titer) in the host. Whereas, if the encoded silencing suppressor is weaker in its activity, then the viral accumulation will be lower (Lu *et*

al., 2003). A systemic viral infection develops if the viral vector is quicker in its replication and movement then the mobile silencing supressor signal. But if, however, the latter rapidly invades distal host tissue, then the RNA silencing will prevail and the subsequent viral secondary infection and systemic spread will be restricted (Kasschau and Carrington, 1998; Vance and Vaucheret, 2001). Induction, viral-suppression, and the various routes of RNA-silencing have been reviewed by Zamore (2004), Roth *et al.* (2004), Voinnet (2005a and b), and Brodersen and Voinnet (2006).

The success of VIGS is essentially dependent upon the persistence of the viral-vector. Only stably integrated transgenes can sustain silencing without a replicating and moving VIGS-vector. The mobile gene silencing can reach, via the phloem, tissues that are at a far distance from the site of signal initiation. The silencing signal may consist of either siRNAs, abnormal RNA transcripts or dsRNA. These progenitors of RNA silencing act as primers in the amplification of the mobile silencing signal for its further spread (Ruiz *et al.*, 1998; Mlotshwa *et al.*, 2002). VIGS does not cause complete eradication of the targeted mRNA from the host cytoplasm rather it has a partial effect and can be useful for studying genes that are involved in the embryonic development of the plant. A number of DNA and RNA viruses have been adapted to allow their utilization as protein expression or gene-silencing vectors. e.g., the DNA viruses Tomato golden mosaic virus (TGMV) and Cabbage leaf curl virus (CaLCuV) are suitable vectors for VIGS in *N. benthamiana* and Arabidopsis plants, respectively. Among RNA viruses, TMV and TRV are suitable for gene silencing in both *N. benthamiana* and *Arabidopsis* plants. TRV can additionally be used for silencing genes in tomato plants. The hordeivirus BSMV is able to silence genes in barley. The introduction of modifications in the virus-vectors for improvement in VIGS efficiency must not weaken the multiplication and movement properties of the virus. Although the DNA virus-vectors are more simple and robust with respect to the inoculation process, they have limited application due to their intrinsic genome size limitations for movement within the host plant.

(Robertson, 2004). TMV was the first known viral vector effective for VIGS (Kumagai *et al.*, 1995). PVX (Ruiz *et al.*, 1998) was the second viral-vector for VIGS but cannot invade the meristematic-tissue of the host plant (Benedito *et al.*, 2004). Later, modification of TRV to function as an efficient VIGS vector (Ratcliff *et al.*, 2001; Purkayastha and Dasgupta, 2009), made it possible to systemically invade the meristematic tissue and cause silencing of target gene in the meristems of the plant. TRV as a VIGS vector has great utility due to its wide host range and production of usually mild symptoms in the infected plant. The original TRV-VIGS constructs derived from TRV isolate PpK20 (pTRV1, RNA1 and pTRV2, RNA2, Liu, *et al.* 2002a) have a duplicate copy of the 35S promoter region at their 5′ end. In the later modified version of these viral constructs (pBINTRA6 and pTV00, Ratcliff *et al.*, 2001), pTRV1 was cloned into pBINTRA6 by introducing intronic sequence (from arabidopsis) in the RdRP gene that made the clone more stable in *Escherichia coli*. This version of TRV was more efficient in gene silencing than the previously used PVX and TMV vectors. Gene silencing in the meristematic regions such as floral differentiating cells of the *N.benthamina* was also shown by using this TRV construct. The pTRV2 (pYL156, Liu, *et al.* 2002a) construct was further modified (to pTRV2-attR2-attR1) by exploiting the GATEWAY cloning strategy. The multiple cloning site (MCS) of pYL276 (obtained by cloning pYL156 into pBin19) was replaced with the GATEWAY recombination cassette to allow directional, restriction digestion and ligation-free cloning. The pTRV2-attR2-attR1 construct was used for silencing the constitutive triple response-1,-2 and PDS genes in tomato. VIGS in tomato plants proved effective when TRV constructs (in *Agrobacterium tumefaciens* cultures) were inoculated by a spray technique. A further modification of TRV vectors was the TRV-2b-GFP vector, where the viral 2b gene was tagged with GFP gene and several root-specific genes were cloned into the vector, to induce VIGS in the roots of *N.benthamiana*, tomato and *Arabidopsis* (Valentine *et al.*, 2004). In addition to the TRV-based VIGS work in tomato, *Arabidopsis*, and *N. benthamiana*, this virus has also been used for gene silencing in several genetically diverse potato

species. Brigneti *et al.,* (2004) carried out TRV-VIGS of the PDS gene, in diploid (S. *bulbocastanum* and *S. okadae*) and hexaploid realtives (*S. nigrum*) of potato and also in the cultivated tetraploid potato (*S. tuberosum* c.v. Cara). They also silenced disease resistance genes (R-genes) in tetraploid *S. tuberosum* c.v. Cara (R1 and Rx genes) and wild potato *S. bulbocastanum* (RB gene). Their work serves as a guide for the utilization of VIGS in both cultivated and wild species of potato. VIGS can perpetuate until the final developmental stage or physiological maturity of the host. Faivre-Rampant *et al.* (2004) used PVX to achieve effective VIGS in both the foliar and tuber-tissue of potato. They obtained PDS silencing that ranged from 70% to 84% in the leaves of *S. tuberosum* c.v Desiree and S. *bulbocastanum*, respectively. Also, the silencing of PDS mRNA was quantified in tissue-culture generated microtubers of *S. tuberosum* c.v Desiree. The PDS mRNA was reduced to 70% and 63% in the subcultures 1 and 3 of the microtubers. Their parallel experiments of inducing VIGS in the cultivars of *S. tuberosum*, using the TRV constructs of Ratcliff *et al* (2001), were not successful as the accumulation of TRV in these cultivars was not sufficient to induce VIGS. The merits and demerits of VIGS, the bottlenecks of the technique along with suitable remedial measures, new improvements and the guiding rules for the VIGS application have been discussed by Robertson (2004), Benedito *et al.* (2004), Bernacki *et al.* (2010), Senthil-Kumar and Mysore (2011a), and Ramegowda *et al.* (2013, 2014) .

1.10. Rationale for the project

Potato cultivars differ in their response to TRV infection and spraing development. It is not yet clear whether spraing is caused by NM- or M-type infection and whether it is an extreme resistance (ER) or a hypersensitive resistance (HR) response of potato (Harrison and Robinson, 1981; Robinson *et al*., 2004; Ghazala and Varrelmann, 2007). Although, Harrison *et al*. (1983) have reported spraing being mostly due to NM-type infection of TRV. In some experiments RT-PCR, using RNA-1 sequence-based primers, failed to detect TRV from spraing-affected tubers whereas,

sometimes, this technique gave positive results from symptomless tubers (Xenophontos *et al*., 1998; Crosslin *et al*., 1999; Brown *et al*., 2000). These reports prompted us to explore the distribution of TRV within spraing-affected potato and to investigate the role of RNA-2 in spraing induction. Martin-Hernandez and Baulocombe (2008) tested the distribution of TRV in *N.benthamiana* by *in-situ* hybridisation studies using an RNA-1-based probe and found that it moves to the growing point within 6-7 days after inoculation. No similar studies of TRV in potato or following the infection pathway of TRV RNA-2 have been reported.

The present studies have been planned to:-

1. Assess whether RNA-2 specific genes encoded by a range of TRV isolates influence the infection of different potato cultivars.
2. Examine the genetic and / or biochemical nature of spraing.
3. Test the hypothesis that spraing is a hypersensitive response to TRV infection.
4. Identify TRV-susceptible potato species suitable for developing a system to conduct functional analysis of potato genes.

TRV infection studies in potato are challenging due to the lack of an easy system to develop infection. Researchers have to rely on viruliferous trichodorid-nematodes to deliver the infection. But the nematode-challenge is difficult due to inability to culture trichodorid nematodes and the lack of suitable *in-vitro* systems for carrying-out studies dealing with virus-vector association (Brown and Boag, 1987, 1988; Brown *et al*., 1989) as TRV is transmitted in a precise species-specific association. We in the current studies will investigate whether it is possible to develop an easy-system to initiate TRV infection by mechanically inoculating potato leaves with a range of recombinant (pseudorecombinant) TRV isolates. The systemic infection of these pseudorecombinant isolates, differing in their encoded-genes, will be evaluated by northern-blot analysis of the infected *N. benthamiana* plants and RT-PCR of the infected tetraploid potato species. A suitable susceptible species from the wild-

relatives of potato will be identified and the possibility of inducing TRV-VIGS of the tuber genes in this species will be evaluated. The genetic and biochemical nature of the spraing disease of potato has not been studied experimentally. A microarray analysis of spraing-affected tissue will be performed to explore the genetic nature of the disease and the data will be validated by qRT-PCR of selected genes. The biochemical nature of spraing will be ascertained by various histological staining techniques.

2. Materials and Methods

2.1. Materials

The materials used in the studies are given below and have been referenced in the text where required.

2.1.1. Acquisition of TRV RNA-1 (NM-type) isolates

Three different TRV RNA1 (NM-type) isolates (SYM, Pp-O85, and PpK-20) were kindly provided by Dr. Stuart MacFarlane. This preserved virus inoculum was created by the selection and isolation of well separated single lesions (as defined by Robinson and Harrison, 1985 b) from *C. amaranticolor* plants which were inoculated with a highly diluted M-type inoculum (containing both RNA-1 and-2) of TRV.

2.1.2. Acquisition and culturing of potato germplasm

The certified, in-vitro propagated, microplants of four tetraploid cultivars (i.e; Pentland Dell (PD30), Maris Bard (MB81), Shepody (SY9) and Saxon, SX9) were purchased from GenTech Propagation Ltd., Dundee. Mother-plants of each cultivar were produced by culturing the microplants in potting media. Two tetraploid cultivars i.e.; Bintje and Wilja were raised, respectively, from the new Pre Basic-3 and Basic seed-potato stock (tuber-stock) at JHI, kindly provided by Mr. Ralph Wilson (Field -Trial Officer).

General purpose and Intercept-mixed compost, commonly used in the glasshouse, was used as the culturing medium. Apical-stem cuttings (about 12 cm long, Fig. 2.1, a) from the mother-plants were used for further propagation and experimentation. Leaf-disc sampling was done as shown in Fig. 2.1, b.

The seedlings of diploid potatoes (see chapter No.4 for accession Nos.) were grown from true-seeds stored in the JHI Commonwealth Potato Collection (CPC), being curated by Dr. Gavin Ramsay.

All the other plant material used in the experiments such as *N. benthamiana, C. amaranticolor, and C. quinoa* plants were grown and provided by the JHI glass-house support staff as required.

2.1.3. Acquisition and sampling of tubers

Pentland Dell (PD) is a known spraing-sensitive cultivar (produces spraing symptoms). For gene expression studies using microarray-analysis, the tubers of PD were kindly collected and provided by Dr. Finlay Dale from commercial fields known to be highly infested with viruliferous trichodorid nematodes. These tubers were collected as part of the end-of-season harvest and transported to the JHI for further examination. Tubers were rinsed thoroughly with tap water to remove any adhering dust or soil particles and dried overnight on paper towels. Visual inspection for any spraing symptoms was done by dicing the individual tubers into slices of about 0.5 cm thickness. Small pieces of about 5 mm^3, exhibiting visible spraing symptoms, were excised from different slices of the same spraing-affected tuber (Fig. 2.2, a), and collected together to make a single composite spraing sample. Similarly, to represent spraing-free samples, tissue was collected from separate individual tubers without visible spraing but which possibly could be TRV infected (Fig. 2.2, b), since the tuber was harvested from a disease plot of TRV. Likewise, to represent healthy samples, tissue was collected from individual tubers harvested from a field-plot that was historically known to be free from TRV disease and processed as before. In total there were twelve different composite tuber-samples, four samples with TRV and spraing (i.e.; spraing samples, S1-S4), four samples with TRV but no spraing (i.e.; spraing-free samples, SF1-SF4) and four samples with neither TRV nor spraing (i.e.; healthy samples, H1-H4). Each composite sample was collected from a

different tuber and processed separately. The excised tissue was snap-frozen in liquid nitrogen to prevent any subsequent alteration in tuber gene expression and immediately freeze-dried in an Edwards Modulyo® Freeze Dryer, at 10^{-1} mbar pressure and -30°C temperature for 48 hours, until the samples were dried enough for pulverization. The freeze-dried samples were ground separately using sterile pestles and mortars to a fine powder and stored at -80°C, in air-tight 50 ml conical falcon tubes, until further processed for RNA extraction.

2.1.4. Collection of spraing-affected tubers with genetically diverse background

For verification of the up-regulation of the HR-related genes from an expanded range of potato tubers, two further sources of germplasm were acquired for PMTV testing and analysis. One of these was provided by Mrs. Louise Sullivan of the JHI, comprising 11 tubers (designated No. L1 to L11), that were collected from a PMTV field-trial showing spraing symptom. These tubers were sampled as before to collect two sets of spraing-affected and one set of spraing-free tissue samples. One of these sets, comprising the spraing-affected tissue (LS1-LS11), was assayed by Mr. Graham Cowan, of JHI, for PMTV detection by ELISA. The other two sets of spraing and spraing-free samples were freeze-dried for total RNA extraction and assayed by qRT-PCR, at later time, to look for possible up-regulation of HR-related genes.

The other source, comprising 12 tubers, was provided by Dr. Christophe Lacomme from the Science and Advice for Scottish Agriculture (SASA). All these 12 tubers, seven of the variety Electra and five of the variety Burren (Table No. 2.1), were initially examined and tested at SASA. Some of them had been sliced at SASA for assessment of spraing symptoms, while others had been cored for real-time RT-PCR testing. Based on the high severity of spraing symptoms, five tubers designated BT3, ET, EP1, EP2 and EP3, were selected at JHI and sampled for further RT-PCR and PMTV testing, as described above.

Table 2.1. Health-status of the potato tubers received from the virus-testing service of SASA

S. No.	Variety	Labelling code of tuber	Health-status	Detected Virus (PMTV or TRV)
1.	**Electra**	EH3	Healthy	NIL
2.		EH5	Healthy	NIL
3.		EH14	Healthy	NIL
4.		EP1	Diseased	PMTV
5.		EP2	Diseased	PMTV
6.		EP3	Diseased	PMTV
7.		ET	Diseased	TRV
8.	**Burren**	BH29	Healthy	NIL
9.		BH30	Healthy	NIL
10.		BT1	Diseased	TRV
11.		BT2	Diseased	TRV
12.		BT3	Diseased	TRV
13.	**Pooled Healthy**	**PEBH**	Healthy	NIL

Potato variety Electra (EH: Electra Healthy; EP: Electra PMTV infected; ET: Electra TRV infected); Potato variety Burren (BH: Burren Healthy; BP: Burren PMTV infected; BT: Burren TRV infected); PEBH: All the healthy tuber samples of Electra (E) and Burren (B) were pooled, at JHI, with a healthy tuber (H1) sample of Pentland Dell.

The freeze-dried samples from tubers BH29, BH30, EH3, EH5 and EH14 were pooled with freeze-dried sample H1 (from a Pentland Dell healthy-tuber, which tested negative for spraing and virus-infection at JHI) to make a combined representative healthy-tuber sample (PEBH).

2.1.5. Primers

The primers used for the studies on the different TRV isolates are detailed in Appendix 1. The primer sets for the VIGS-related studies and quantitative RT-PCR (qRT-PCR) validation of the spraing microarray data are detailed in Appendices 8 and 22, respectively. Whereas, the primers for full-length sequencing of I6 RNA-2 are given in Appendix 3.

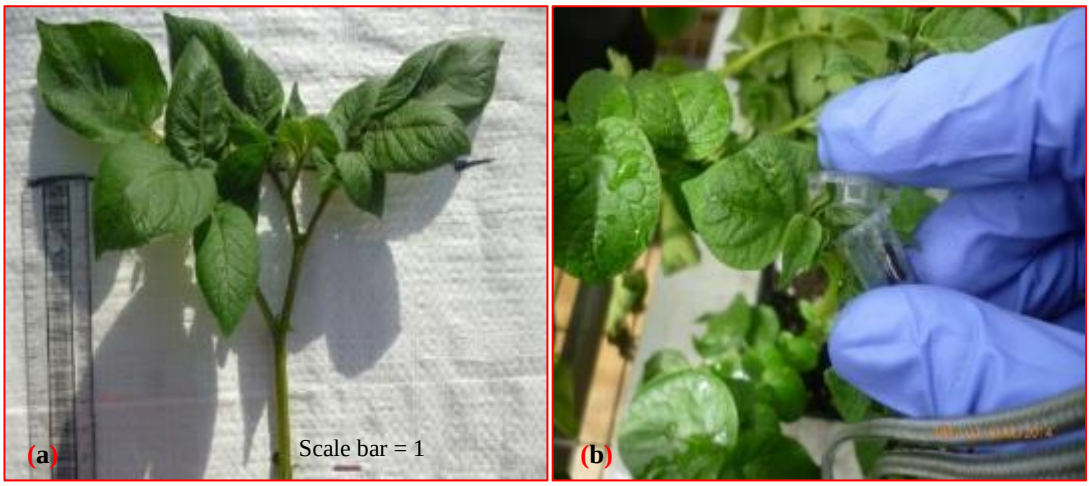

Figure 2.1. Raising of potato cuttings and sampling of potato leaf tissue. (a) apical-stem cutting made from a mother-plant **(b)** collection of leaf-disc samples from the topmost non-inoculated leaves of potato. Scale bar = 1 cm

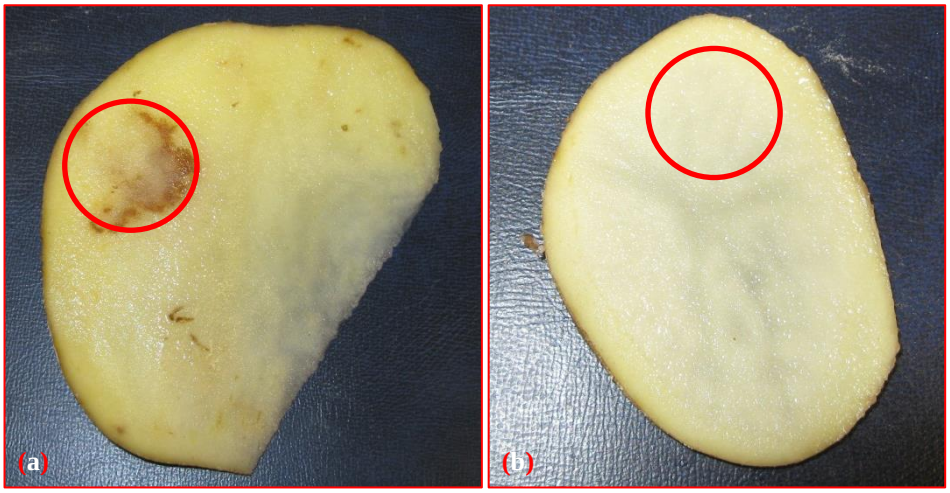

Figure 2.2. Sections of TRV-infected tuber (c.v. Pentland Dell). (a) with spraing **(b)** spraing-free. Red-circle marks the area selected to excise the tuber tissue.

2.2. Methods

All the methods followed throughout the course of studies are given in the following sections.

2.2.1 Multiplication and extraction of TRV RNA-1 isolates

RNA isolated from plants infected with the different TRV RNA-1 (NM-type) isolates was mechanically inoculated to carborundum-dusted leaves of two plants each of *N. clevelandii* and *N. benthamiana*. Additionally, two *N. clevelandii* plants, one inoculated only with 1X PBS buffer and the other inoculated with a TRV SYM M-type RNA inoculum, were the mock and positive control plants, respectively. The plants were given 10 days for symptom expression to occur. Leaf-discs were harvested, using 1.5 ml eppendorf tubes, at 4 days post-inoculation (dpi) from the inoculated and top-most non-inoculated (systemically infected) leaves and at 8 dpi from the top-most systemic leaves only for virus testing. Additionally, the top-most infected whole leaves were harvested separately, at 8 dpi, from the inoculated plants and pooled separately for each virus isolate. The collected leaf tissue was weighed, snap-frozen in liquid nitrogen and stored in a -80°C freezer, until further processed for total RNA isolation to confirm virus infectivity and for further experimental usage.

1. Small-scale total RNA isolation

TRV infection in the inoculated plants was confirmed by RT-PCR detection of the virus in the collected leaf-disc samples. For this purpose, the small-scale total RNA extraction involving phenol chloroform extraction and LiCl precipitation was done according to the protocol of Verwoerd *et al*. (1989).

2. Large-scale total RNA isolation and quantification

The whole leaf tissue samples from the TRV-positive *N. benthamiana* plants were processed for large-scale extraction of total RNA as detailed below:-

1. Each snap frozen sample was pulverized to a fine powder, using liquid nitrogen, and immediately mixed with TLES Extraction Buffer (0.1M LiCl, 100mM Tris HCl (pH 8.0), 10mM EDTA, 1% SDS; 2 ml/g of leaf tissue) and buffer-saturated phenol, pH 4.5 (in a ratio of 1:1). The mixture was vigorously homogenized for 20 minutes using a ‘‘Heidolph™-Multi Reax machine’’.
2. The sample was centrifuged for 10 minutes in a SANYO Mistral 2,500 at 2,500 rpm and 4°C, the supernatant transferred to a new 50 ml conical centrifuge tube, and mixed with an equal volume of phenol (pH 4.5) and chloroform (1:1), followed by vortexing for 2 minutes.
3. The mixture was again centrifuged and the water phase (supernatant) transferred into a new centrifuge tube. The phenol-chloroform extraction was repeated and the supernatant gently mixed with an equal volume of 4M LiCl, followed by overnight precipitation in a -20°C freezer. The mixture was centrifuged for 45 minutes and the supernatant discarded.
4. The RNA pellet was washed with 2 ml of 70% ethanol by spinning for 5 minutes, the supernatant was discarded and the RNA was air-dried for about 30 minutes before being re-suspended in 100 µl of RNAse-free water and quantified using a spectrophotometer.
5. 3M Na-Acetate (0.1 volume) and absolute-ethanol (2 volume) was added to each RNA sample and stored (100 µg RNA sample / tube) in a -80°C freezer, until further use.

2.2.2 Detection of TRV using RT-PCR beads

5 µg of total RNA (section 2.2.1) and 1 µl of each 20 µM primer (0.400 µM final concentration) was added in a 50 µl RT-PCR reaction containing a single *Ready-To-Go™ RT-PCR bead* (GE Healthcare). Primers # 1760 and 1761 (Robinson, 1992; Appendix 1.) were used to amplify the 16K gene (463 bp amplimer) of TRV RNA1. The RT-PCR programme comprised one hour incubation at 42°C, followed by one cycle of initial denaturation (95°C, for 5 minutes) and 40 cycles of denaturation (95°C, for 2 minutes), annealing (52°C, for 1 minute) and extension (72°C, for 1 minute). A final extension cycle (72°C) of 10 minutes was done. 5 µl of the PCR product was resolved on a 1.1% agarose gel and the DNA was visualised by ethidium bromide staining.

2.2.3 First strand cDNA synthesis

cDNA synthesis was done according to the suppler protocol for ‘‘Superscript™ III Reverse Transcriptase Enzyme kit’’ (Invitrogen© Corporation). Reactions contained 1 µg of total plant RNA (except that RT-PCR testing of tetraploid potatoes used 5 µg RNA). Also, 1 µl each of 100 µM oligo dT_{17} (Primer # 967) and random-hexamer (Primer # 1458) primers were added to a 20 µl reaction, followed by incubation at 55°C for 1 hour. The cDNA was treated with RNase H, following the protocol of New England BioLabs® Inc. (NEB), U.K. The cDNA aliquots (1/25 dilution) were stored in a -80°C freezer, until required.

2.2.4 Infectivity confirmation of TRV RNA-1 isolates by using a GFP engineered RNA-2 transcript

100 µg total RNA of each RNA1 isolate (section 2.2.1, sub-section 2) was mixed with 15 µl of capped RNA-2 transcript (Cap94T, 1 µg/µl, kindly provided by Dr. Stuart MacFarlane) and mechanically inoculated to carborundum-dusted (4-5 leaf-stage) leaves of *N. benthamiana* plants. The Cap94T construct was engineered for

GFP expression. The GFP expression was visualized using a hand operated U.V transilluminator (BLAK-RAY®, Long-wave, 365 nm spot, Ultraviolet Lamp, Model B100 AP), and the GFP-signals were captured with a camera.

2.2.5 Infectivity confirmation of TRV RNA-1 isolates by using indicator-plant

100 µg RNA1 of each of the three isolates (section 2.2.1, sub-section 2) was serially diluted to 10^{-1}-10^{-4} and mechanically inoculated onto the leaves (4-5 leaf stage) of the indicator plant (*Chenopodium quinoa*). Data of average number of necrotic lesions produced on three inoculated leaves of each plant were recorded at 4 dpi.

2.2.6 Extraction and quantification of total proteins from TRV-GFP infected plants

5 µg of p0049 was linearized by digesting with 4 µl of *Sma1* restriction enzyme (NEB) for 4 hours, as recommended. The protocol for Phenol-Chloroform extraction, precipitation of the linearized DNA template, transcription (49T) and capping of the transcript (Cap49T) was the same as detailed in section 2.2.7 and 8.

Total RNA (5 µg) of each RNA-1 isolate (viz; SYM, PpO-85 and PpK-20) was mixed separately with 5 µg of the Cap49T transcript and mechanically inoculated onto carborundum-dusted leaves, at 4-5 leaf-stages, of *N. benthamiana* plants. The strength of GFP-signal in the inoculated and the systemically infected leaves was observed by exposure to U.V. light at 4 and 8 dpi, respectively and the images recorded using a Canon EOS 350D camera. Samples (about 1 g) of the top-most systemically infected leaves, collected from one set of plants at 4 dpi and from the other set of plants at 8 dpi were snap-frozen in liquid nitrogen and stored in a -80°C freezer, until processed for protein extraction.

The leaf proteins were isolated by following the protocol kindly provided by Dr. Hazel McLellan (CMS group, JHI) and is given below:-

1. Each frozen leaf sample (1 g for fluorometry and 0.5 g for western-blot assay) was separately pulverized using a pestle and mortar and mixed with chilled Extraction-buffer (1.5 ml, supplemented with Proteinase Inhibitor (PI) cocktail, Appendix 2.). Maceration was continued until the formation of dark-green pulp, which was transferred with a 1 ml pipette into two separate 1.5 ml Eppendorfs and allowed to rest on ice for 15 minutes.
2. The samples were spun, at $13.2x10^3$ rpm and room temperature, for 2 minutes and the supernatant (total proteins) removed into a new Eppendorf tube for use in a fluorometric assay to be quantified by the Bradford protein assay and used in a western-blotting assay.

1. Fluorometric assay

For the fluorometric assay, 200 µl of each leaf protein extract was loaded into duplicate wells of black (opaque) assay plates. The data for GFP expression were collected by the *SoftMax Pro 5* package of the ‘‘Spectramax M5 spectrophotometer’’. The instrument was instructed for top read fluorescence mode (10 reads / well) with the excitation-wavelength of 395, emission-wavelength of 519 and auto cut-off of the wavelength in an ON mode. The data were generated in the form of arbitrary fluorescence units (AFU). In order to subtract the effect of background fluorescence and get the normalized AFU data, the mean AFU of the mock-inoculated *N. benthamiana* samples was manually subtracted from the mean AFU of the test samples.

2. Western-blot assay

The leaf-protein extract, before being analysed by the western-blot method, was quantified by the Bradford protein assay (also known as the Coomassie dye-binding method). The bovine serum albumin (BSA, 10 mg/ml, NEB) was used as a reference protein for preparation of the relative standards by adopting the protocol of ‘‘Bio-Rad Protein Assay kit’’. The BSA stock (10 mg/ml) was diluted with protein

extraction buffer to prepare five BSA standards (relative standards) containing 0.2, 0.4, 0.6, 0.8, and 0.9 mg BSA per ml. The diluted Bradford-dye reagent (900 µl) was separately mixed, by vortexing, with 100 µl of each BSA standard and every leaf-protein sample. Each protein mixture was pipetted (100 µl) into fresh and dry spectrophotometer cuvettes and incubated at ambient temperature for not less than 5 minutes. Each sample was evaluated in duplicate and the absorbance (A°) was measured at 595 nm wavelength (A° 595).

The absorbance for the extraction buffer only (blank reading) was subtracted from the absorbance of the test samples to get a normalized absorbance for the samples. The protein concentration of the samples was determined by plotting a standard-curve for absorbance ($A^{\circ}595$) vs. concentration (mg/ml) of the protein (BSA) standards. Some of the test samples were diluted to bring the $A^{\circ}595$ within the range of the BSA standard curve.

2.5 µg of each leaf extract was mixed separately with the dissociation buffer (1 ml Tris (0.5M, pH 6.8), 1.6 ml SDS (10%), 400 µl 2-Mercaptoethanol, 0.1% Bromophenol blue, 0.8 ml Glycerol, and 4ml distilled H_2O), to a volume of 20 µl. The denatured protein samples (placing in boiling water for five minutes) were resolved on a 10% Poly Acrylamide Gels (PAGE) and transferred to a nitrocellulose-membrane. Before blocking the blot, the transferred proteins were visualized by staining with Ponceau S. The blot (s) was blocked with 5% non-fat dry milk and immuno-labelled with PpK-20 CP-specific primary antibody (PLB antiserum, 1:5,000 dilution). The PLB antibody was kindly provided by Dr. Stuart MacFarlane (from the collection of Dr. David Robinson). It was cross-absorbed with leaf-sap from healthy *N. benthamiana* plants and incubated with Alkaline Phosphatase Conjugate (1:2,500 dilution). The details of the protocol for developing the blot are explained in section 2.2.13.

5 µl PageRuler™ Pre-stained Protein Marker (ThermoFisher Scientific©) was run in each PAGE gel. The detection of TRV-CP was done by staining of the blots with 10 ml solution of the detection reagent (BCIP / NBT, 1 tablet per 10 ml H_2O) and

allowed for sufficient colour development to occur. The stained blots were washed with H_2O to stop the staining reaction and the images captured with a Panasonic DMC-FS18 digital camera.

2.2.7 Preparation of DNA templates for transcription

The five full-length TRV RNA-2 infectious clones (Table No. 2.2.) used in the studies were kindly provided by Dr. Stuart MacFarlane. All these clones viz: p0214 (PpK-20), p0215 (I-6), p0216 (PaY4), p0217 (TpO-1) and p0218 (SYM) allow the synthesis of infectious TRV RNA2 by *in vitro* transcription using T7 or SP6 Polymerase.

Table 2.2. Full-length TRV RNA-2 infectious clones of five different isolates

Sr.No.	Infectious Clone No.	TRV isolate (size of full-length RNA-2); genes present	Cloning vector (size)	Size of infectious clone
1.	p0214	PpK-20 (3,855 bp); CP, 2b, 2c.	pUC18 (2,686 bp)	6,538 bp
2.	p0215	I-6 (3,410 bp); CP, 9K, 2b, 2c.	pT7 Blue (2,887 bp)	6,261 bp
3.	p0216	PaY-4 (3,926 bp); CP, 2b, 2c.	pT7 Blue (2,887 bp)	6,843 bp
4.	p0217	TpO-1(3,216 bp); CP, 9K, 2b, 2c.	pT7 Blue (2,887 bp)	6,133 bp
5.	p0218	SYM (3,898 bp);CP not at 5′, Δ2b	pGEM-T Easy(3,015 bp)	6,930 bp

The clones were separately transformed, by the heat-shock method, into chemically competent *E.coli* (DH5-α strain) cells, following the standard protocol (Sambrooke *et al.,* 1989). The transformants were selected on LB agar-plates supplemented with ampicillin. The picked colonies were re-cultured in 10 ml LB tubes, supplemented with 10 µl of ampicillin (100 mg/ml). Incubation was done at 37°C for overnight. The plasmid DNA (s) were isolated and purified (Miniprep) by the spin-column purification method, following the protocol of New England Biolabs® (NEB) kit. 5 µg (200 ng/µl) of each of plasmid DNAs was digested (60 µl reaction) with 3.0 µl of *Sma-1* restriction endonuclease (NEB), following 4 hours of incubation at room-temperature (25°C). The linearized plasmids were recovered by the phenol / chloroform extraction and precipitated with 0.1 volumes of 3M Na-Acetate and 2.5

volumes of absolute ethanol (Sambrooke *et al.*, 1989). The precipitated linearized-plasmid DNAs were resuspended in distilled H_2O to a concentration of more than 500 ng/µl. The linearization efficiency was confirmed by resolving plasmid DNAs (1 µl) on a 1.1% agarose gel and staining with ethidium bromide. The samples were stored in a -20°C freezer, until further use, or alternatively they could be transcribed immediately.

2.2.8 Transcription and capping of the transcripts

All the five linearized plasmid DNA-templates (each ~1 µg / 2 µl) were transcribed (20 µl reaction), following the recommended protocol of the ''MEGAscript® T-7 promoter Kit (Ambion®-Applied Biosystems)''. The reagents were assembled at room temperature and incubated at 37°C for 4 hours. The transcripts were precipitated with LiCl, re-suspended in 40 µl of RNase-free water, quantified and stored in a -20°C freezer, for further processing. The quality of the transcripts was validated on a 1.0% denaturing agarose-gel in 1X MOPS running-buffer and resolved under an electric field of 100 volts.

The transcripts were capped by following the ''Standard Cap 0 Capping Protocol'' of the ''Script Cap™ m7G capping system, CELLSCRIPT™ Kit'' and stored in a -80°C freezer, until mechanically inoculated onto *N. benthamiana* plants.

2.2.9 Reconstitution and making of TRV recombinant isolates

A total of 15 TRV recombinants (henceforth referred to as ''isolates'') including two *in-vitro* recombinant isolates (KK20 and SS, that generated the parental isolates PpK-20 and SYM isolates, respectively) and thirteen pseudorecombinant isolates were assembled in the laboratory. These isolates were prepared by mixing separately 5 µg of each of the three TRV RNA-1 isolates (viz: SYM, PpK-20 and PpO-85) with 5 µg of the *in-vitro* transcribed and 5′ capped RNA-2s (section 2.2.8, T214, T215, T216, T217, and T218) of the five different TRV isolates (viz: PpK-20, I-6,

PaY4, TpO-1 and SYM RNA-2), respectively. Infectious sap of each TRV isolate was prepared by macerating the whole leaf tissue, collected at 8 dpi from systemically infected leaves, with 1X PBS buffer (1 g tissue / ml of buffer) and stored in a -80°C freezer for further studies.

2.2.10 RT-PCR to confirm the identity of TRV recombinant isolates

RNA was isolated from plants infected with either of the fifteen TRV isolates. First-strand cDNA was synthesized by following the protocol given in section 2.2.3 except the oligo (dT) (Primer # 967) and random hexamer (Primer # 1458) primers were replaced by 1 µl (100 µM) of the tobravirus 3′ end universal primer (Primer No.1759, Appendix 1). A 1/100 dilution of each cDNA sample was used as a template in a 30-cycle PCR reaction.

Primer-sets (Appendix 1.) specific to each of the five different TRV RNA-2 species were designed to produce amplicons of less than 1,000 bp. Each amplicon (2.5 µl) was resolved on a 1.1% agarose-gel and visualized by Ethidium Bromide staining.

2.2.11 Preparation of the ribo-probes and the dot-blot hybridization for northern blot analysis

The systemic movement and accumulation of all the 15 TRV recombinant and three RNA1 isolates was further documented by northern blot analysis.

1. Preparation of ribo-probes

The p0040 (PpK-20-CP), p1494 (I6-CP), p225 (PaY4-CP), p1496 (TpO-1-CP), p0073 (SYM-MP), and p1497 (SYM-CP) plasmids were linearized (following NEB protocol) by digesting 1 µg of plasmid with 3 µl of *Pst-1* (p0040), *Nco-1* (p1494, p225, p1496 and p0073) and *Spe-1* (p1497) in a 50 µl reaction, for 2 hours. The protocol for phenol-chloroform extraction, precipitation, storage and re-suspension of the linearized plasmid DNAs was the same as discussed before. The linearized

plasmid DNAs were transcribed following the recommended protocol of the ‘‘MEGAscript SP 6 promoter Kit’’ (p0073, p1494, p225, p1496) and the ‘‘MEGAscript T-7 promoter Kit’’ (p0040 and the p1497) of the Ambion®-Applied Biosystems. The quality of transcripts was assessed by resolving 1 µg of each transcript on a denaturing agarose gel, according to the protocol previously discussed.

The anti-sense transcripts were labelled with alkaline phosphatase by physical cross-linking using the ‘‘Amersham Gene Images AlkPhos Direct Labelling and Detection System Kit (Code RPN3680)’’.

2. Dot-blot hybridization of the ribo-probes

The detection efficiency of the ribo-probes was assayed by dot-blot hybridization. The linearized plasmid DNAs (p0072, p0040, p1494, p225, p1496 and p1497, each of 100 ng) were spotted at 2-2.5 cm separation onto positively charged nitrocellulose membrane and cross-linked with UV light (at 1200 µJoules x 100) using a ‘‘UV Statalinker 2400’’. The membrane was pre-hybridized at 55°C for 30 minutes in AlkPhos hybridization buffer (0.25 ml/cm^2). The labelled probes (20 ng/ml of hybridization buffer) were added to the buffer and the membranes were incubated overnight at 55°C. The blot was washed sequentially with primary and secondary buffer before the addition of 1 ml of the chemiluminescent detection reagent (CDP-star). Exposure of X-Ray film (Fujifilm©) to the blot was initially for one hour, followed by later 1-5 minutes exposures. The autoradiograph was developed in a dark-room using ‘‘Xograph Compact X4’’ film-developer of ‘‘Xograph Imaging Systems Ltd’’.

2.2.12 Northern blot analysis of *N. benthamiana* plants

The systemic accumulation of TRV isolates in the *N. benthamiana* plants was evaluated by northern blot analysis. The total RNA extracted (section 2.2.1, sub-

section 1) from the leaf-discs of transcript inoculated plants (section 2.2.9) was loaded (5 µg/lane) on a denaturing 1.1% agarose gel, following the standard protocol (Sambrooke et al., 1989). RNAs were transferred, overnight, to pre-equilibrated positively-charged nitrocellulose membrane (Amersham Hybond-N^+). After overnight-transfer, the samples were UV-cross linked (on both sides), and the fixed RNAs were hybridized with the labelled riboprobe (s) according to the method already explained. Following overnight hybridization, the blots (s) were washed and developed as already discussed in above section.

2.2.13 Tissue-print immunoblotting of the TRV infected plants

The protocol of Más and Pallás (1996) was adopted for tissue-print immunoblotting. The TRV-infected leaves were manually pressed, for 1 minute, onto nitrocellulose membrane (Amersham Hybond-ECL). After printing, the membrane was washed for 20 minutes in 3% Bovine Serum Albumin (BSA) and TBS (20 mM Tris-HCl, pH 7.5, and 150 mM NaCl) solution, followed by another 20 minutes washing in 3% BSA and TBS solution containing 0.1% Nonidet P-40, and a final washing in 3% BSA and TBS solution without Nonidet P-40.

Healthy leaf tissue (0.5 g) macerated in an Eppendorf, containing 0.5 ml of TBS solution, was spin-filtered to rescue the supernatant (leaf sap) in a separate Eppendorf. The virus-specific primary antibody (4 µl, PLB serotype of PpK20 RNA-2) was added to the collected sap and cross-absorbed by incubating, in an ice-box, for half an hour. The cross-absorbed PLB antibody (3 µl) was diluted to 1:5,000 (3 µl in 15 ml of 3% BSA and TBS solution) and added to the press-blot, followed by incubation at room temperature for 2 hours. The blot was washed twice with TBS solution and incubated at room temperature with a 1:2,500 dilution (24 µl in 60 ml of 3% BSA and TBS solution) of the secondary antibody i.e., Anti Rabbit IgG with Alkaline Phosphatase Conjugate (Sigma Anti-Rabbit IgG (whole molecule)-Alkaline Phosphatase Conjugate, developed in Goat). Following 2 hours of incubation, the

blot was washed twice with TBS solution as before and lastly rinsed with tap-water. TRV-CP was detected by treating the tissue-blot with substrate solution (1 tablet of BCIP / NBT per 10 ml H_2O) and the colorimetric reaction was stopped by rinsing the blot with tap-water. The greenish (Chlorophyll content) background on the blot was removed by treating the developed blot with 10% NaHClO (Chlorox, commercial bleach). The images were taken with a digital camera.

2.2.14 Preparation of frameshift mutants of the CP, 2b and 2c genes of PpK-20 RNA-2

The plasmids of the wild type PpK20 RNA-2 (i.e., p0214) was separately treated with restriction endonucleases *BsRG1*, *BstE11*, and *NgoMIV* to cut the CP (P2a), 2b (P2b) and 2c (P2c) genes, respectively, at 422 nts, 297 nts and 459 nts downstream of the respective genes (Fig. 2.3).

The plasmid DNA (466 ng/µl) was digested (in a 10 µl reaction) for 2 hours with 0.75 µl of the respective restriction enzyme, according to the NEB recommended protocol.

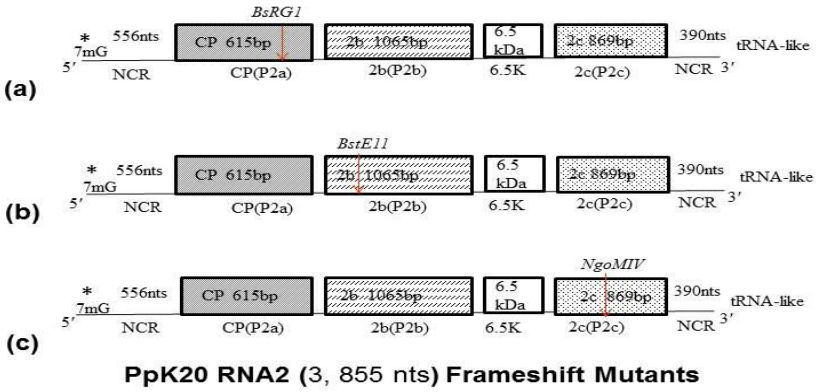

Figure 2.3. Illustration of the restriction digestions to create frameshift mutants of PpK-20 RNA-2. The CP (P2a, 615 bp), 2b (P2b, 1065 bp), and the 2c (P2c, 869 bp) genes were restricted (site marked by an arrow) at 978 nts (*BsRG1*), 1636 nts (*BstEII*) and 3045 nts (*NgoMIV*), respectively.

The enzyme was inactivated, the plasmid DNA phenol: chloroform extracted, and precipitated using Na-Acetate. The DNA pellet was washed with 70% ethanol. Complete digestion of the plasmid was confirmed by agarose-gel electrophoresis of the digestion-reaction. The digested plasmid DNA (200 ng/µl) was made blunt-ended in a 20 µl Klenow (Fill-In) reaction, using 0.5 µl Klenow DNA Polymerase, following the NEB recommended protocol. The reaction was terminated after 20 minutes.

The plasmid DNA (3 µl) was ligated, in a 10 µl reaction; using Promega T4 DNA Ligase (3U / 1.0 µl) and 10X T4 DNA Ligase Buffer (1.5 µl), following incubation at room temperature for 3 hours. DNA transformation of *E.coli* competent cells, selection of transformants and plasmid isolations were done as described before. Frame-shift mutations were confirmed by restriction digestion and DNA sequencing of the clones.

2.2.15 Plate trapped antigen (PTA) ELISA

Leaf-samples (0.5 g) were extracted with 5 ml of coating-buffer using a sap-press machine (Erich Pollähne GmBH). The extract was filtered through a double-layered muslin cloth to remove the tissue-debris and the filtrate of each test-sample, positive and negative control samples was loaded (100 µl) in duplicate into the wells of an ELISA-plate. The primary antibody (PLB serotype) diluted to 1:5,000 and the secondary antibody (Sigma Anti-Rabbit IgG (whole molecule)-Alkaline Phosphatase Conjugate developed in Goat) diluted to 1:2,500 were used for TRV-detection, by adopting the recommended protocol of ‘‘ADGEN Phytodiagnostics’’.

The microtitre plate was scanned by a spectrophotometer (Multiskan Ascent, Thermo Labsystems) and the readings were recorded at 405 nm absorbance. Samples with an absorbance-value twice the absorbance-value of the negative control sample were considered to be infected with virus.

2.2.16 RT-PCR evaluation of the systemic infection of various TRV isolates in potato

The infectious sap of each TRV recombinant isolate was mechanically applied (at 10 days post-planting) to the fully-expanded leaves of the potato apical-stem cuttings (section 2.1.2, Fig. 2.1, a). Each TRV recombinant isolate was inoculated on three leaves of each plant and three plants per treatment.

Leaf-discs (Fig. 2.1, b) were collected from the inoculated (at 5 dpi) and the top-most non-inoculated (at 15 dpi and 30 dpi) leaves. Leaf-samples from the positive control *N. benthamiana* plants were collected at 4 dpi (inoculated and non-inoculated leaves) and at 8 dpi (non-inoculated leaves only). The samples were snap-frozen in liquid nitrogen and stored in a -80°C freezer. Total RNA isolations were done by following the recommended protocol of the TRIZOL reagent (Sigma™). The RNA preparations of all the three plants for each type of sample were pooled together. The cDNA synthesis, using 5 µg total RNA of each pooled RNA preparation, was done by following the protocol given in section 2.2.3.

The RT-PCR reaction (25 µl) contained 5 µl of 5X Green Go-Taq Reaction Buffer, 1 µl of the cDNA template of each sample, 0.3 µl of each 20 µM primer (forward and reverse) to give each primer a final concentration of 0.240 µM, 1.5 µl of 25 mM $MgCl_2$ to make a final concentration of 1.5 mM $MgCl_2$. Also 2.5 µl of 2 mM dNTP mixture was added to make a final concentration of 0.2 mM in each reaction-mixture and the reaction-volume was made up to 25 µl with distilled, HPLC purified, sterile water. Finally, 0.125 µl of the Go-Taq Polymerase was added to a 25 µl reaction-volume. The primer-set of each target-gene (TRV1 16K, MP, or replicase gene and the respective TRV2 gene) is given in Appendix 1.

The PCR cycle comprised an initial denaturation at 95°C for 5 minutes; followed by 40 cycles of 2 minutes denaturation (95°C), 1 minute annealing and 1 minute extension (72°C).

2.3. Methods related to VIGS studies

Previous TRV VIGS studies focused on the use of *N. benthamiana, Arabidopsis* and tomato plants but the use of potato-plant in VIGS-related work is of limited occurrence. We have attempted to develop an efficient potato-based system for conducting VIGS-related studies. The potato genes *Phytoene desaturase* (PDS), *Granule bound starch synthase* (GBSS) and the *Zeaxanthin epoxidase* (ZEP) were selected for VIGS in potato.

2.3.1 Making of VIGS-constructs to silence potato-genes

The PDS, GBSS, and ZEP genes were first cloned into pGEMT-Easy, then recombined into pDONR and finally into the Gateway-TRV vector for inoculation to potato plants.

1. Cloning of ZEP and GBSS DNA fragments into pGEMT-Easy

Potato cDNA from healthy *S. jamesii* was synthesized (section 2.2.3) and diluted with distilled water to make aliquots (of 1/25 dilution). The DNA fragments of ZEP (408 bp) and GBSS (441 bp) genes were amplified by ‘‘Finnzymes Phusion™ High-Fidelity DNA Polymerase’’ (NEB), by adopting a PCR programme of 1 cycle of initial denaturation (at 98°C for 30 seconds), followed by 40 cycles of denaturation (at 98°C for 10 seconds), annealing of 30 seconds (at 62°C for ZEP, or 61°C for GBSS), and extension (at 72°C for 20 seconds). The PCR reaction (50 µl) for each targeted gene comprised 5X Phusion HF-buffer (10 µl), 10 mM dNTPs (1µl), 20 µM forward and reverse primers of the targeted gene (1µl of each primer), template cDNA (1/50 dilution, 2 µl), and Phusion Polymerse (1 µl).

The primer numbers (2296 and 2297) and (2298 and 2299, Appendix 8.) were used for the amplification of ZEP (408 bp) and GBSS (441 bp) fragments, respectively. The single-band amplicons were purified by agarose gel-electrophoresis and were A-

tailed using Go-Taq Polymerase. The A-tailing reaction (10 µl) comprised 5X Go-Taq colourless buffer (2 µl), 2 mM dNTP mixture (1 µl), 25 mM $MgCl_2$ solution (0.5 µl), Go-Taq Polymerase (0.2 µl) and the Gel-purified PCR product (6.3 µl), with 20 minutes incubation at 72°C in a PCR machine.

The A-tailed amplicons were ligated (3:1 molar ratio) into the pGEMT-Easy vector. The ligation reaction (10 µl) comprised pGEMT-Easy vector (1 µl), 10X ligation buffer (1 µl), A-tailed gel-purified PCR product (1 µl), T4 DNA Ligase (1 µl), and distilled H_2O (6 µl), followed by overnight incubation at 4°C and transformation into *E. coli* DH5α. The transformants were selected by overnight culturing on LBAIX plates and the clones were multiplied overnight in LB medium containing Ampicilin; plasmid DNA isolation and quantification was the same as discussed before. Orientation of the cloned DNA fragments of ZEP and GBSS was confirmed by DNA sequencing.

The ZEP and GBSS clones were re-amplified in a 2-step PCR procedure to add firstly ½ att sequences and secondly full att sequences to the gene fragments. The primers used for this cloning are listed in Appendix 8. These re-amplified clones were, thus, suitable for insertion into a TRV RNA2 vector (pTRV2 Gateway-vector) following the suggested protocol of the ‘‘*Invitrogen*™ Gateway-Technology’’ kit.

2. LR recombination (attL x attR) reaction

The LR recombination-reactions (10 µl) were performed by adding the reagents in separate 1.5 ml microfuge tubes, following the suggested protocol of the kit. p0697, a pTRV2 Gateway-vector with *att*-sites in antisense-orientation, was the destination vector (Liu *et al*., 2002). The LR reactions were set-up at room temperature and incubated, at 25°C, for overnight. The protocols for Proteinase-K treatment, transformation, selection and culturing of the transformants and plasmid isolation were as described in ‘‘*Invitrogen*™ Gateway cloning’’ manual.

2.3.2 Agrobacterium-transformation and agro-infiltration of *N. benthamiana* plants

The TRV RNA2 binary vector clones (p1294, PDS; p1390, ZEP; p1391, GBSS; and p1402, virus-control) were transformed into Agrobacterium-GV3101 by heat-shock at 37°C for 5 minutes, chilling on ice for 5 minutes, followed by addition of LB medium (400 µl) to each culture and 3 hours of shaking at 28°C. The transformants were selected by plating onto $LB_{Kan50Rif50}$ culture-plates, and incubated at 28 °C for 2 days.

All these TRV RNA2-VIGS clones along with the TRV1 infectious clone (p0695) were separately cultured at 28°C in LB medium (5 ml) supplemented with Kanamycin (50 µg/ml) and Rifampicin (50 µg/ml). Each overnight-grown culture was amended with 20 ml fresh LB medium, containing 150 µl of MES (1 M), 5 µl of Acetosyringone (0.1 M), 20 µl of Kanamycin (50 mg/ml), and 20 µl of Rifampicin (50 mg/ml) and grown at 28°C in a shaking-incubator overnight. The cultures were pelleted, at 3,000 rpm, for 15 minutes and the supernatants discarded. The pellets were resuspended in 5 ml of infiltration-buffer [1 ml MES (1 M), 1 ml $MgCl_2$ (1 M), 150 µl Acetosyringone (100 mM) and 98 ml of distilled H_2O]. The optical density (O.D600) of the cultures was adjusted to 0.5 and the cultures were allowed to sit at room temperature for 3 hours. Each TRV RNA2-VIGS culture was mixed with an equal volume of TRV1 culture and infiltrated into 3 fully-expanded leaves of *N. benthamiana* plants to initiate infection.

2.3.3 Extraction and staining of potato starch

Potato starch was extracted from the tubers of plants infected with the different VIGS-constructs, and was evaluated by staining of the isolated starch granules with Lugol's iodine solution.

1. Extraction of potato-starch

Tuber-slices from washed, air-dried, and peeled tubers were cut and pooled to make a representative sample of all TRV-VIGS infected samples. Tuber-flesh (0.5 g) was crushed in a sterile 2 ml centrifuge-tube, using a sterile pestle, with 1 ml of starch extraction buffer [10 mM EDTA, 1 mM DTT, 50 mM Tris-base, pH 7.5, 0.1% $Na_2S_2O_5$; Kuipers *et al*., 1994]. The macerate was passed through double-layered muslin cloth to remove the fibrous debris and the filtrate collected in a new 2 ml tube before being allowed to settle for 4 hours at 4°C. The supernatant was removed and the starch deposits re-suspended in 1 ml of starch extraction buffer. The flow-through was again passed through double-layered muslin, the starch allowed to deposit under gravity and the supernatant removed as before. The starch-deposits were resuspended in 500 µl of deionized water and again allowed to settle for over-night. The supernatant was removed and the starch-deposits finally resuspended in 500 µl of deionized water.

2. Staining of potato-starch

Lugol's solution (20 µl, 2-3 drops; Fluka, Chemie GmbH, CH-Buchs) was added to 100 µl of the starch-granule suspension. 50 µl of this stained suspension was placed on a microscope slide and observed at 20X magnification using a Leica DMLFS microscope.

Staining of whole tuber slices was done in separate petri-dishes. Each dish was half-filled with Lugol solution and the tuber slice submerged for 1minute.

2.3.4 Tuberization from stem-cuttings

The mother plants (s) were placed for two weeks in a growth cabinet adjusted to 18°C temperature and short-day conditions (8 hours / 16 hours light / dark cycle) to induce tuberization. After two weeks, the mother-plants were shifted to the glass-house with long-day conditions (16 hours / 8 hours light / dark cycle). Apical stem-cuttings (section 2.1.2) were planted in Intercept treated compost with normal watering and allowed to grow for one week to promote better shoot and leaf-growth for improved virus infection. The plantlets were mechanically inoculated with viral inoculum within 7-10 days of planting.

2.4. Methods related to spraing studies

All the methods followed throughout the course of studies related to spraing are given in the following sections

2.4.1 Total RNA extraction from freeze-dried tuber tissue

The air-tight falcon-tubes (section 2.1.3) containing the freeze-dried and finely pulverized tuber tissue were warmed to room temperature. The two protocols used for the isolation of large and small quantities of RNA, were adapted from the protocol suggested by Ducreaux *et al.,* (2008), and are given below:-

1. *Small-scale extraction of total RNA from freeze-dried potato tuber*

This protocol is suitable for isolation of small to medium amounts of total RNA (usually less than 1 µg).

1. Each sample was transferred to four sterile 2 ml microfuge-tubes (each tube containing 0.05 g tissue) and mixed with 650 µl of hot (80°C) extraction buffer (1:1 with phenol, Appendix 11), by vortexing for 1 minute. Sterile-distilled water (460 µl) was added to each tube which was again vortexed for 1 minute,

followed by the addition of 750 µl of chloroform: isoamyl alcohol solution (24:1) and another vortexing.

2. The tubes were centrifuged at 14,000 rpm and 4°C for 15 minutes and the upper aqueous layer was transfered to a new, sterile microfuge-tube containing an equal volume (ca. 750 µl) of 4 M LiCl. The contents of each tube were mixed-well, by shaking, and incubated overnight in a -80 °C freezer.
3. Following centrifugation of the tubes as before, for 30 minutes, the supernatant was discarded and the RNA pellet was resuspended in 250 µl sterile, distilled water; reprecipitated by adding 0.1 volume (ca. 25 µl) of 3 M NaOAc, pH 5.2, and 3 volumes (ca. 750 µl) of 100% ethanol and incubated at -80°C overnight. The RNA was pelleted by centrifugation (as before) and washed with ice-cold 70% (v/v) ethanol. The RNA pellet was air-dried at room temperature for 10-20 minutes, followed by resuspension in 50 µl sterile HPLC purified water.
4. The RNA in each of the four tubes was combined to form a total volume of 200 µl for each sample. Each RNA sample was quantified using the NanoDrop™ 1000 and the quality of sample was tested by resolving it on a denaturing agarose-gel and by using a microfluidic chip (Agilent 2100 bioanalyzer).
5. The RNA isolations were further cleaned of any impurities by passing 100µg of each sample through the spin-columns (pink) of the ‘‘Qiagen RNeasy® Mini kit’’ (section 2.4.3) as suggested in the RNA cleanup protocol.
6. Each column-purified total RNA sample (10 µg) was further treated with DNase 1 following the suggested protocol of the ‘‘Ambion TURBO DNA-free™ kit’’ (section 2.4.4).
7. Aliquots of the RNA (20 µg/tube) were stored in a -80°C freezer, until required for further use.

2. Large-scale extraction of total RNA from freeze-dried potato tuber

This protocol is suitable for experiments requiring higher amounts of tuber RNA (usually more than 1 µg).

1. Each pulped tuber sample (1 g) was transferred to a 50 ml Sorvall® tube, together with 14 ml of hot (80°C) extraction buffer (1:1 with phenol) and mixed by shaking using a ‘‘Heidolph-Multi Reax’’ machine for 2 minutes, at full speed. Sterile distilled water (10 ml) was added to each tube and mixed as before for a further 1 minute, followed by addition of 16 ml of ice-cold chloroform: isoamyl alcohol (24: 1) and mixed as before for 2 minutes.
2. The tubes were centrifuged at 14,000 g (10,900 rpm) and 4°C, for 20 minutes and the upper aqueous layer was transfered to fresh, sterile 50ml tubes, containing an equal volume (ca. 16 ml) of 4 M LiCl. The tubes were vortexed to mix and stored in a -80°C freezer, for overnight.
3. The tubes were centrifuged as before for 40 minutes, the supernatant was discarded and the RNA pellet resuspended in 5 ml sterile HPLC-purified water and reprecipitated in 0.1 volumes (ca. 500 µl) of 3 M NaOAc, pH 5.2, and 3 volumes (ca. 15 ml) of absolute ethanol followed by overnight incubation in a -80°C freezer. The RNA was pelleted by centrifugation as before for 40 minutes, washed with 10 ml of ice-cold 70% ethanol following by centrifugation for 20 minutes. The ethanol was removed, the RNA pellet air-dried, and resuspended in 300 µl sterile HPLC-purified water.
4. The protocol for RNA quantification, quality confirmation, clean-up, DNase treatment and storage was the same, as described before.

2.4.2 Total RNA extraction from tuber using QIAGEN RNeasy® Mini kit

Each snap-frozen tuber sample (~ 100 mg) was ground to a powder and transferred to a 2 ml, sterile, microfuge tube. RLT Buffer (supplemented with the β ME) was added to each tube, followed by 1 minute incubation (without heating) and constant vortexing. The recommendations of the column-purification protocol of the QIAGEN RNeasy® Mini Kit (‘‘for the purification of total RNA from plant cells and tissues and filamentous fungi’’) were followed for rest of the procedure. The isolated RNA was concentrated by adding 0.1 volume of 3 M NaOAc, pH 5.2, and 3 volumes of absolute ethanol, followed by storage overnight in a -80°C freezer. The RNA was pelleted by centrifuging for 30 minutes, washed with 70 % ethanol, air-dried for 10-15 minutes at room temperature, and resuspended in 30 µl nuclease-free water.

2.4.3 RNA cleanup

Each RNA sample (100 µg), adjusted to 100 µl with nuclease-free water, was purified from any contaminants such as cellular-debris or any residual contaminants of the extraction process, by passing it through the pink coloured spin-column of the ‘‘QIAGEN RNeasy® Mini kit’’ following the suggested protocol.

2.4.4 DNase digestion

None of the existing RNA isolation methods can extract RNA without any traces of contaminating DNA (Anonymous, 2009). Therefore, the RNA preparations were cleaned from any contaminating DNA by DNase-digestion in solution using the suggested protocol of the ‘‘Ambion® TURBO DNA-free™ kit’’. The RNA (10 µg) in a 50 µl reaction-volume was mixed with 5 µl (0.1 volume) of 10X TURBO DNase Buffer and 1 µl (2 Units) of TURBO DNase enzyme, followed by gentle mixing and incubation at 37 °C for 20 minutes. The DNase Inactivation-Reagent (5 µl, 0.1 volume) was incubated for 5 minutes, at ambient-temperature, with repeated mixing

of the tube contents. Finally, the DNA-free RNA was transfered to fresh tubes and quantified using a ‘‘NanoDrop™ 1000 spectrophotometer’’.

2.4.5 RT-PCR detection of PMTV in tuber samples

For detection of PMTV in tuber samples, the PMTV primer-set (PTGB2 FOR, CGTCGACAA**ATGGTCCGGAATAACGAAATTG** and PTGB2REV, CCTCGAGTTAA**CCTCCATATGACCTGCAGC**) based on the triple gene block (TGB2) of PMTV RNA-3, was kindly provided by Mr. Graham Cowan (JHI). The virus sequence within this primer set, complementary to the TGB2 of PMTV (Swedish isolate), is in bold and underlined letters. The rest of the primer sequences comprised supplementary bases added for restriction digestion of the TGB2 gene. A plasmid clone of PMTV-TGB2 was used as a positive-control and water as negative-control (NTC). The rest of the reagents and conditions of the PCR were the same as given in the TRV detection protocol (see section 2.2.2.).

2.4.6 One colour microarray-based gene expression analysis

Experiments were performed using a custom designed Agilent gene expression microarray, referred to as the Potato Oligo Chip Initiative (POCI) array, which consists of 60-mer oligonucleotide probes representing 42,034 potato unigenes in 4x 44K format (A-MEXP-1117; http://www.ebi.ac.uk/arrayexpress). Experimental design and data can be accessed at ArrayExpress (E-MTAB-4670; http://www.ebi.ac.uk/arrayexpress). Potato tuber RNA samples were converted to Cy3-labelled cRNA using the ‘‘Low Input Quick Amp Labeling kit’’ (Agilent), following the One-Color Microarray-Based Gene Expression Analysis v 6.5 protocol.

Labelled cRNAs were hybridised to the POCI arrays overnight and scanned as recommended using a G2505B scanner (Agilent). Four replicates of each of the twelve RNA samples (themselves representing four biological replicates of the three

tuber types) were processed on the array. Data were extracted from each of the arrays using Feature Extraction v 10.7.3.1 software (Agilent) and default parameters, prior to importing into Genespring v 7.3 software (Agilent) for normalisation, QC and analysis.

2.4.7 Preparation of cDNA standards and validation of the quantitative RT-PCR (qRT-PCR) primer sets

The cDNA aliquots (1/25 dilution) of all the twelve RNA samples viz; spraing (S1, S2, S3, and S4), spraing-free (SF1, SF2, SF3 and SF4) and healthy (H1, H2, H3 and H4) were pooled together to make a composite sample (300 µl).The pooled cDNA sample (300 µl) was of concentration 100 ng/µl and then serially diluted (1:4 with H_2O) to make 300 µl of the diluent 1 (25 ng/µl), diluent 2 (6.25 ng/µl), diluent 3 (1.56 ng/µl), and diluent 4 (0.39 ng/µl). 5 µl of the pooled and the serially diluted cDNAs (diluents, standards) were loaded into a qRT-PCR plate. The cDNA template in the NTC was replaced by nuclease-free water. The primer-sets for the target gene, alongwith the recommended concentrations of the primers are given in Table No. 5.5. The rest of the qPCR reagents and the thermal cycling programme was the same as mentioned in section 2.4.8. Each sample was assayed in duplicate using the standard-curve function of the ‘‘StepOne Plus’’ package (Applied Biosystems) for data analysis.

2.4.8 qRT-PCR validation of potato gene expression

Quantitative RT-PCR reactions comprised 12.5 µl of the ‘‘Power SYBR® Green PCR Master Mix’’ (Life Technologies Corporation) per 25 µl reaction. The forward and reverse primers (10 µM each) were added to the PCR-mixture to a final concentration as mentioned in Table No. 5.5. The Elongation factor-1 alpha (Ef-1 α) and Cyclophilin (CyP) genes were the internal-control (house-keeping) genes in these assays to comply with the ‘‘Minimum information for publication of quantitative real-time experiments’’ (MIQE) guidelines (Bustin *et al*., 2009). The

1/25 diluted cDNA of each sample was thawed on ice, just prior to the loading of 5µl into the corresponding well of the qRT-PCR plate. Each cDNA sample was assayed in triplicate. The total reaction volume was made up with nuclease-free water. For the NTC the template was replaced with the water.

The thermal cycling parameters were as follows: - Holding stage at initial denaturation of 95°C for 15 minutes, followed by 40 cycles of denaturation at 95°C (for 15 seconds), annealing at 59°C (for 40 seconds) and extension at 72°C (for 30 seconds). The DNA amplification data were extracted by the software at the annealing stage of each cycle. Melt-curve analysis was done in continuous run mode with denaturation at 95°C (for 15 seconds), followed by annealing at 59°C (for 40 seconds) and again denaturation at 95°C (for 15 seconds). The qPCR was performed using an ‘‘Applied Biosystems’’ StepOne Plus™ machine and the data were collated by the ‘‘StepOne Plus’’ package.

2.4.9 Staining of tuber sections for histological confirmation of HR

Pentland Dell tubers were collected from a field affected with spraing disease. The tubers ranging a diameter of 4.5 to 6 cm were checked to ensure they were free of any injury, bruising and morphological abnormalities. Tubers were washed with tap-water to remove any adhering soil-particles, air-dried on paper towels and cut in cross-sections with a knife. Small tuber sections including spraing symptoms were collected, using a cork-borer, and the tuber sections lacking any disease symptoms were also collected from healthy tubers. The sections were trimmed to a 2 mm thickness with a vibroslicer and stained to confirm the histological occurrence of HR. Three sections from both healthy and spraing-affeccted tubers were stained simultaneously by dipping in a beaker containing the stain solution. Images before and after the staining were examined using a Leica MZFL III stereoscope and captured by ‘‘Moticam 3000’’ camera.

1. *Trypan Blue staining*

The tuber-sections were washed for 2 minutes with deionized and distilled water, and then stained by boiling in a lactophenol trypan-blue solution (10 mg of trypan-blue, 20 ml of absolute-ethanol, 10 ml of buffer-saturated phenol pH 4.5, 10 ml of lactic acid (Sigma L-1250), and 10 ml of deionized water) for 2 minutes (Keogh *et al*., 1980; Koch and Slusarenko, 1990; Miles *et al*., 2010). The stained sections were washed with 70% ethanol, rinsed in distilled water, and finally destained over three weeks by submerging in 40 ml of chloral hydrate solution (500 g / 200 ml distilled water) with weekly changes of the solution until the background staining was removed. Chloral hydrate solution was prepared by dissolving chloral hydrate overnight in boiled, sterile, distilled water with continuous stirring for hours. Once the background stain was removed, the tuber-sections were rinsed with sterile and distilled water and examined using a stereoscope.

2. *Phloroglucinol staining*

Acidic phloroglucinol is used as a general stain for the detection of lignin (Wiesner reaction) that is stained temporarily pink to red. The freshly prepared tuber-sections were dipped simultaneously in 2% phloroglucinol / ethanol (70%) solution at room temperature and incubated for 30 minutes, followed by replacing the staining solution with the 25% HCl solution (Liljegren, 2010; Miles *et al*., 2010). The stained sections were rinsed with distilled water and immediately examined with a stereoscope.

3. *DAB staining*

The generation of Reactive Oxygen Species (ROS) such as H_2O_2 can be visualized by staining with 3, 3′-Diaminobenzidine (DAB), as DAB produces dark-brown precipitates when it is oxidized by H_2O_2 in the presence of peroxidases (Thordal-Christensen *et al.*, 1997; Daudi *et al.*, 2012). The DAB stain was prepared in HPLC-purified water, following the suggested protocol of SIGMAFAST™ 3, 3′-

Diaminobenzidine tablets (Sigma-Aldrich™, Inc.). The tuber slices were simultaneously submerged in the DAB-stain solution. As soon as the tuber-tissue started to develop a background of brown-coloured precipitates, the staining was stopped by washing with PBS. The samples were finally washed with sterile distilled water and the images captured with a Canon EOS Ultrasonic camera.

3. Systemic Infection of TRV isolates

3.1. Aim

TRV can move systemically from the mechanically-inoculated foliage down to the roots of susceptible hosts (Chen *et al.,* 1969). In the field, TRV is transmitted from an infected to a healthy plant by trichodorid nematodes which transmit it in a species-specific association (van Hoof, 1968; MacFarlane *et al*., 1999). RNA-1 of TRV is highly conserved in different isolates (Robinson and Harrison, 1989; Sudarshana and Berger, 1998; Visser and Bol, 1999; Crosslin *et al*., 2003; MacFarlane, 1999, 2010), whereas RNA-2 is extremely variable among different isolates in the size, nucleotide-sequence and organization of the encoded-genes (Robinson *et al*., 1983; Bergh *et al.,* 1985; Cornelissen *et al*., 1986; Angenent *et al*., 1986; Goulden *et al*., 1990; Sudarshana and Berger, 1998). The contribution of RNA-1 and RNA-2 to virus infection was examined in a series of experiments. Firstly, three different RNA-1 molecules (SYM, PpO-85 and PpK-20) were separately combined with a GFP-expressing PpK-20-derived RNA-2 and any differences caused in the expression of GFP and CP were quantified by fluorometric and western-blot assay, respectively. In another set of experiments, all three RNA-1 isolates were separately mixed with full-length, wild-type, RNA-2 transcripts of five different TRV isolates to form 15 different TRV recombinant isolates. All 15 laboratory isolates were mechanically inoculated to *N. benthamiana* plants. The replication and systemic movement of the RNA-1 and -2 of these TRV recombinants (hereafter refereed as TRV isolates) was evaluated by northern blotting. We have also investigated the infection and systemic movement of all 15 TRV isolates in six different cultivars of tetraploid potato. As part of this work the full-length sequence of the I6 RNA-2 was also determined.

Before proceeding to prepare the recombinant TRV isolates, the infectivity of the three TRV RNA-1 inocula was confirmed as follows:-

3.1.1. Infectivity confirmation of the TRV RNA-1 isolates

Total plant leaf RNA containing each of the three TRV RNA1 species was mechanically inoculated to *N. benthamiana* and *N. clevelandii* plants (section 2.2.1). RNA1 multiplication was confirmed by RT-PCR amplification of the TRV 16K gene as described in section 2.2.2 (Fig. 3.1). RNA was then isolated from these plants to produce a stock of infectious RNA1 of each TRV isolate for use in genome reconstitution experiments.

Infectivity of all these RNA-1 isolates was further tested by inoculation onto *Chenopodium quinoa* (section 2.2.5). The RNA-1 isolates produced necrotic-flecks (Fig. 3.2) on *C. quinoa* and were found to be infectious up to a dilution of 1:100. However, no infectivity was noticed at dilutions of 1:1000 and 1:10,000 (Table No. 3.1). The mock-inoculated plants remained asymptomatic.

Table 3.1. Infectivity score of TRV RNA-1 (NM-type) isolates assessed by bioassay

Sr. No.	Dilution factor	Average number of necrotic-lesions produced on three inoculated leaves of each plant			
		SYM RNA-1	Pp0-85 RNA-1	PpK-20 RNA-1	Mock
01-	Undiluted	23	11	64	00
02-	1 :10 dil.	08	08	18	00
03-	1 :100 dil.	04	03	07	00
04-	1:1000 dil.	00	00	00	00
05-	1:10,000 dil.	00	00	00	00

The given values are average of two individual plants

The undiluted inoculum of PpK-20 RNA-1 produced the highest average number of necrotic-lesions (64), followed by the SYM RNA-1 (23). Whereas, the PpO-85 RNA-1 was least capable of producing infection (an average of 11 necrotic-spots).

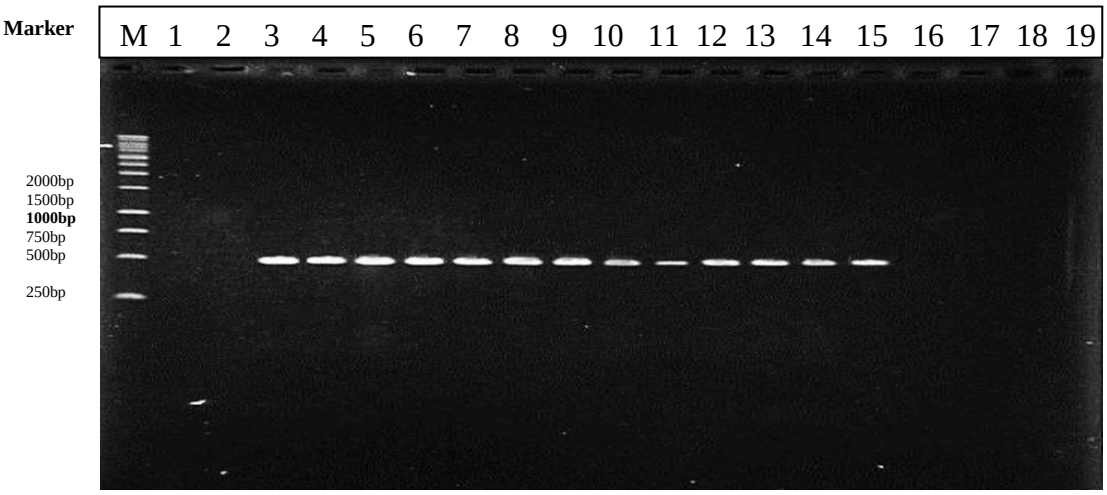

Figure 3.1. RT-PCR detection of TRV in plants inoculated with RNA-1 isolates. **Lane M**: 1Kb Promega DNA marker; **Lane 1**: Non-Template control; Plants inoculated with, Lane **2**: 1X PBS only; **Lane 3**: SYM, M-type; **Lane 4-7**: SYM RNA-1; **Lane 8-11**: PpO-85 RNA-1; and **Lane 12-15**: PpK-20 RNA-1 isolates; **Lane 16-19**: Blank. The first two lanes of each RNA-1 isolate are from *N. benthamiana* and the latter two are from *N. clevelandii* plants.

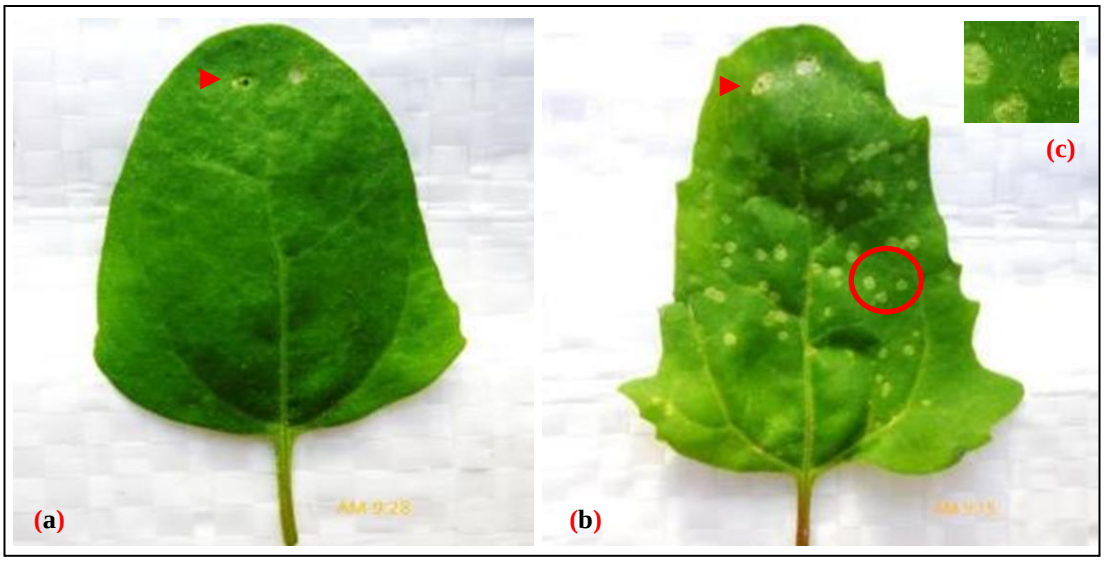

Figure 3.2. TRV RNA-1 infection on the indicator plant *Chenopodium quinoa*. Leaves of *Ch. quinoa* inoculated with **(a)** 1X PBS only, showing no symptoms. **(b)** undiluted inoculum of PpK-20 RNA-1 isolate, showing necrotic-lesions. **(c)** Close-up of encircled-tissue elaborating TRV-induced necrotic lesions. Arrow-head (►) indicates the marks to differentiate the inoculated from the non-inoculated leaves. Images were captured at 4 dpi.

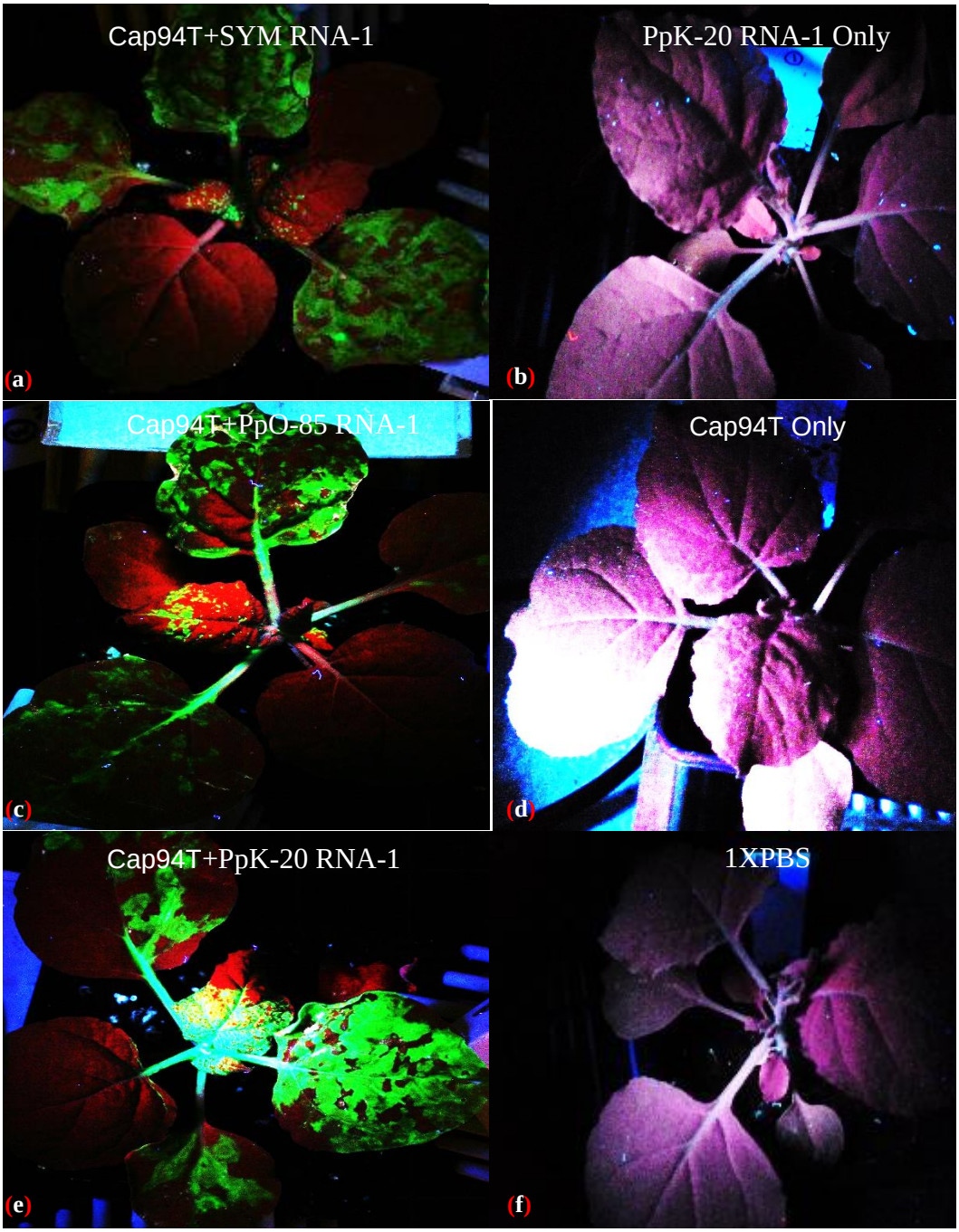

Figure 3.3. GFP expression in *Nicotiana benthamiana* plants infected by TRV RNA-1 isolates. Plants inoculated with Cap94T and **(a)** SYM RNA-1; **(c)** PpO-85 RNA-1; and **(e)** PpK-20 RNA-1 isolates. Plants inoculated only with **(b)** PpK-20 RNA-1; **(d)** Cap94T; and (**f)** 1X PBS (mock-inoculation). Images were captured at 4 dpi.

The viability of the TRV RNA-1 preparations was further tested by mixing each separately with an RNA-2-GFP transcript (Cap94T) as given in section 2.2.4. This RNA mixture was mechanically inoculated to 4-5 leaf stage *N. benthamiana* plants and the effect of RNA-1 isolates on the systemic infection of RNA-2 was documented by recording the GFP expression at 4 dpi. GFP fluorescence was seen in all the plants inoculated with Cap94T and any of the TRV RNA-1 isolates. The results presented in Fig. 3.3 are representative of the experiment repeated three times. The GFP expression was stronger in the plants inoculated with PpK-20 RNA-1 (Fig. 3.3, e) and weaker in the plants inoculated with SYM RNA-1 (Fig. 3.3, a) and PpO-85 RNA1 (Fig. 3.3, c). The plants inoculated with only PpK-20 RNA-1 or Cap94T, or the1X PBS (mock-inoculation) did not show any GFP-expression (Fig. 3.3, b, d, and f), thus confirming the viability of these RNA-1 preparations (as the RNA-2 transcript cannot replicate and express GFP by itself).

3.1.2. Quantitation of GFP expression in TRV-GFP infected plants

The replication and gene expression of TRV RNA-2 is dependent on the TRV RNA-1 and thus is indirectly indicative of the level of replication and infectivity of the supporting RNA-1 molecule. Therefore, a GFP-engineered TRV RNA-2 was exploited to assess the infectivity of the three different supporting RNA-1 molecules of the virus. The images of *N. benthamiana* plants (inoculated by the method given in section 2.2.6) were captured at 4 dpi and 8 dpi, and are presented in figure 3.4. and 3.5., respectively. The presented images are representative of three plants for each treatment.

All the mock inoculated *N. benthamiana* plants, used as negative controls for the experiment, remained GFP-free (Fig. 3.4, e) and the GFP transgenic *N. benthamiana* (CB28) plants, served as positive control for the experiment, were documented with good strength of GFP signal (Fig. 3.4, a). At 4 dpi, much stronger GFP expression was recorded in the top systemic leaves of the plants co-inoculated with GFP engineered TRV RNA-2 (Cap49T) and the PpK-20 RNA-1 isolate (Fig. 3.4, d). The

Figure 3.4. GFP expression in *Nicotiana benthamiana* recorded at 4 dpi. (a) GFP transgenic *N. benthamiana* plant, CB28. Non-transgenic *N. benthamiana* plants inoculated with GFP-engineered Cap49T (TRV RNA-2) and **(b)** SYM RNA-1 **(c)** PpO-85 RNA-1 **(d)** PpK-20 RNA-1 isolates and **(e)** 1X PBS only.

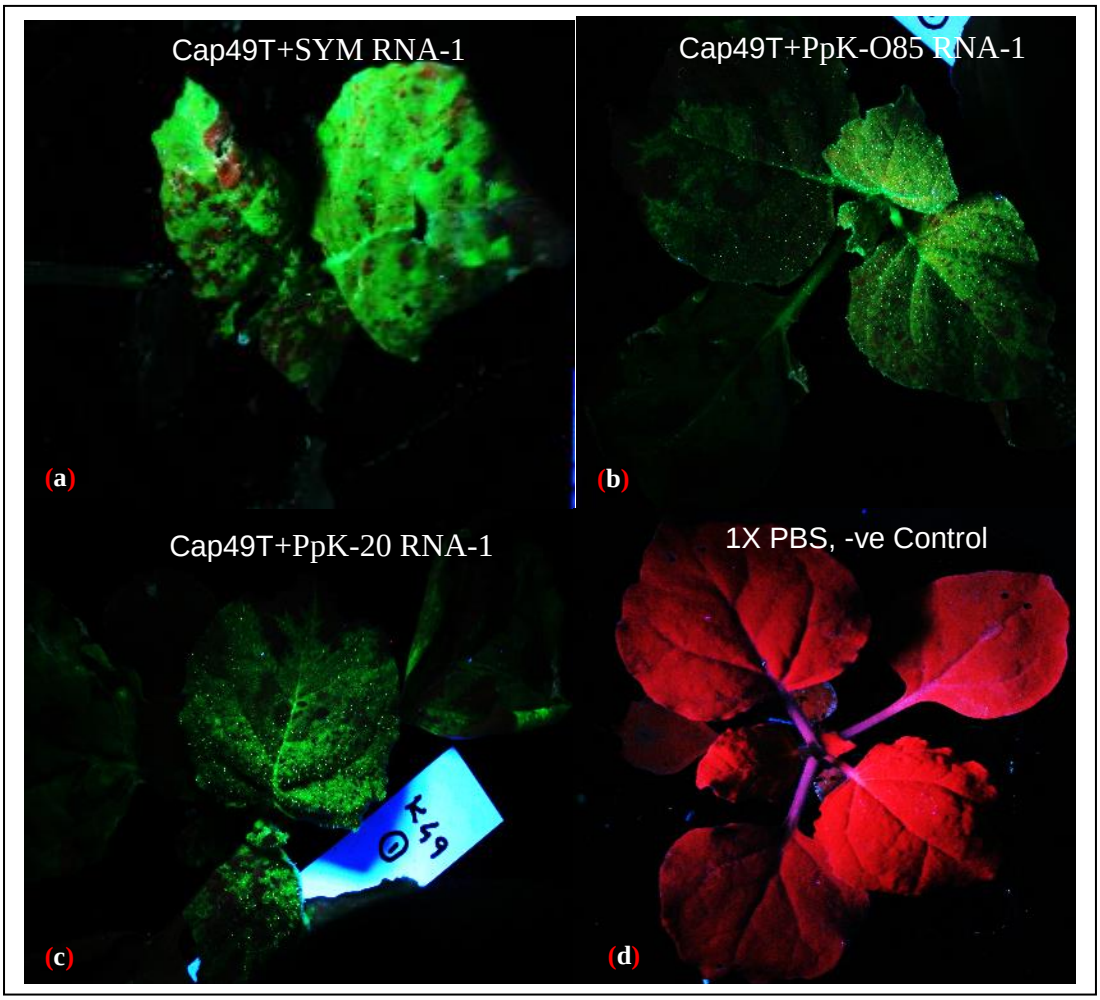

Figure 3.5. GFP expression in *Nicotiana benthamiana* recorded at 8 dpi. Non-transgenic *N. benthamiana* plants inoculated with GFP-engineered Cap49T (TRV RNA-2) and **(a)** SYM RNA-1, **(b)** PpO-85 RNA-1, **(c)** PpK-20 RNA-1 isolates, and **(d)** 1X PBS only (mock-inoculation).

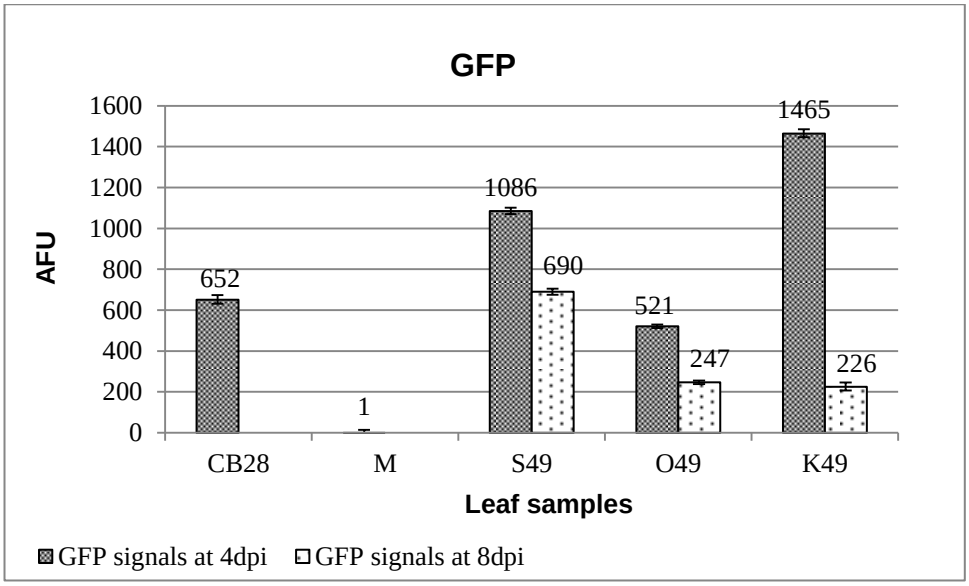

Figure 3.6. GFP expression with relevance to the TRV RNA-1 isolates. CS28: GFP transgenic plants; M: Mock-inoculated plants; Plants inoculated with GFP engineered TRV RNA-2 (Cap49T) and SYM RNA-1 (S49) or PpO-85 RNA-1 (O49) or PpK-20 RNA-1 (K49). "ɪ" is the error-bar representing standard deviation of the mean; value above bar is normalized AFU of GFP expression from three plants.

next strongest intensity of GFP expression was observed in the plants inoculated with Cap49T and SYM RNA-1 (Fig. 3.4, b). However, the least GFP expression was observed in the plants inoculated with Cap49T and PpO-85 RNA-1 (Fig. 3.4, c).

GFP expression was reduced at 8dpi, with the greater reduction being observed in the plants inoculated with PpK-20 RNA-1 (Fig. 3.5, c), followed by the PpO-85 RNA-1(Fig. 3.5, b) and the SYM RNA-1(Fig. 3.5, a), respectively.

The total proteins from the leaf samples were extracted (section 2.2.6) and the differential GFP expression was quantified (Appendix 7), using a fluorimeter. The mean arbitrary fluorescence unit (AFU) for the four blank (empty) wells and six wells loaded with the extraction buffer only was 50.027 and 112.434, respectively (Appendix 7). Whereas, the mean AFU of the three mock-inoculated *N. benthamiana* plants (M-1,-2, and -3) was 276.12. The mean AFU of mock plants was subtracted from the mean AFU of the test samples to get the normalized (nor.) AFU. The nor.

AFUs were rounded to the nearest unit. For example, the mean AFU of the three GFP transgenic *N. benthamiana* plants (CB28-1,-2 and -3) was 928. Subtracting the mean AFU of mock plants (276.12) from the mean AFU of the CB28 (928) produced the nor. AFU (i.e., 652) of CB28.

At 4dpi, the highest GFP expression was recorded in the plants infected with PpK-20 RNA1 (K49, nor. AFU of 1465), followed by the plants infected with the SYM RNA1 (S49) and PpO85 RNA1 (O49) with nor. AFUs of 1086, and 521, respectively (Fig. 3.6). However, at 8 dpi, the nor. AFU in all the plants was reduced by over 50% of that recorded at 4dpi, resulting a nor. AFU of 226 in the K49 plants. 247 was in O49 and 690 was in S49 plants, respectively. So at 8 dpi, the GFP expression and therefore RNA-2 replication was maintained best in the S49 (SYM RNA-1) plants.

The PpO-85 RNA-1 appeared less infectious than the other two RNA-1 isolates (SYM and PpK-20).

3.1.3. Western blot assay of the TRV-CP expression

Expression of virus CP in these experiments was examined by western blotting. For this purpose, two sets of *N. benthamiana* plants (Set I and II; three plants per treatment) were inoculated and treated as given in section 2.2.6. These were the same plants as above in section 3.1.2 and the relative GFP expression in these plants was the same, as described already. The plants inoculated with PpK-20 RNA-1, at 4 dpi, had the highest GFP expression in the top-systemic leaves, followed by the plants infected with SYM RNA-1 and O-85 RNA-1, respectively. The GFP after reaching its peak expression was found progressively to decline after 6 dpi.

Both the inoculated and top systemic leaf samples were collected at 4 dpi from one set of plants (Set I). Whereas, from the other set of plants (Set II), only the top systemically infected leaves were collected at 6 and 10 dpi. The total proteins of these samples were extracted (section 2.2.6) and quantified by the Bradford protein assay. Equal amounts of total protein from each sample were separated by denaturing

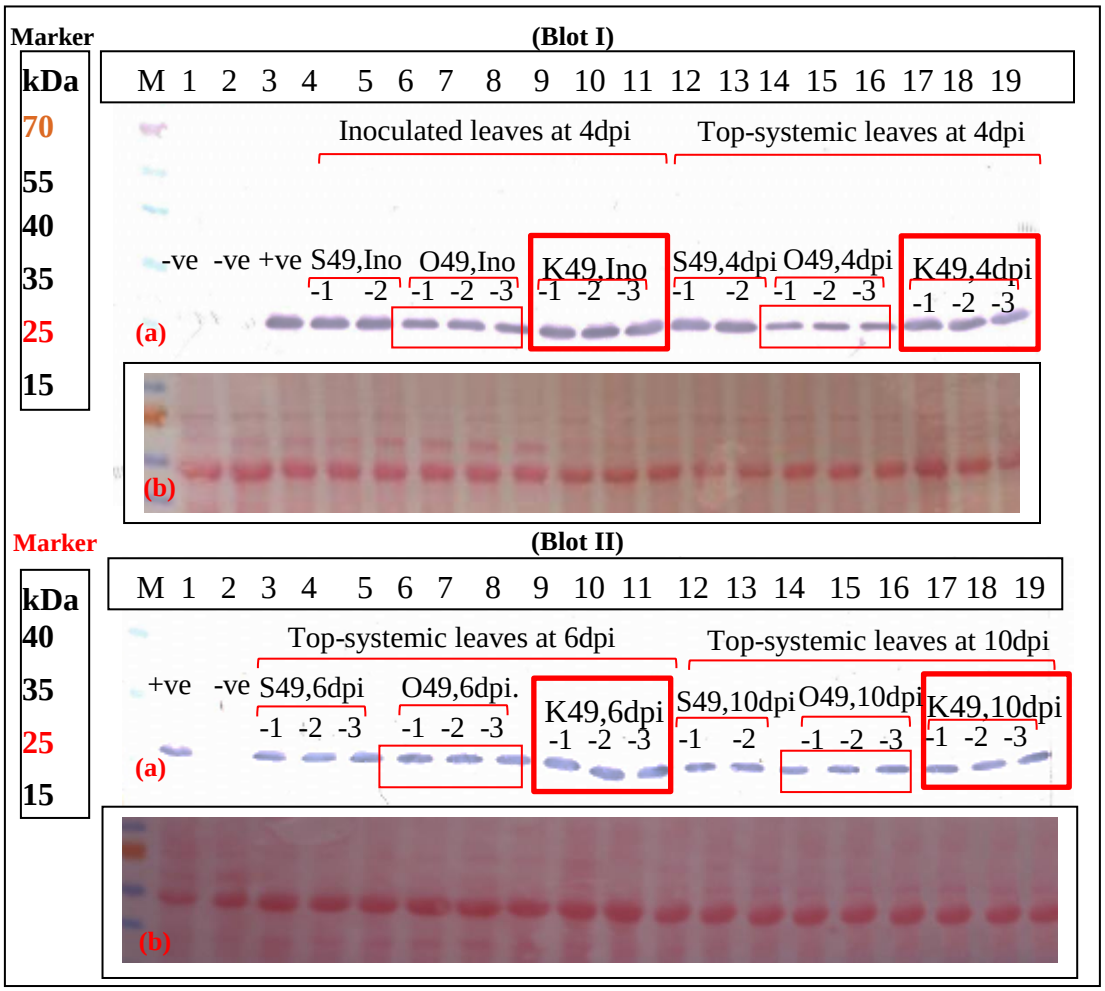

Figure 3.7. Western blots of the GFP expressing *N. benthamiana* infected with TRV-GFP and various RNA-1 isolates, probed with CP antibody. Lane M: Precision Pre-stained Protein Marker;

(Blot I) *N. benth* **Set-1**, sampled at 4 dpi**. Lane 1**: CB28, -ve control; **Lane 2**: *N. benth* Mock, -ve control; **Lane 3-11**: Inoculated (Ino.) leaf samples at 4 dpi; **Lane 3**: K20 Ino, +ve; **Lane 4-5**: S49, Ino; **Lane 6-8**: O49, Ino; **Lane 9-11**: K49, Ino, respectively. **Lane 12-19**: systemically infected leaf samples at 4 dpi; **Lane 12-13**: S49, 4 dpi; **Lane 14-16**: O49, 4 dpi; **Lane 17-19**: K49, 4 dpi, respectively.

(Blot II) *N. benth* **Set-2**, sampled at 6 dpi and 10 dpi**. Lane 1**: PpK20, 6 dpi, +ve control; **Lane 2**: CB28, -ve control; **Lane 1-11**: systemically infected leaf samples at 6 dpi; **Lane 3-5**: S49, 6 dpi; **Lane** TRV-CP **6-8**: O49, 6 dpi; **Lane 9-11**: K49, 6 dpi, respectively. **Lane 12-19**: systemically infected leaf samples at 10 dpi; **Lane 12-13**: S49, 10 dpi; **Lane 14-16**: O49, 10 dpi; **Lane 17-19**: K49,10 dpi, respectively; Ino., 4, 6, and 10 dpi: represents sample collected from inoculated leaf at 4 dpi and top-systemic leaves at 4, 6, and 10 dpi, respectively; -1, -2, and -3: represents individual plant numbers. **Panel a** is the blot stained for CP detection and **panel b** is the Ponceau S staining of the respective blot.

PAGE and the TRV CP proteins were detected using CP-specific antibodies (Fig. 3.7).

The CP (22kDa) was detected in the positive control samples (plants inoculated with PpK-20 infectious sap), and all the test samples (S49, 1-3; O49, 1-3; and K49, 1-3). The CP was undetectable in the samples from the GFP transgenic (CB28) and the mock-inoculated *N. benthamiana* plants (negative controls of the experiment).

The blot of the samples from Set I is presented in Fig. 3.7, Blot I. The CP (22kDa), besides being strongly detected in the positive control plant (K20, Lane 3), was also strongly detected in the plants inoculated with virus carrying SYM RNA-1 (S49,Ino.; Lane 4 and 5) and PpK20 RNA-1 (K49, Ino.; Lane 9 -11). Whereas, it was weakly detected in the plants inoculated with the PpO-85 RNA-1 virus (O49, Lane 6 -8). Similar to the detection in the inoculated leaves, CP was also relatively strongly detected (at 4dpi) in the top systemically infected leaves (K49, Lane 17 -19) of all the plants infected with the PpK20 RNA-1 containg inoculum and was also strongly detected in the plants (S49, Lane 12 -13) infected with the SYM RNA-1 containing virus. However, the CP detection in all three plants infected with PpO-85 RNA-1 (O49, Lane 14 -16) virus was weaker compared to the plants infected with the other two TRV RNA-1 isolates.

The blot of samples from Set II is presented in Fig. 3.7, Blot II. The CP accumulation in all the three plants (K49, 6dpi, Lane 9 -11) inoculated with virus comprising PpK-20 RNA-1 was still stronger at 6dpi, compared to the plants inoculated with the other two RNA1 isolates. However, at 10dpi the CP detection decreased in the top-systemically infected leaves of all three plants inoculated with PpK-20 RNA-1 virus (K49, 10,-1,-2, and -3 ; Lane 17 -19) and it was difficult to differentiate the level of CP accumulation in the plants inoculated with the SYM RNA-1(S49, 10,1,-2, and -3 ; Lane 12 -14) and PpO-85 RNA-1 (O49, 10,1,-2, and -3; Lane 15 -17) containing virus. The TRV CP accumulation in association with PpK-20 RNA-1, at various

time intervals, is highlighted in square blocks (Fig. 3.7) for quick comparison with the other two RNA-1 isolates.

In general, the results of the western-blot analysis, for the systemic accumulation of the virus at 4 and 6dpi, were in agreement with the fluorometric analysis. However, some dissimilarity in the relative systemic accumulation of the viruses at 8dpi and 10dpi was recorded when comparing the GFP and the CP expression, respectively. The reasons for this are not known.

3.2. Utilization of full-length TRV RNA-2 infectious clones

The full-length RNA-2 infectious clones of five different isolates (viz, PpK-20, I6, PaY4, TpO1, and SYM; Table No. 2.2) were available in the laboratory (section 2.2.7). Full-length RNA-2 transcripts of these clones were synthesized that were separately mixed with the three RNA-1 isolates to form TRV recombinant isolates. These isolates were then tested on various hosts including tetraploid potato varieties. Investigations for any influence of the RNA-2 encoded genes on the systemic movement and accumulation of TRV were conducted by northern-blot analysis.

3.3. TRV recombinant isolates

An overview of the constituents and the names (acronyms) of all the TRV recombinant isolates examined here is given in Table No. 3.2. For each virus three individual N. *benthamiana* plants were inoculated and kept in the glass-house for more than a week to observe any symptomatological difference(s). In total 45 plants were inoculated with 15 different TRV isolates and three plants were inoculated with 1X PBS buffer as controls.

All nine plants inoculated with the three different isolates containing PpK-20 RNA-2 (viz: SK20, OK20 and KK20), developed systemic necrosis that progressed from the inoculated leaves to the systemically-infected leaves (Fig. 3.8). The inter- and intra-veinal necrosis of the top leaves was more prominent and severe (Fig. 3.8, c and d) in

the plants inoculated with KK20 (KK20 is an *in-vitro* generated recombinant of the parental PpK-20 isolate). However, the plants inoculated with the other two TRV recombinant isolates, reconstituted using the SYM RNA-1 (SK20) and O-85 RNA-1 (OK20), produced less severe symptoms (Fig. 3.8, a and b, respectively). The systemic necrosis induced by KK20 was lethal as it killed the plants within 8-10 days of inoculation (dpi).

Table 3.2. The constituents and acronyms of TRV recombinant isolates

Sr.No.	Constituents of TRV isolates		Acronym of recombinant isolates
	TRV RNA-1 isolate (Total RNA)	TRV RNA-2 isolate (Transcript)	
1.	SYM	PpK-20 (T214)	pseudorecombinant isolate SK20
2.		I6 (T215)	pseudorecombinant isolate SI6
3.		PaY4 (T216)	pseudorecombinant isolate SY4
4.		TpO1 (T217)	pseudorecombinant isolate ST
5.		SYM (T218)	parental recombinant isolate **SS**
6.	PpO-85	PpK-20 (T214)	pseudorecombinant isolate OK20
7.		I6(T215)	pseudorecombinant isolate OI6
8.		PaY4 (T216)	pseudorecombinant isolate OY4
9.		TpO1 (T217)	pseudorecombinant isolate OT
10.		SYM (T218)	pseudorecombinant isolate OS
11.	PpK-20	PpK-20 (T214)	parental recombinant isolate **KK20**
12.		I6 (T215)	pseudorecombinant isolate KI6
13.		PaY4 (T216)	pseudorecombinant isolate KY4
14.		TpO1 (T217)	pseudorecombinant isolate KT
15.		SYM (T218)	pseudorecombinant isolate KS

The plants inoculated with the isolates containing I6 RNA-2, produced vein-yellowing and chlorosis in the systemically-infected leaves. These symptoms were more severe in the plants inoculated with the isolate reconstituted using SYM RNA-1 (SI6, Fig. 3.8, e) and PpK-20 RNA-1 (KI6) as compared to the isolate derived from PpO-85 RNA-1 (OI6).

The plants inoculated with the three recombinant isolates containing PaY4 RNA-2

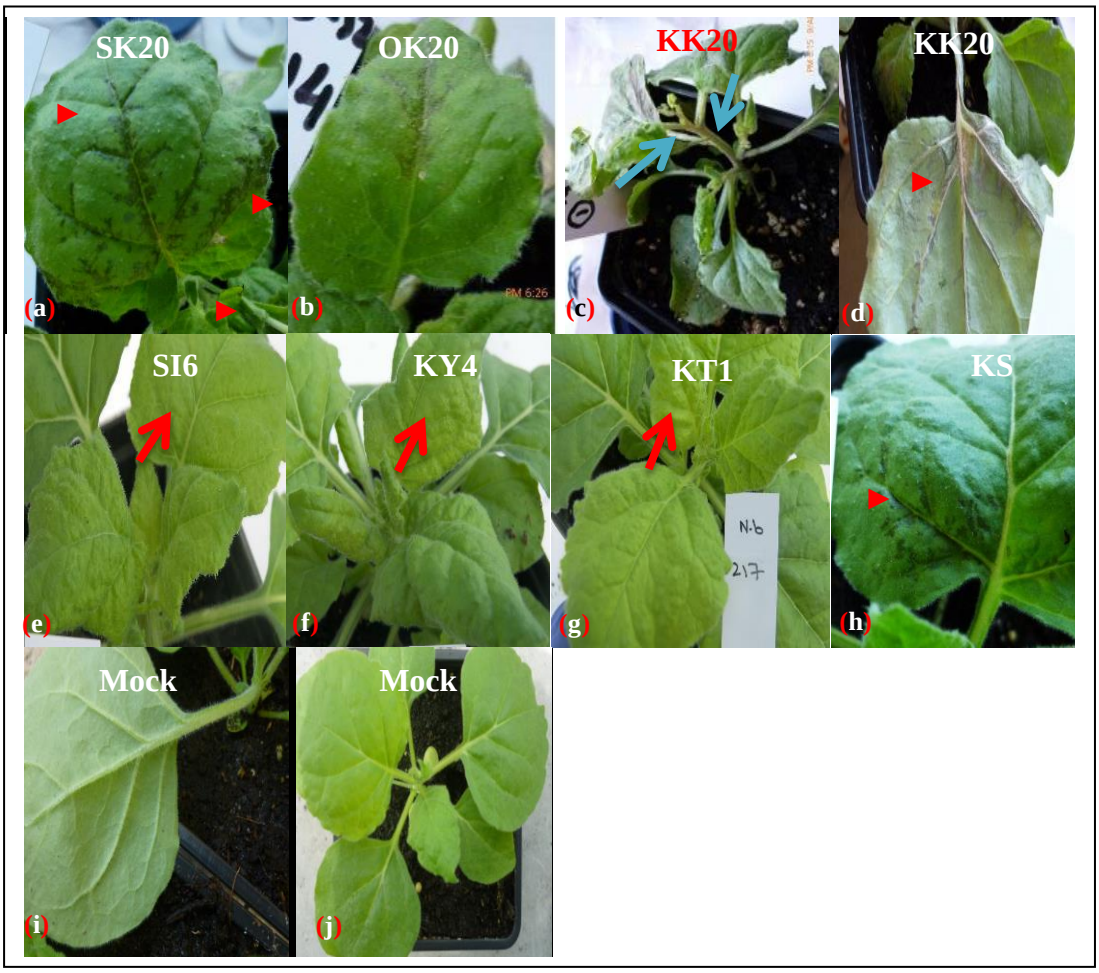

Figure 3.8. Systemic symptoms induced by various TRV recombinant isolates. Top system-infected leaves of *N. benthamiana* plants inoculated with the isolate **(a)** SK20, **(b)** OK20, **(c)** KK20, **(d)** close-up image of the abaxial-surface of a top-leaf from **c**, elaborating the veinal-necrosis; **(e)** SI6, **(f)** KY4, **(g)** KT1, and **(h)** KS. Arrow-head (►) indicates the symptoms of vein-necrosis, the blue-arrow (→) points to the spreading systemic-necrosis, and the red-arrow (→) points to the vein-yellowing symptoms. **(i)** abaxial-surface of a leaf from **(j)** mock-inoculated plant. Images were captured at 8 dpi.

(SY4, OY4 and KY4) produced light chlorosis and curling of the top, systemically-infected leaves (Fig. 3.8, f). These symptoms were rather milder than those produced by the isolates containing I6 RNA-2. However, the plants inoculated with the KY4 inoculum displayed relatively more severe symptoms than the plants inoculated with the SY4 and OY4 inocula.

Among all the three recombinant isolates containing TpO-1 RNA-2 (ST1, OT1, and KT1), the induced symptoms resembled in pattern and severity to the symptoms produced by the I-6 RNA-2-containing inoculum (Fig. 3.8, g).

All the three recombinant isolates containing SYM RNA-2 (SS, OS, and KS), produced veinal-necrosis on the top, non-inoculated leaves, but these symptoms were much weaker in intensity and prevalence (Fig. 3.8, h) than the symptoms produced

Table 3.3. Overview of the symptoms induced by various TRV recombinant isolates on *Nicotiana benthamiana* plants

Sr.No.	TRV recombinant isolate (Acronym)	Symptoms	
			Intensity
1.	SK20	Systemic necrosis, veinal necrosis	+
2.	OK20	----------Same as above---------	++
3.	KK20	----------Same as above---------	+++, Plant death
4.	SI6	Systemic vein-yellowing and chlorosis	+++
5.	OI6	----------Same as above---------	++
6.	KI6	----------Same as above---------	+
7.	SY4	Light chlorosis and curling of the top leaves	+
8.	OY4	----------Same as above---------	++
9.	KY4	----------Same as above---------	+++
10.	ST	Systemic vein-yellowing and chlorosis	+
11.	OT	----------Same as above---------	++
12.	KT	----------Same as above---------	+++
13.	SS	Veinal necrosis of top leaves	++
14.	OS	----------Same as above---------	++
15.	KS	----------Same as above---------	+

+, ++, and +++ denotes mild, milder and severe intensity of the symptoms.

by the inoculum containing PpK-20 RNA-2. All the three mock-inoculated plants remained asymptomatic (Fig. 3.8, i and j), confirming that the environmental conditions were not the cause of any visible symptoms. A brief summary of the various symptoms induced by these isolates is given in Table No. 3.3.

Over-all, the symptomatological observations showed that among all the fifteen recombinant isolates, the TRV-inoculum representing the parental form of the PpK-20 isolate was the most pathogenic as it caused the most severe symptoms and killed the infected plants when other isolates did not.

3.3.1. Confirmation of the identity of TRV recombinant isolates in the infected *N. benthamiana* plants

The identity of all the 15 isolates was confirmed by RT-PCR detection (section 2.2.10) of the respective TRV-RNA-2 in systemically infected *N. benthamiana* plants. After confirming the systemic movement and identity of all the 15 infecting isolates (Fig. 3.9), infectious-sap of the plants containing these viruses was prepared and stored as given in section 2.2.9.

3.4. Preparation of the ribo-probes for dot-blot hybridization

The systemic accumulation of all the 15 TRV isolates in the *N. benthamiana* plants was also evaluated by northern blot analysis (section 2.2.12). The RNA-1 and -2 of all 15 isolates were detected using MP-specific (TRV-1) and CP-specific (TRV-2) ribo-probes which were prepared by the following the protocol described in section 2.2.11. As a quality check (QC), each of these probe transcripts (1 µg) was resolved on a denaturing agarose gel (Fig. 3.10). All the six transcripts (T1, T2, T3, T4, T5, and T6) produced a single, sharp RNA band on the gel without any smearing which confirmed their suitability for use in northern blot analysis.

The template specificity and detection efficiency of the labelled transcripts (ribo-

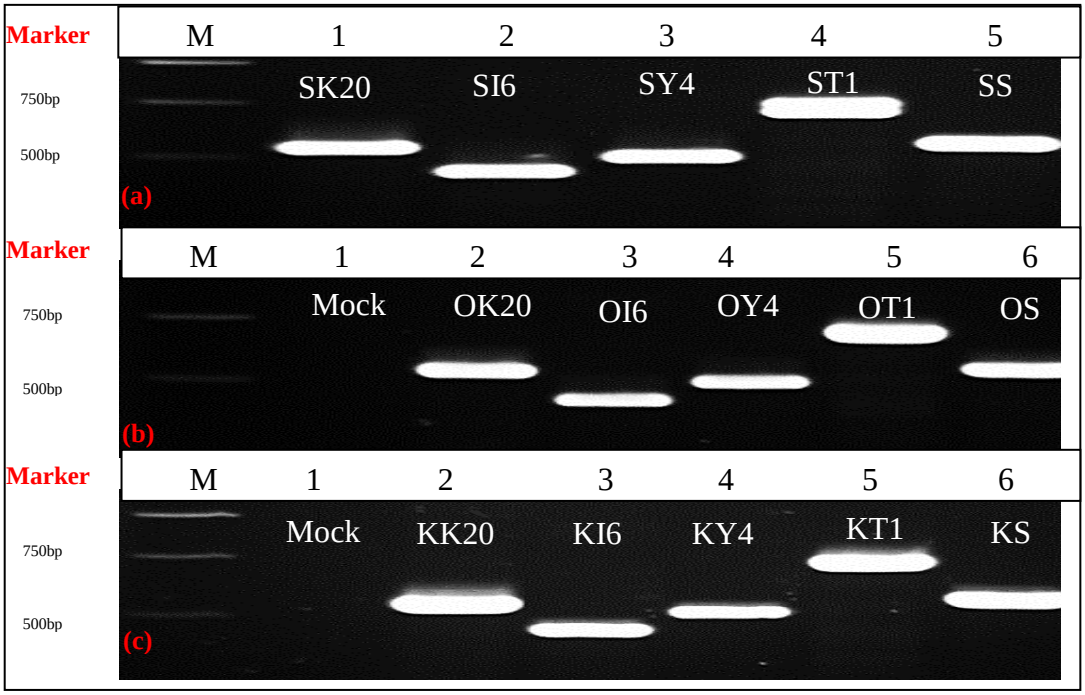

Figure 3.9. RT-PCR detection of various TRV RNA-2 in the top systemic-leaves of *N. benthamiana.* **Lane M**: 1Kb Promega DNA marker. Samples from plants inoculated with TRV isolates **Panel a**: SYM RNA-1; **Lane 1**: SK20; **Lane 2**: SI6; **Lane 3**: SY4; **Lane 4**: ST1; and **Lane 5**:SS; **Panel b**:O-85 RNA-1; **Lane 1**: mock inoculation; **Lane 2**: OK20; **Lane 3**: OI6; **Lane 4**: OY4; **Lane 5**: OT1; and **Lane 6**: OS; **Panel c**: PpK-20 RNA-1; **Lane 1**: mock inoculation; **Lane 2**: KK20; **Lane 3**: KI6; **Lane 4**: KY4; **Lane 5**: KT1; and **Lane 6**: KS. The amplicons of SK20, OK20, KK20 (PpK-20 RNA-2); SI6, OI6, KI6 (I6 RNA-2); SY4, OY4, KY4 (PaY4 RNA-2); ST1, OT1, KT1 (TpO-1 RNA-2); and SS, OS, KS (SYM RNA-2) were of 540 bp, 450 bp, 503 bp, 708 bp, and 559 bp, respectively.

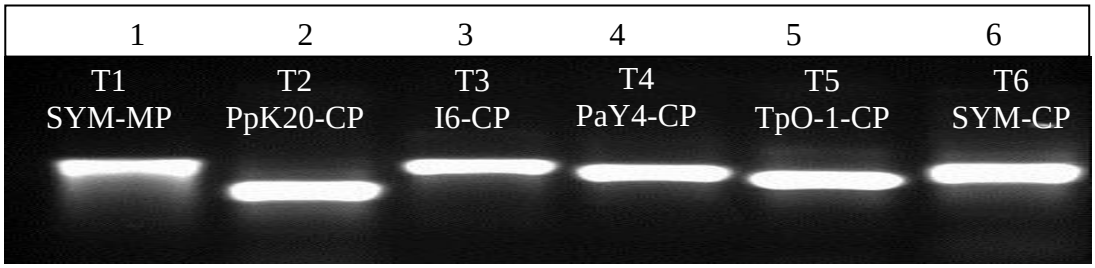

Figure 3.10. Quality of the transcripts for use in the northern blot analysis. Transcript **Lane 1**: T1 (SYM-MP); **Lane 2**: T2 (PpK-20 CP); **Lane 3**: T3 (I6 CP+NCR); **Lane 4**: T4 (PaY4-CP); **Lane 5**:T5 (TpO-1 CP); and **Lane 6**:T6 (SYM-CP).

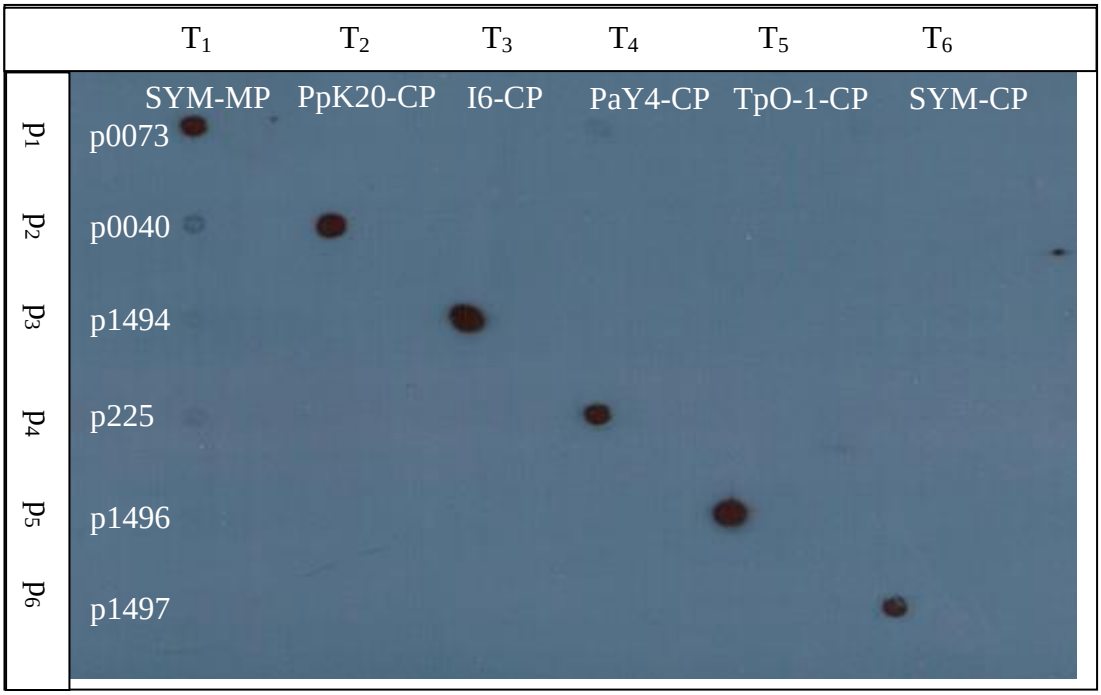

Figure 3.11. Dot-blot hybridization of the SYM-MP and the CP-specific riboprobes. Lanes $T_{1\text{-}6}$ were the labelled transcripts. **Lane T_1**: T1 (SYM-MP); **Lane T_2**: T2 (PpK-20 CP); **Lane T_3**: T3 (I6 CP+NCR); **Lane T_4**: T4 (PaY4-CP); **Lane T_5**: T5 (TpO-1 CP); **Lane T_6**: T6 (SYM-CP). Rows $p_{1\text{-}6}$ were the linearized plasmid-templates. **Row p_1**: p0073 (SYM-MP); **Row p_2**: p0040 (PpK-20 CP); Row **p_3**: p 1494 (I6 CP+NCR); **Row p_4**: p225 (PaY4-CP); **Row p_5**: p1496 (TpO-1 CP); **Row p_6**: p1497 (SYM-CP).

probes) was assessed by the dot-blot hybridization method described in section 2.2.11, sub-section 2. The autoradiograph presented in Fig. 3.11 is the result of a 1 minute exposure of the film to the blot.

The results show that ribo-probe T6 (for the detection of SYM-CP) was relatively weaker in the detection of the target-gene as compared to the other five ribo-probes. However, all the ribo-probes were highly-specific in detecting the targeted genes cloned into the plasmids. In another dot-blot test, none of the ribo-probe reacted with total RNA isolated from healthy *N. benthamiana* plants. Therefore all these ribo-probes were selected for utilization in the northern blotting.

3.5. Systemic accumulation of TRV isolates in the *N. benthamiana* plants

Northern blot analysis has been used previously for evaluation of TRV recombinant isolates (Robinson and Harrison, 1985b). Leaf discs were collected from infected *N. benthamiana* plants (three plants per isolate) and RNA isolation from these samples were done as given in section 2.2.1, sub-section 1.

Robinson *et al.,* (1987) showed by electron microscopy, that in TRV infected leaf-sap the RNA-1 and 2 were found in a 1:10 ratio. This was apparent in the northern-blots in the current studies where a stronger RNA-2 signal was seen as compared to the RNA-1 signal.

Examination at 4 dpi of the systemically-infected leaves of all three plants infected with any of the three TRV isolates containing PpK-20 RNA-2 (SK20, OK20, and KK20, Fig. 3.12) showed that the KK20 isolate had the highest level of viral RNA accumulation (Fig. 3.12, II).

Thus, the KK20 isolate was faster in systemic movement and accumulated to higher levels than the isolates SK20 and OK20. At 8 dpi, the isolate OK20 accumulated to higher levels in 2 out of 3 plants (Lane 9 and 10, Fig. 3.12, III).

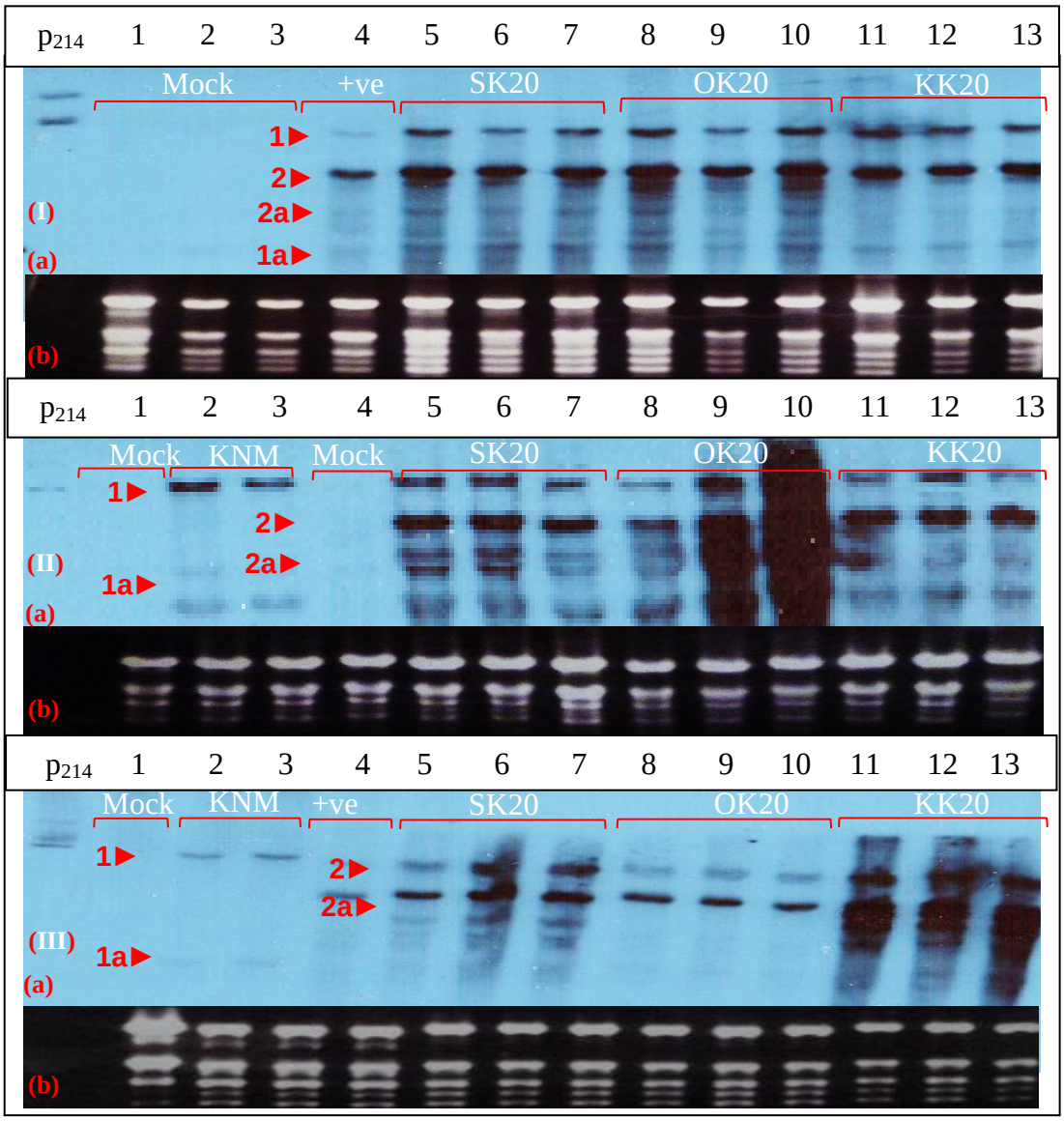

Figure 3.12. Northern blots of the plants inoculated with the TRV isolates comprising PpK-20 RNA-2. Mock-inoculated plants (Lane 1-3, Panel Ia; Lane 1, Panel IIa and Lane 1 and 4, Panel IIIa); Undigested plasmid 214 (Lane p214). Plants inoculated with, PpK-20 infectious sap (positive control, Lane 4, Panel Ia and IIa), PpK20 RNA-1 (Lane 2 and 3, Panel IIa and IIIa), recombinant isolate, SK20 (Lane 5-7 , Panel Ia, IIa, and IIIa); OK20 (Lane 8-10, Panel Ia, IIa, and IIIa), and KK20 (Lane 11-13 Panel Ia, IIa, and IIIa). Samples from the inoculated leaves were collected at 4 dpi (**Panel Ia**) and the systemically infected leaves at 4 dpi (**Panel IIa**) and 8 dpi (**Panel IIIa**). **Panel Ib, IIb, and IIIb** are the gel-images of the ribosomal (r) RNAs of the samples in Panel Ia, IIa, and IIIa, respectively. Arrow-head (▶) indicates the positions of individual TRV-RNA species.

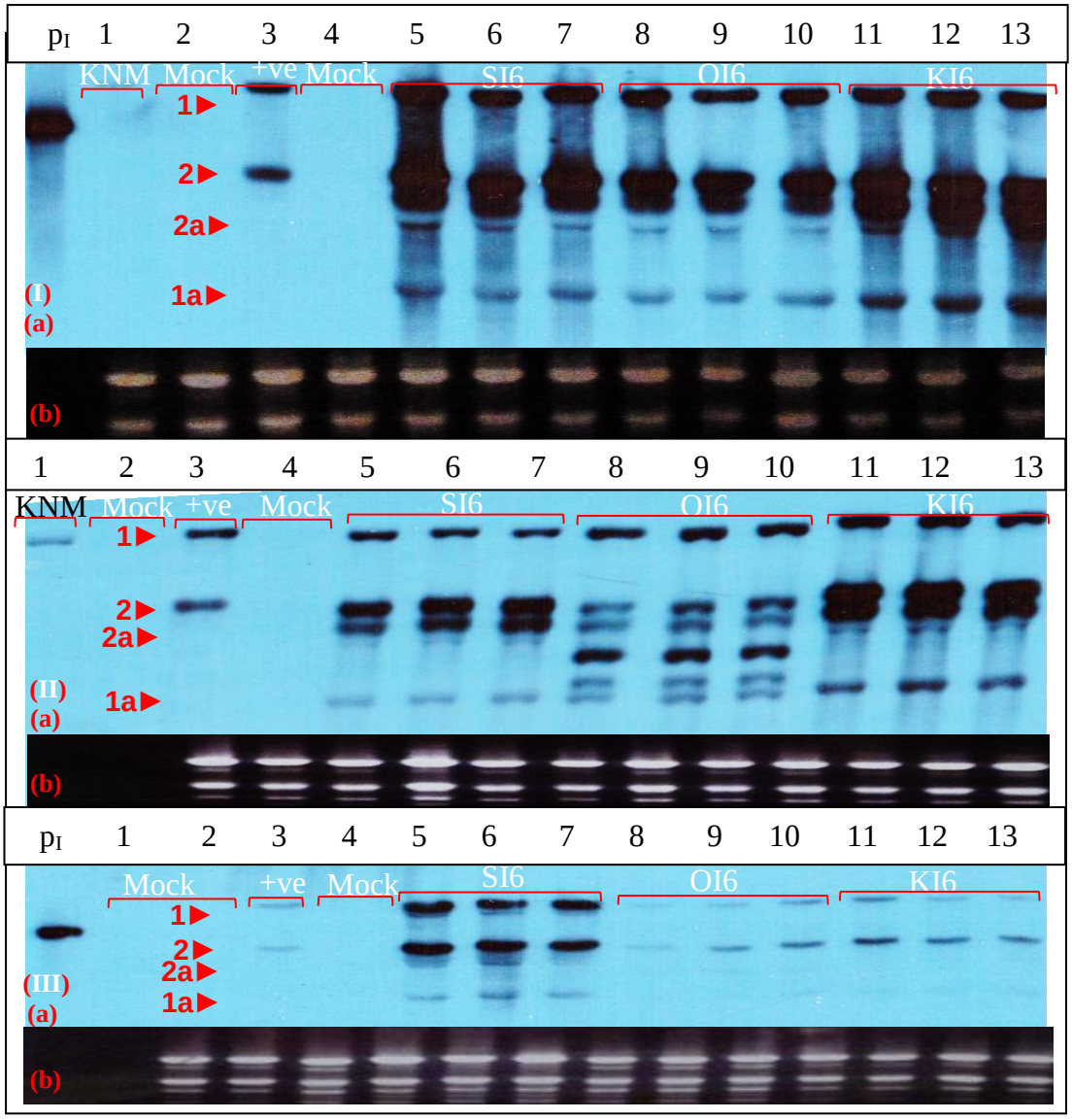

Figure 3.13. Northern blots of the plants inoculated with the TRV isolates comprising I6 RNA-2. Mock-inoculated plants (Lane 2 and 4, Panel Ia and IIa; Lane 1,2 and 4, Panel IIIa); Linearized plasmid 0073 (Lane p_I); Plants inoculated with, I6 infectious sap (positive control, Lane 3, Panel Ia, IIa and IIIa), PpK20 RNA-1 (Lane1, Panel Ia and IIa), recombinant isolate, SI6 (Lane 5-7 , Panel Ia, IIa, and IIIa); OI6 (Lane 8-10, Panel Ia, IIa, and IIIa), and KI6 (Lane 11-13 Panel Ia, IIa, and IIIa). Samples from the inoculated leaves were collected at 4 dpi (**Panel Ia**) and the systemically infected leaves at 4 dpi (**Panel IIa)** and 8 dpi (**Panel IIIa)**. **Panel Ib, IIb, and IIIb** are the gel-images of the ribosomal (r) RNAs of the samples in Panel Ia, IIa, and IIIa, respectively. Arrow-head (▶) indicates the positions of individual TRV-RNA species.

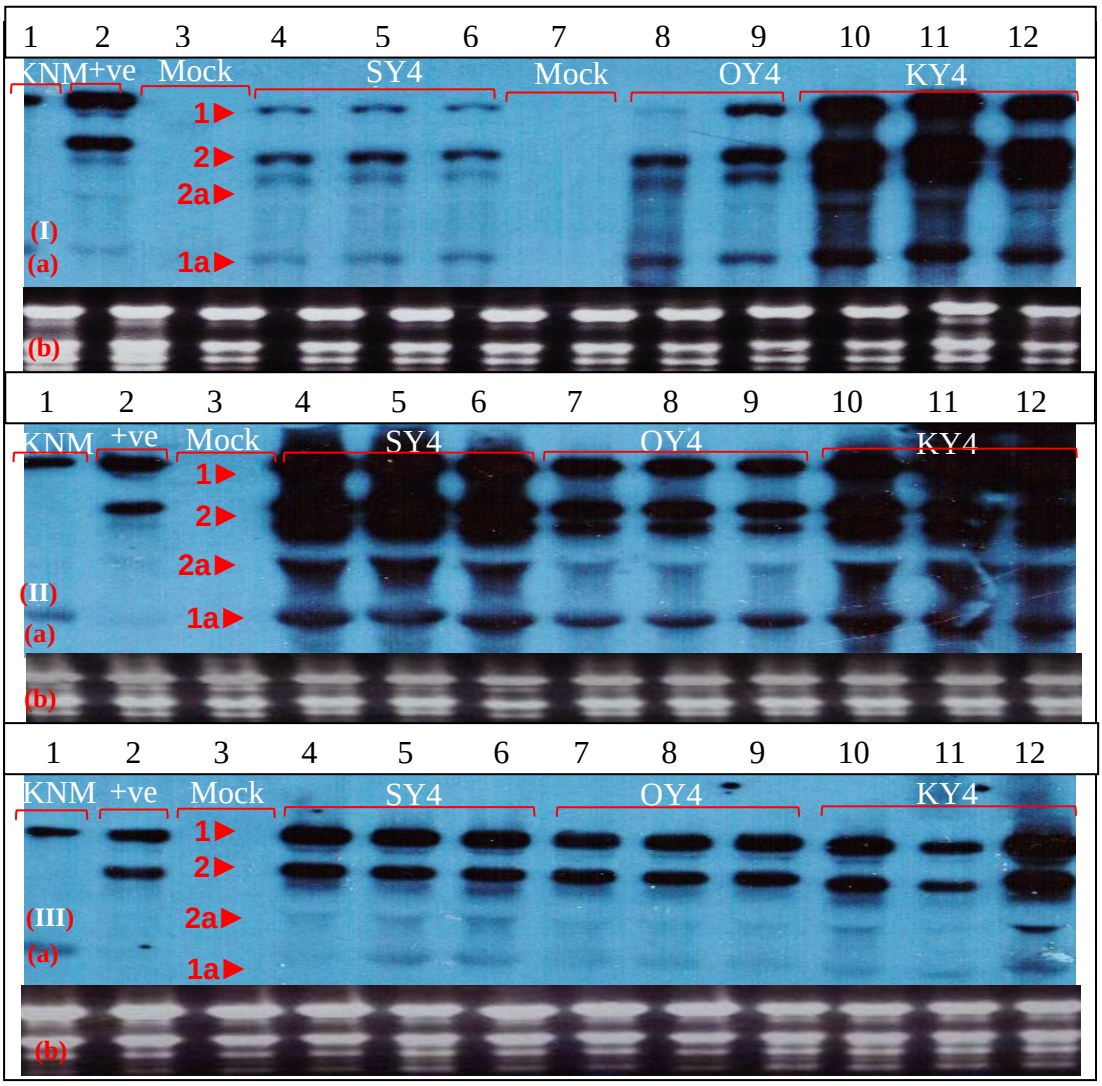

Figure 3.14. Northern blots of the plants inoculated with the TRV isolates comprising PaY4 RNA-2. Mock-inoculated plants (Lane 3 and 7, Panel Ia; Lane 3, Panel IIa and IIIa); Plants inoculated with, PaY4 infectious sap (positive control, Lane 2, Panel Ia, IIa and IIIa), PpK20 RNA-1 (Lane1, Panel Ia, IIa and IIIa), recombinant isolate, SY4 (Lane 4-6 , Panel Ia, IIa, and IIIa); OY4 (Lane 8-9, Panel Ia, Lane 7-9, Panel IIa and IIIa), and KY4 (Lane 11-12Panel Ia, IIa, and IIIa). Samples from the inoculated leaves were collected at 4 dpi (**Panel Ia**) and the systemically infected leaves at 4 dpi (**Panel IIa**) and 8 dpi (**Panel IIIa)**. **Panel Ib, IIb, and IIIb** are the gel-images of the ribosomal (r) RNAs of the samples in Panel Ia, IIa, and IIIa, respectively. Arrow-head (►) indicates the positions of individual TRV-RNA species.

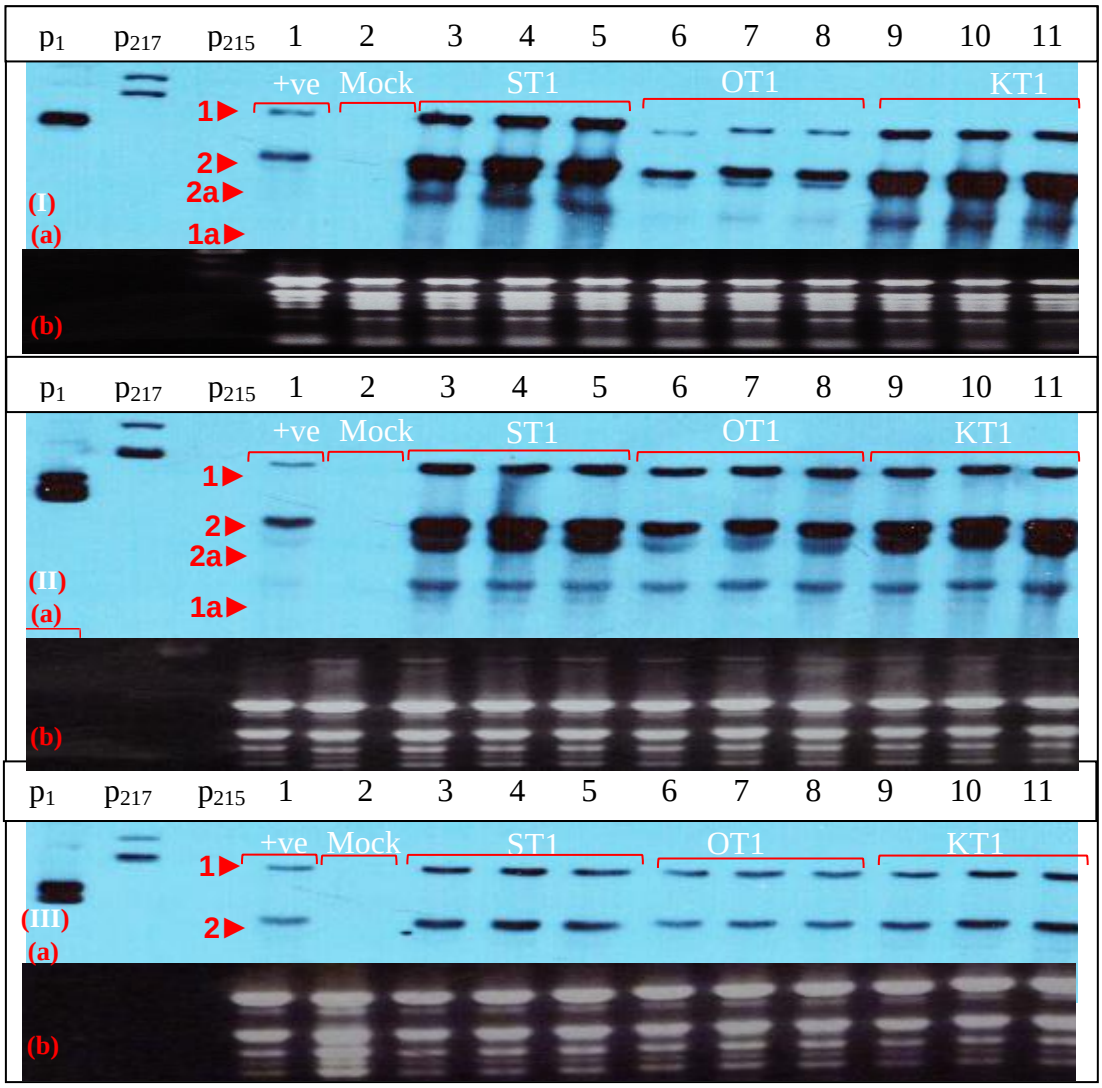

Figure 3.15. Northern blots of the plants inoculated with the TRV isolates comprising TpO1 RNA-2. Mock-inoculated plant (Lane 2 Panel Ia, IIa and IIIa); Linearized plasmid 0073 (Lane p_l); Undigested plasmid 217 (Lane p217) and 215 (Lane p215); Plants inoculated with, TpO1 infectious sap (positive control, Lane 1, Panel Ia, IIa and IIIa), recombinant isolate, ST1 (Lane 3-5 , Panel Ia, IIa, and IIIa); OT1 (Lane 6-8, Panel Ia, IIa and IIIa), and KT1 (Lane 9-11 Panel Ia, IIa, and IIIa). Samples from the inoculated leaves were collected at 4 dpi (**Panel Ia**) and the systemically infected leaves at 4 dpi (**Panel IIa**) and 8 dpi (**Panel IIIa**). **Panel Ib, IIb, and IIIb** are the gel-images of the ribosomal (r) RNAs of the samples in Panel Ia, IIa, and IIIa, respectively. Arrow-head (▶) indicates the positions of individual TRV-RNA species.

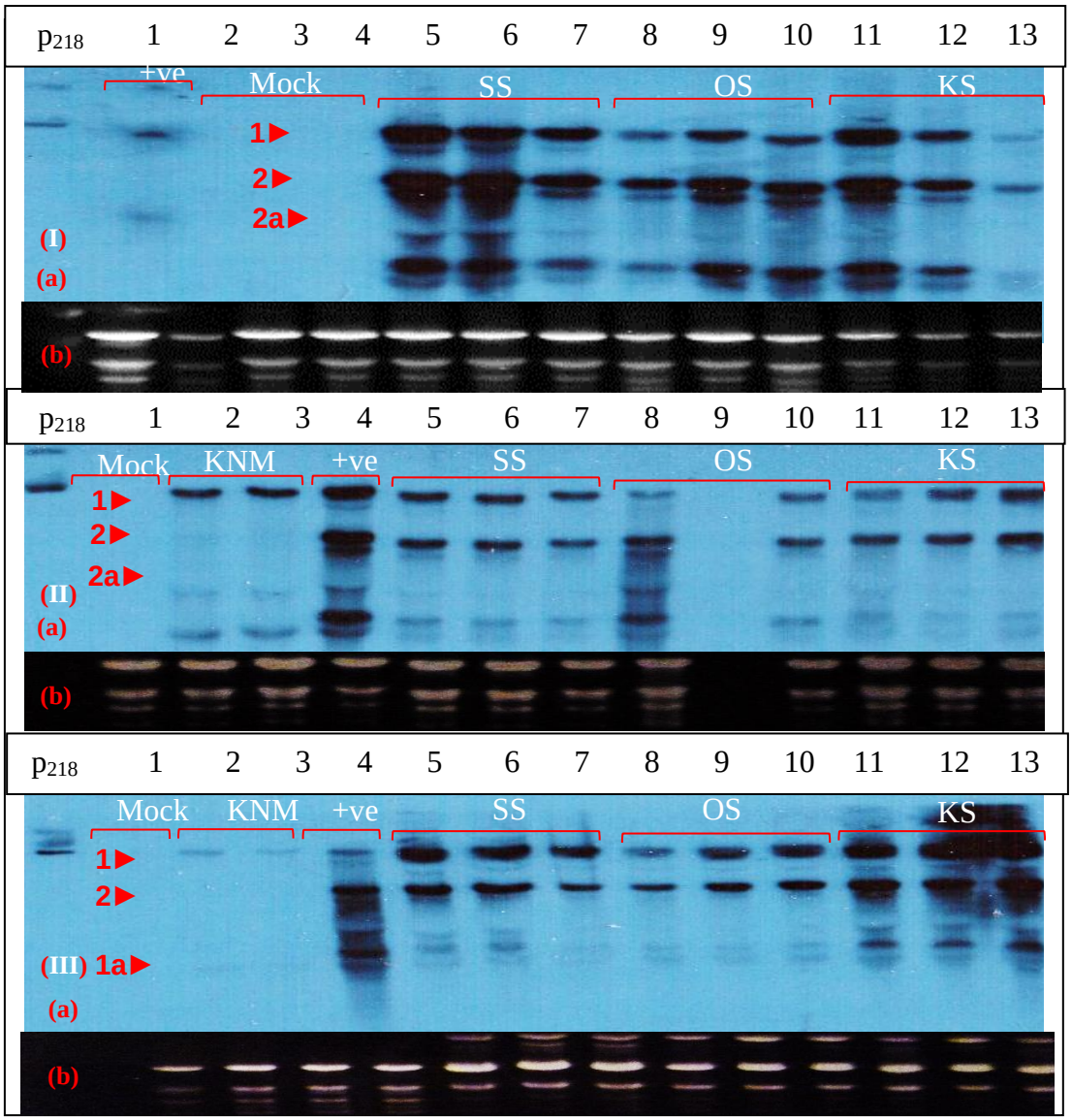

Figure 3.16. Northern blots of the plants inoculated with the TRV isolates comprising SYM RNA-2. Mock-inoculated plants (Lane 2, 3 and 4, Panel Ia, Lane 1, Panel IIa and IIIa); Undigested plasmid 218 (Lane p_{218}, Panel Ia, IIa and IIIa); Plants inoculated with, SYM infectious sap (positive control, Lane 1, Panel Ia, Lane 4, Panel IIa and IIIa), PpK20-RNA-1 (Lane 2 and 3, Panel IIa and IIIa), recombinant isolate, SS (Lane 5-7 , Panel Ia, IIa, and IIIa); OS (Lane 8-10, Panel Ia, IIa and IIIa), and KS (Lane 11-13 Panel Ia, IIa, and IIIa). Samples from the inoculated leaves were collected at 4 dpi (**Panel Ia**) and the systemically infected leaves at 4 dpi (**Panel IIa** and 8 dpi (**Panel IIIa)**. **Panel Ib, IIb, and IIIb** are the gel-images of the ribosomal (r) RNAs of the samples in Panel Ia, IIa, and IIIa, respectively. Arrow-head (▶) indicates the positions of individual TRV-RNA species.

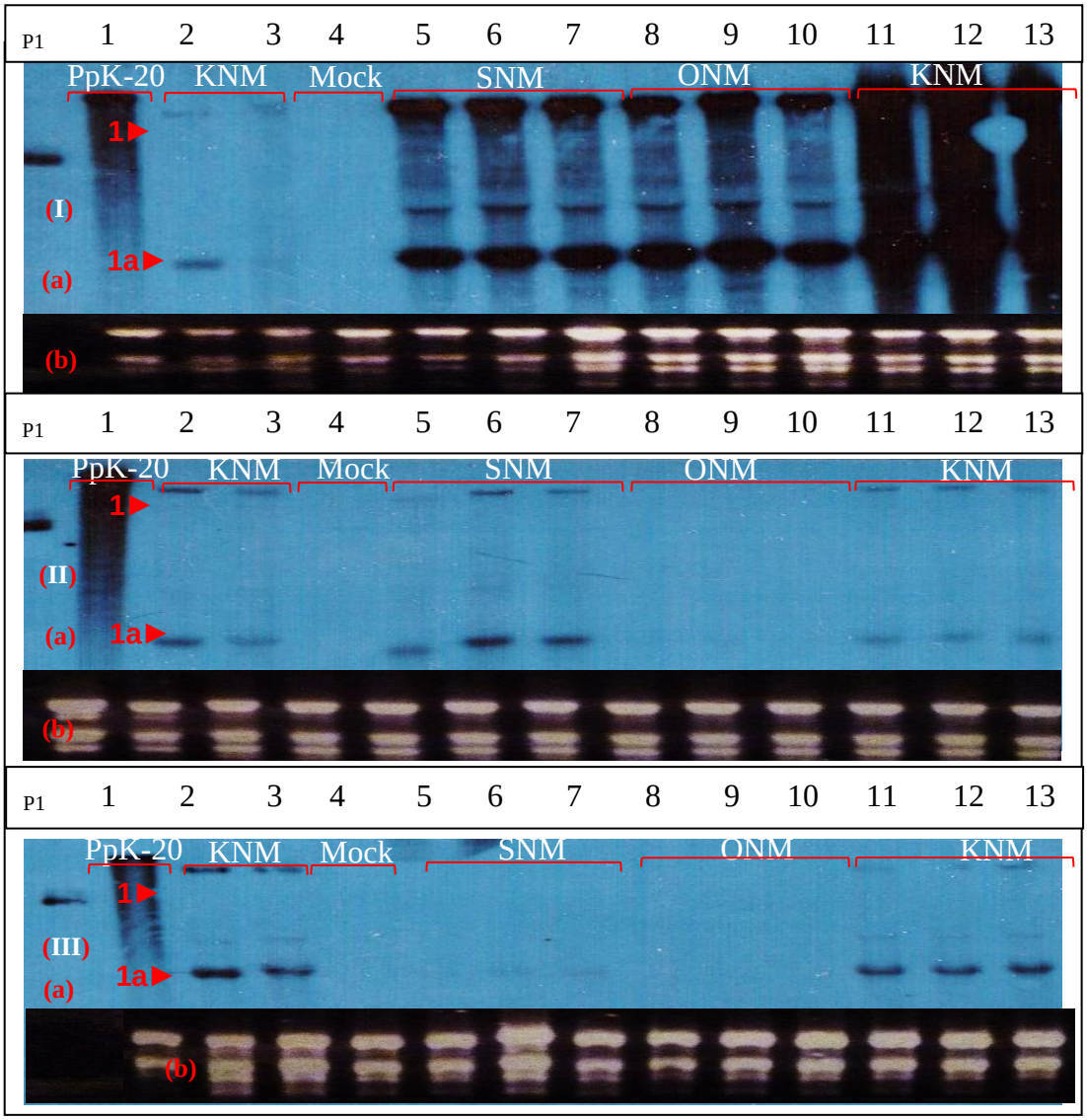

Figure 3.17. Northern blots of the plants inoculated with the TRV RNA-1 isolates. Mock-inoculated plant (Lane 4, Panel Ia, IIa and IIIa); Linearized plasmid 0073 (Lane p_1, Panel Ia, IIa and IIIa); Plants inoculated with, PpK-20 infectious sap (positive control, Lane 1, Panel Ia, IIa and IIIa), PpK-20 RNA-1 (KNM, Lane 2 and 3, Panel Ia,IIa and IIIa); RNA-1 isolate, SNM (Lane 5-7 , Panel Ia, IIa, and IIIa); ONM (Lane 8-10, Panel Ia, IIa and IIIa), and KNM (Lane 11-13 Panel Ia, IIa, and IIIa). Samples from the inoculated leaves were collected at 4 dpi (**Panel Ia**) and the systemically infected leaves at 4 dpi (**Panel IIa**) and 8 dpi (**Panel IIIa)**. **Panel Ib, IIb, and IIIb** are the gel-images of the ribosomal (r) RNAs of the samples in Panel Ia, IIa, and IIIa, respectively. Arrow-head (►) indicates the positions of individual TRV-RNA species.

However, analysis of the three recombinant isolates containing I6 RNA-2 (SI6, OI6, and KI6, Fig. 3.13) showed that at 4 dpi the isolate KI6 accumulated to higher levels in the inoculated- and the systemically-infected leaves of all three plants (Lane 11 - 13, Fig. 3.13, I, and II, respectively) as compared to the isolates SI6 and OI6. But at 8 dpi the isolate SI6, accumulated to higher levels in the systemically-infected leaves (Lane 11 -13, Fig. 3.13, III).

For the three recombinant isolates containing PaY4 RNA-2 (SY4, OY4, and KY4, Fig. 3.14) at 4 dpi KY4 accumulated to higher levels than the other two isolates (Lane 10 -12, Fig. 3.14, I and II). But at 8 dpi all these three isolates (SY4, OY4, and KY4, Fig. 3.14, III) accumulated to almost equal levels in the top, systemically-infected leaves.

Northern blot analysis of the plants infected with the recombinant isolates containing TpO1 RNA-2 (ST1, OT1, and KT1), SYM RNA-2 (SS, OS, and KS) and the RNA-1 isolates (SNM, ONM, and KNM) is presented in figures 3.15-3.17. In general, the PpO-85 RNA-1 accumulated to lower levels than the PpK-20 or SYM RNA-1s, regardless of whether this was RNA-1 only (NM) infections or RNA-1+RNA-2 (M) infections (Lane 10 -12, Fig. 3.17, I and II).

3.6. Infection of TRV isolates in tetraploid potatoes

Mostly the TRV infection studies in the past were conducted in *N. benthamiana* plants and other glasshouse plants. In the current studies, I have examined TRV infection in tetraploid potatoes. Two cultivars from the spraing reactant or TRV sensitive group (c.vs. Maris Bard and Pentland Dell), three cultivars from the tolerant or TRV susceptible group (c.vs. Shepody, Saxon and Wilja), and one cultivar from the TRV resistant group (i.e.; Bintje) were included in the studies (see details in section 1.8.). Apical-stem cuttings were mechanically inoculated at 10 days post planting and the RT-PCR evaluation of the infection was done as described in section 2.2.16.

3.6.1. Local symptoms induced by the TRV isolates

The potato leaves displayed genotype-specific symptoms. The symptomatological observations were recorded during the winter season (short day length period). In the summer season (longer day length period), the symptoms were either masked or erratic. The TRV recombinant isolates comprising I6 RNA-2 (i.e; SI6, OI6, and KI6) produced milder symptoms or remained asymptomatic and were also found to be the least pathogenic among all the fifteen recombinant isolates. Robinson *et al*. (1987) had also reported the I6 isolate to produce milder symptoms on *N. clevelandii* plants. Among all the 15 recombinant isolates, the PpK-20 RNA-2 containing isolates (SK20, OK20 and KK20) were more severe in symptom production and amongst these three, the KK20 isolate was found to be the most pathogenic (virulent). Representative foliar symptoms induced by the KK20 isolate on all the six potato cultivars are presented in figure 3.18. Observations were recorded at 5 dpi.

Among the TRV-sensitive cultivars a mixture of the characteristic symptoms of annulus-like and disc-shaped necrotic lesions was produced on the inoculated leaves of Pentland Dell (Fig. 3.18, a). Cadman (1959) had described similar TRV-induced symptoms on the leaves of a tobacco (*N. tabacum* var. White Burley) plant. The non-inoculated leaves were either asymptomatic or displayed mild leaf-distortion and the mock-inoculated leaves remained asymptomatic (Fig. 3.18, b). However, the inoculated leaves of Maris Bard displayed ‘‘spreading necrosis’’ and ‘‘yellowing’’; and the systemic necrosis progressively reached to the mid-vein of the leaf and the stem (Fig. 3.18, c). The inoculated leaves died within 7-10 dpi. Similar symptoms were reported on the leaves of the cultivar Russet Burbank when inoculated with the infectious leaf-sap of TRV-DsRed, an engineered PpK20 isolate (Ghazala and Varrelmann, 2007). The TRV-resistant cv. Bintje displayed small necrotic-lesions on the inoculated leaves (Fig. 3.18, k) that resembled the HR-like response, reported by Ghazala and Varrelmann (2007). The non-inoculated and mock-inoculated foliage was asymptomatic (Fig. 3.18, l). However, in some instances in virus infected plants,

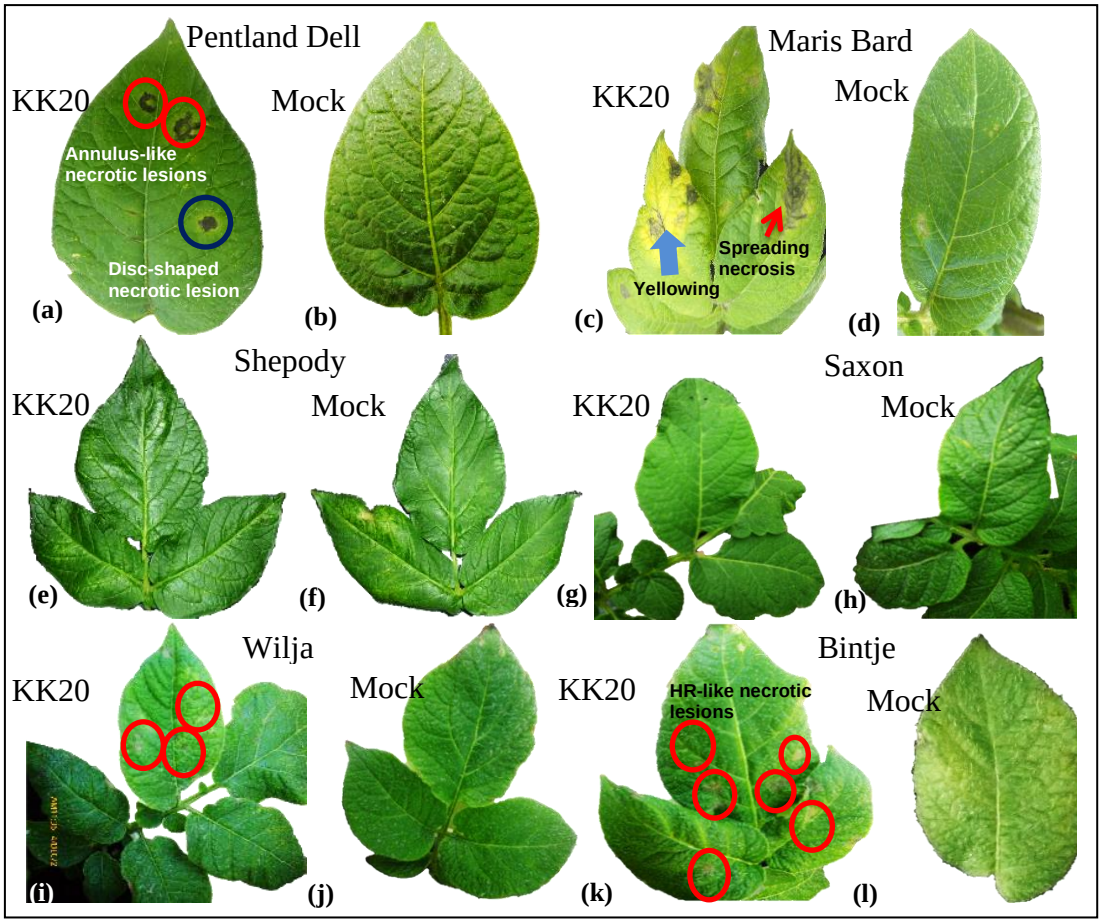

Figure 3.18. Foliar symptoms induced by KK20 isolate on various cultivars of tetraploid potato. KK20 inoculated leaves of c.v. **(a)** Pentland Dell, exhibiting typical annulus-like (encircled red) and disc-shaped (encircled blue) necrotic lesions, **(c)** Maris Bard, displaying ‘‘spreading necrosis’’ (red-arrow) and ‘‘yellowing’’ (blue-arrow), **(e)** Shepody, asymptomatic, **(g)** Saxon, asymptomatic, **(i)** Wilja and **(k)** Bintje, both exhibiting HR-like necrotic lesions, (encircled red). Mock-inoculated and asymptomatic leaves **(b, d, f, h, j, and l)** of a, c, e, g, i, and k**,** respectively. Leaves were rub-inoculated with the infectious sap of KK20 recombinant isolate. Pictures were taken at 5 dpi.

systemic necrosis progressing along the petiole to the stem was also observed.

Among the TRV-susceptible cultivars, the inoculated, non-inoculated and mock-inoculated leaves of both Shepody and Saxon, remained asymptomatic (Fig. 3.18, e-h). However, one of the three plants of the cultivar Wilja produced small HR-like necrotic lesions on the inoculated leaves. Whereas, the non-inoculated and the mock-inoculated leaves were asymptomatic (Fig. 3.18, i-j).

3.6.2. Systemic infection of TRV isolates in potato

The symptoms induced by the TRV recombinant isolates on some of the potato plants were not extensive or apparent. The systemic movement of the virus, from the inoculated to the top-most non-inoculated leaves of the plant, was investigated by RT-PCR (section 2.2.16). These studies were conducted during the summer season. The amplification of the potato reference gene, EF-1α, was also assessed to confirm the integrity of the RNA preparation from each test sample. An overview of this diagnostic test is given in Table No. 3.4.

The TRV RNA-2 of all the 15 recombinant isolates was detected in the inoculated leaves of Maris Bard (Fig. 3.19, I, d) but the TRV RNA-1 from the same potato samples was not detectable (c) by using the 16K gene flanking primer-set (DJR16K primer-set). Rather a smeared pattern of TRV1 amplification was observed in all the potato samples collected at 5, 15 and 30 dpi (I, II, III, c). However, the same primer-set successfully amplified the 16K gene from the *N. benthamiana* positive control samples. At 15 dpi, the RNA-2 of the I6 isolate was detected in the non-inoculated leaf-samples of the plants inoculated with the SI6, OI6 and KI6 isolates (I6 RNA-2 containing recombinant isolates) and in one sample, each, of the plants inoculated with OT1 (TpO1 RNA-2) and OS (SYM RNA-2). The detection of RNA-2 in these non-inoculated leaves confirmed the systemic infection of Maris Bard potato by these viruses (Fig. 3.19, II, d). At 30dpi, besides the detection of I6 RNA-2, TpO1 RNA-2 from all the three isolates (ST1, OT1 and KT1), and SYM RNA-2 from one

sample (SS) were also detected from the top non-inoculated leaves (Fig. 3.19, III, d). The SYM RNA-2 of the OS isolate, previously detected at 15 dpi, could not be detected at 30 dpi from the top, non-inoculated leaves of the same plants. The reference gene (Ef-1α) was amplified from all these samples, confirming the integrity of the RNA preparations. This detection of RNA-2 from the systemically-infected leaves, but not the RNA-1 encoded 16K gene, suggested that it was necessary to change the RNA-1-specific primer-set in further diagnostic tests. RNA-1 must be present in tissue where RNA-2 has accumulated.

The RNA-2 was also detected (at 5 dpi) in Wilja plants inoculated with SK20, OK20, and KK20 (isolates containing PpK20 RNA-2), SS, OS, and KS (isolates containing SYM RNA-2) and the I6 RNA-2 isolates. However, the detection of SYM RNA-2s was weaker than that of the RNA-2 of the other isolates. No RNA-2 could be detected in any of the Wilja plants inoculated with isolates containing PaY4 and TpO1 RNA-2 (Fig. 3.20, I, d). At 15 dpi and 30 dpi in non-inoculated leaves (II, III), the RNA-2 was detected only from plants inoculated with I6 RNA-2 containing isolates (IId, IIId). In this case, the RNA1 also could not be amplified from any of these samples (IIc, IIIc).

Both the RNA-1 and -2 of all fifteen recombinant isolates were amplified, at 5 dpi, from the inoculated leaves of Bintje (Fig. 3.21, I, c, d). At 15 dpi, the RNA-2 was detected in one sample of the non-inoculated leaves from plants inoculated with the SK-20 isolate (containing PPK-20 RNA-2), two samples of the plants inoculated with SS, and KS isolates (containing SYM RNA-2, II, d) and all three plants inoculated with the I6 RNA-2 isolates. The RNA-1 was detected (II, c) from almost all samples. At 30 dpi, the RNA-2 was detected from all three systemic leaf samples of plants inoculated with the I6 RNA-2 containing isolates and one of the plants (ST1) inoculated with the TpO1 RNA-2 comprising isolate. The RNA-1 was amplified from all of the plants that tested positive for the RNA-2.

Table 3.4. Overview of RT-PCR evaluation of tetraploid potatoes inoculated with various TRV isolates, at 30 dpi.

Sr. No.	Potato Cultivar	Gene Amplification	TRV- isolates containing														
			PpK-20 RNA-2			I6 RNA-2			PaY4 RNA-2			TpO1 RNA-2			SYMRNA-2		
			SK20	OK20	KK20	SI6	OI6	KI6	SY4	OY4	KY4	ST1	OT1	KT1	SS	OS	KS
1.	M.B	TRV1	×	×	×	×	×	×	×	×	×	×	×	×	×	×	×
		TRV2	×	×	×	√	√	√	×	×	×	√	√	√	√	×	×
		Ef-1α	√	√	√	√	√	√	√	√	√	√	√	√	√	√	√
2.	P.D	TRV1	--	--	×	--	--	×	--	--	×		--	×	--	--	×
		TRV2	--	--	×	--	--	√	--	--	×	--	--	×	--	--	×
		Ef-1α	--	--	√	--	--	√	--	--	√	--	--	√	--	--	√
3.	Bintje	TRV1	√	×	×	√	√	√	×	×	√	√	√	×	√	×	×
		TRV2	×	×	×	√	√	√	×	×	×	×	×	×	×	×	×
		Ef-1α	√	√	√	√	√	√	√	√	√	√	√	√	√	√	√
4.	Wilja	TRV1	×	×	×	×	×	×	×	×	×	×	×	×	×	×	×
		TRV2	×	×	×	√	√	√	×	×	×	×	×	×	×	×	×
		Ef-1α	√	√	√	√	√	√	√	√	√	√	√	√	√	√	√
5.	Saxon	TRV1	--	--	√	--	--	√	--	--	√	--	--	√	--	--	√
		TRV2	--	--	×	--	--	√	--	--	×	--	--	×		--	×
		Ef-1α	--	--	√	--	--	√	--	--	√	--	--	√	--	--	√
6.	Shepody	TRV1	--	--	√	--	--	√	--	--	√	--	--	√	--	--	√
		TRV2	--	--	×	--	--	√	--	--	×	--	--	×	--	--	×
		Ef-1α	--	--	√	--	--	√	--	--	√	--	--	√	--	--	√

M.B: Maris Bard; P.D: Pentland Dell; TRV1: Tobacco rattle virus-replicase gene or Movement protein; Ef-1α: House-keeping Elongation-factor -1 α; √: Detection; ×: No detection; --: Not tested. The presented results are of RT-PCR detection at 30dpi from the top-most non-inoculated leaves.

The TRV recombinant isolates containing PpK-20 RNA-1 (especially the KK20 isolate), were found to be more aggressive, virulent in pathogenicity and symptom production. Therefore, the rest of the investigations were carried-out focusing on PpK-20 RNA-1 containing isolates. Thus, the cultivars Pentland Dell, Saxon and Shepody mechanically inoculated with the TRV isolates containing PpK20 RNA-1 and each of the five different RNA-2s (KK20, KI6, KY4, KT1, and KS) were analysed. The RNA-2 of all five isolates was detected from the inoculated leaf

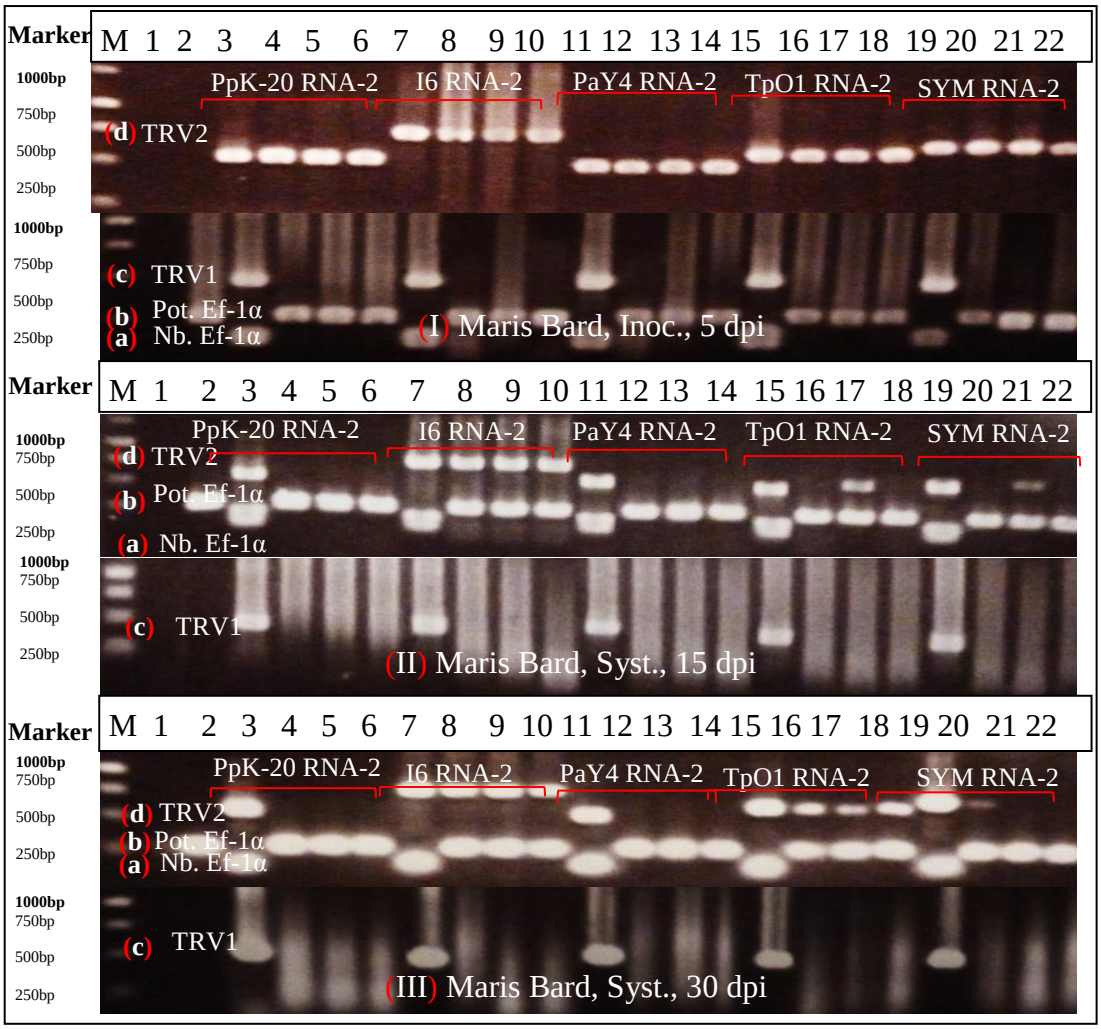

Figure 3.19. RT-PCR evaluation of the systemic infection of TRV isolates in Maris Bard. Lane M: 1Kb Promega DNA marker; **Lane 1**: NTC, Non template control; **Lane 2**: Mock inoculated Maris Bard. Plants inoculated with recombinant isolate containing **Lane 3-6**: PpK-20 RNA-2, Lane 3: KK20, Lane 4: SK20, Lane 5: OK20, Lane 6: KK20; **Lane 7-10**: I6 RNA-2, Lane 7: KI6, Lane 8: SI6, Lane 9: OI6, Lane 10:KI6; **Lane 11-14**: PaY4 RNA-2, Lane 11: KY4, Lane 12: SY4, Lane13: OY4, Lane 14:KY4; **Lane 15-18:** TpO1 RNA-2, Lane 15: KT1, Lane 16: ST1, Lane 17: OT1, Lane 18:KT1; **Lane 19-22**: SYM RNA-2, Lane 19: KS, Lane 20: SS, Lane 21: OS, Lane 22:KS. Samples were collected at 5 dpi from inoculated leaves **(Panel I),** and at 15 dpi **(Panel II),** and 30 dpi **(Panel III)** from systemically infected leaves. *N. benthamiana* samples (Lane 3, 7, 11, 15 and 19) were collected at 5 dpi from non-inoculated leaves. House-keeping, Ef-1α, amplicon from (**a**) *N. benthamiana* (150 bp) and (**b**) potato (255 bp). (**c**) TRV1 16K amplicon (463 bp) and (**d**) TRV2 amplicons of PpK20 RNA-2 (540 bp), I6 RNA-2 (751 bp), PaY4 RNA-2 (503 bp), TpO-1 RNA-2 (591 bp), and SYM RNA-2 (650 bp), respectively.

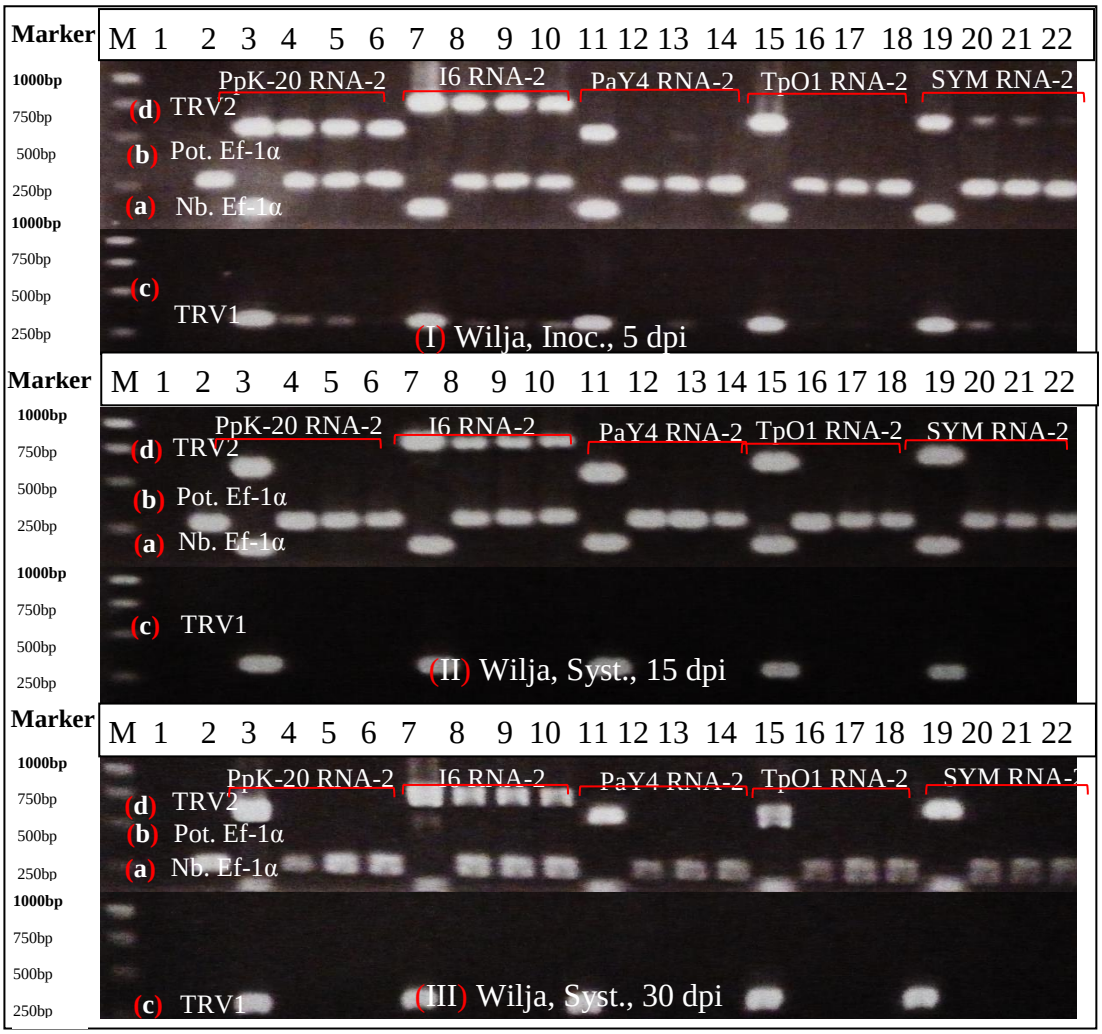

Figure 3.20. RT-PCR evaluation of the systemic infection of TRV isolates in Wilja. Lane M: 1Kb Promega DNA marker; **Lane 1**: NTC, Non template control; **Lane 2**: Mock inoculated Wilja. Plants inoculated with recombinant isolate containing **Lane 3-6**: PpK-20 RNA-2, Lane 3: KK20, Lane 4: SK20, Lane 5: OK20, Lane 6: KK20; **Lane 7-10**: I6 RNA-2, Lane 7: KI6, Lane 8: SI6, Lane 9: OI6, Lane 10:KI6; **Lane 11-14**: PaY4 RNA-2, Lane 11: KY4, Lane 12: SY4, Lane13: OY4, Lane 14:KY4; **Lane 15-18:** TpO1 RNA-2, Lane 15: KT1, Lane 16: ST1, Lane 17: OT1, Lane 18:KT1; **Lane 19-22**: SYM RNA-2, Lane 19: KS, Lane 20: SS, Lane 21: OS, Lane 22:KS. Samples were collected at 5 dpi from inoculated leaves **(Panel I),** and at 15 dpi **(Panel II),** and 30 dpi **(Panel III)** from systemically infected leaves. *N. benthamiana* samples (Lane 3, 7, 11, 15 and 19) were collected at 5 dpi from non-inoculated leaves. House-keeping, Ef-1α, amplicon from (**a**) *N. benthamiana* (150 bp) and (**b**) potato (255 bp). (**c**) TRV1 MP amplicon (318 bp) and (**d**) TRV2 amplicons of PpK20 RNA-2 (540 bp), I6 RNA-2 (751 bp), PaY4 RNA-2 (503 bp), TPO-1 RNA-2 (591 bp), and SYM RNA-2 (650 bp), respectively.

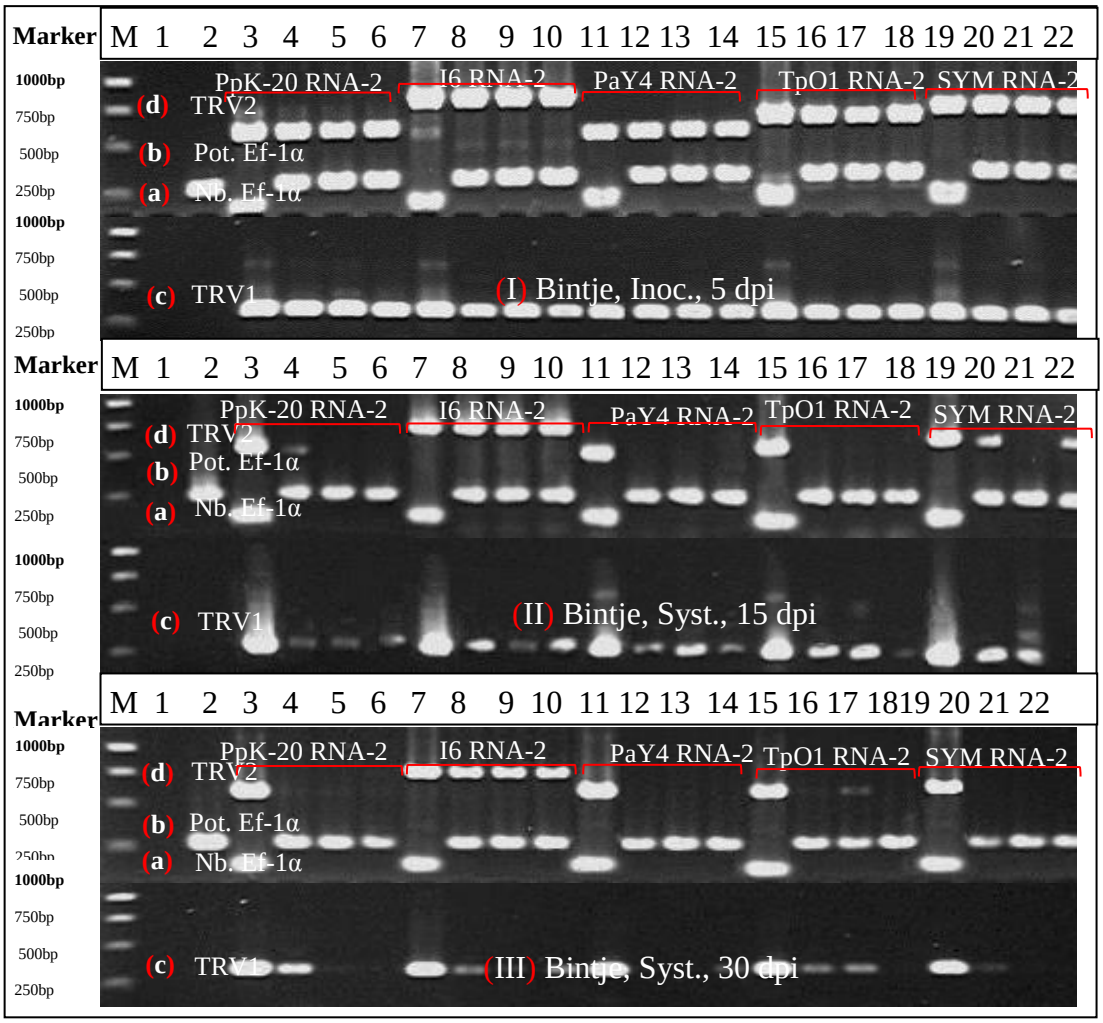

Figure 3.21. RT-PCR evaluation of the systemic infection of TRV isolates in Bintje. Lane M: 1Kb Promega DNA marker; **Lane 1**: NTC, Non template control; **Lane 2**: Mock inoculated Bintje. Plants inoculated with recombinant isolate containing **Lane 3-6**: PpK-20 RNA-2, Lane 3: KK20, Lane 4: SK20, Lane 5: OK20, Lane 6: KK20; **Lane 7-10**: I6 RNA-2, Lane 7: KI6, Lane 8: SI6, Lane 9: OI6, Lane 10:KI6; **Lane 11-14**: PaY4 RNA-2, Lane 11: KY4, Lane 12: SY4, Lane13: OY4, Lane 14:KY4; **Lane 15-18:** TpO1 RNA-2, Lane 15: KT1, Lane 16: ST1, Lane 17: OT1, Lane 18:KT1; **Lane 19-22**: SYM RNA-2, Lane 19: KS, Lane 20: SS, Lane 21: OS, Lane 22:KS. Samples were collected at 5 dpi from inoculated leaves **(Panel I),** and at 15 dpi **(Panel II),** and 30 dpi **(Panel III)** from systemically infected leaves. *N. benthamiana* samples (Lane 3, 7, 11, 15 and 19) were collected at 5 dpi from non-inoculated leaves. House-keeping, Ef-1α, amplicon from (**a**) *N. benthamiana* (150 bp) and (**b**) potato (255 bp). (**c**) TRV1 MP amplicon (318 bp) and (**d**) TRV2 amplicons of PpK20 RNA-2 (540 bp), I6RNA-2 (751 bp), PaY4 RNA-2 (503 bp), TPO-1 RNA-2 (591 bp), and SYM RNA-2 (650 bp), respectively.

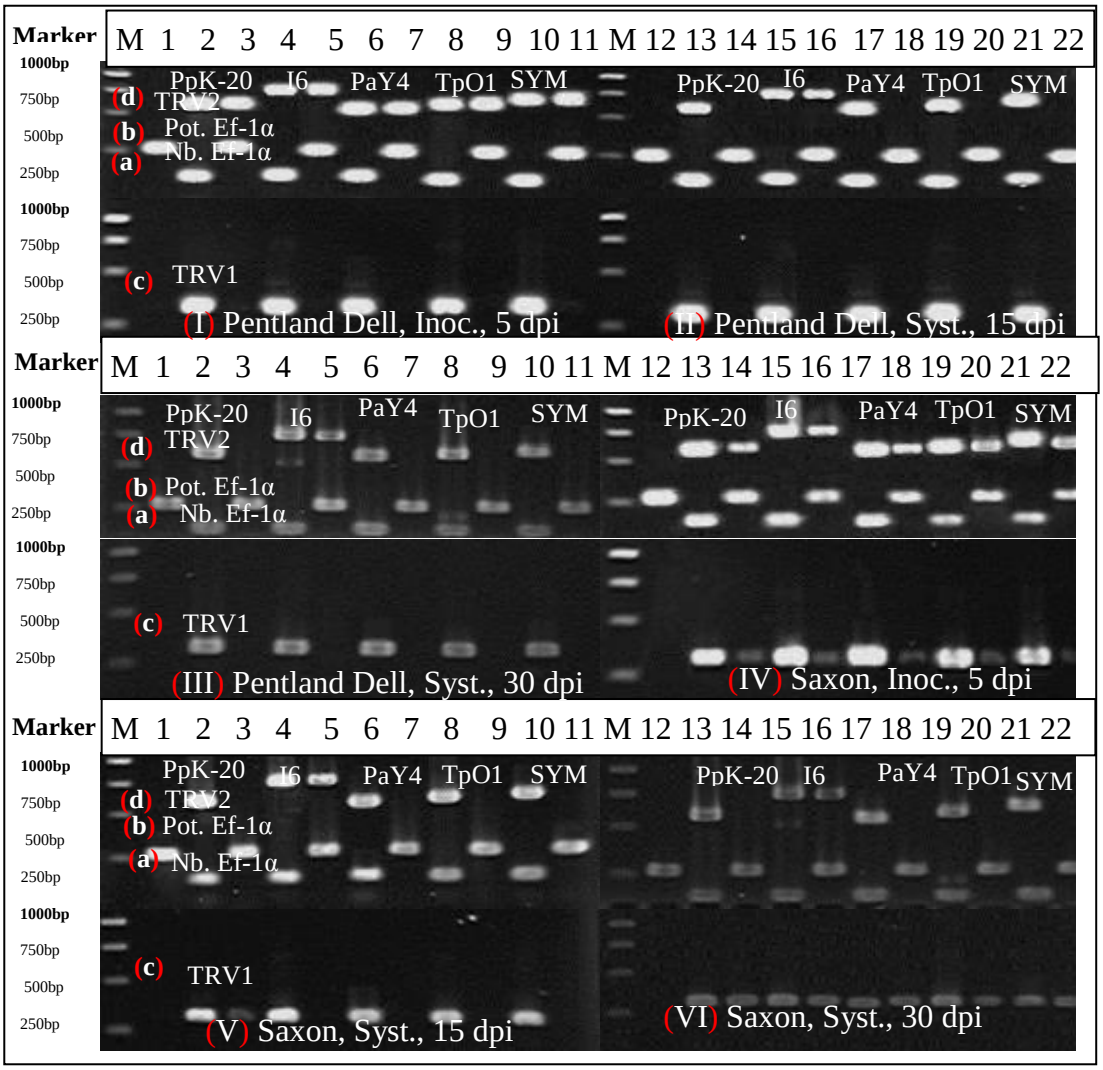

Figure 3.22. RT-PCR evaluation of the systemic infection of TRV isolates in Pentland Dell and Saxon. Lane M: 1Kb Promega DNA marker; **Lane 1 and 12**: Mock inoculated Pentland Dell (Panel I, II, and III) and Saxon (Panel IV, V, and VI). Plants inoculated with recombinant isolate containing **Lane 2-3, 13-14**: PpK-20 RNA-2, KK20; **Lane 4-5, 15-16**: I6 RNA-2, KI6; **Lane 6-7, 17-18**: PaY4 RNA-2, KY4; **Lane 8-9, 19-20:** TpO1 RNA-2, KT1; **Lane 10-11, 21-22**: SYM RNA-2, KS. Samples were collected at 5 dpi from inoculated leaves **(Panel I, and IV),** and at 15 dpi **(Panel II and V),** and 30 dpi **(Panel III and VI)** from systemically infected leaves. *N. benthamiana* samples (Lane 2, 4, 6, 8, 10, 13, 15, 17, 19 and 21) were collected at 5 dpi from non-inoculated leaves. House-keeping, Ef-1α, amplicon from (**a**) *N. benthamiana* (150 bp) and (**b**) potato (255 bp). (**c**) TRV1 MP amplicon (318 bp) and (**d**) TRV2 amplicons of PpK20 RNA-2 (540 bp), I6 RNA-2 (751 bp), PaY4 RNA-2 (503 bp), TPO-1 RNA-2 (591 bp), and SYM RNA-2 (650 bp), respectively.

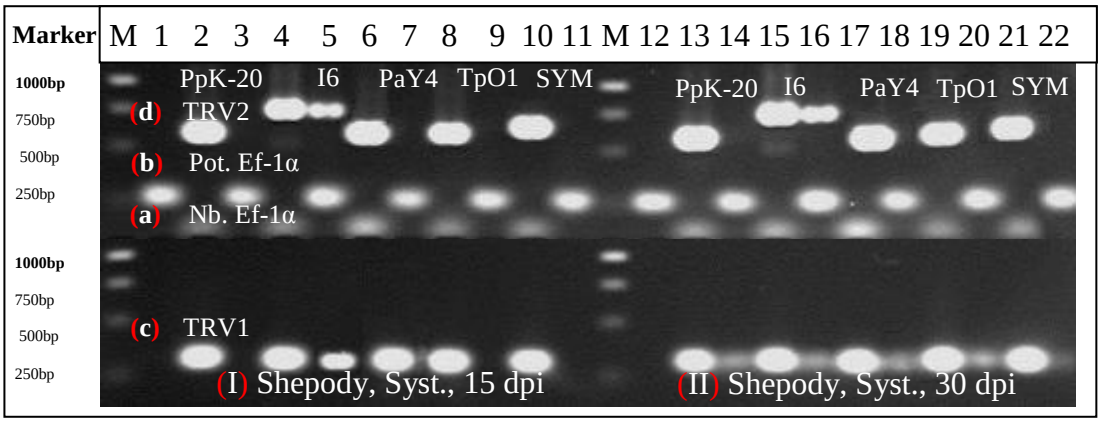

Figure 3.23. RT-PCR evaluation of the systemic infection of TRV isolates in Shepody. Lane M: 1Kb Promega DNA marker; **Lane 1, and 12:** Mock inoculated Shepody. Plants inoculated with recombinant isolate containing **Lane 2-3, 13-14**: PpK-20 RNA-2, KK20; **Lane 4-5, 15-16**: I6 RNA-2, KI6; **Lane 6-7, 17-18:** PaY4 RNA-2, KY4; **Lane 8-9, 19-20:** TpO1 RNA-2, KT1; **Lane 10-11, 21-22**: SYM RNA-2, KS. Samples were collected at 15 dpi (**Panel I**), and at 30 dpi **(Panel II)** from systemically infected leaves. *N. benthamiana* samples (Lane 2, 4, 6, 8 and 10, **Panel)** and (Lane 13, 15, 17, 19 and 21, **PanelI**) were collected at 5 dpi from systemically infected leaves. House-keeping, Ef-1α, amplicon from **(a)** *N. benthamiana* (150 bp) and **(b)** potato (255 bp). **(c)** TRV1 MP amplicon (318 bp) and **(d)** TRV2 amplicons of PpK20 RNA-2 (540 bp), I6 RNA-2 (751 bp), PaY4 RNA-2 (503 bp), TPO-1 RNA-2 (591 bp), and SYM RNA-2 (650 bp), respectively.

samples (collected at 5 dpi) of Pentland Dell and Saxon (Fig. 3.22, Id, and IVd). The RNA-1 was not detected from the inoculated leaves of Pentland Dell. However, it was detected from most of the inoculated leaves of Saxon (Ic, and IVc). At 15 and 30 dpi, the RNA-2 was only detected from the non-inoculated leaf samples of the plants inoculated with the isolates comprising I6 RNA-2 (IIc, IIIc, Vc and VIc).

Similarly, I6 RNA was detected, at 15 and 30 dpi, from the non-inoculated leaves of Shepody plants infected with the recombinant isolate KI6 (Fig. 3.23). The RNA-1 (c) was detected from all the samples infected with KI6, at 15 dpi (II) and 30 dpi (III).

3.6.3. Assessment of the tubers harvested from mechanically-inoculated plants

The plants in section 3.6.2 (foliage-inoculation) were allowed to grow and tuberize. Tubers were harvested, washed with tap-water, dried on paper-towels and diced in cross-section to observe for any noticeable symptom-production. The aim of this investigation was to examine whether TRV inoculated to the leaves moved to the tubers and could induce spraing disease.

The RT-PCR detection of the KI6 isolate in the top, non-inoculated leaves indicated systemic movement of the virus in these plants. The tubers harvested from both KI6-infected and mock-inoculated plants were examined for the spraing symptoms (Fig. 3.24). Not many tubers were produced during these experiments and the Shepody did not tuberize. Some variation was found for the tuber size and shape (a-e). However, it was not determined in the current studies that whether these abnormalities were solely due to the effect of virus or to the growth conditions of the inoculated plants. The symptoms were more obvious on the tubers harvested from Wilja plants. One of the three Pentland Dell tubers had an internal symptom similar to spraing (f). All the infected and mock-inoculated tubers of the other cultivars were spraing-free.

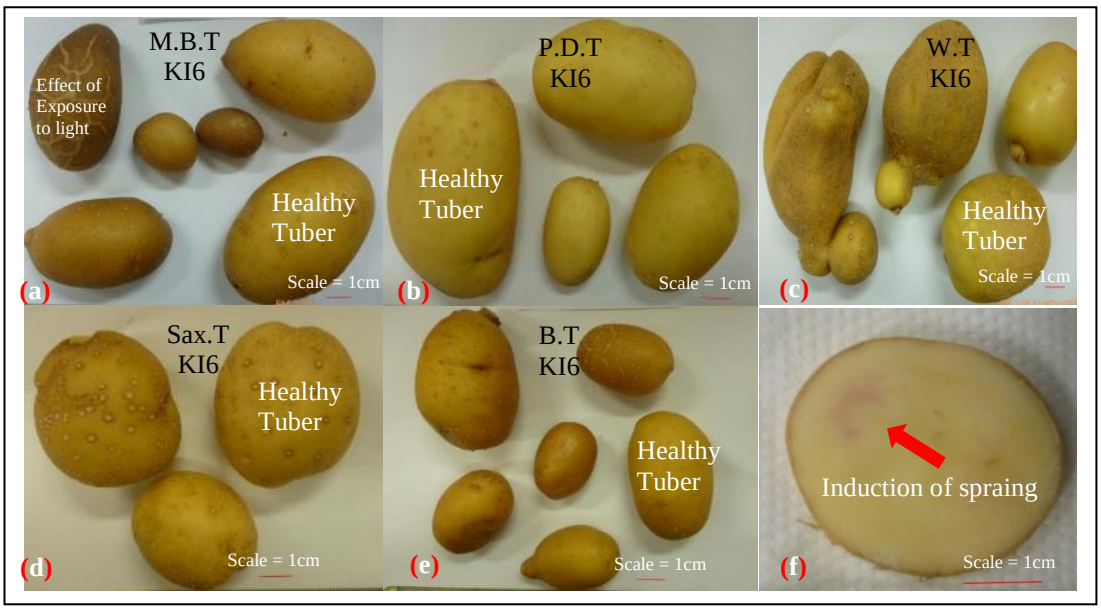

Figure 3.24. Tubers from various potato cultivars infected with the KI6 isolate. Tubers of cultivar **(a)** Maris Bard **(b)** Pentland Dell **(c)** Wilja **(d)** Saxon and **(e)** Bintje. **(f)** Tuber-section from **b** exhibiting spraing-induction. Tubers from mock-inoculated plants are denoted as ‘‘Healthy Tuber’’.

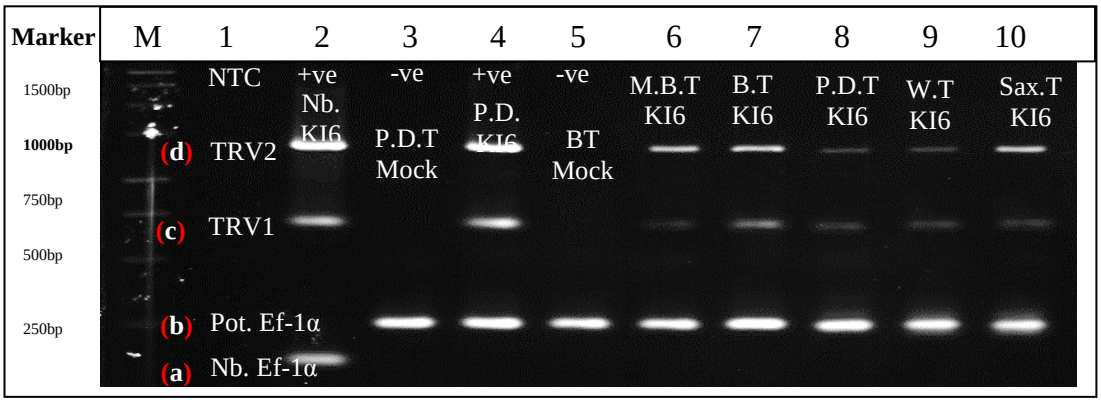

Figure 3.25. RT-PCR confirmation of TRV in the tubers of KI6 infected plants. Lane M: 1Kb Promega DNA marker; **Lane 1**: NTC, Non template control; **Lane 2 and 4:** positive control samples, KI6 infected *N.benthamiana* leaf sample (Nb.,Lane 2) and Pentland Dell leaf-sample (P.D., Lane 4); **Lane 3 and 5**: negative controls, Tuber-samples from mock-inoculated Pentland Dell (P.D.T, Mock, Lane 3) and Bintje (BT Mock, Lane 5); **Lane 6-10**: Tuber-samples from KI6 infected plants of Maris Bard (M.B.T, Lane 6), Bintje (BT, Lane7), Pentland Dell (P.D.T, Lane 8), Wilja (W.T, Lane 9) and Saxon (Sax.T, Lane 10); House-keeping gene, Ef-1α, amplicon from **(a)** *N. benthamiana* (150 bp) and **(b)** potato (255 bp). **(c)** TRV1 KU amplicons (655 bp) and **(d)** TRV2 amplicons (I6 RNA-2, 627 bp), Due to almost equal amplicon-size of TRV1 and -2, the TRV2 amplicons were loaded, after the TRV1 amplicons had sufficiently resolved on the gel.

TRV-infection in these tubers was confirmed by RT-PCR. The tuber-tissue of all the three plants of each cultivar was freeze-dried, methodology discussed in section 2.1.3, and pooled for each cultivar to represent a single biological sample. The cDNA synthesis and protocol for 40 cycles of PCR was the same as already described. TRV1 (RNA-1) was detected by using the primer-set (Primer No. 2371 and 1759) designed within the 16K gene and the 3′ UTR of TRV RNA-1. The TRV2 (I6 RNA-2) was detected by using the CP-specific primers (Primer No. 2422 and 2423). Both the TRV1 (655 bp) and TRV2 (627 bp) were amplified from the tubers of all the five cultivars (Fig. 3.25), confirming the tuber-infection.

3.6.4. Evaluation of the systemic infection of KI6 isolate in individual potato plants

In the initial studies described above the TRV recombinant isolate KI6 was found to move systemically in various tetraploid cultivars of potato. In a second experiment ten cuttings each of Pentland Dell and Bintje plants were rub-inoculated, at 10 days post planting, with infectious sap of KI6. The top, non-inoculated leaf samples were separately collected at 15 dpi from the individual plants and processed for cDNA synthesis and RT-PCR analysis (section 2.2.16). TRV1 detection was done by using the MP-based primer set (Primer No.2369 and 2370) and the TRV2 amplification was done by using an I6 CP-based primer-set (2422 and 2423). In addition to the amplification of EF-1α gene (255 bp), the RNA-1 (318 bp) was detected in all 10 samples each of Pentland Dell (P.D. 1-10) and Bintje (B1-10). The systemic infection of I6 RNA-2 (627 bp) was detected in six of ten Pentland Dell (Fig. 3.26, I) and nine of ten Bintje samples (II).

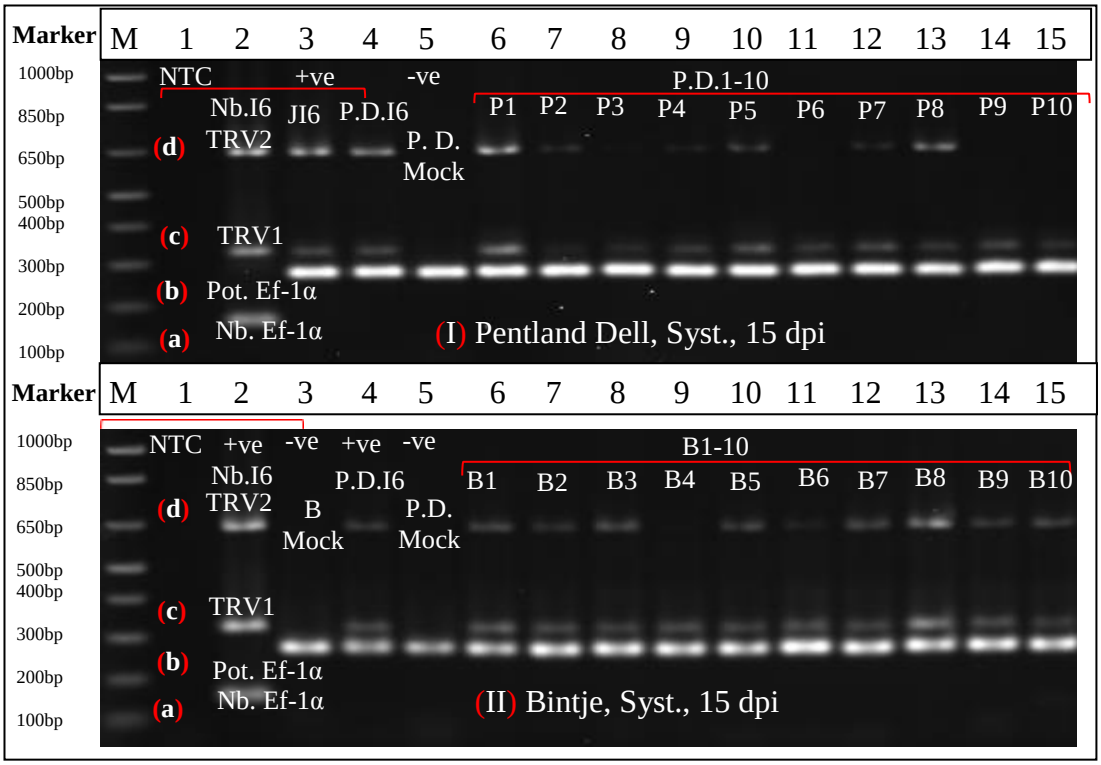

Figure 3.26. Evaluation of the systemic infection of KI6 isolate in 10 individual potato plants. Lane M: 1Kb Plus Promega DNA marker; **Lane 1**: NTC, Non template control; **Lane 2–4:** positive controls; KI6 infected leaf-samples of *N. benthamiana* (Nb. I6, Lane 2, Panel 1 and II) , *Solanum jamesii* (JI6, Lane 3, Panel 1), and Pentland Dell (P.D. I6, Lane 4, Panel 1 and II); **Lane 3 and 5:**negative controls, mock inoculated leaf-samples of Pentland Dell (P.D., Mock, Lane 5, Panel 1 and II) and Bintje (Bintje, Mock, Lane 3, Panel 1); **Lane 6-10**: KI6 infected leaf-samples from plants 1-10 of Pentland Dell (P1-10, Panel I) and Bintje (B1-10,Panel II); House-keeping gene, Ef-1α, amplicon from **(a)** *N. benthamiana* (150 bp) and **(b)** potato (255 bp). **(c)** TRV1 MP amplicon (318 bp) and **(d)** TRV2 amplicon (I6-CP, 627 bp), Potato leaf-samples were collected at 15 dpi

3.7. Full-length sequencing of I6 RNA-2 (p0215)

TRV I6 is a natural isolate originating by recombination between the RNA-2 segments of unknown TRV and PEBV isolates. It is an Italian isolate transmitted by *T. viruliferous* and was originally isolated, by van Hoof *et al* (1966), from soil-samples collected from Italy. A full-length clone of I6 RNA-2 had previously been prepared (S. MacFarlane, unpublished) but its sequence had not been determined. The nucleotide sequence of the 5′ and 3′ termini of I6 were published by Robinson (1994; accession number S72875.1). The 5′ (375 nts) region of I6 RNA-2 is most closely related to TRV-TCM strain and the 3′ (376 nts) region of I6 RNA-2 is very similar to the RNA-2 of PEBV isolates SP5 and TpA56 (93% identical if a single nucleotide gap is inserted into the 5′ NCR and a 6 nts gap is inserted into the 3′ NCR). Likewise, the 5′ NCR of a recently identified natural recombinant, AL TRV RNA-2, is also derived from TRV-TCM strain (Koenig *et al*., 2011). The 25nts at the 3′ terminus of I6 and PEBV-SP5 (Swaffham P5 isolate) RNA-2 are identical and like the TRV TC3′ PE are thought to be derived from a British isolate of PEBV. The demonstration of long-lived systemic infection of I6 RNA-2 within tetraploid potatoes (in the earlier studies of this Ph.D) motivated us to sequence the full-length RNA-2 of this strain.

The nucleotide sequence of I6 RNA-2 from clone p0215 was completely sequenced in the current studies by using the primers given in Appendix 3 and was determined to be of 3,410 nts. The GenBank database accession number is KT964816. I6 RNA-2 encodes four ORFs; the first ORF (of 627 nts) encodes the CP, followed by 240 nts encoding a putative-9K protein, 768 nts encoding the 2b protein (29kDa) and 627 nts encoding the 2c protein (23kDa; Fig. 1.4). The 5′ and 3′ NCR are of 551 nts and 487 nts, respectively. Analysis of the complete sequence shows that I6 RNA-2 has a TRV-like 5′ untranslated region (UTR) but PEBV-like coding sequence and 3′ UTR.

Although, it is very closely related in its particle properties to the particles of the PEBV, it is included in the TRV-group as the replication of I6 RNA-2 is dependent

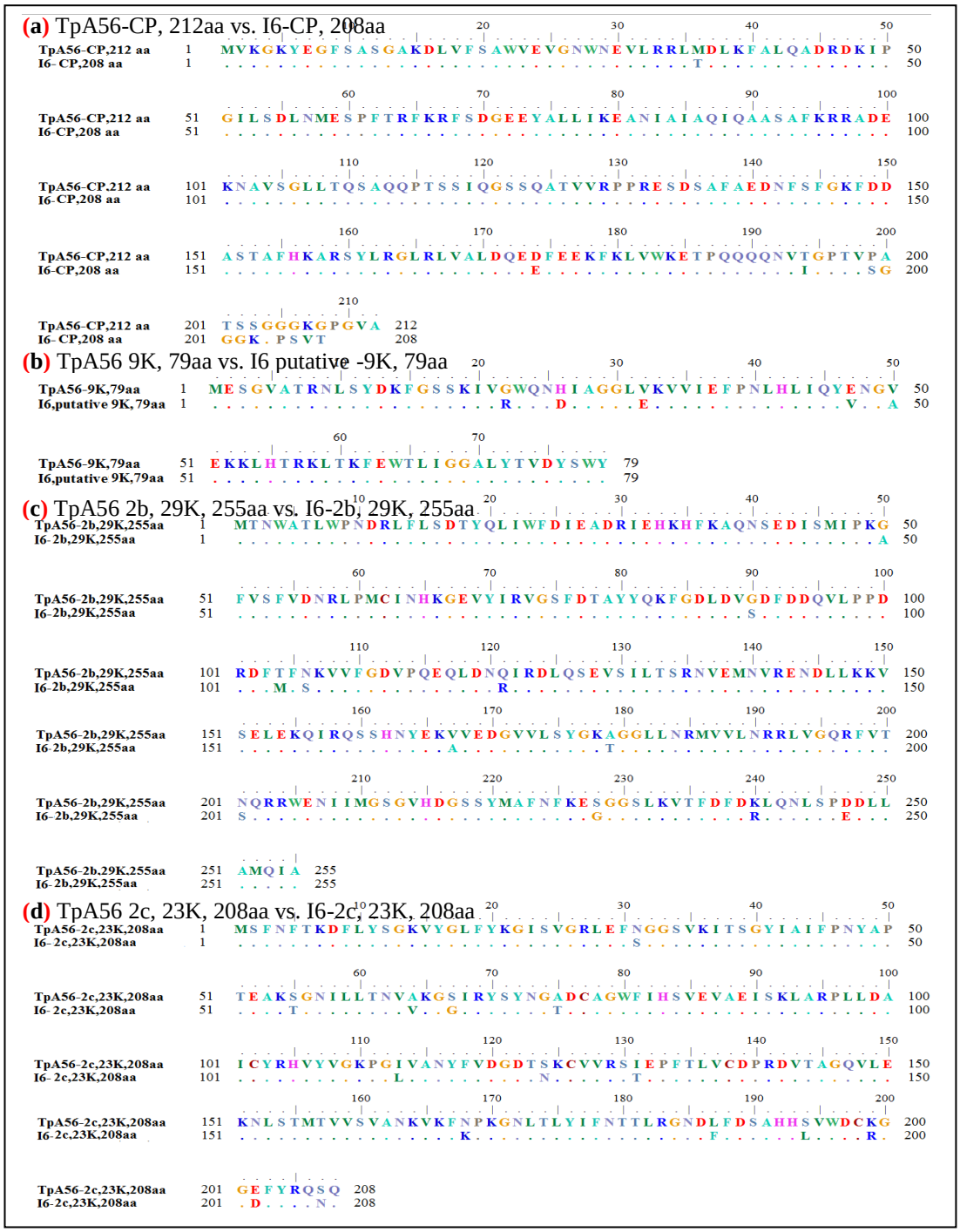

Figure 3.27. Amino acid sequence of CP, 2b, and 2c proteins of I6 RNA-2 compared with the PEBV (TpA56) proteins. (a) TpA56 CP, 212aa vs. I6-CP, 208aa **(b)** TpA56 9K, 79aa vs. I6 putative-9K, 79aa **(c)** TpA56 2b, 29K, 255aa vs. I6-2b, 29K, 255aa **(d)** TpA56 2c, 23K, 208aa vs. I6-2c, 23K, 208aa.

upon the TRV RNA-1 encoded replicase proteins and the PEBV isolates cannot be replicated by the replicase of TRV RNA-1.

Comparison of the I6-CP, 2b, and 2c proteins with the corresponding proteins of the PEBV (TpA56 isolate) is given in the Fig. 3.27. The I6-CP (208 amino acid (aa) residues) differs in only 12 aa residues from the TpA56 CP (212 aa residues), most of these dissimilarities are in the carboxy terminus of the protein (a). The I6 putative-9K protein (79 aa residues) differs in five aa residues from the TpA56 9K protein (79 aa residues, b). The 29K, 2b protein of the I6 isolate (255 aa residues) differs in 11 aa residues from the 29K, 2b protein of TpA56 (255 aa residues, c). The I6-23K, 2c protein (208 aa residues) was found to differ in 14 aa residues from the TpA56 23K, 2c protein (208 aa residues, d). Thus, the TRV I6 genes and their encoded proteins are highly similar to those of PEBV SP5 (CP [gene / protein % identity] 92/94; 9K 95/92; 2b 94/95; 2c 94/92). This analysis clarifies the previous serological and nucleic acid hybridization studies of TRV I6, and confirms that TRV I6 is a true natural recombinant between TRV and PEBV.

3.8. Detection capability of replicase and 16K gene-based primer-sets

Attempts to detect TRV from upper, non-inoculated and sometimes from the inoculated leaves of tetraploid potatoes, by using the primer-set flanking the 16 K gene were not successful in most of the cases. This necessitated designing different primer-sets around diverse genes, along the length of RNA-1, and evaluating their detection efficiency.

TRV1 detection capability of the replicase and the 16K primer-sets was evaluated by using the template cDNA from the *N. benthamiana* plants infected with KK20 isolate. Both these primer-sets were found to be almost equally capable of detecting TRV1 from the *N. benthamiana* plants (Fig. No. 3.28, I and II). In fact, the replicase

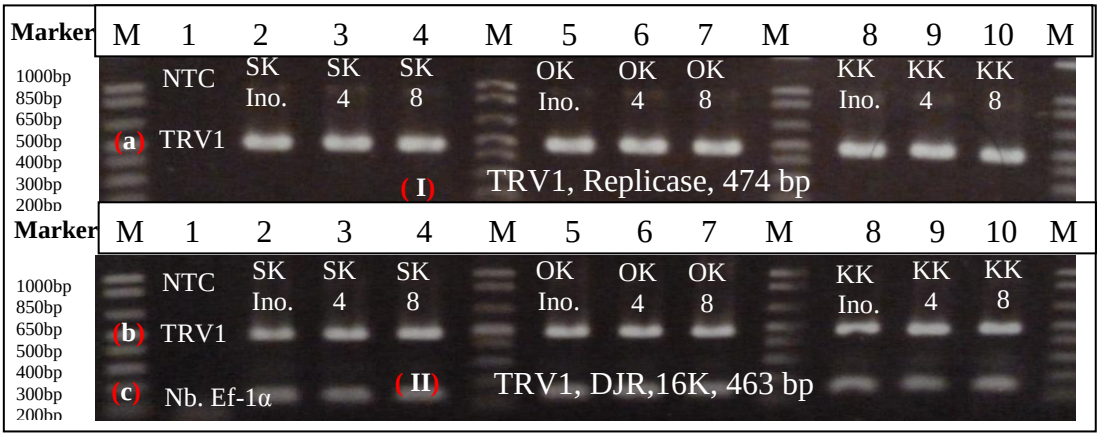

Figure 3.28. Detection of TRV1 in *N. benthamiana* by replicase primer-set vs. 16K primer-set. Lane M: 1Kb Plus Promega DNA marker; **Lane 1:** NTC, Non-Template control; Plants inoculated with Lane **2-4**: SK; **Lane 5-7:** OK; and **Lane 8-10:** KK isolates. **Panel I** TRV1 **(a)** Replicase-amplicon (474 bp), and **Panel II (b)** 16K flanking-amplicon (463 bp, not line-up with marker); **(c)** Ef-1α amplicon (Nb. Ef-1α, 150 bp). Sample-labels represent the samples collected from the inoculated leaves (Ino.) at 4 dpi and systemically infected leaves at 4 and 8 dpi.

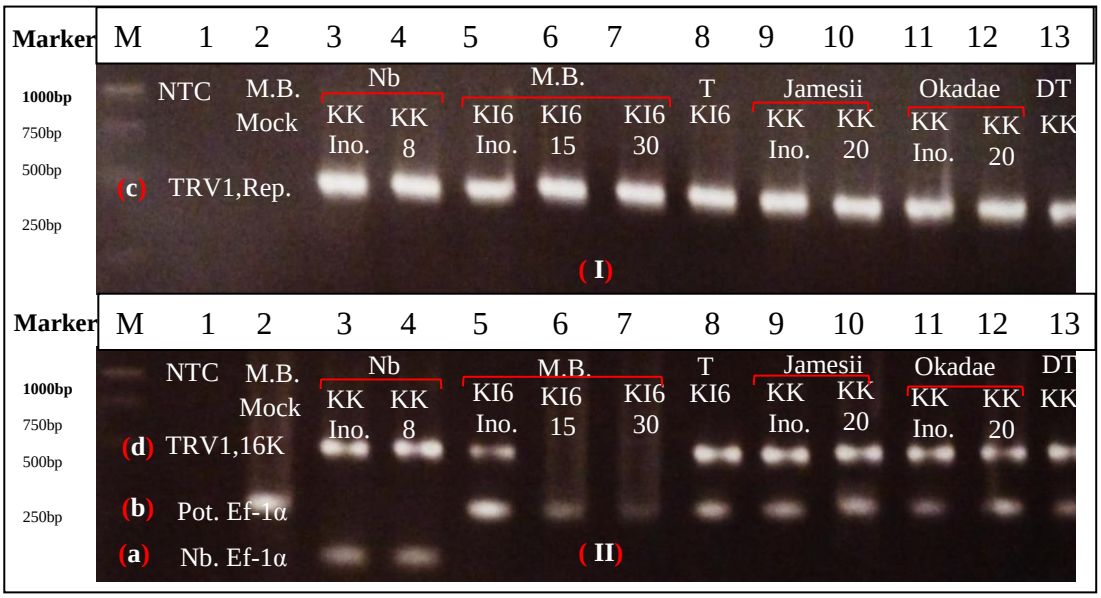

Figure 3.29. Evaluation of detection capability of replicase primer-set vs. 16K primer-set in a range of TRV infected plants. Lane M: 1Kb Promega DNA marker; **Lane 1:** NTC, Non-Template control; Lane **2**: M.B, Mock, Mock-inoculated Maris Bard. Plants inoculated with **Lane 3-4, 9-13:** KK20 isolate and **Lane 5-8:** KI6 isolate. Ef-1α amplicon of **(a)** *N. benthamiana* (Nb. Ef-1α, 150 bp) and (**b)** Potato (Pot. Ef-1α, 255 bp). TRV1 amplicon of **(c)** replicase gene (474 bp, **Panel I**), and **(d)** 16K Flanking-gene (463 bp, **Panel II**). Sample labels M.B., Nb., Jamesii, Okadae, T, and DT, represent the leaf samples collected from Maris Bard, *N. benthamiana*, *Solanum jamesii*, *S. okadae*, and tuber samples from tetraploid and diploids tuber, respectively. Sample labels represent the samples collected from the inoculated leaves (Ino.) at 5 dpi and systemically infected leaves at 8, 15, 20 and 30 dpi, respectively.

gene based amplicons were slightly brighter in fluorescence than the 16K based amplicons.

The utility of both the primer-sets to detect virus in a range of samples including the TRV-infected leaf samples of *N. benthamiana*, Maris Bard, *S. jamesii*, *S. okadae*, and the tuber samples from tetraploid and diploid potatoes was also investigated. The replicase gene based primer set detected TRV1 (474 bp) from all the test samples except the negative controls (Fig. No. 3.29, c and d). However, the 16K primer-set either failed or weakly detected TRV1 (at 15 and 30 dpi) from the systemic leaves of KI6-infected Maris Bard (Lane 6 and 7) producing a smear rather than a discrete amplicon. This suggests that the replicase gene-based primer-set is most effective for detection of TRV in a range of plant hosts.

3.9. Discussion

In the current studies, although variation was seen between plants, the PpK-20 RNA-1 isolate was found to be more infectious than the other two isolates (SYM RNA-1 and PpO-85 RNA-1) and to promote greater expression of GFP and CP from co-replicating GFP-RNA-2. Not only was its accumulation level higher but this isolate was also more pathogenic in symptom production, sometimes causing death of the infected plants. However, the production of severe symptoms is not always associated with a higher accumulation rate of an infecting virus. For example, a natural mutant of *Tobacco streak virus* (genus Ilarvirus) with only one nucleotide variation from the parental virus produced more severe and long-lasting symptoms than the parental virus, although its accumulation in the infected tobacco plants was lower than the parental isolate (Xin and Ding, 2003; Whitham and Wang, 2004).

All the 15 TRV recombinant isolates (including two parental *in-vitro* recombinant isolates and thirteen pseudorecombinant isolates) examined in this work were able to cause systemic infection in *N. benthamiana* plants, however, some differences in

symptom production were noticed during the infection, with the PpK-20 RNA-2 (KK20 isolate) producing more noticeable vein-necrosis than the other RNA-2 species in systemically infected leaves. The KK20 isolate was more severe in symptom production and also its accumulation in the systemically infected leaves was higher, as revealed by northern-blot analysis of the infected plants, than all the other fourteen recombinant isolates and the three TRV RNA-1 only (SYM, PpO-85 and PpK-20) isolates.

Spraing disease is of economic significance in the potato industry but research studies using molecular techniques to investigate the infection of potato by TRV are very few (Harrison and Robinson, 1982; Crosslin *et al.*, 1999; Ghazala and Varrelmann, 2007). Naturally, TRV infection in the potato fields is caused by two routes, either by feeding of the viruliferous ‘‘trichodorid’’ nematodes on the underground tissues of the plant or by planting of virus-infected seed-tubers in the field and the consequent spread of the virus into the emerging tissues or daughter tubers of the plant. Studies focusing on mechanical inoculation of the aerial parts of potato and the subsequent successful movement of TRV into the underground parts are lacking in the literature. Systemic infection by TRV has been achieved by planting tubers of susceptible cultivars in fields infested with viruliferous nematodes. But the nematode transmission of TRV occurs in a species-specific association (Ploeg *et al.*, 1992 a, b; Vassilakos *et al.*, 2001) and for many of the TRV-isolates vector nematode species is not known. Therefore, it would be impossible to use nematode vectors to do comparative infection studies in potato with the 15 recombinant isolates constructed in this Ph.D. study.

The genetic details of spraing disease and TRV infection in potato are not known, although, quantitative trait loci (QTL) and a molecular marker associated with the development of spraing symptoms in tubers have been identified (Khu *et al.*, 2008). These QTLs might be associated with virus symptom production rather than reflect

real resistance or susceptibility to TRV as the tubers in this study were not evaluated for the actual presence of TRV.

Potato cultivars have broadly been categorised into resistant, spraing sensitive and tolerant. The resistant varieties (including Bintje) do not produce spraing symptoms and the virus is not recovered from these plants. Spraing sensitive varieties (Maris Bard, and Pentland Dell) produce visible spraing symptoms and virus is detectable. The third group of tolerant varieties (Wilja, Saxon, and Shepody) do not produce classic spraing symptoms, but the systemic infection of M-type virus (both RNA-1 and -2) is known to occur in these plants (Robinson and Dale, 1994; Dale *et al.*, 2004) that with repeated propagation can cause reduction in the uniformity and size of infected tubers.

The recombinant isolates in the current study produced different types of symptoms on the inoculated leaves of potatoes. Each variety exhibited different types of symptoms that included annulus-like or disc-shaped necrotic lesions, yellowing, spreading necrosis, HR-like necrotic lesions or no symptoms. Robinson and Harrison (1985b) in their experiments, conducted on pseudorecombinant isolates of PEBV (Broad Bean Yellow Band Virus isolate), proved that some of the symptoms induced in the test plants were determined by the RNA-2 segment of the pseudorecombinant isolate. In similar studies it was demonstrated that RNA-1 controlled lesion formation and systemic invasion of infected plants, whereas, RNA-2 could influence the symptom type (Lister and Bracker, 1969; Robinson, 1977). In the current studies, the TRV recombinant isolates comprising PpK-20 RNA-2 were more severe in symptom production as compared to the I6 RNA-2-containing isolates. Robinson *et al.*, (1987) also found the TRV I6 isolate to induce systemic symptoms in infected *N. clevelandii* plants; these symptoms were milder than the symptoms produced by another recombinant isolate (N5) that caused severe necrosis resulting in the death of infected plants. In the current studies, we also found that I6 RNA-2-containing

recombinant isolates produced milder symptoms than all the other fourteen recombinant isolates.

Some TRV isolates can overcome tuber-resistance in potato. Robinson (2004) reported a TRV variant (PpO-85 RNA-1) isolate that was a resistance-breaker in Bintje. He produced pseudorecombinant isolates comprising PpO-85 RNA-1 and PpK-20 RNA-2 or PpK-20 RNA-1 and PpO-85 RNA-2 and using nematodes was able to challenge Bintje plants to these isolates. In his study, only the isolate comprising PpO-85 RNA-1 was able to infect and induce spraing symptoms in the tubers of Bintje. Ghazala and Varrelmann (2007) agro-infiltrated the leaves of Bintje with various mutants to advocate that the movement-protein (MP) of PpO-85 does not trigger the HR-response of Bintje, thus allowing the isolate to overcome the TRV-resistance mechanism in Bintje. RT-PCR was used in this work to detect RNA-1 of TRV PpK-20 and PpO-85 isolates in the mechanically inoculated leaves of Bintje, Russet Burbank, and Saturna. However, RNA-1 of PpK-20 isolate was detected in the systemically infected leaves of Russet Burbank only.

The current study provides more details of TRV infection in different potato varieties, following leaf inoculation. All the 15 recombinant isolates could infect the inoculated leaves of six different potato varieties, including Bintje, which is considered to be resistant to TRV. Moreover, RNA-2 of some isolates was sometimes found at low levels in the non-inoculated leaves of Bintje and Maris Bard, suggesting a sporadic and weak infection. It seems that the TRV-resistance mechanism in Bintje primarily targets some stage in the delivery of virus to the tubers by nematodes, or, it does not operate with the same efficiency in the leaves as it does in the tubers. Furthermore, in the current work, three of the varieties that belong to the tolerant group (Wilja, Saxon and Shepody) and where TRV infection starting in the tubers can spread throughout the aerial parts of the plant (Xenophontos *et al.,* 1998) did not become systemically infected by most of the viruses, following leaf-inoculation. This again suggests that there might be difference in the resistance

or susceptibility mechanisms that are operating in the leaves as compared to the roots and tubers. We did not examine whether any of the isolates that did not move to the systemic leaves were, nevertheless, able to move directly to the tubers.

Interestingly, in contrast to most of the viruses examined here, the recombinant isolates comprising I6 RNA-2 were able to spread systemically and persist for at least 30 days in the leaves of all six potato varieties. The I6 isolates were then able to move into the tuber (s) that developed from the infected plants. This indicates that either the RNA-2 of I6 isolate encodes a sequence or expresses a protein that is helpful for the persistence of the virus or more likely RNA-2 escapes the host surveillance mechanism that recognises and targets an as yet identified component of the RNA-2 of other isolates. Analysis of the stem mottle affected plants revealed that such plants were largely infected by the RNA-1 isolates only (Cadman, 1959; Harrison and Robinson, 1982), suggesting that replication and movement of RNA-2 in these plants was somehow prevented.

Viral movement through the plasmodesmata (cytoplasmic channels) is controlled by virus-encoded proteins that are commonly known as movement proteins (MP). In addition to MP, some of virus-encoded proteins related to particle formation or viral replication are also found to be associated with short or long distance transport of viruses (Carrington *et al.*, 1996; Cruz., 1999). However, it is primarily the MP that is associated with cell-to-cell transport of viruses, and long distance transport may or may not be dependent upon the structural protein (CP). The difference in the particle (CP) properties of the KI6 recombinant isolate from the other TRV-isolates may account for the enhanced systemic movement of the KI6 isolate. In the current studies Bintje was also susceptible to the KI6 isolate. This isolate is different in its serological properties (PEBV serotype) to the other TRV-isolates (van Hoof *et al*., 1966; Robinson *et al*., 1987). I6 RNA-2 carries the coding sequences and the 3′ UTR from PEBV. Perhaps, these PEBV-specific RNA-2 components are not recognized

by the potato surveillance system that allows the virus to persist and spread in the field.

The viral MPs attach non-specifically to nucleic acids and form viral ribonucleo-protein complexes (vRNPC) that aid viral-transport (Hull, 1989; Lucas, 2006). Thus cellular trafficking of the viruses can be either in the form of vRNPC or as virus particles. In short-distance (cell-to-cell) movement of the viruses, the plasmodesmata are provisionally modified to allow the virus to transit in the form of nucleic acids or vRNPC (e.g.; TMV RNA) molecules. In some cases modification of the plasmodesmata allows the transit of virions (e.g.; CMV) through a tubule-like structure formed in the plasmodesmata (McLean *et al.,* 1993). The MP also modifies the ‘‘size exclusion limit (SEL)’’ of the plasmodesmata and thus facilitates transport of the virus. It seems to be more likely that the TRV KI6 isolate remains non-encapsidated in the tetraploid potatoes and its systemic trafficking in these potatoes is in the form of vRNPC.

Larger-scale inoculations of Bintje and Pentland Dell plants, performed in long-day conditions, reveal that the systemic movement of KI6 varies from plant to plant. In order to make a more generalized understanding about systemic infection by KI6, large-scale replicated experiments including more number of plants need to be done under varied environmental conditions. Light and temperature could have profound effects on the symptom expression and viral-titre in the inoculated plants (Harrison and Jones, 1971a, b). The RNA-2s of all the isolates should be detected using CP-specific primers as the non-structural genes could be lost during multiplication**,** preventing the viral RNA-2 from being detected if primers located in these areas are used for RT-PCR (Hernandez *et al.,* 1996).

It was apparent that the detection of RNA-1 became more difficult as the systemic infection proceeded. In a TRV infection, RNA-1 is known to accumulate to less than one tenth the level of RNA-2, which would make the detection of RNA-1 more

difficult to achieve. Improved TRV RNA-1 detection using a primer-set targeting the replicase gene is one outcome of this work, which will allow further experiments to be done with greater confidence.

4. Utilizing Diploid Potatoes for VIGS

4.1. Aim

Our initial attempts to find tetraploid potato cultivars that were fully susceptible to systemic infection by TRV had faced difficulties (see chapter no. 3, section 3.6. pp. 100-114). This led us to explore other genetic sources of potato including diploid species. Our purpose was to find genotypes that were highly susceptible to TRV and perhaps could be practically exploited for functional-genomics analysis using virus-induced gene silencing (VIGS). Investigations were conducted to identify the genotypes in which TRV could move systemically and accumulate to a sufficient level to be useful for TRV infection and VIGS-related studies. For this purpose the 98 accessions of the Commonwealth Potato Collection (CPC) were screened by mechanical leaf inoculation with TRV (PpK-20 isolate) and virus was detected by Plate Trapped Antigen (PTA) ELISA, leading to the identification of seven susceptible genotypes. The susceptible accessions were further evaluated for the systemic accumulation of TRV by the tissue-print method and the accessions with the highest accumulation of TRV were selected for further studies.

The systemically-infected leaves of *Solanum okadae* were found to exhibit chevron-like symptoms. The accumulation of TRV RNA-1 and -2 in these symptomatic leaves was quantified and its relevance to the induction of the symptoms was evaluated. Frameshift mutants of the coat-protein (CP), 2b, and 2c genes of the PpK-20 RNA-2 were made and assessed for any effects on virus infection.

The effectiveness of TRV for the functional analysis of potato tuber genes was assessed by evaluating VIGS constructs of the *Phytoene desaturase* (PDS), *Zeaxanthin epoxidase* (ZEP), and *Granule bound starch synthase* (GBSS) genes. These studies led us to recommend *Solanum jamesii* as a model species for

investigating gene function related to tuber development and virus infection of potato.

4.2. Screening of Commonwealth Potato Collection (CPC)

The seedlings (section 2.1.2.) of 98 accessions of the Commonwealth Potato Collection (CPC) were screened by Ms. Wendy McGavin (JHI). These seedlings were mechanically inoculated, at the 4-5 leaf stage (2 weeks post emergence), with infectious-sap of the KK20 isolate. The inoculated and top, non-inoculated leaves of each plant were collected and extracted separately at 7 dpi. The leaf extracts were screened by PTA ELISA (section 2.2.15.), using the TRV-PLB antiserum. Among these 98 accessions, seven were found to be susceptible to TRV systemic infection viz.; ACL 7098, BST 3822, GND 3534, JAM 7653, MGA 2482, OKA 7327, and TOR 3705 (Table No. 4.1). All of these are diploid (2n) potatoes with 100 %

Table 4.1. TRV susceptible diploid potatoes (CPC).

Sr.No.	CPC Accession	Taxonomic Nomenclature	Symptoms produced on		ELISA +ve
			Inoculated leaves	Systemic leaves	
1.	ACL 7098	*Solanum acaule* Bitt.	Few chlorotic and necrotic lesions	Asymptomatic	4/4 plants
2.	BST 3822	*Solanum brachistotrichum* (Bitt.) Rydb.	Chlorotic lesions	Asymptomatic	4/4 plants
3.	GND 3534	*Solanum gandarillasii* Cárd.	Large chlorotic and necrotic lesions	Asymptomatic	3/3 plants
4.	JAM 7653	*Solanum jamesii* Torr.	Asymptomatic	Asymptomatic	3/3 plants
5.	MGA 2482	*Solanum megistacrolobum* Bitt.	Asymptomatic	Asymptomatic	4/4 plants
6.	OKA 7327	*Solanum okadae* Hawkes et Hjerting	Asymptomatic	Asymptomatic	3/3 plants
7.	TOR 3705	*Solanum toralapanum* Cárd. et Hawkes	Asymptomatic	Asymptomatic	3/3 plants

infection incidence and none of them produced any symptoms on the systemically infected leaves (when infected with the KK20 isolate). However, three of these CPC accessions (viz.; ACL 7098, BST 3822 and GND 3534) developed some chlorotic and/or necrotic symptoms, at 3-4 dpi, on the inoculated leaves. The symptoms were more evident on the inoculated leaves of GND 3534 as compared to the other two

Table 4.2. Brief botanical description of the TRV susceptible diploid potatoes (CPC).

Sr.No.	Diploid potato species (Acronym)	Natural Habitat & (Country of origin)	Brief botanical characteristics
1.	*Solanum acaule* Bitt. (**ACL**)	Alpine-meadows, puña-grassland and roadsides 3,500 to 4,600 m. (**Argentina; Peru**)	Plant low; rosette forming; stoloniferous and tuber-bearing. Leaves odd pinnate; lateral leaves obtuse. Flower corolla rotate, purple to white. Fruit sub-globoid to ovoid.
2.	*Solanum brachistotrichum* (Bitt.) Rydb. (**BST**)	Dry piñon-scrub vegetation at 1,750-2,500 m. (**Mexico**)	Plant slender and erect; 0.25-0.8 m tall. Leaves pinnate, short and single leaflet at the apex. Stem downward pointing. Corolla stellate white or cream coloured, occasionally tinged purple. Berries globular green with white mottling; around 1 cm diameter.
3.	*Solanum gandarillasii* Cárd. (**GND**)	Under bushes and cacti in dry summer-green woodland at 1,800 - 2,500 m (**Bolivia**)	Plant erect; 10-35 cm tall. Stems pale green, with narrow wing. Leaves odd-pinnate; glabrous with enlarged terminal. Flowers white, pentagonal. Berries globular to ovoid 2 - 2.5 cm diameter.
4.	*Solanum jamesii* Torr. (**JAM**)	Rocky hillsides, ravines at 1,400-2,900 m. (**Mexico; USA**)	Plant, erect to bushy; 0.2-0.5 m tall. Leaves odd-pinnate, bluish-grey, generally pubescent with 3-4 pairs of leaflets. Flowers borne in 10 flowered inflorescence; white with petals often tinged lavender. Fruits 1 cm in diameter, globose, green throughout.
5.	*Solanum megistacrolobum* Bitt. (**MGA**)	High mountain grassland and field margins at 3,500-4,500 m. (**Argentina; Peru**)	Plant low, rosette forming with straggling stems; stoloniferous and tuber bearing. Leaves odd-pinnate with coarse hairs on upper surface and terminal leaf often larger than laterals; often greyish-green. Flower corolla rotate to broadly stellate; generally pale blue-lilac. Berries green and globular. Foliage often has parsley-like leaf odour.
6.	*Solanum okadae* Hawkes et Hjerting (**OKA**)	High mountain rainforest at 2,600-3,200 m. (**Argentina; Bolivia**)	Plant 20-80 cm tall, erect. Leaves odd-pinnate with leaflets in pairs. Flower corolla white, rotate to pentagonal. Berries globular to 2 cm in diameter.
7.	*Solanum toralapanum* Cárd. et Hawkes (**TOR**)	Rocky and grassy slopes, field margins and puña-grassland at 3,000-4,100 m. (**Argentina; Bolivia**)	Plant low, rosette forming; stoloniferous and tuber bearing. Leaves odd-pinnate; rather coarse and thick; similar to *S. megistacrolobum* but with very long curved spathulate terminal lobe. Flower corolla generally dark violet rotate-pentagonal to rotate-stellate. Berries globose to somewhat ovoid.

(Source: - Mrs. Jane Robertson, CPC Research Assistant, JHI; Hawkes, 1990)

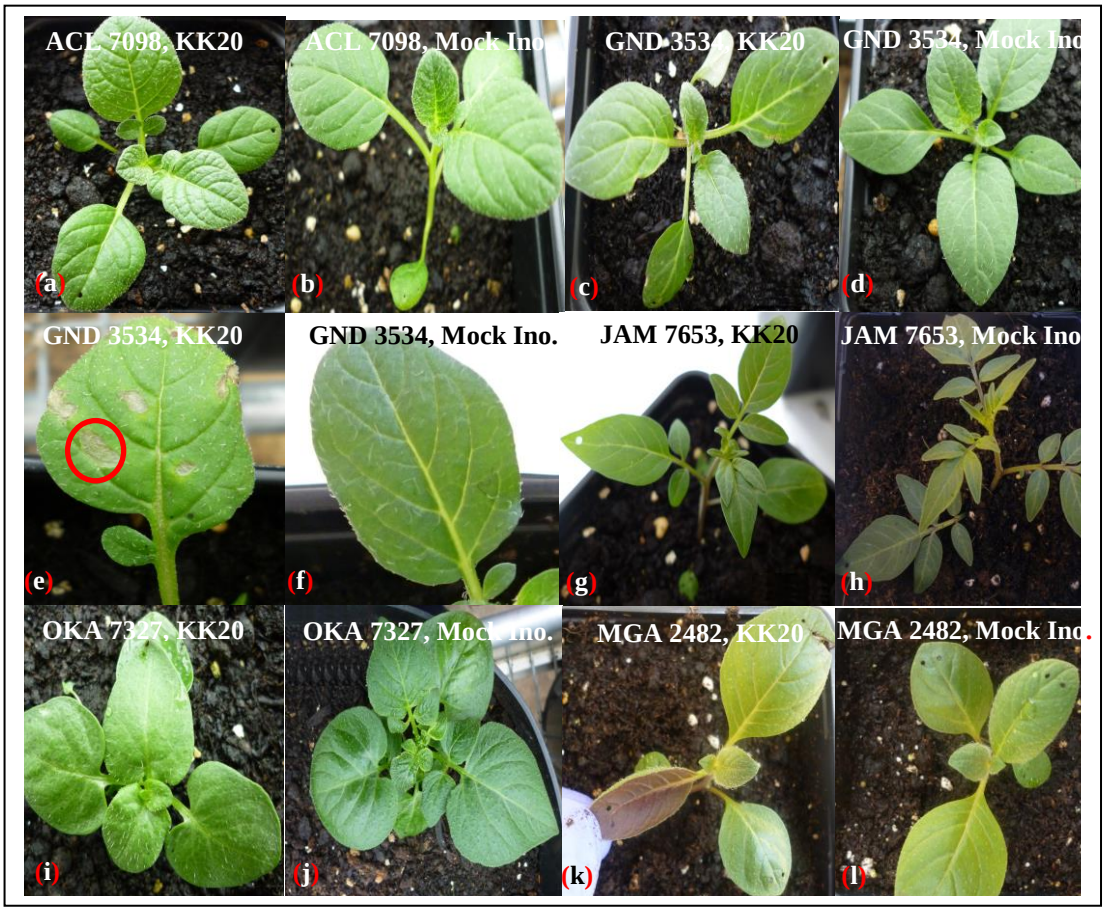

Figure 4.1. TRV-susceptible diploid potatoes (CPC) inoculated at the 4-5 leaf seedling stage. Inoculated (KK20) seedlings of **(a)** *Solanum acaule* (ACL 7098), **(c)** *Solanum gandarillasii* (GND 3534), **(e)** necrotic lesion (encircled) on the inoculated leaf of c **(g)** *Solanum jamesii* (JAM 7653), **(i)** *Solanum okadae* (OKA 7327), and **(k)** *Solanum megistacrolobum* (MGA 2482) with the violet coloured lower surface of the leaf exposed to show its morpho-genetic trait. Mock-inoculations of **(a), (c), (e), (g), (i),** and **(k)** are shown in **(b), (d), (f), (h), (j),** and **(l)**, respectively.

accessions. A brief botanical description of all of these seven TRV susceptible accessions (CPC) is given in Table No. 4.2.

Further seeds of all the seven accessions (Table No. 4.1) were sown to obtain more plants for RT-PCR analysis. The seed germination of BST 3822, and TOR 3705 was very poor, giving insufficient numbers of plants for carrying-out more studies. Therefore, these accessions were excluded from further studies.

Five seedlings of each of the remaining five accessions (ACL 7098, GND 3534, JAM 7653, MGA 2482 and OKA 7327) were mechanically inoculated, at the 4-5 leaf stage (Fig. 4.1.), with the infectious sap of the OK20 isolate which is less virulent than the KK20 isolate (section 2.2.9; Fig. 3.8, a-d).

4.2.1. RT-PCR evaluation of the systemic infection of TRV in the diploid potatoes (CPC)

Leaf-discs collected from the inoculated leaves (at 4 dpi) and from the systemically-infected leaves (at 6, 12, and 24 dpi) of each of three individual plants of each accession were processed for total RNA extractions by the method given in section 2.2.16. Virus was detected using TRV replicase (RNA-1, 474 bp) and CP (RNA-2, PpK-20, 360 bp)-specific primers given in appendix 1.

The RT-PCR results (Fig. 4.2.) confirmed the systemic infection of TRV as RNA-1 was detected in all of the positive control (*N. benthamiana*) and potato samples. Systemic infection of RNA-2 was confirmed in all the five diploid species with some variability in GND 3534, as only a weak amplicon of RNA-2 was detected at 12 dpi in the systemically infected leaves (Panel 1**,** Lane 12) and it remained undetected at 6 dpi and 24 dpi. The disparity in the RT-PCR result and the earlier ELISA result (showing full susceptibility) for this species (Table No. 4.1) was possibly due to the use of different infecting TRV-isolates (i.e.; OK20 in RT-PCR vs. KK20 in ELISA).

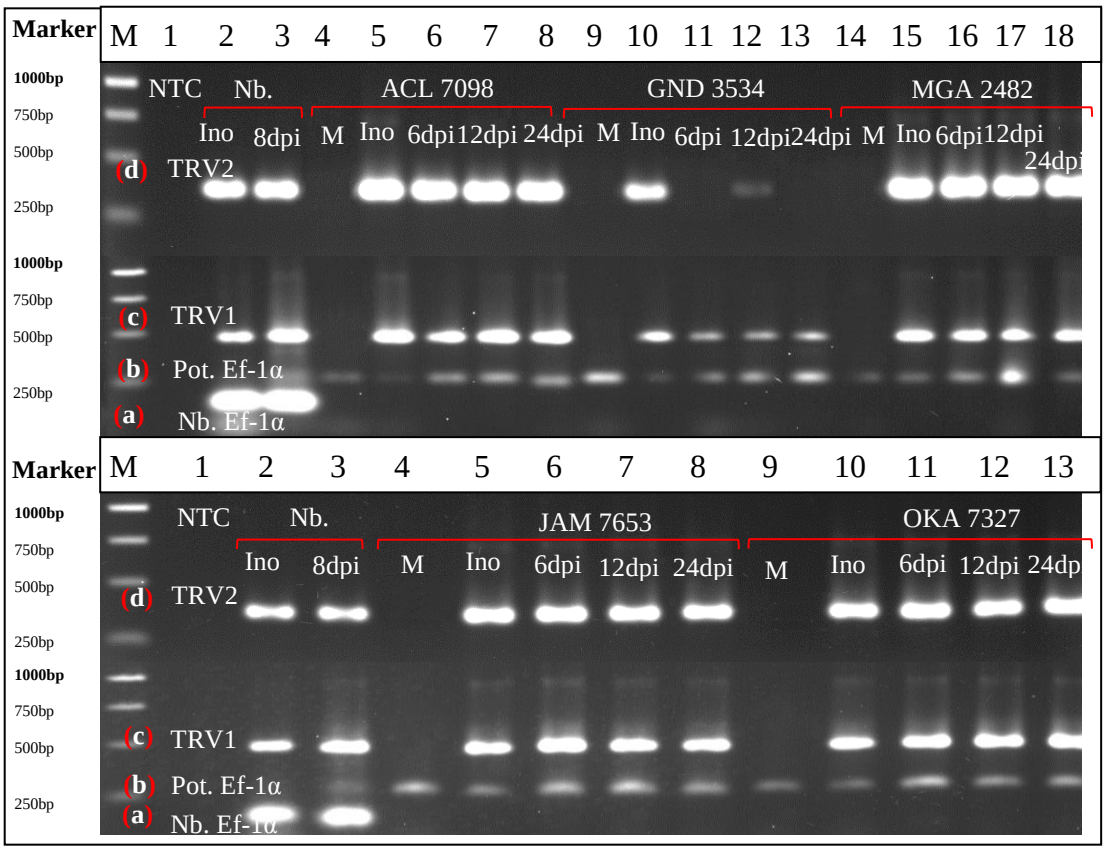

Figure 4.2. RT-PCR evaluation of the systemic infection of TRV RNA-2 (KK20 isolate) in the diploid potatoes. Lane M: 1Kb Promega DNA marker; **Lane 1**: NTC, Non template control; **Lane 2–3:** positive controls; OK20 infected *N. benthamiana* (Nb. Ino, Inoculated leaf, Lane 2; systemically-infected leaf, 8 dpi, Lane 3); **Lane 4, 9,** and **14:** negative controls, mock-inoculated (M) seedlings of respective accession. OK20 infected diploid accession, **Panel I:** ACL 7098 **(Lane 5-8,)**, GND 3534 **(Lane 10-13),** MGA 2482 **(Lane 15-18), and Panel II:** JAM 7653 **(Lane 5-8),** and OKA 7327 **(Lane 10-13).** Leaf-samples were collected at 4 dpi from the inoculated leaves **(Lane 2, 5, 10** and **15)** and from the systemically-infected leaves at 6 dpi **(Lane 6, 11,** and **16),** 8 dpi **(Lane 3),** 12 dpi **(Lane 7, 12,** and **17),** and 24 dpi **(Lane 8, 13,** and **18)**; House-keeping gene, Ef-1α, amplicon from **(a)** *N. benthamiana* (150 bp) and **(b)** potato (255 bp). **(c)** TRV1 replicase amplicon (474 bp) and **(d)** TRV2 amplicon (K20-CP, 358 bp).

4.2.2. Systemic accumulation of TRV in the diploid potatoes

The systemic accumulation of TRV in these diploid potatoes was further examined by the detection of the virus CP, using the tissue-printing method. Two seedlings of each of four diploid accessions (ACL7098, GND 3534, JAM 7653 and OKA 7327) were mechanically-inoculated (at 4-5 leaf stage) with the infectious-sap of the KK20 isolate. The press-blots of the whole infected seedling were prepared at 6, 12 and 30 dpi and developed by the method given in section 2.2.13. The tissue-print analysis of the seedlings at 6 dpi, given in Fig. 4.3. shows that TRV had accumulated to a detectable level in the positive control plant(s) of *N. benthamiana* (a) and the test seedlings of all the four diploid accessions (ACL7098 (c), GND 3534 (d), JAM 7653 (e) and OKA 7327 (f). The CP was not detected in the mock-inoculated (1X PBS) plants of ACL7098 (b). At 12 dpi (data not shown) and 30 dpi (Fig. 4.4.), the TRV-CP was detected only in the press-blots of JAM 7653 (a) and OKA 7327 (b) suggesting these accessions could be suitable for use in VIGS-related studies. Interestingly, the roots and stolons of the infected *S. jamesii* plants were also found to be infected with TRV.

4.3. TRV infection and production of chevron-like symptoms in *Solanum okadae*

Five individual plants of *Solanum okadae* were mechanically-inoculated with the OK20 isolate (section 2.1.2 and 4.2.), as this isolate produced systemic symptoms in *S. okadae*, whereas, the KK20 isolate did not. All the five plants developed chevron-like and mottling symptoms on the systemically infected leaves (Fig. 4.5.). The symptoms were more conspicuous at 21 dpi and started to diminish at 35 dpi. Leaf disc samples were collected from the asymptomatic (AS) and the symptomatic leaves of three individual plants (OK2, -3 and -5). Samples from the asymptomatic (green region, G) and the symptomatic area (region with chevron-like symptoms, CH) of the symptomatic leaves of infected plants and healthy samples from mock-inoculated (healthy, OH) plants were collected at 25 dpi. The total RNA extraction using

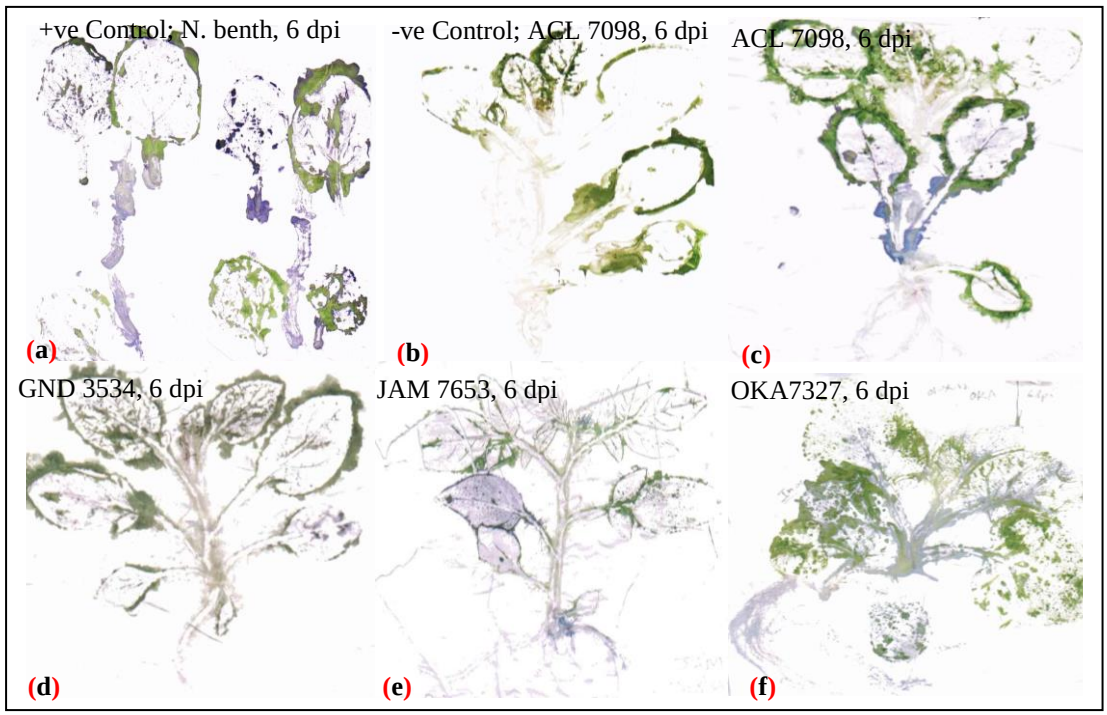

Figure 4.3. Tissue-print analysis of the diploid potato seedlings at 6 dpi. Press-blot of the positive control (**a**) *N. benthamiana*, and the negative control (**b**) ACL 7098 plants. Test seedlings of diploid potato (**c**) ACL 7098 (**d**) GND 3534 (**e**) JAM 7653 and (**e**) OKA 7327. Blue-colour is the TRV-CP detection.

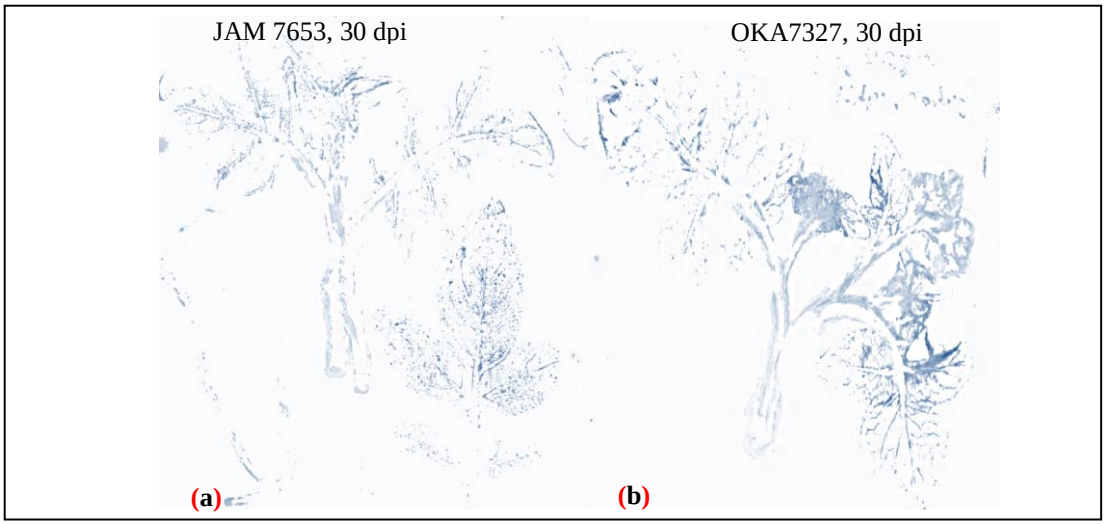

Figure 4.4. Tissue-print analysis of the diploid potatoes at 30 dpi. Press-blot of the test seedlings of diploid potato (**a**) JAM 7653 and (**d**) OKA 7327. Blue colour is the TRV-CP detection.

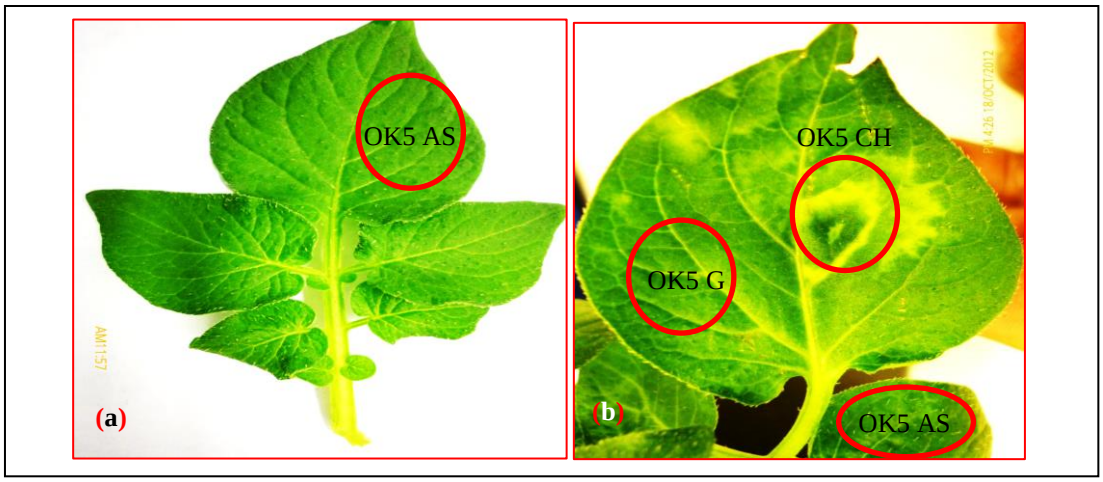

Figure 4.5. Symptomatic leaves of *Solanum okadae*. Systemically-infected **(a)** asymptomatic and **(b)** symptomatic leaf with Chevron-like symptoms. Red-circles mark the sampling-sites. Pictures were taken at 25 dpi.

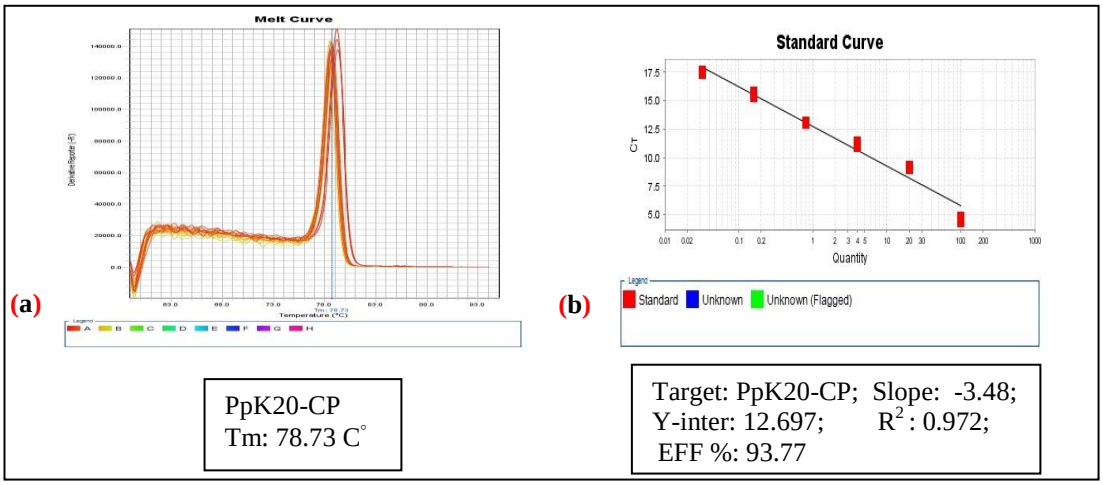

Figure 4.6. Melt-curve and standard-curve analysis of the primer-set for the qRT-PCR of TRV-CP gene (PpK-20 isolate). (a) Melt-curve and **(b)** Standard-curve analysis; Y-inter: Y-intercept; R2: correlation coefficient or regression line coefficient; EFF %: amplification efficiency.

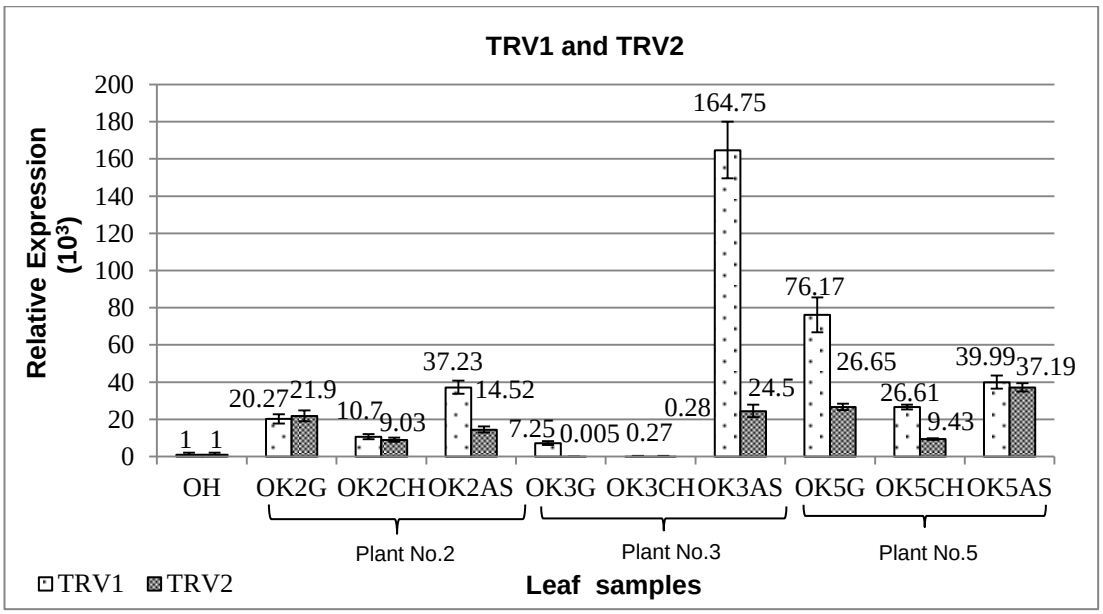

Figure 4.7. Relative quantitation of TRV RNA-1 and RNA -2 in the symptomatic leaves of *Solanum okadae*. OH: Mock-inoculated, healthy plant; OK2, OK3, and OK5: TRV-infected *S.okadae* plant no. 2, 3 and 5, respectively. G: asymptomatic or green area and; CH: chevron-like area from symptomatic leaves; AS: asymptomatic leaves. "ɪ" is the error-bar representing standard error of ΔΔCT measurements.

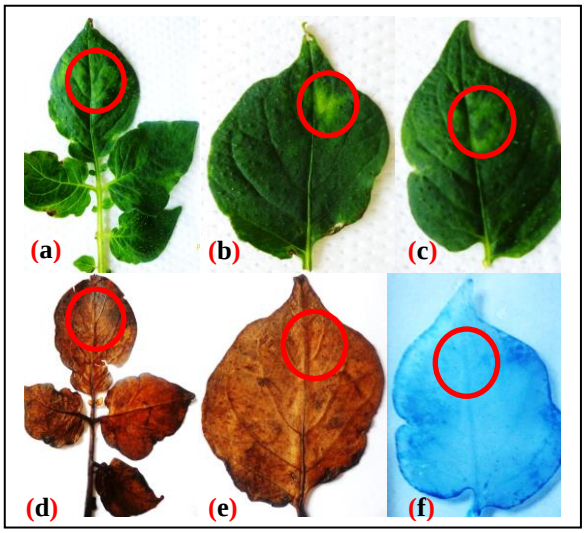

Figure 4.8. Symptomatic leaves of *Solanum okadae* stained with DAB and Trypan-blue. Leaves **(a-b)** before and **(d-e)** after staining with DAB; leaf **(c)** before and **(f)** after staining with Trypan-blue. Circles mark the chevron and mosaic-like regions of the symptomatic leaves.

TRIZOL, RNA purification, DNase treatment, cDNA synthesis and qRT-PCR protocols were the same as given in Chapter No.5 (sections 2.4.3-4; 2.2.3 and 2.4.8.) The relative amounts of TRV RNA-1 and -2 in all the three types of infected (AS, G, and CH) and virus-free (OH) samples were quantified by qRT-PCR and correlated according to the various symptoms. The concentration optimization and validation of the TRV2 (KK20-CP) primer-set (Primer no. 2357 and 2358, Appendix 1) was done by following the same protocol as given in Chapter No. 5 (section 2.4.7). The melt-curve and standard curve analysis of this primer-set gave a single Tm peak (Fig. 4.6, a) with a regression co-efficient (R^2) of 0.972, a regression line slope of -3.48 and an amplification efficiency (EFF %) of 93.772 (b). Details of the TRV1 primer-set (Primer no. 2353 and 2354) are given in Chapter No. 5.

The qRT-PCR of these samples, using Cyclophilin (CyP) as the internal-control gene (Hunter, 2013), showed that TRV1 accumulated to higher levels in most of the asymptomatic (AS) leaves (Fig. 4.7.). However, the accumulation of both the RNA-1 and RNA-2 was suppressed in the leaf regions producing the chevron-like symptoms (CH) as compared to the asymptomatic regions (G) of the same leaves.

The ‘‘green islands’’ and mosaic or chevron-like symptoms induced in plants infected with non-seed-transmitted viruses are the result of localized-resistance (Sheerwood, 1988; Ratcliff *et al*., 1997) to defend against viruses. The symptomatic leaves were stained with DAB and trypan-blue to look for the production of H_2O_2 (ROS species) and the cell-death response, respectively. The staining results (Fig. 4.8.) indicated that the induction of the chevron-like symptoms was an independent response as neither H_2O_2 production nor cell-death could be found in the vicinity of the symptomatic regions.

4.4. Infection of the CP-frameshift mutant (KCPfs)

TRV accumulation in the tetraploid potatoes was extremely low (see Chapter No. 3, section 3.6), therefore, this germplasm was not used for further systemic infection

studies. Identification of the TRV-susceptible diploid potato species provided us with a more preferable genetic source for investigating the systemic infection of the virus in potato. In order to observe any possible effect of the RNA-2 encoded proteins on the co-ordinated systemic infection of RNA2 together with RNA-1, I introduced separate mutations into the RNA-2-encoded genes. The mutants were created by the insertion or deletion of one or more nucleotides at unique restriction sites within the RNA-2 genes. These mutations create a translational frameshift in each of the RNA-2-encoded proteins. The frameshift (fs) mutants of the CP, 2b and 2c genes of the PpK-20 RNA-2 were made by following the protocol given in section 2.2.14 and the frameshift-mutations were confirmed by DNA-sequencing of the mutant clones p1295 (KCPfs), p1296 (K2bfs), and p1299 (K2cfs), respectively. Full-length transcripts of these mutant clones were synthesized by following the protocol given in Chapter No.3 (sections 2.2.7-8.) and rub-inoculated together with RNA-1 on carborundum-dusted leaves of *N. benthamiana* (three plants per mutant clone). The infectious sap was collected at 6 dpi, stored at -20°C, and later rub-inoculated to diploid potatoes for further experimentation.

Besides the wild-type isolate of the virus (K20 wt., M-type isolate), the KCPfs mutant was also found to form a stable inoculum that caused infection in *N. benthamiana* plants (Fig. 4.9, c). The viability of this mutant was confirmed by the freeze-thawing test as described by Harrison *et al*. (1983). Thus after being subjected to two cycles of freeze-thawing the KCPfs mutant-containing leaf sap remained capable of causing infection in *N. benthamiana* plants (d). This treatment is expected to differentiate encapsidated viral RNAs from non-encapsidated viral RNAs, with the latter being destroyed during the repeated freeze-thawing. Western-blot analysis (e) of the total proteins extracted from the plants inoculated with RNA1 only (a), K20 wt. isolate (b), KCPfs without freeze-thawing (c), and with freeze-thawing (d) showed that the K20-CP was only detected in the plants inoculated with the K20 wt. isolate (e, Lane 1, 4 and 5). The KCPfs mutant was made by shifting the frame (ORF) at 193 nts upstream of the carboxy-terminal of the CP and would be expected

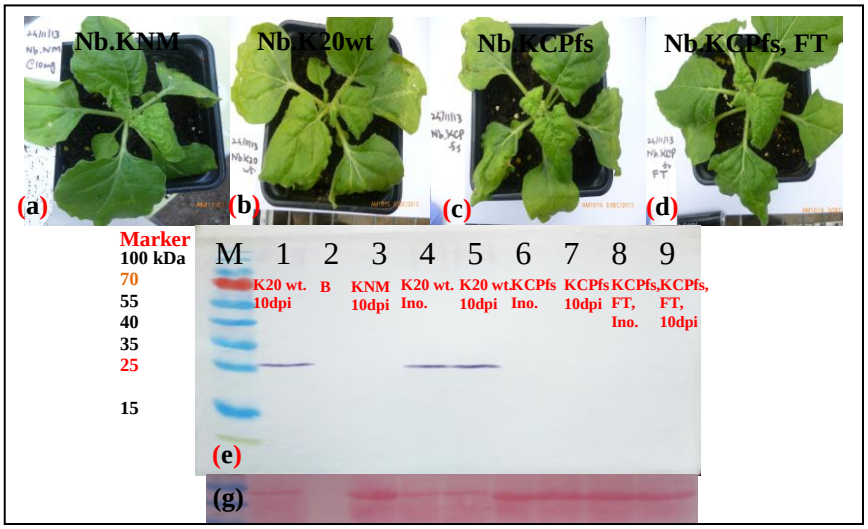

Figure 4.9. *N. benthamiana* infected with TRV inoculum and the western-blot of infected plants. Plants inoculated with **(a)** PpK-20 RNA1 only (KNM), **(b)** PpK-20 M-type (K20 wt.), **(c)** KCPfs without freeze-thaw, and **(d)** with freeze-thaw treatment (KCPfs, FT); **(e)** Western-blot for detection of TRV-CP in **a**-**d**, **Lane M**: Precision Pre-stained Protein Marker; Plants infected with **Lane 1**: K20 wt., positive control; **Lane 2**: loading-buffer (B) only; **Lane 3**: KNM only; **Lane 4**: K20 wt. inoculated (Ino.) and, **Lane 5**: systemically-infected leaves; **Lane 6**: KCPfs inoculated and, **Lane 7**: systemically-infected leaves; **Lane 8**: KCPfs, FT inoculated and, **Lane 7**: systemically-infected leaves **(f)** is the Ponceau S staining of **e**. Samples from inoculated and systemically infected leaves were collected at 4 and 8 dpi, respectively. Lane 2 and 3 are the negative controls of the experiment. Pictures of infected plants were taken at 10 dpi.

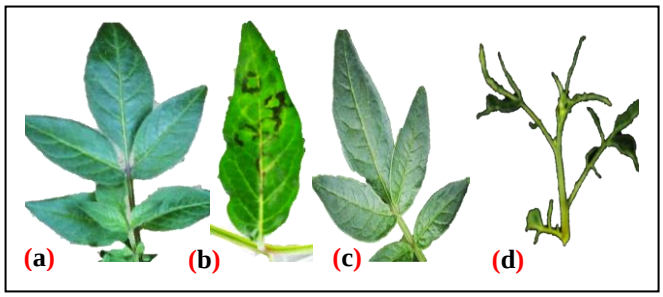

Figure 4.10. Symptoms induced by the TRV inoculum in *Solanum jamesii*. (a) Leaf of a mock-inoculated plant. Leaf inoculated with **(b)** PpK-20 RNA-1 (KNM) isolate, inducing characteristic TRV ring-shaped lesions, and **(c)** PpK-20 M-type (K20 wt.) isolate producing no symptoms (**d**) Top, systemically-infected leaf infected with CP frameshift mutant (KCPfs), displaying leaf-malformation and shoe-string- like symptoms. Pictures were taken at (**a-c**) 7 dpi and (**d**) 30 dpi.

to delete most of the antigenic sites of the TRV CP. The region at the C-terminus of the CP does not affect the particle stability of the virus, but possesses the epitopes that are actively involved in determining the serological properties of the virus. The N-terminal portion and the central 110-121 amino acid residues are weaker in their antigenic properties as compared to the C-terminal region of the CP (Legorburu *et al*., 1995 and 1996). Inoculation of PpK20 RNA-1 only (KNM) on to the leaves of *S. jamesii* produced ring-shaped necrotic lesions on the inoculated leaves, at 4-5 dpi, but the systemically-infected leaves remained asymptomatic (Fig. 4.10, b). The inoculated and systemically-infected leaves of the plants inoculated with K20 wt. isolate were asymptomatic (c).

However, the plants inoculated with the KCPfs mutant produced malformation and shoe-string-like symptoms (Fig. 4.10., d), at 21 dpi, on the top, systemically-infected leaves. The symptom expression was reduced in both severity and incidence at 45 dpi. The mock-inoculated plants remained asymptomatic (a). Infection in these *S. jamesii* plants was confirmed by RT-PCR (section 2.2.16, Fig. 4.11.). The RNA-1 inoculated plants were verified to be free from RNA-2, suggesting the production of characteristic ring-shaped necrotic lesions (b) was associated with RNA-1. Robinson and Harrison (1985b) had also associated the RNA1 of the virus with the production of necrotic lesions in *C. amaranticolor* plants. In the current study the M-type isolate (K20 wt.), containing both RNA-1 and-2, was found to be asymptomatic on *S. jamesii* plants.

The RT-PCR analysis given in Fig. 4.11 showed that even after freeze-thawing of the inoculum, RNA2 of the KCPfs mutant had accumulated systemically within the *N. benthamiana* control plants. Although, very weak amplicons of TRV1 and TRV2 were detectable.

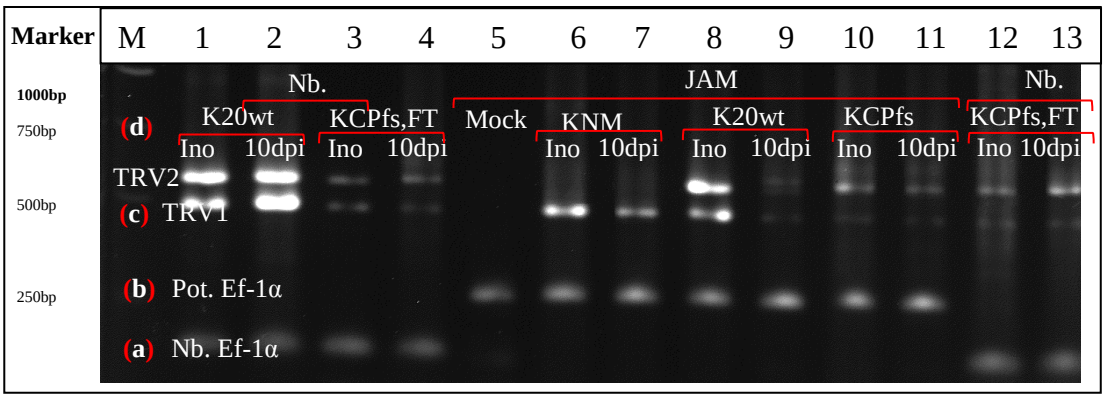

Figure 4.11. RT-PCR assay of the KCPfs mutant infection in *Solanum jamesii*. **Lane M**: 1Kb Promega DNA marker; **Lane 1-4**: positive controls, *N. benthamiana* infected with wild-type PpK20 RNA-2, K20 wt. (Lane 1-2) and the CP frame-shift mutant, KCPfs (Lane 3-4); **Lane 5:** negative control, mock-inoculated *Solanum jamesii (*Mock*)*; **Lane 6-11:** *Solanum jamesii* infected with KNM (Lane 6-7), K20 wt. (Lane 8-9), and KCPfs (Lane 10-11); **Lane 12-13:** *N. benthamiana* infected with freeze-thawed KCPfs inoculum; Leaf-samples were collected at 4 dpi from the inoculated leaves **(Lane 1, 3, 6, 8, 10** and **11)** and from the systemically-infected leaves at 10 dpi **(Lane 2, 4, 7, 9, 11** and **13)**; House-keeping gene, Ef-1α, amplicon from **(a)** *N. benthamiana* (150 bp) and **(b)** potato (255 bp). **(c)** TRV1 Replicase amplicon (474 bp) and **(d)** TRV2 amplicon (K20-CP, 574 bp).

Table 4.3. Optimal concentration of the primer-pair(s) for the qRT-PCR of PDS, ZEP and GBSS genes of potato

S.No.	Targeted gene	Primer name	Primer number	Opt.Conc. (nM)	C_T mean	C_T S.D
1.	PDS	qPDSf	2459	300	22.367	0.102
		qPDSr	2460	300		
2.	ZEP	qZEPf	2461	300	19.954	0.199
		qZEPr	2462	300		
3.	GBSS	qGBSSf	2463	300	27.762	0.268
		qGBSSr	2464	300		

Opt.Conc. Optimal concentration; nM: Nano-Molar C_T mean: Cyclic threshold; C_T S.D: C_T Standard Deviation; PDS: *Phytoene desaturase*; ZEP: *Zeaxanthin epoxidase*; GBSS: *Granule bound starch synthase*.

4.5. Functional analysis of potato genes using virus-induced gene silencing (VIGS)

The effectiveness of VIGS needs the virus to infect the plant, preferably without any symptom production, and to also be capable of multiplying and spreading throughout the plant system. Screening of the 98 CPC accessions identified two diploid potato species viz., *S. jamesii* and *S. okadae* as being very susceptible to TRV and, therefore, as potentially useful for the functional analysis of potato genes using VIGS. Previous studies have demonstrated the utility of TRV for VIGS analyses in an extensive range of plant species. In this current study, the potato genes *Phytoene desaturase* (PDS), *Granule bound starch synthase* (GBSS) and the *Zeaxanthin epoxidase* (ZEP) were selected for VIGS in potato. The relative expression of these genes differs in potato leaves and tubers, and so separate analyses of VIGS in leaves (which can be completed in a few weeks) and VIGS in tubers (which requires several months to complete) were done. The results are presented in separate sections that follow:-

4.5.1. Infection of the TRV VIGS constructs in *N. benthamiana*

Each pTRV2 carrying a silencing-inducing gene fragment (section 2.3.2) was separately mixed with the TRV1 binary-clone (p695) and infiltrated into three *N. benthamiana* plants. The plants that were agro-infiltrated with the PDS construct developed photo-bleaching symptoms at 10 dpi (Fig. 4.12, a and e) and the plants inoculated with the VIGS-clones of ZEP, GBSS, and a virus-control construct showed typical TRV-induced leaf-curling symptoms of the top-most, non-inoculated leaves (b, c, and d). At 6 dpi, infectious sap was prepared from the systemically-infected leaves and stored at -80°C for later use as virus inoculum in the potato silencing experiments.

4.5.2. Concentration-optimization and validation of the primer-sets(s), for qRT-PCR of the PDS, ZEP, and GBSS genes of potato

The concentration optimization and validation of the primer-sets for PDS, ZEP, and GBSS genes was done by following the already explained method (section 2.4.7). The optimal concentrations (Opt. Conc.) of the tested primer-pairs with the lowest C_T means and acceptable C_T S.Ds (< 0.167) are given in Table No. 4.3. Since, the GBSS is lower in its expression in potato leaves as compared to the tubers (Visser *et al*., 1991; Kuipers *et al*., 1994), therefore, cDNA was synthesized from total RNA isolated from tubers of *S. jamesii* and a 1/25 dilution of this cDNA was used as a template in the GBSS gene standardization experiments.

The melt-curve analysis, gave a single Tm peak for each primer-set (Appendix 10, I, a-c) that ruled-out any possibility of non-specific amplification. The standard-curve analysis (II, a-c) gave regression co-efficients (R^2) of 0.962, 0.998, and 0.989; regression line slopes of -3.478, -3.073, and -3.26; and amplification efficiencies (EFF%) of 93.856, 111.566, and 102.673 for the primer-sets of PDS, ZEP, and GBSS, respectively. Thereafter, qRT-PCR analysis of PDS, ZEP, and GBSS expression was done in both leaves and tubers, following TRV-VIGS treatment (section 4.5.3 and 4.5.4).

4.5.3. Gene-silencing in potato leaves.

The *S. jamesii* and *S. okadae* (section 2.1.2) plants were mechanically inoculated at the 4-5 leaf stage with the infectious sap of the *N. benthamiana* plants infected with the VIGS-constructs of PDS, ZEP, GBSS, and the virus-control (section 4.5.1). Each construct was inoculated onto three plants of each potato species that were grown in two batches. One batch (Batch No.1) consisting of both *S. jamesii* and *S. okadae* seedlings. Whereas, the second batch (Batch No.2; grown the following year) was comprising only of *S. jamesii* plantlets that were raised through apical stem-culture of healthy *S. jamesii* plants (i.e.; JH1 and JH2, retained as mother plants for further

experimentation) from the Batch No. 1 experiment. The seedlings of *S. jamesii* exhibited photo-bleaching of the top, systemically-infected leaves 11 days after infection with the TRV-PDS construct (Fig. 4.13, a). These symptoms appeared at almost the same time as in the similarly treated *N. benthamiana* plants. However, the appearance of photo-bleaching in the systemically-infected leaves of *S. okadae* was delayed until 16-17 dpi and the symptoms were weaker in both their incidence and intensity. The plants inoculated with the other VIGS-constructs remained asymptomatic (b-d). The severity and incidence of the photo-bleaching in the PDS-silenced plants of *S. jamesii* (at 12, 23, and 40 dpi) and *S. okadae* (at 18, 23, and 40 dpi) are shown in Fig. 4.14. The photo-bleaching symptoms appeared 4-5 days later on the *S. jamesii* plants that were raised through apical-stem culture than from seed (c vs. g) and also the symptoms were weaker in severity. Leaf disc samples from the top, systemically-infected leaves were collected at 22 dpi (Batch No.1) and 40 dpi (Batch No. 1 and 2). Sampling of the leaf-tissue was done as shown in Fig. 4.14, i.

The 22 dpi RNA samples from all the three plants inoculated with each treatment were combined in a composite sample prior to cDNA synthesis and qRT-PCR. The optimal primer concentration and primer-details are given in Table No. 4.3. and Appendix 8, respectively. The qRT-PCR quantification was done by the comparative C_T ($\Delta\Delta C_T$) quantitation method. The fluorescence signals of the targeted genes were normalized with the cyclophilin gene (Hunter, 2013).

1. *VIGS in seed-derived plants (Batch No.1)*

The qRT-PCR quantification of the seed-derived plants (Batch No.1) at 22 dpi (Table No. 4.4 and Fig. 4.15), showed that the expression of PDS mRNA relative to the calibrator was knocked down (KD) by 57% and 76% (a) in *S. jamesii* and *S. okadae*, respectively. The expression of ZEP was KD by 37% (b) but only in the *S. jamesii* plants. The silencing of ZEP was not successful in *S. okadae*. The expression of GBSS was reduced to 42% and 47% (c) in *S. jamesii* and *S. okadae*, respectively.

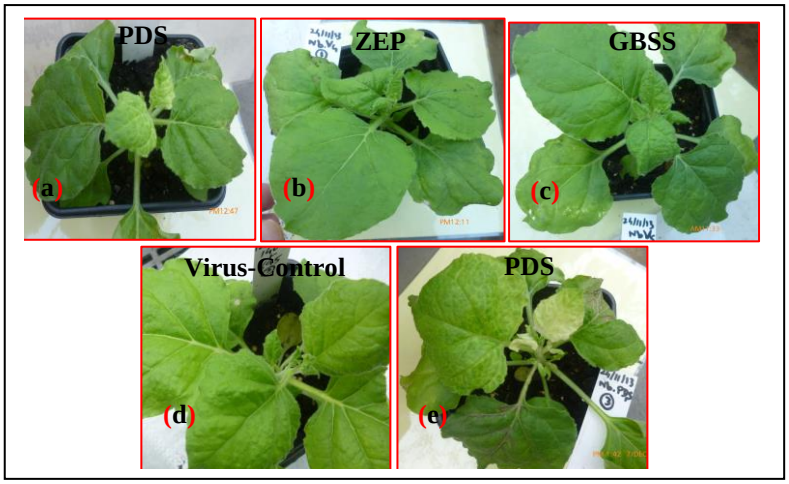

Figure 4.12. *N. benthamiana* plants infected with various VIGS-constructs. Plants infected with TRV1 and VIGS-construct of **(a)** PDS **(b)** ZEP **(c)** GBSS and **(d)** Virus-Control, empty-TRV **(e)** same plant in **a**. Pictures were taken at 10 dpi (**a-c**) and 13 dpi (**d and e**).

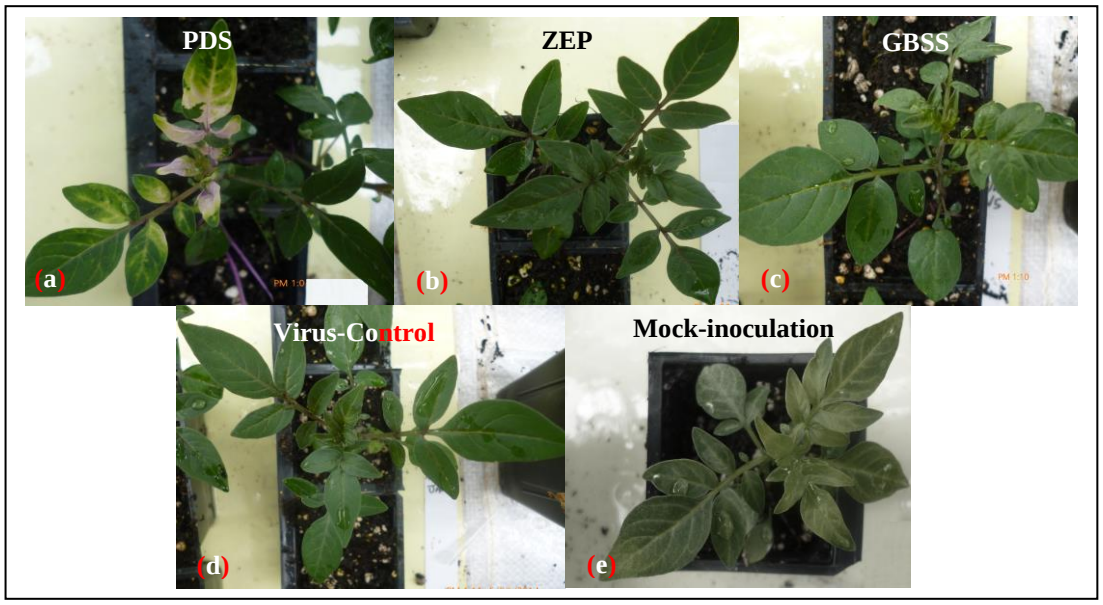

Figure 4.13. *S. jamesii* plants infected with various VIGS-constructs. Plants infected with TRV1 and VIGS-construct of **(a)** PDS **(b)** ZEP **(c)** GBSS and **(d)** Virus-Control, empty-TRV **(e)** Mock-inoculation (1X PBS). Pictures were taken at 12 dpi (Batch No.1).

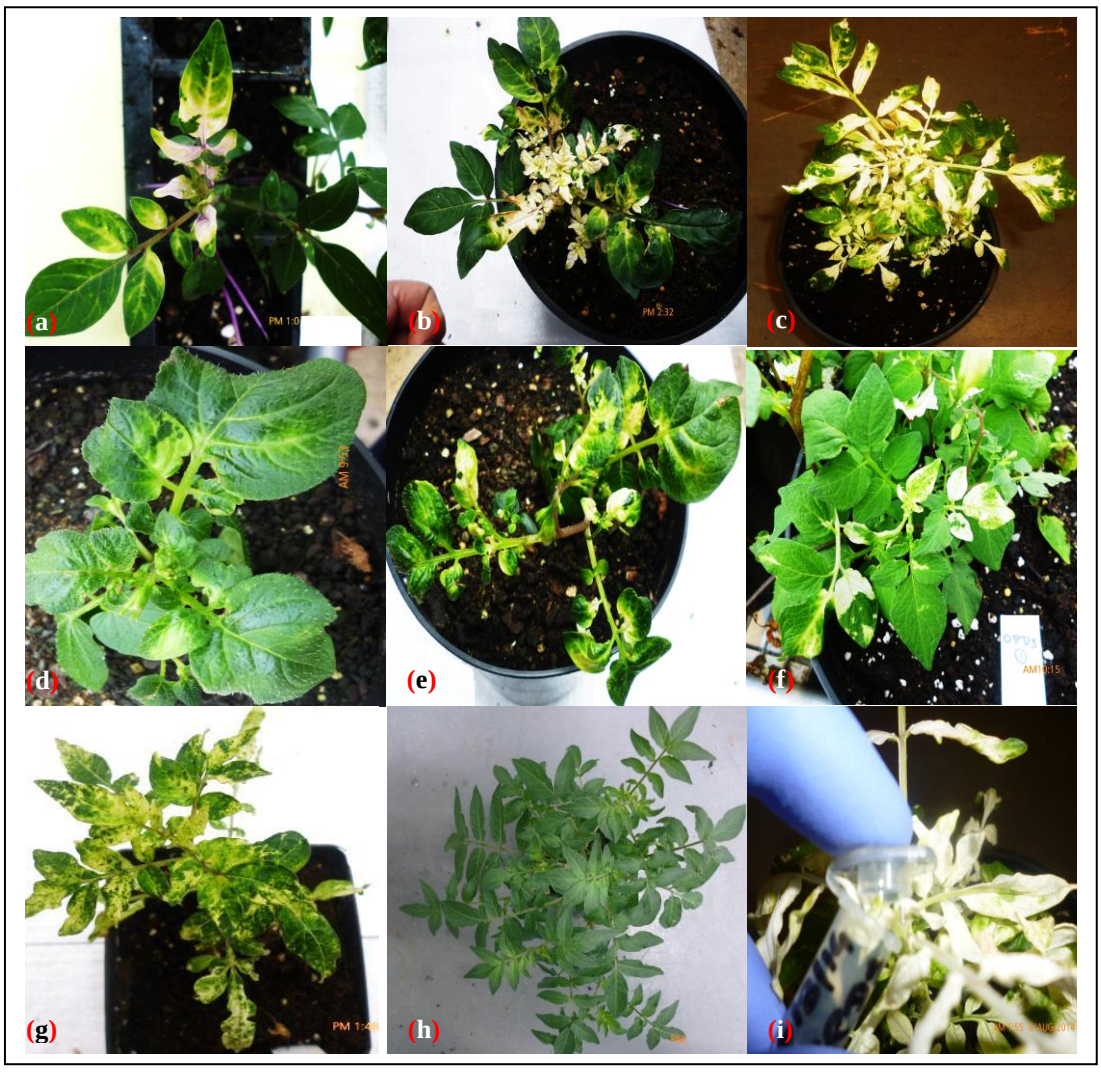

Figure 4.14. PDS-silenced *S. jamesii* and *S. okadae* plants. PDS-silenced plants of *S. jamesii* at **(a)** 12 dpi **(b)** 23 dpi and **(c, g)** 40 dpi; and *S. okadae* at **(d)** 18 dpi **(e)** 23 dpi and **(f)** 40 dpi. **(h)** Mock-inoculation (1X PBS), *S. jamesii* at 40 dpi **(i)** sampling of PDS-silenced leaf-tissue. Plants in **a-f** and **h** were raised from true-seeds (Batch No.1) and in **g, h** from apical stem-cutting (Batch No.2).

Although greater reduction of PDS and GBSS gene expression was recorded in the *S. okadae* plants compared to the *S. jamesii* plants. *S. okadae* was not selected for further VIGS experiments. This was because of the failure of the ZEP-based construct to induce the silencing of ZEP in *S. okadae* and because of the delayed expression of photo- bleaching symptoms, with a 5-6 days delayed appearance, in *S. okadae* as compared to *S. jamesii*. Moreover, the incidence of photo-bleaching was less uniform in *S. okadae* (Fig. 4.14, b vs. e, and c vs. f). Therefore, *S. jamesii* was considered as the preferred host for carrying out further VIGS-related studies in potato.

Following the promising results of potato gene-silencing, more leaf-disc samples were collected at 40 dpi from *S. jamesii* plants only. In order to observe the response of each individual potato plant to the VIGS-construct, the RNA samples from these plants were not bulked together and each qRT-PCR reaction was done with a different individual plant.

The qRT-PCR quantification at 40 dpi (Fig. 4.15, d-f) showed a 50 to 68 % reduction in the PDS expression with a mean % KD of 56 (Table No. 4.4). The targeting of the ZEP mRNA revealed silencing of 67 to 90% (e) with a mean silencing of 52%. The ZEP mRNA in one (JZ2) of these plants was not silenced. The silencing of the GBSS mRNA ranged from 24-95%, (f) with a mean of 62% KD.

2. *VIGS in plants raised by stem-cutting (Batch No.2)*

The following season a new batch (Batch No.2) of *S. jamesii* plants was raised by planting of apical-stems from the healthy (mother) plants (section 2.3.4). This approach significantly reduces the period required for completion of VIGS-studies. This technique produced single tubers at the stem-nodes and was effective in overcoming plant to plant variation in tuber production that could affect functional analysis of the tuber genes. Inoculations and sample processing was done by the methods already described. The leaf-disc samples collected at 40 dpi from three

biological replicates of each treatment were analysed by the qRT-PCR (Fig. 4.16, a-c) to reveal a % KD of PDS ranging from 42 to 88% (a) with a mean % KD of 66% (Table No. 4.4). The silencing of ZEP ranged from 57 to 60% (b) with a mean % KD of 58%.The VIGS of GBSS revealed a % KD of 20 to 50% (c), with a mean % KD of 40%. It appears from these results that infection by TRV itself (the empty-virus control (JC, C) sometimes increases expression of the targeted genes (Fig. 4.15-17).

4.5.4. Gene-silencing in the potato tubers.

The tubers harvested from these *S. jamesii* plants (Batch No. 2) were also evaluated for the efficacy of VIGS. The qRT-PCR quantification (Fig. 4.17, a-c) revealed % KD of 81 to 92 %, (a) with mean % KD of 88% for the expression of PDS mRNA (Table No. 4.5). The silencing of ZEP showed % KD of 2 to 79% (b) with a mean % KD of 44%. The expression of GBSS gene was silenced 9 to 85% (c) with a mean % KD of 39%. The impact of this gene-silencing on the normal physiological functions of these tubers was assayed by evaluating the carotenoids (Phytoene) and sugar-metabolism (staining for starch) of the tubers.

Carotenoids are vital constituents of all organisms that use a photosynthetic system for their survival, as they shield the photosynthetic machinery from the photo-bleaching (chlorophyll bleaching) effects of high intensity light. Carotenoids are also involved in the biosynthesis of Abscisic acid (ABA) and also provide different colours to the fruits and flowers that attract animals and insects (Hirschberg, 2001). *Phytoene desaturase* (PDS) is an important carotenoid that protects the photosynthetic apparatus of the plants. The gene-silencing of PDS results in increased expression of phytoene and the appearance of photo-bleaching. The major carotenoids from the gene-silenced tubers were chromatographically quantified by examining the peak heights of component carotenoids in the tubers. The carotenoid analysis revealed a noticeable increase (Table No. 4.6, Fig. 4.18) in the phytoene-content of the PDS-silenced tubers.

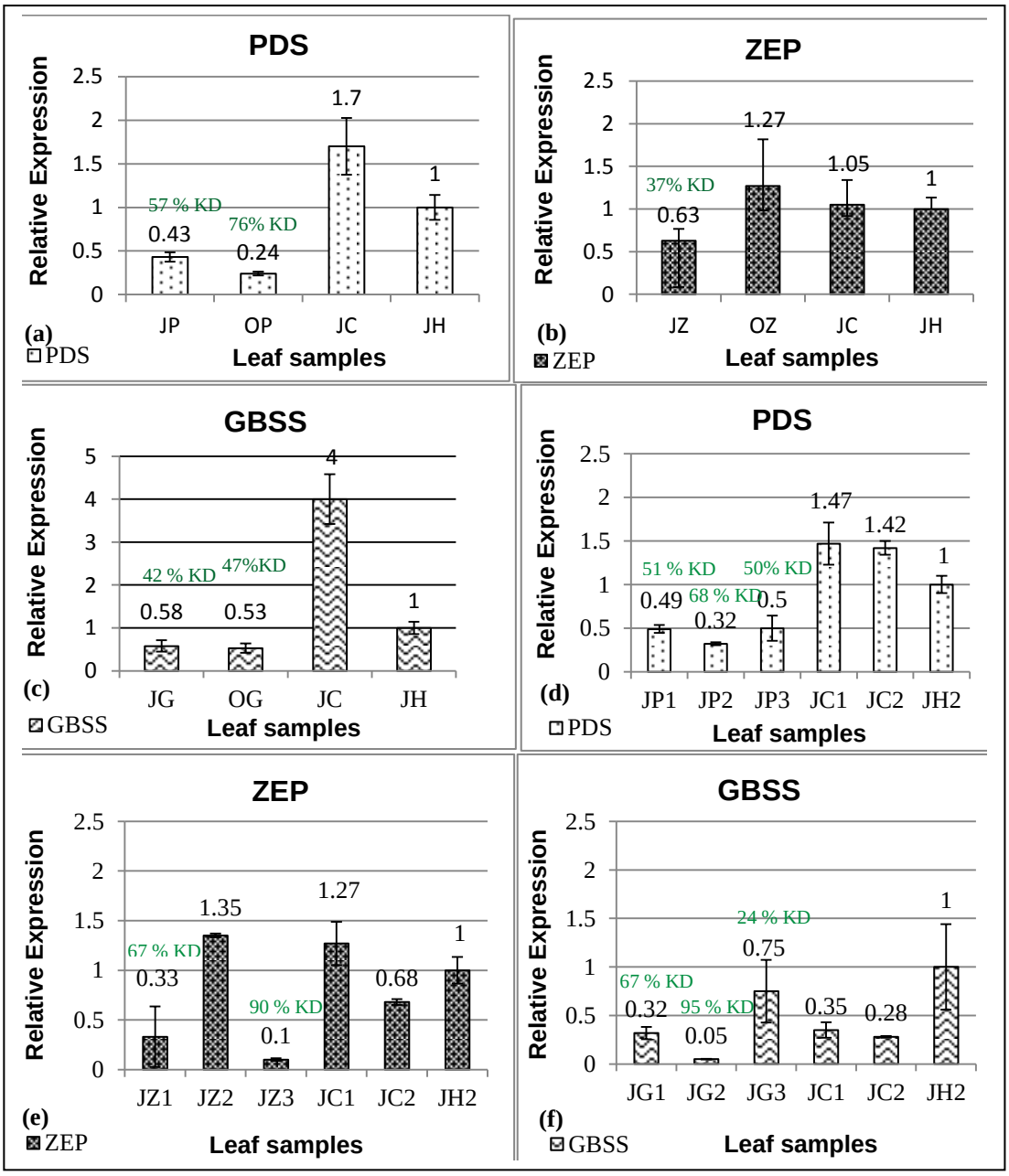

Figure 4.15. Knock-down of gene expression in the leaves of seed-derived plants (Batch No.1), at 22 dpi (a-c) and 40 dpi (d-f). (a, d) PDS-silencing **(b, e)** ZEP-silencing and **(c, f)** GBSS-silencing. Three plants of targeted gene combined in each sample **(a-c)** and analysed separately **(d-f)**. J: *S. jamesii*, and O: *S. okadae* plants. C: empty TRV-vector, H: mock-inoculated, P: PDS-VIGS, Z: ZEP-VIGS and G: GBSS-VIGS.1, 2, and 3 denotes the individual plants or biological replicates. ''ɪ'' is the error-bar representing standard error of ΔΔCT measurements; value above bar is % KD of the gene. Sample H2 is the calibrator.

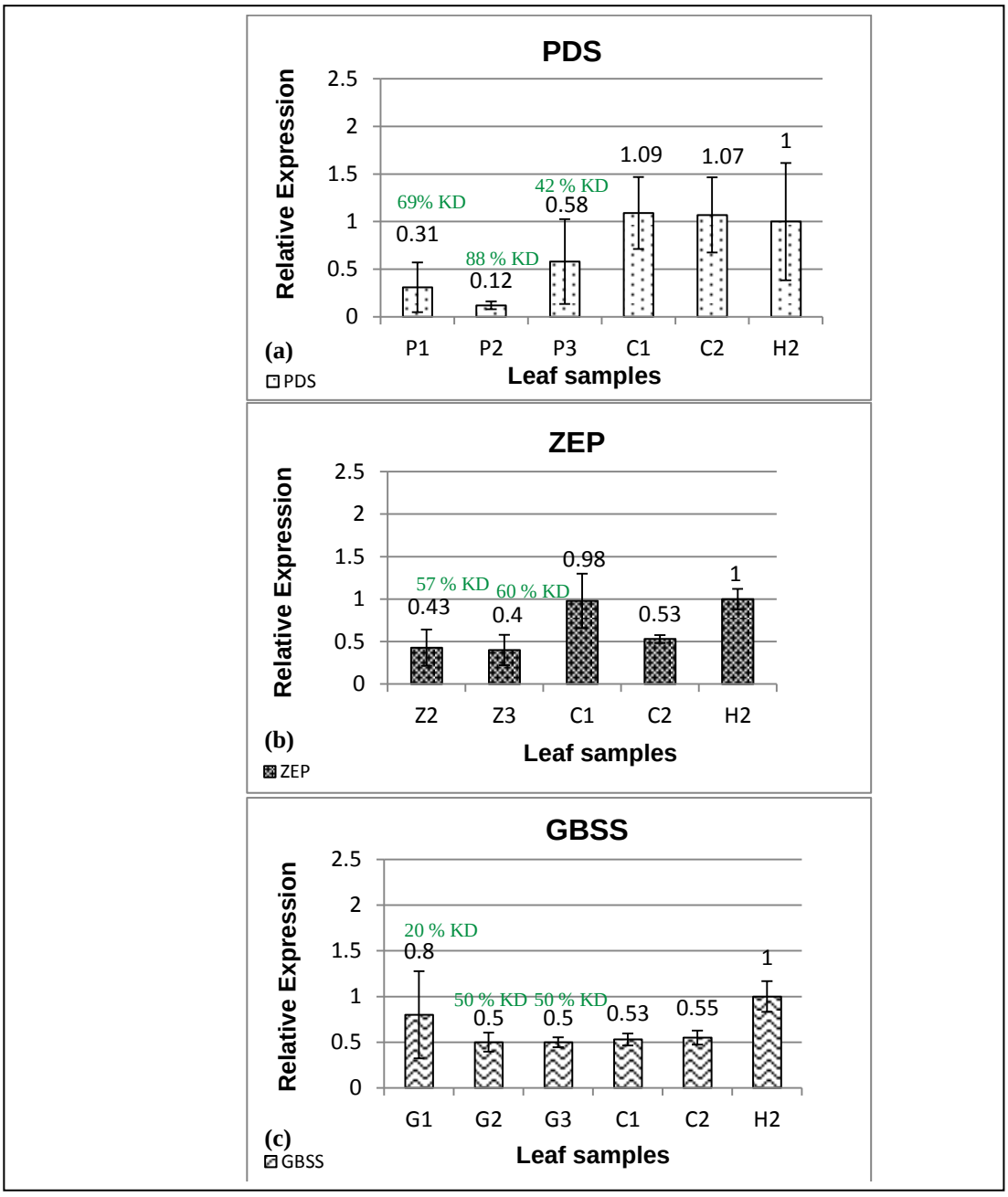

Figure 4.16. Knock-down of the gene expression in the leaves of apical-stem cultured *S. jamesii* plants (Batch No.2), at 40 dpi. (a) PDS-silencing **(b)** ZEP-silencing and **(c)** GBSS-silencing. C: empty TRV-vector, H: mock-inoculated, P: PDS-VIGS, Z: ZEP-VIGS and G: GBSS-VIGS. 1, 2, and 3 denotes the individual plants or biological replicates. ''ɪ'' is the error-bar representing standard error of ΔΔCT measurements; value above bar is % KD of the gene. Sample H2 is the calibrator.

Table 4.4. VIGS in the potato leaves

S.No.	Targeted gene	VIGS at 22dpi in seedling raised plants (Batch No.1)			VIGS at 40dpi in seedling raised plants (Batch No.1)			VIGS at 40dpi in apical stem cultured plants (Batch No.2)		
		Sample	**Relative mRNA**	**% KD of gene**	**Sample**	**Relative mRNA**	**% KD of gene**	**Sample**	**Relative mRNA**	**% KD of gene**
1.		JP	0.43	57	JP1	0.49	51	P1	0.31	69
		OP	0.24	76	JP2	0.32	68	P2	0.12	88
		JC	1.7	N/A	JP3	0.5	50	P3	0.58	42
		JH	1	N/A	**Mean**	**0.44**	**56.33**	**Mean**	**0.34**	**66.33**
	PDS				JC1	1.47	N/A	C1	1.09	X
					JC2	1.42	N/A	C2	1.07	X
					Mean	**1.44**	N/A	**Mean**	**1.15**	X
					JH2	1	N/A	H2	1	N/A
2.		JZ	0.63	37	JZ1	0.33	67.44			
		OZ	1.27	X	JZ2	1.35	-----	Z2	0.43	57
		JC	1.05	X	JZ3	0.1	90.02	Z3	0.4	60
		JH	1	N/A	**Mean**	**0.59**	**52.49**	**Mean**	**0.41**	**58**
	ZEP				JC1	1.27	X	C1	0.98	2
					JC2	0.68	32	C2	0.53	47
					Mean	**0.97**		**Mean**	**0.75**	
					JH2	1	N/A	H2	1	N/A
3.		JG	0.58	42	JG1	0.32	67	G1	0.8	20
		OG	0.53	47	JG2	0.05	95	G2	0.5	50
		JC	4	X	JG3	0.75	24	G3	0.5	50
		JH	1	N/A	**Mean**	**0.37**	**62**	**Mean**	**0.60**	**40**
	GBSS				JC1	0.35	65	C1	0.53	47.16
					JC2	0.28	72	C2	0.55	44.52
					Mean	0.31		**Mean**	**0.54**	**45.84**
					JH2	1	N/A	H2	1	N/A

PDS, *Phytoene desaturase*; ZEP, *Zeaxanthin epoxidase*; GBSS, *Granule bound starch synthase*. mRNA: messenger RNA; J: *S. jamesii*, and O: *S. okadae* plants. C: empty TRV-vector, H: mock-inoculated, P: PDS-VIGS, Z: ZEP-VIGS and G: GBSS-VIGS. 1, 2, and 3 denotes the individual plants or biological replicates. X: not determined; N/A: not applicable; JH, JH2 and H2 are the calibrator or reference samples for relative quantitation. **%** KD: % Gene Knock down.

Most higher plants store their reserve carbohydrates in the form of starch. This storage carbohydrate mainly consists of amylose (a linear-glucan) and amylopectin (a branched-glucan). The configuration of the starch granules is formed by the amylopectins that are interspersed with the amylose molecules. The growth of these main constituents of the starch granules is promoted by a group of enzymes that are generally known as ‘‘Starch synthases’’. These enzymes are further categorised into soluble starch synthases (SSS) and granule-bound starch synthases (GBSS). Amylose synthesis involves the enzymatic activity of GBSS. The potato starch contains nearly 20% amylose and 80% amylopectin (Kuipers *et al.*, 1994; Smith *et al.*, 1997, 2001). Silencing of the GBSS always suppresses amylose production.

Tubers from plants infected with the VIGS-constructs were harvested, sliced using a vibroslicer and stained with Lugol’s solution (section 2.3.3). The images of the stained tuber-slices presented in Fig. 4.19. are representative of three biological replicates for each silenced gene. The whole-tuber sections (a-e) were differentially stained with Lugol’s iodine solution, producing an intensely stained slice from the healthy tuber (a) with less intense staining in the PDS silenced tubers (c). The tuber slices from the GBSS-silenced tubers were faintly stained (e). More critical observation showed that the slices from the virus-control (b) and ZEP-silenced tubers (d) were also less strongly stained than tubers from untreated plants.

Table 4.5. VIGS in the potato tubers (Batch No.2)

S.No.	Targeted gene	VIGS in the potato-tubers		
		Sample	**Relative mRNA**	**% KD of gene**
1.		PT1	0.1	90.07
		PT2	0.07	92.38
		PT3	0.18	81.57
		Mean	**0.12**	**88.01**
	PDS	CT1	0.11	89.13
		CT2	0.14	86.19
		CT3	0.93	6.93
		Mean	**0.39**	**60.75**
		HT2	1	N/A
2.		ZT1	0.49	50.47
		ZT2	0.98	2.14
		ZT3	0.21	78.79
		Mean	**0.56**	**43.8**
	ZEP	CT1	0.51	49.39
		CT2	1.69	-----
		CT3	1.3	-----
		Mean	**1.17**	**16.38**
		HT2	1	N/A
3.		GT1	0.15	84.63
		GT2	0.76	23.81
		GT3	0.90	9.46
		Mean	**0.60**	**39.3**
	GBSS	CT1	5.22	-----
		CT2	3.52	-----
		CT3	2.64	-----
		Mean	**3.79**	**-----**
		HT2	1	N/A

PDS, *Phytoene desaturase*; ZEP, *Zeaxanthin epoxidase*; GBSS, *Granule bound starch synthase*. mRNA: messenger RNA; T: denotes cDNA of tuber-tissue; C: empty TRV-vector, H: mock-inoculated, P: PDS-VIGS, Z: ZEP-VIGS and G: GBSS-VIGS. 1, 2, and 3 denotes the individual plants or biological replicates. -----: not determined; N/A: not applicable; H2 is the calibrator or reference samples for relative quantitation. **%** KD: % Gene Knock down.

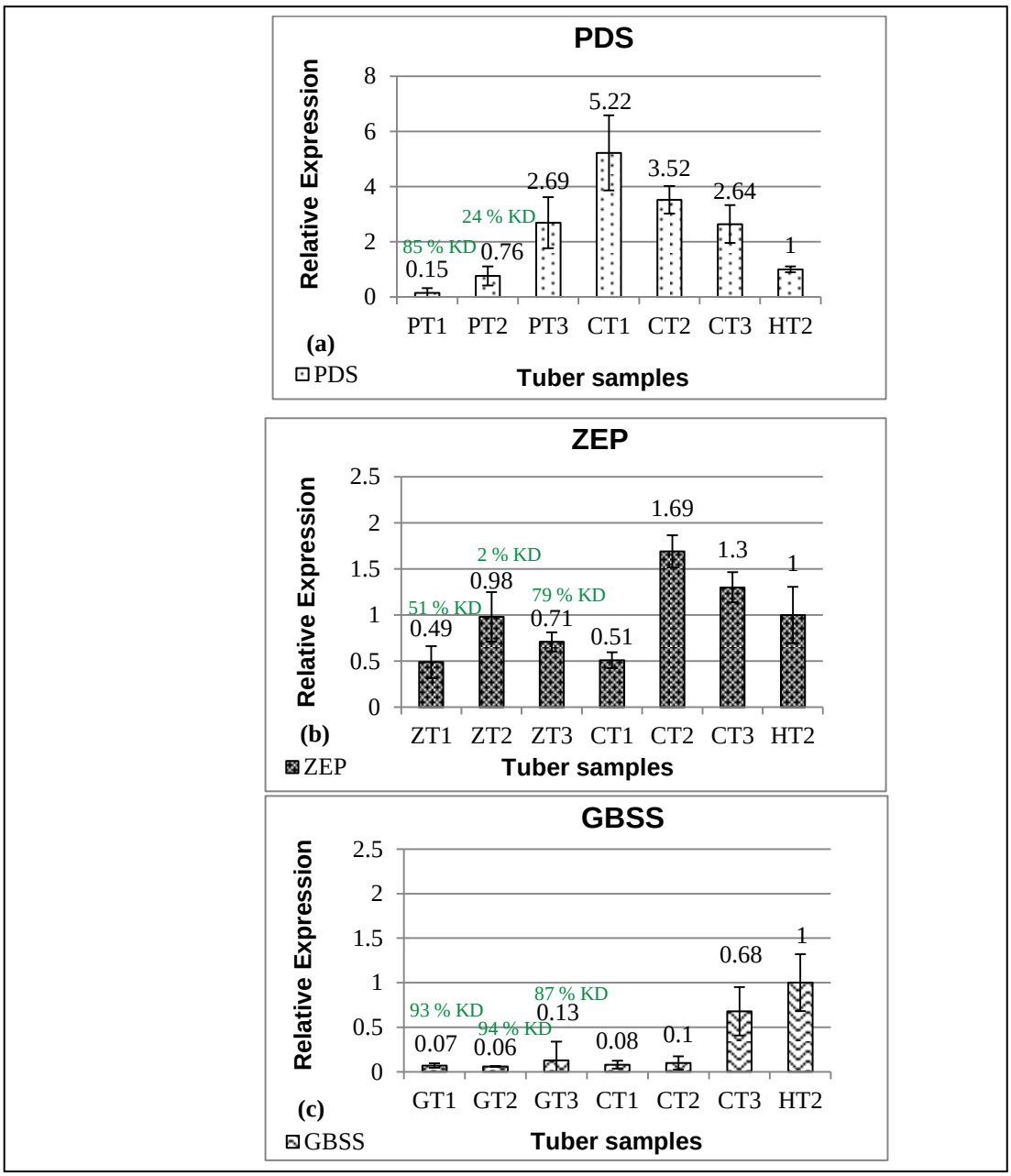

Figure 4.17. Knock-down of gene expression in the tubers of apical-stem cultured *S. jamesii* plants (Batch No.2). (a) PDS-silencing **(b)** ZEP-silencing and **(c)** GBSS-silencing. C: empty TRV-vector, H: mock-inoculated, P: PDS-VIGS, Z: ZEP-VIGS and G: GBSS-VIGS. T1, T2, and T3 denote the tubers from individual plants or biological replicates. ''ɪ'' is the error-bar representing standard error of ΔΔCT measurements; value above bar is % KD of the gene. Sample H2 is the calibrator.

Table 4.6. Phytoene in the PDS-silenced tubers

S.No.	Targeted gene	Gene-silenced tuber collected from biological replicate no.	Phytoene (mAU*min 285nm)	Std. Dev.	Std. Error
1.	PDS	JP1	12.01	11.588	6.690
		JP2	6.36		
		JP3	28.65		
		Mean	**15.673**		
2.	ZEP	JZ1	1.45	0.442	0.255
		JZ2	1.60		
		JZ3	0.77		
		Mean	**1.273**		
3.	Virus-control (JC)	JC1	0.16	0.726	0.419
		JC2	0.00		
		JC3	1.33		
		Mean	**0.497**		
4.	Healthy control (JH)	JH1	0.23	0.382	0.221
		JH2	0.94		
		JH3	0.83		
		Mean	**0.667**		

PDS: *Phytoene desaturase*; ZEP: *Zeaxanthin epoxidase*; Std. Dev.: Standard Deviation; Std. Error.: Standard Error. The total carotenoid analysis was done by Dr. Wayne Morris, JHI.

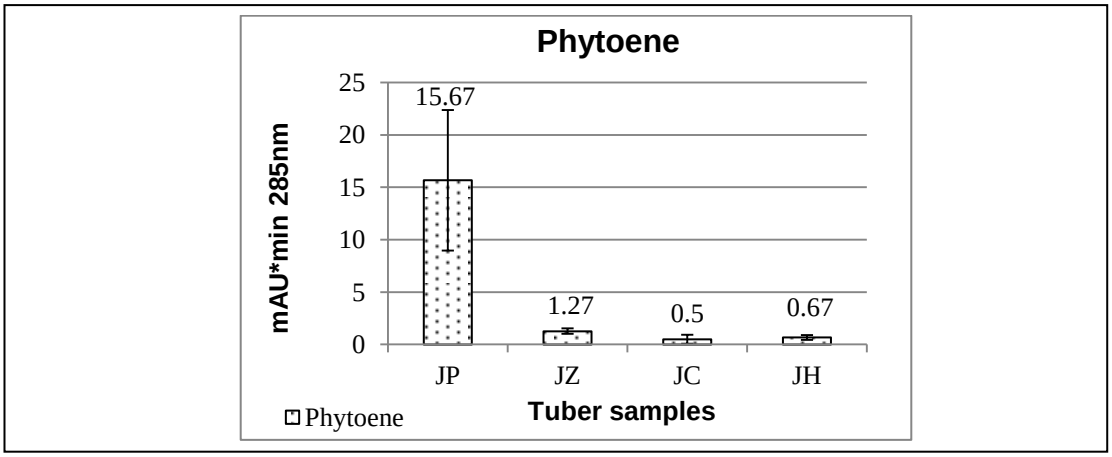

Figure 4.18. Effect of PDS-silencing on tuber-carotenoids. Amount of Phytoene in the *Solanum jamesii* tubers harvested from PDS-silenced (JP), ZEP-silenced (JZ), TRV-control (JC) and mock-inoculated (JH) plants.

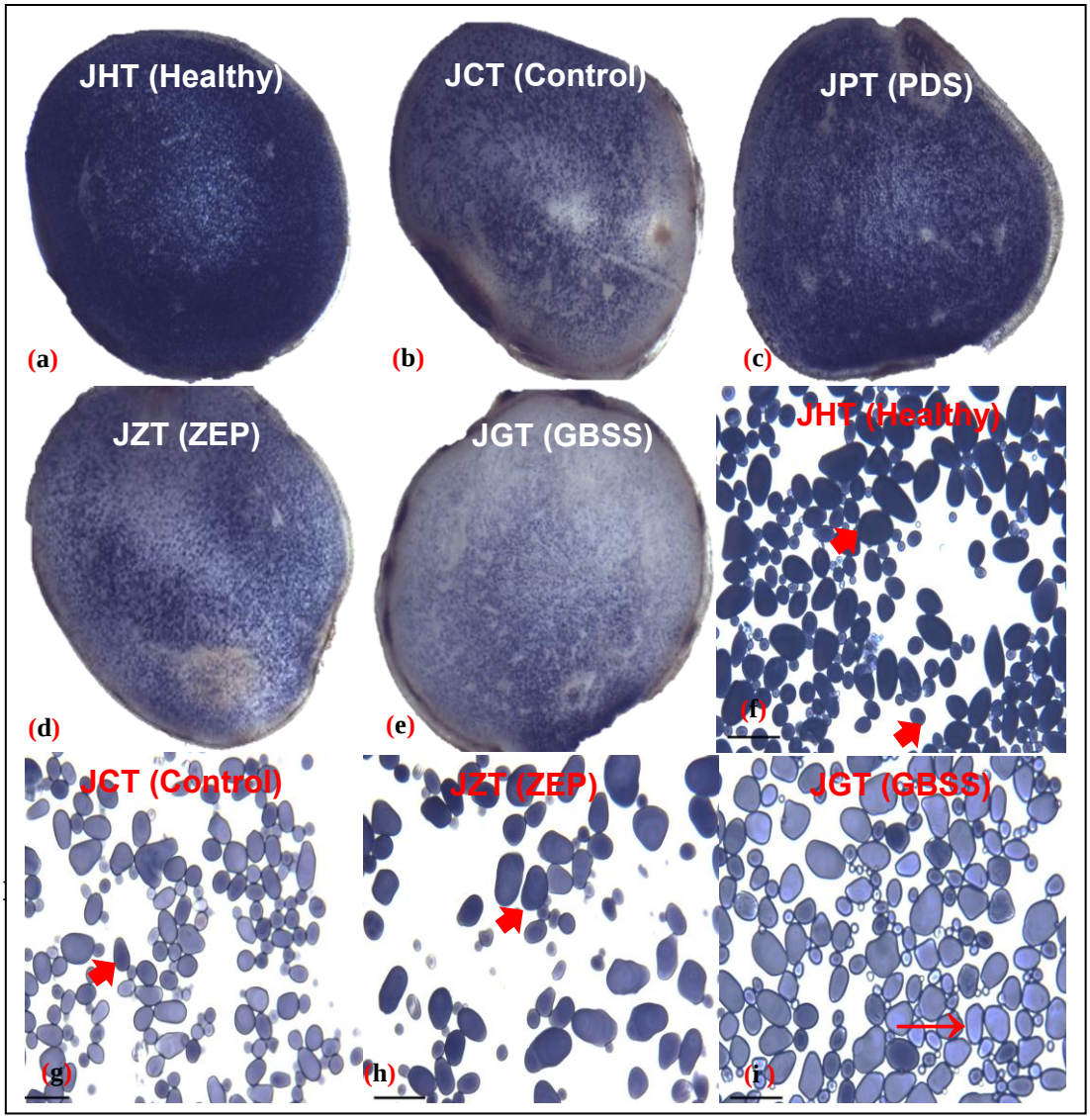

Figure 4.19. Staining of tuber starch. Lugol's stained sections of the tubers infected with **(a)** JH, healthy, mock-inoculated, **(b)** JCT, virus-control **(c)** JPT, PDS-silenced **(d)** JZT, ZEP-silenced and **(e)** JGT, GBSS-silenced tubers. Lugol's stained starch-granules **(f-i)** from the tubers in **a**, **b**, **d**, and **e**, respectively. Arrow (→) points to the GBSS-silenced and arrow-head to the non-silenced starch granules. Scale bar = 50 µm

Starch granules from these tubers were extracted by following the protocol given in section 2.3.3 and the isolated granules were stained with Lugol's solution. The amylose in the starch granule is stained dark blue by the Lugol's solution. The GBSS-silenced starch granules of the transgenic potatoes are either opaque or reddish-brown due to the complete absence of amylose or are stained light to dark-blue depending upon the efficacy of the GBSS–silencing (Anonymous, 2011). Amylose in the starch granules affected by the silencing of GBSS is intensely deposited in the co-central rings of the granules and is localised to the centre of the granule rather than the peripheral part of the granule. The starch granules isolated from the healthy tubers were intensely stained (Fig. 4.19, f), followed with the granules from ZEP-silenced tubers being slightly less stained (h). However, the granules from the GBSS-silenced tubers were stained least intensely and comprised a mixture of granules that were lightly stained to varying degrees (i) as silencing is never 100% efficient (Velasquez *et al.*, 2009) when using the VIGS. Silencing modifies the gene-expression to varying levels but it never eliminates the gene-expression (Robertson, 2004). Similarly, some of the granules isolated from the tubers infected with the empty-virus construct (virus-control) were also lightly stained suggesting that some reduction in the GBSS expression could also be caused by the virus itself.

4.6. *Solanum jamesii* as a model potato species for TRV infection studies

Solanum jamesii is an erect to spreading-type diploid species (Fig. 4.20, a) that is amenable to both cabinet and glass-house culturing and can also be produced through apical-stem cuttings (f). It develops profuse stolons bearing abundant numbers of tubers (b, and c). An apical stem-cutting with developing tuber is shown in Fig. 4.20, g. The fully developed tubers are about 1-1.5 cm^2 in diameter (d) and can be used for investigating the functional analysis of genes related to tuber development. In the current studies, *S. jamesii* proved to be a good host for investigating TRV infection

Figure 4.20. *Solanum jamesii* as a model potato species for TRV-infection. (a) Healthy three months old mother plant **(b)** tuberization in **a (c)** cleaned tubers **(d)** close-up of a tuber from **c,** Scale bar = 0.5 cm **(e)** Sprouts from healthy vs. PDS-silenced tubers. Tuberization in the plants raised by apical stem-planting **(f)** Tuber developing at the stem-node **(g)** close-up of tuber in **f**

of potato.

The tubers harvested from plants infected with the gene-silencing constructs (section 4.5.4) were sown in compost and examined for the regeneration of VIGS symptoms in emerging sprouts. Thus, the tubers infected with the PDS-silencing construct produced photo-bleached sprouts (Fig. 4.20, f). A total of 50 tubers from TRV-PDS-infected plants were sown, 44 of these tubers produced photo-bleached sprouts and six of the tubers produced sprouts without any photo-bleaching. Among the photo-bleached sprouts, some were completely albino and stunted in growth. However, sprouts from the healthy (mock-inoculated) tubers were normal in growth (Fig. 4.20, a). Sprouts emerging from GBSS-silenced tubers were with sparse foliage and some of the tubers produced sprouts with shoe-string-like and mottling symptoms.

4.7. Discussion

VIGS is one of the most widespread techniques used across the world for plant functional genomics analysis. The effectiveness of VIGS needs the virus to infect the plant, preferably without any symptom production, and to also be capable of multiplying and spreading throughout the plant system. TRV has a wide host-range (more than 400 plant species), systemically infect many plant species, produces few or mild symptoms and does not express a strong silencing suppressor protein (Ratcliff *et al*., 2001; Padmanabhan and Dinesh-Kumar, 2009; Senthil-Kumar and Mysore, 2011a). VIGS analysis using TRV has been successfully demonstrated in an extensive range of plant species, including members of the family Solanaceae notably the model-plant *Nicotiana benthamiana* (Ratcliff *et al*., 2001; Liu *et al*., 2002a; Lu *et al*., 2003), *S. lycopersicum* (Liu *et al*., 2002b; Ekengren *et al*., 2003; Fu *et al*., 2005), *Capsicum annum* (Chung *et al*., 2004), *Papaver somniferum* (Hileman *et al*., 2005), *Petunia* (Chen *et al*., 2004; Spitzer *et al*., 2007), *Solanum nigrum* (Hard *et al*., 2008) and some *Solanum* species of potato (Brigneti *et al*., 2004, Dobnik *et al*., 2016). TRV has also been effectively employed in non-Solanaceous host systems as well such as *Arabidopsis thaliana* (Burch-Smith *et al*., 2006), *Aquilegia* species

(Gould and Kramer, 2007), *Thalictrum* species (Di Stilio *et al*., 2010) and *Gladiolus grandifloras* (Singh *et al*., 2013). Among the advantages of using TRV in VIGS are the capability of the virus to systemically infect the meristematic tissue of the host and its ability to infect different Solanaceous hosts (Burch-Smith *et al*., 2006, Mártin-Hernández and Baulcombe, 2008). However, there are only a few publications dealing with the use of TRV for VIGS in potato (Dobnik *et al*., 2016) showing that there are practical problems in using TRV as a VIGS vector in potato.

Published studies of TRV VIGS have used constructs derived from the PpK20 isolate. Brigneti *et al*. (2004), using this vector-system, had reported the highest efficiency of VIGS (PDS) in a hexaploid relative of potato (*S. nigrum*) and two diploid potato species viz., *S. bulbocastanum* (60-70% PDS silencing) and *S. okadae*. However, in tetraploid *S. tuberosum* c.v. Cara, TRV VIGS was less effective. The authors stated that, besides the type of virus-vector (construct), the efficiency of VIGS was also influenced by the inoculation technique, the plant growth-stage and the genetics of the potato plant. The discovery of additional susceptible diploid potato species, in which TRV can multiply and move systemically from the mechanically-inoculated leaves down into the roots and the developing tubers, led us to revisit the TRV-vector system for functional analysis of tuber genes.

Most of the wild relatives of potato, naturally growing in the Andes, are a good resource against the biotic (insect pest and diseases) and biotic stresses (drought, frost and heat). These quality traits can be exploited by incorporating them in potato breeding programmes to develop improved varieties (Machida-Hirano, 2015). This work has shown that the diploid potato, *S. jamesii*, is a good genetic source for investigating the infection and systemic movement of TRV. The virus in the systemically-infected leaves of seed-derived plantlets was detectable at 6 dpi by the tissue-print technique, suggesting rapid accumulation in the tissue. The species is amenable to be grown under glass-house conditions for carrying-out further virus-infection studies. With good husbandry practices a single plant can bear a sufficient

number of tubers to conduct tuber-related infection studies. The TRV RNA-1 was found to be associated with the production of ring-shaped necrotic lesions on the inoculated leaves of *S. jamesii*. But the plants inoculated with the M-type of TRV were generally asymptomatic. This response of *S. jamesii* to TRV-infection was of advantage because our purpose was to exploit this species for VIGS studies. Another diploid species, *Solanum okadae*, was used to investigate the production of Chevron-like symptoms during TRV-infection. The qRT-PCR quantification of TRV RNA-1 and -2 within the Chevron-like regions of the symptomatic leaves revealed that these symptoms correlated with reduced virus-infection, as mostly virus was present at a low titre in the symptomatic areas compared to adjacent asymptomatic areas. The association of an HR with the Chevron-like symptoms could not be verified by DAB and Trypan-blue staining techniques. Unlike *S. jamesii*, *S. okadae* was found to be poor in tuberization in the conditions used in the current studies.

In potato leaves, the PDS gene, *Phytoene desaturase*, was silenced to 57% (at 22 dpi), 56% (at 40 dpi, Batch No. 1), and 66% (at 40 dpi, Batch No. 2). The ZEP gene, *Zeaxanthin epoxidase*, was silenced to 36% (at 22 dpi), 52% (at 40 dpi, Batch No. 1), and 59% (at 40 dpi, Batch No. 2). The GBSS gene, *Granule bound starch synthase*, was silenced to 42% (at 22 dpi), 5% (at 40 dpi, Batch No. 1), and 40% (at 40 dpi, Batch No. 2).

The reduction in expression of these genes in the tubers was 88% (PDS), 44% (ZEP), and 39% (GBSS). The exploitation of *S. jamesii* for VIGS-related studies has given promising results, though, in some instances, the empty virus-control construct also affected the targeted genes. The use of empty control virus vectors in VIGS experiments (as in Tomato) has been shown to affect the growth and development of the host plant more strongly than virus-control constructs carrying an insert of a non-silenced gene e.g.; GFP or GUS (Wu *et al*., 2011).

It is thought that the empty-vectors can replicate more efficiently and put more stress on the host than the vectors containing a inserted non-targeted gene fragment and

thus could possibly influence the experimental out-comes (Hartl *et al*., 2008). TRV has also been reported to affect the cell metabolism in *Arabidopsis* that change the susceptibility of the infected plant to the virus. Besides affecting the protein content, the sugar and starch metabolism has also been influenced by TRV in these plants. The *Starch Synthase* 2 (SS2) and the *Granule-bound Starch Synthase 1* (GBSS1), both genes involved in sugar-metabolism, were down-regulated in TRV infected plants (Fernández-Calvino *et al*., 2014). Thus, for VIGS-related experiments the use of healthy (mock-inoculated) and empty-virus controls is recommended as a minimum requirement for phenotypic analysis (Bernacki *et al*., 2010). Most of the past studies on VIGS have used empty-TRV (virus-control) as a calibrator or reference sample, but in the current studies we have used the healthy control for normalization of the gene-expression signal. This modification, in some of the current instances, revealed the effect of the virus-control construct on the expression of the genes under study. However, the results of phytoene quantification and staining of the potato-slices and the starch-granules were in general agreement with the qRT-PCR quantitation of the silenced genes.

We conclude that the VIGS-studies conducted here on *S. jamesii* have revealed potential improvements in the capability of VIGS in potato.

5. Molecular Studies of Spraing Disease of Potato

5.1. Aim

Spraing has been described in the literature as a hypersensitive response (HR), however, the genetic and biochemical nature of spraing has not been tested experimentally. Microarray and quantitative RT-PCR analyses of potato pathogen defence-related genes (which are known to be up-regulated during the HR) were done to see whether spraing is in fact a hypersensitive response. In addition to this, other biochemical tests such as staining for HR-related compounds or production of reactive oxygen species were done to detect any HR-related processes that might be active in spraing-affected potato tubers.

Production of spraing disease under controlled environmental conditions such as in the glass-house is very difficult and time-consuming. Vector-specific transmission of the virus and the associated problems of maintaining a viruliferous-nematode population complicate these studies (Brown and Boag, 1987, 1988; Brown *et al*., 1989; Dale and Barker, 2007). Spraing-resembling symptoms can also be produced by direct mechanical-inoculation of the virus to the tubers but is too inefficient (Eibner, 1959; Xenophontos *et al*., 1998) for exploitation in spraing-related studies. Therefore, for gene expression studies by microarray analysis, field-grown tubers of potato c.v. Pentland Dell (known for sensitivity to spraing disease) were collected and examined for spraing by the method of Alonso and Preece (1970). Spraing-affected (S1-4) and spraing-free (SF1-4) tuber-tissue was excised separately from different individual spraing-affected tubers to produce four samples of each tissue-type. Likewise, healthy tuber-tissue (H1-4) from four TRV-free tubers of Pentland Dell was collected to produce four samples of healthy tuber tissue. Since these tubers were grown under field-conditions they could have significant variation in their individual transcriptome expression profiles.

Moreover, information about the infecting TRV isolate from the field was not available. The sampled tubers could have been infected by either a single TRV isolate or a mixture of isolates. All of these factors might introduce variability into the data from these experiments. In additional work, we have investigated the distribution of TRV across a spraing-affected tuber and examined the expression of some spraing-associated genes in relation to TRV infection levels.

5.2. Potato tuber samples and quality of RNA preparations

RNA of all the 12 tuber samples representing four different biological replicates of three tuber types (S1-S4, SF1-SF4, and H1-H4; sample preparation method explained in section 2.1.3) was extracted as described in section 2.4.1 sub-section 2. After successive precipitations with lithium chloride and then ethanol, the RNA preparations were further cleaned using QIAGEN RNeasy® columns (section 2.4.3) and treatment with Ambion® TURBO DNase (section 2.4.4), following the supplier's instructions. The RNA was quantified using a ''NanoDrop 1000 spectrophotometer'' (Appendix 12 and 13). All the 12 RNA preparations were diluted with RNase-free water to a concentration of 250 ng / µl and the quality of the samples was confirmed by using an ''Agilent 2100 Bioanalyzer'' (RNA chip method), following the protocol of ''Agilent RNA 6000 Nano kit''.

The Relative Integrity Number (RIN) values for each of these RNA preparations, were within the acceptable range (i.e.; RIN >7.0) specified for good quality RNA preparation. The RIN values are given in parenthesis against each of these samples i.e.; S1(RIN:7.60), S2(RIN:7.60), S3(RIN:7.60), S4(RIN:5.40), SF1(RIN:7.80), SF2(RIN:7.90), SF3(RIN:7.30), SF4(RIN:7.00), H1(RIN:7.70), H2(RIN:7.70), H3(RIN:7.60), and H4(RIN:7.80). The sample S4 was repeated for RNA extraction as it had given poor RIN value of 5.40. This fresh RNA isolation (S4 Rep.) had a

RIN value of 8.10. The analysis of all these RNA preparations, generated by the by the Bioanalyzer software, is given in figure 5.1.

5.3. Detection of TRV and PMTV in tuber samples

The symptoms of spraing disease (section 1.4.2 and 1.8) can be induced by either TRV or PMTV, or by a mixed infection of both viruses (Beuch *et al*., 2014). All of the twelve tuber samples for microarray analysis were screened for the presence or absence of TRV and PMTV by using Illustra Ready-To-Go™ (GE Healthcare) beads that carry out a combined RT-PCR reaction, and virus-specific primers.

5.3.1. RT-PCR testing of TRV in tuber samples

TRV was detected by following the RT-PCR protocol given in section 2.2.2. A 463 bp amplicon of the TRV 16K gene was produced in the positive controls (Fig. 5.2, a, Lane 1 and 7), and also in all the four spraing (Lane 3 to 6) and spraing-free (Lane 9 to 12) samples, demonstrating the presence of TRV in these samples {NB: the spraing-free samples were derived from non-symptomatic regions of tubers that did show some area of spraing, so that TRV was already suspected to be present in these tubers}. The RNA preparations from healthy tubers (Lane 13 to 16) and the non-template controls (Lane 2 and 7) did not produce any RT-PCR product which confirmed the TRV-free status of these samples.

5.3.2. RT-PCR testing of PMTV in tuber samples

PMTV encodes three movement proteins that are known as the Triple Gene Block (TGB) proteins viz; TGB-1,-2 and TGB-3 (Scott, *et al*., 1994; Adams *et al*., 2012; Beuch, 2013). These TGB proteins are encoded by three overlapping genes and they act in a coordinated fashion to regulate the plasmodesmatal and long-distance systemic movement of the virus. Due to the highly conserved nature of TGB2

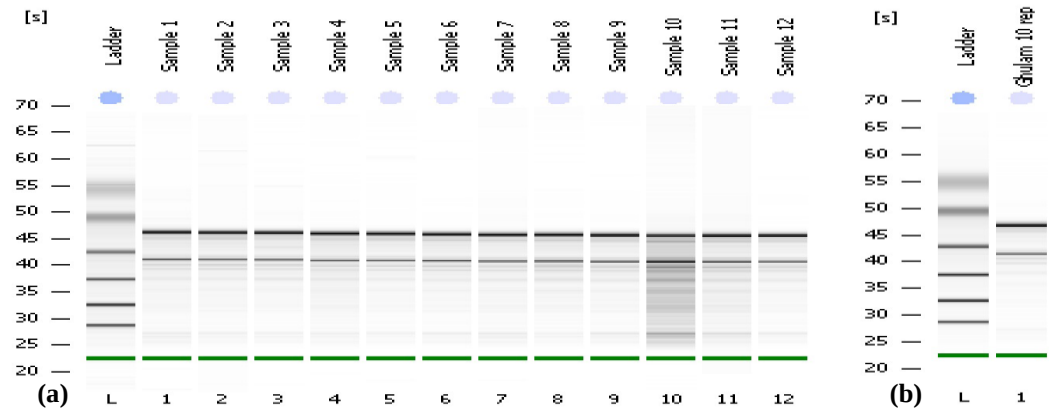

Figure 5.1. Analysis of all the RNA preparations used in microarray analysis. (a) Lane L: RNA Marker; Lane 1: Sample 1, S1; Lane 2: Sample 2, SF1; Lane 3: Sample 3, H1; Lane 4: Sample 4, S2; Lane 5: Sample 5, SF2; Lane 6: Sample 6, H2; Lane 7: Sample 7, S3; Lane 8: Sample 8, SF3; Lane 9: Sample 9, H3; Lane 10: Sample 10, S4; Lane 11: Sample 11, SF4; Lane 12: Sample 12, H4; **(b)** Gel image of re-extracted RNA of sample 10; Lane L: RNA Marker; Lane 1: Ghulam 10 Rep (repeat of extraction of sample S4).

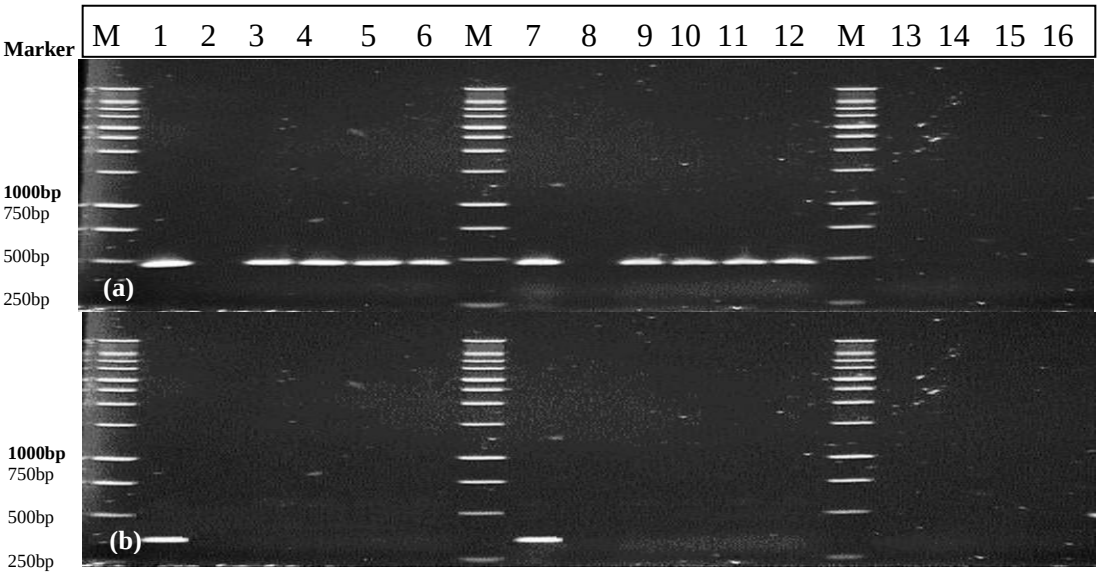

Figure 5.2. RT-PCR detection of TRV and PMTV in the tuber samples selected for gene-expression analysis. Lane M: 1kb Promega DNA ladder; Lane 1 and 7: Positive controls, **(a)** 463 bp amplicon from TRV infected *N. benthamiana* **(b)** 356 bp amplicon from a plasmid clone of PMTV-TGB2. Lane 2 and 8: Non template control; Lane 3-6: Spraing samples, S1-S4; Lane 9-12: Spraing-Free samples, SF1- SF4; Lane 13-16: Healthy samples, H1-H4.

(Andrey *et al*., 2012) a primer set based on the TGB2 gene was used for the detection of PMTV as given in section 2.4.5. A 356 bp amplicon of TGB2 was amplified only from the positive-control sample (Fig. 5.2, b, Lane 1 and 7), revealing the PMTV-free status of the tuber samples prepared here for subsequent microarray analysis.

5.4. Microarray and GeneSpring Analyses

A microrray analysis of all the 12 tuber samples was done as given in section 2.4.6. Data extracted from the arrays was imported into the GeneSpring programme. Default normalisation (Agilent 1-colour) settings were applied and probes flagged as 'absent' in ≥10 of the 12 RNA samples were removed from the analysis, leaving 27,895 probes with reliable gene expression. Each probe on the array is not unique to one potato gene, as the potato genes are represented by multiple probes on the array. Significant differences in gene expression were observed as the samples were taken from tubers that were harvested from the field rather than from a controlled-environment (cubicle or cabinet). However, condition cluster analysis revealed that most of the biological replicates for each condition grouped together (Fig. 5.3) therefore indicating that pattern of relative gene expression was comparatively stable within each tuber type (S v. SF. H). After 1-way ANOVA analysis, the resulting data were subject to a pairwise comparison (Volcano plot) to ascertain the comparative differential gene expression between two contrasting sets of samples; in one analysis spraing (S) and no-spraing (spraing-free, SF) samples, and in a second analysis healthy (H) and spraing-free samples were compared. The Volcano plot displays the –log (p-value) vs. the log (fold change) and thus illustrates the two important parameters of differential gene expression in a single plot. It provides the investigator with a foundation to quickly decide which genes are worthy to be focused on in further research. The pair-wise comparison, performed at a high stringency with a Student's T-test (t-test) probability value (p-value) restriction of ≤0.01, identified

844 differentially expressed probes for the first set of samples (S/SF) and 1,024 probes for the second sample set (H/SF). These pair-wise comparisons were restricted to probes that showed at least a two-fold change in their expression. A gene expression profile for the spraing samples is given in figure 5.4, revealing significantly higher expression of many genes in the spraing samples as compared to the spraing-free and healthy tuber samples. Lastly, comparing healthy versus spraing symptomatic samples, 2,827 differentially expressed probes were identified. The raw data from these experiments has been deposited in the Array Express database (accession number E-MTAB-4670; http://www.ebi.ac.uk/array express). Appraisal of all three pair-wise comparisons show that 630 probes (17.8 % of total number) were associated with spraing production (Fig. 5.5) and 439 probes (12.4 % of total number) were related to TRV-infection, regardless of whether there was or was not spraing formation in the tubers.

The expression of the potato Elongation Factor-1 alpha (Ef-1 α) gene, a commonly selected ‘‘reference gene,’’ was also examined to confirm the integrity of the RNAs isolated from the three types of tuber samples (S, SF and H). The graph (Fig. 5.6) for Ef-1 α expression appeared as a flat-line for all the three sample types and thus suggested the uniform expression of this gene among all the three types of tubers.

The ‘‘gene enrichment analysis’’ assigns a biological ‘‘function’’ to the highlighted genes in the array analysis, and is based on ‘‘gene ontologies’’, where, the organized method of grouping genes with related annotations creates a gene ontology (GO) and where annotation is the process of attaching a note or a comment (phrase or word) to a sequence giving a biological meaning to the annotated sequence. Gene ontology uses a well-ordered vocabulary including a set of accepted terms that can provide functional data either about a gene product (protein) of a single gene or as a ‘‘gene enrichment analysis’’ for the whole proteome and group of proteins (Hill *et al.*, 2008; Huntley *et al.*, 2014). Gene ontology and associated annotations is a useful tool for the extraction of ‘‘biologically relevant’’ information from extensive data sets, such

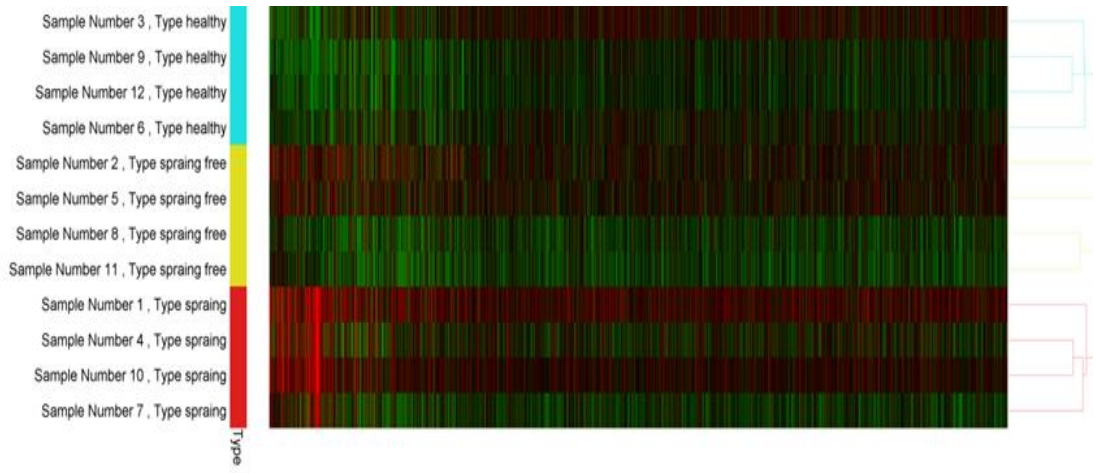

Figure 5.3. Condition tree clustering of QC-filtered normalised expression data of each replicate microarray. Pearson correlation with average linkage was used in GeneSpring v 7.3 (Agilent).

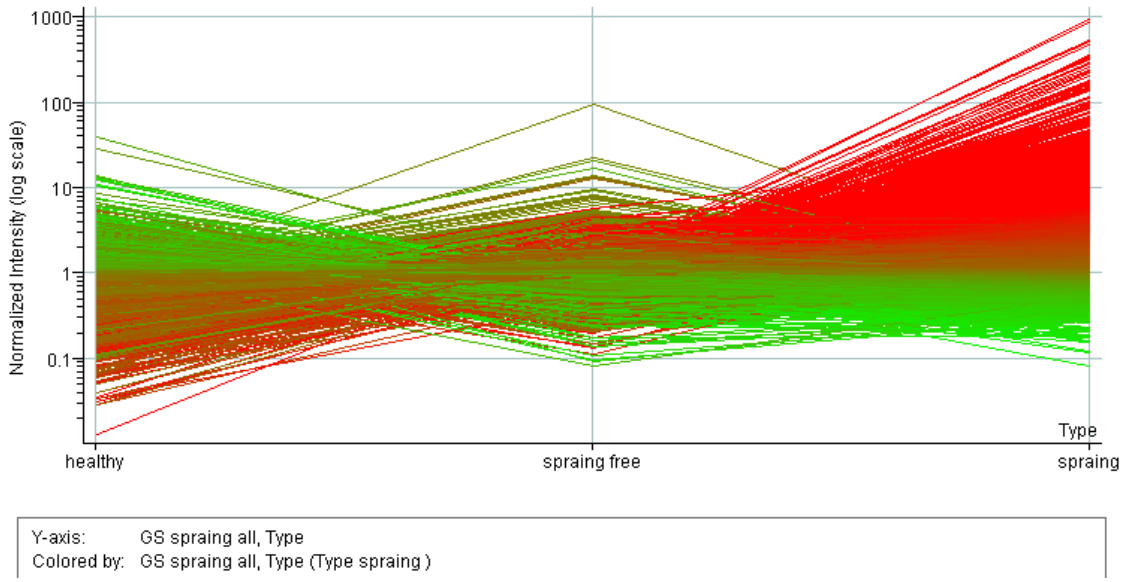

Figure 5.4. Expression profile of potato genome (4x44K array) for spraing tubers. Each line represents a gene (probe). The red-lines denote the up-regulated probes and the green-lines show the down-regulated probes in the spraing-free and spraing volcano plot of the 42,034 potato unigenes present on the array.

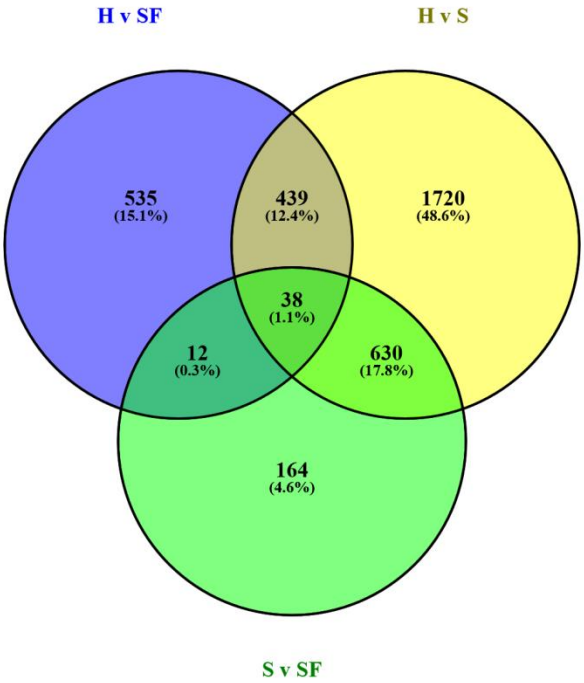

Figure 5.5. Numbers and percentage of differentially (>2-fold) expressed genes in data sets. Comparisons are between healthy (H), virus-infected, spraing free (SF) and virus-infected, spraing symptomatic (S). Regions of overlap denote differentially expressed genes shared between dataset comparisons.

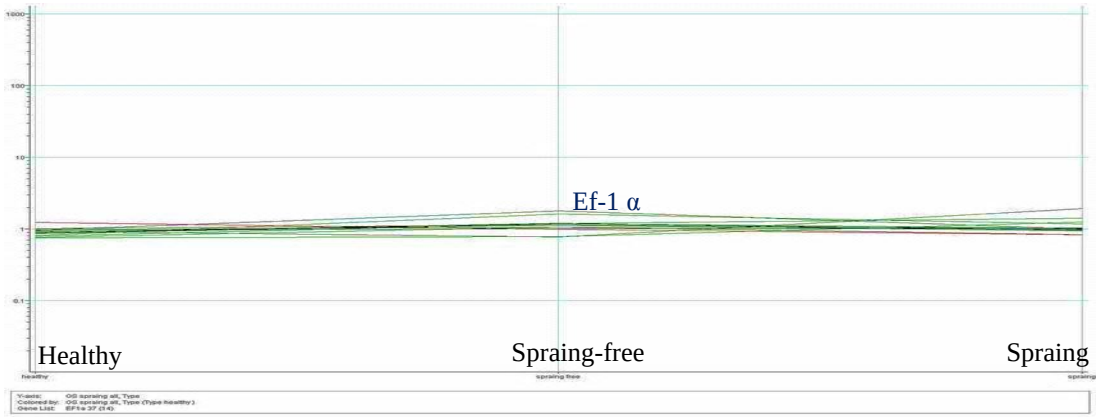

Figure 5.6. Genetic expression of potato Ef-1 α, among all the three types of tuber samples. The expression of potato Ef-1 α, was a flat-line for all the three sample types, suggesting a uniform expression pattern of this gene among all the three tissue types.

as microarray data (Harris *et al.*, 2006). From the total of 27,895 expressed probes detected from the data extracted by Feature Extraction (FE), only 53.84% (15,019) were annotated in the potato genome database, whereas, rest of the probes were without any annotation and therefore have no known function.

The GO presents organized information about the traits of genes and their coded proteins in three significant domains that are shared by all organisms viz., molecular function, biological process and cellular component. The differentially expressed potato genes in the current studies were allocated to these three overarching functional domains according to their GO annotation. This analysis created sub-sets of genes that were related by their expected GO terms, with the highest level domains being Molecular Function (GO: 3674), Biological Process (GO: 8150), and Cellular Component (GO: 5575). The molecular function relates to genes involved in a task or basic activity such as enzymatic or catalytic activity. The biological process defines a broad goal or objective encompassing a chain of events, completed either by a single or a multiple ordered assembly of molecular functions (gene pathways), such as a signal transduction process, or responses to biotic or abiotic stresses, or a cellular-physiological process, and includes many lower level GO term categories related to programmed cell-death (PCD) and associated HR reactions. The cellular component refers to a cellular entity, complex or location where the molecular function or a biological process is performed. Cellular component relates to sub-cellular location where the gene is active. It relates to a bigger object or an organelle such as a mitochondrion, nucleolus or a chloroplast or is a group of proteins (gene-products) such as ribosomes and liposomes.

For the 844 probes differentially expressed in the spraing versus spraing-free samples, only 512 have a predicted function and only 495 have an ascribed GO term annotation. For the 1,024 probes differentially expressed in the healthy versus TRV-infected but spraing-free samples, only 585 have a predicted function and only 422 have an ascribed GO term annotation.

5.4.1. Biological process domain (GO: 8150)

Because our aim was to discover whether spraing production is a defense reaction of the plant to virus infection we did ‘‘gene enrichment analysis’’ focusing on GOs that are related to defence responses. In this analysis, high-level GOs have lower level GOs that are located within them. The pie-chart of the high-level ‘‘biological process domain’’ (GO: 8150) given in figure 5.7, identified 839 genes associated with this GO term in the spraing-affected tubers. The majority of these genes (379 genes, 45.17% of total) had a role in the physiological processes (GO: 7582) of the spraing-tuber. The second largest group of genes (317 genes, 37.78%) in this domain was associated with cellular functions (GO: 9987) of the spraing-tuber, followed by a group of genes involved in the regulation of biological process (GO: 50789), response to the stimulus (GO: 50896) or no known biological role (GO: 4), with 59 genes (7.03%), 56 genes (6.67%), 18 genes (2.14%), respectively. The second smallest group of genes (6 genes, 0.71%) located in this domain play roles in reproduction (GO: 3) and the smallest group of genes (4 genes, 0.48%) was linked to reproductive processes (GO: 7275) in the spraing-tuber.

The total number of genes in each GO term group (genes in list in category) and the actual number of genes in that category that were differentially expressed in the samples, alongwith the GOs identified at a stringency with a student t distribution (t-test) probability value (p-value) restriction of <0.01 are given in Table No. 5.1.

Necessarily, ‘‘biological processes’’ are in train constantly in all tissues, in all organisms. The thorough search of this ontology at the lower hierarchical level revealed some GO terms with direct or indirect relevance to plant defence responses; such as ‘‘response to stimulus’’ GO: 50896, ‘‘cellular physiologic process’’ GO: 50875, etc. The set of genes present in ‘‘response to stimulus’’ was twice the expected frequency (13.33% observed compared to 7.97% expected) in the

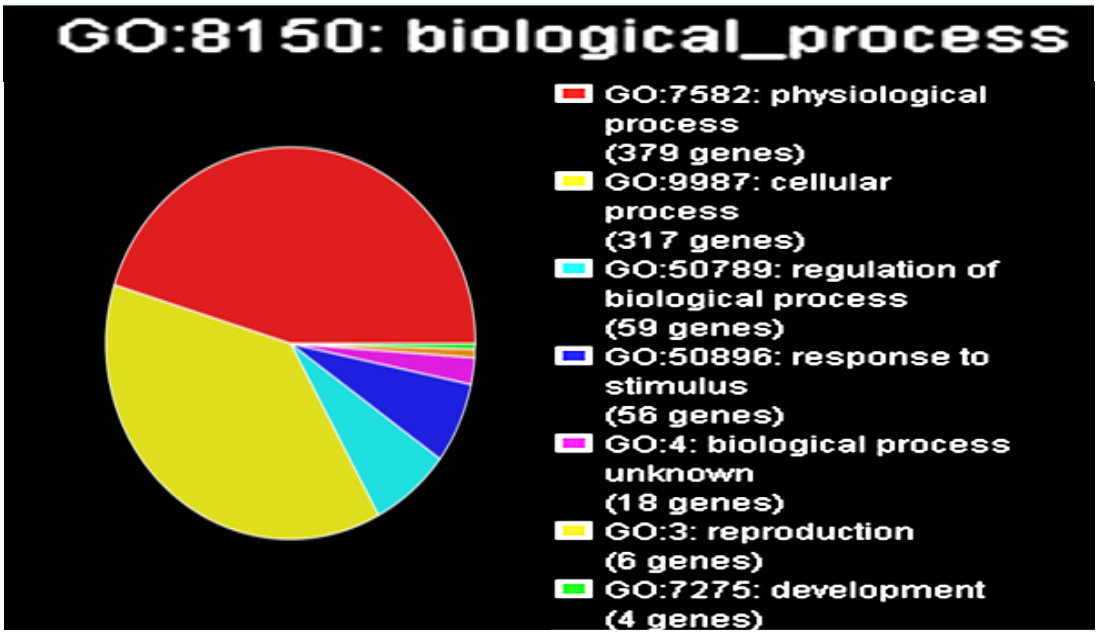

Figure 5.7. Pie-chart of the GO group for biological process. The major class of genes associated with biological role in the spraing-tuber was linked to physiological (45.23%) and cellular activities (37.83%).

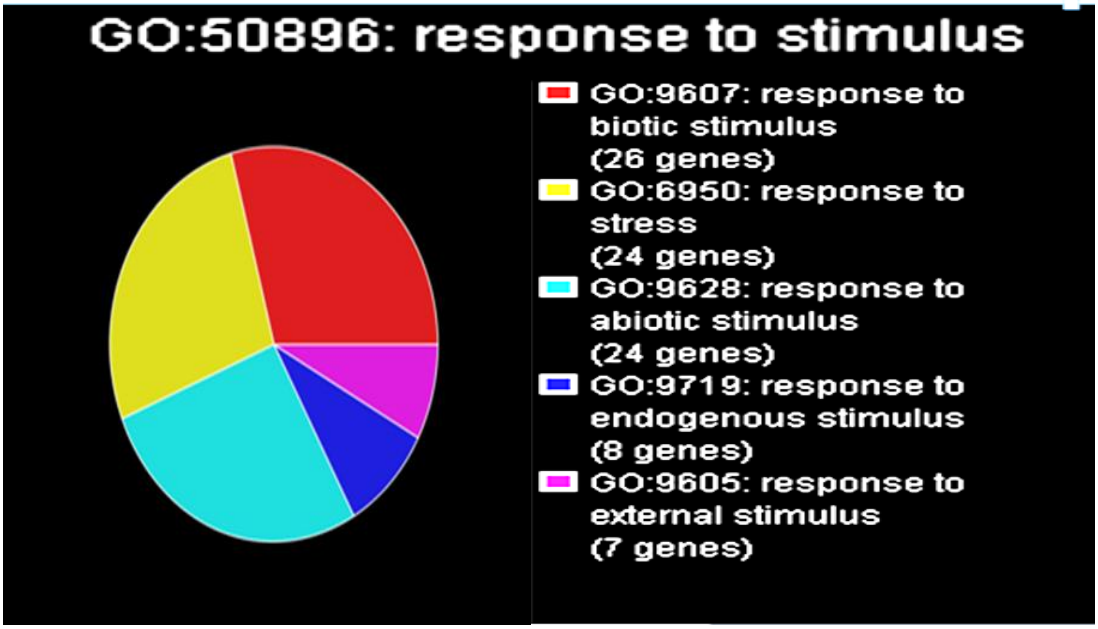

Figure 5.8. Pie-chart of the GO group for response to stimulus. The majority of the genes (29.21%) in this category of studied genes were associated with response to biotic stimulus.

Table 5.1. Over-represented tuber-expressed genes* in the GO: 8150 (biological process)

S.No.	Functional category and GO ID	Genes in Category	% of Genes in Category (expected)	Genes in List in Category	% of Genes in List in Category (observed)	p-Value
1.	Regulation of biological process GO: 50789	1715	11.42	58	16.57	0.00222
2.	Response to stimulus GO: 50896	1197	7.97	56	13.33	9.30E-05
3.	Reproduction GO: 3	81	0.539	6	1.429	0.0258

* Percent genes filtered at p-value restriction of <0.01

transcriptome of spraing-affected tubers compared to spraing-free and also healthy and also healthy tubers.

5.4.2. Response to stimulus (GO: 50896)

The gene ontology associated with ‘‘response to stimulus’’ (GO: 50896, Fig. 5.8) comprised 89 genes that had association with responses to stimuli in the spraing-tuber. The major group of genes (29.12% of total, 26 genes) in this ontology was attached to the response to biotic stimulus (GO: 9607), followed by 26.97% genes (24 genes) linked each with the response to stress (GO: 6950) and abiotic stimulus (GO: 9628), respectively. 8.99% (8 genes) were related to the response to endogenous stimulus (GO: 9719) and the smallest number of genes (7.86%, 7 genes) in this set of studied genes was associated with response to external stimulus (GO: 9605). The percentage of the total number of genes in this set of studied genes (genes in list in category) and the actual number of genes in this category that were present on the microarray (genes in category) are given in table No. 5.2. These genes along with the GOs were filtered at a stringency with student t distribution (t-test) p-value <0.01.

Table 5.2. Over-represented tuber-expressed genes* in the GO: 50896 (response to stimulus)

S.No.	Functional category and GO ID	Genes in Category	% of Genes in Category (expected)	Genes in List in Category	% of Genes in List in Category (observed)	p-Value
1.	Response to biotic stimulus GO: 9607	512	3.409	26	6.19	0.00255
2.	Response to stress GO: 6950	482	3.209	24	5.714	0.00469
3.	Response to abiotic stimulus GO: 9628	507	3.376	24	5.714	0.00859

* Percent genes filtered at p-value restriction of <0.01

5.4.3. Cellular physiological process (GO: 50875)

The gene ontology of the biological processes linked to ‘‘cellular physiological process’’ (GO: 50875, Fig. 5.9) of the spraing-tuber was investigated to search for genes related to cell-death of the tissue.

The GO: 50875 comprised a total of 432 genes in the spraing-tuber. The largest group of annotated genes (246 genes, 56.94% of total) in this ontology was related with cellular metabolism (GO:44237), followed by genes associated with transport processes (GO: 6810, 93 genes, 21.53%), regulation of cellular physiological processes (GO: 51244, 55 genes, 12.73%), cell-death (GO: 8219, 13 genes, 3.01%), cell organization and biogenesis (GO: 16043, 12 genes, 12.73 %), and hormone-mediated signalling (GO: 9755, 7 genes, 1.62%), respectively. The group of genes linked to the cell cycle (GO: 7049) and cell homeostasis (GO: 19725) had 2 genes (0.46%) in each ontology. The smallest number of the genes (0.46%) were in the cell proliferation (GO: 8283) and cell division (GO: 51301) ontologies, each consisting of one gene in the ontology.

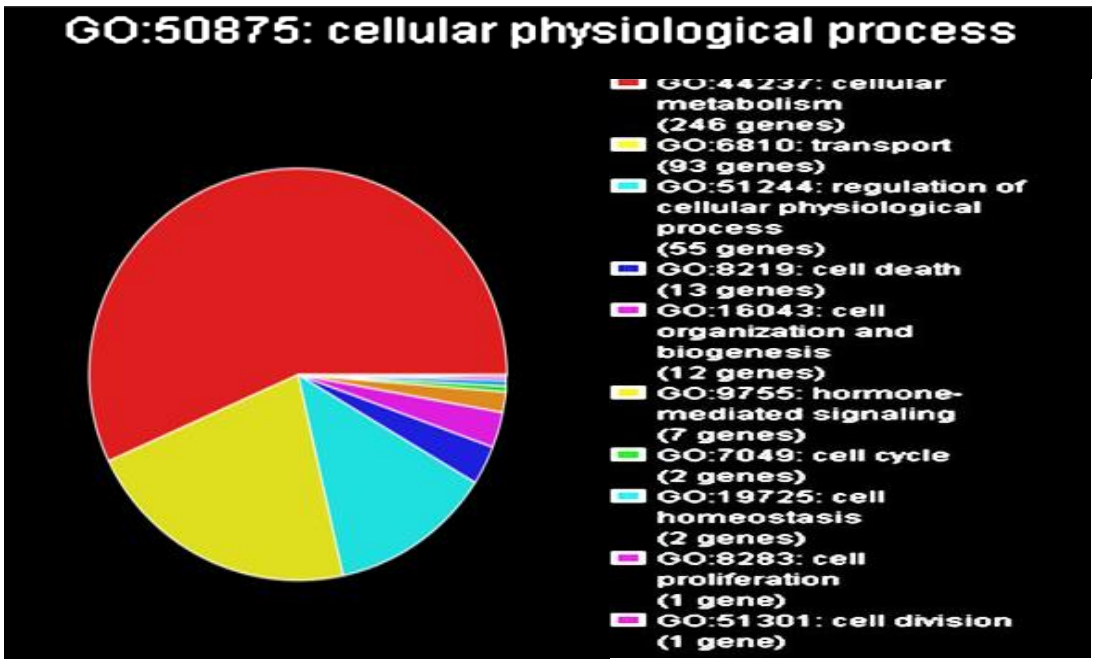

Figure 5.9. Pie-chart of the GO group for cellular physiological process. The largest number of genes (56.94%) in this group were associated with the cellular metabolism of the spraing-tuber.

5.4.4. Selected gene ontologies

Using GOs to identify genes that are significant players in any biological phenotypic process is a subjective exercise, and focussing on genes whose expression is up-or down-regulated by two-fold or more may lead to important changes in gene expression being overlooked. Nevertheless, we have used this process to try to identify some important genes for spraing production and reaction to virus infection in potato tubers. Some GOs, where differential expression occurs, from the spraing vs. spraing-free volcano plot and the spraing-free vs. healthy volcano plot are given in appendix 14 and 15, respectively.

5.5. HR-related gene ontologies

The gene ontologies comprising the HR-related annotations (Table No. 5.3) were selected from the gene enrichment analysis of both volcano plots given in appendix 14 and 15. Some important HR-related GO's in the spraing vs. spraing-free volcano plot include GO: 6952 (defense response); GO: 6979 (response to oxidative stress); GO: 6800 (oxygen and reactive oxygen species metabolism); GO: 302 (response to reactive oxygen species) and GO: 42542 (response to hydrogen peroxide). Some important HR-related GO's in the spraing-free vs. healthy volcano plot include GO: 45454 (cell redox homeostasis); GO: 6800 (oxygen and reactive oxygen species metabolism); and GO: 9615 (response to virus). Closer examination of these various GOs reveals that particular individual genes are included in more than one GO gene list (see Table No. 5.3) and are thus over-represented.

Table 5.3. Selection of HR-related gene ontologies from the *gene enrichment analysis*

S.No.	GO ID and term	Genes in Category	% of Genes in Category (expected)	Genes in List in Category	% of Genes in List in Category (observed)	p-Value
	Spraing vs. Spraing-free volcano					
1.	GO:6952: defense response	488	3.249	26	6.19	0.00131
2.	GO:6979: response to oxidative stress	161	1.072	12	2.857	0.00191
3.	GO:6800: oxygen and reactive oxygen species metabolism	189	1.258	12	2.857	0.00697
4.	GO:42542: response to hydrogen peroxide	48	0.32	5	1.19	0.0107
5.	GO:302: response to reactive oxygen species	50	0.333	5	1.19	0.0126
6.	GO:9627: systemic acquired resistance	1	0.00666	1	0.238	0.028
7.	GO:42828: response to pathogen	47	0.313	4	0.952	0.0418
8.	GO:42744: hydrogen peroxide catabolism	37	0.246	5	1.19	0.00348
9.	GO:42743: hydrogen peroxide metabolism	37	0.246	5	1.19	0.00348
10.	GO:9693: ethylene biosynthesis	27	0.18	3	0.714	0.0387
11.	GO:9692: ethylene metabolism	27	0.18	3	0.714	0.0387
	Spraing-free vs. Healthy volcano					
12.	GO:45454: cell redox homeostasis	146	0.972	9	2.571	0.00724
13.	GO:19725: cell homeostasis	160	1.065	9	2.571	0.0128
14.	GO:6979: response to oxidative stress	161	1.072	12	2.857	0.00191
15.	GO:42592: homeostasis	179	1.192	9	2.571	0.0246
16.	GO:6800: oxygen and reactive oxygen species metabolism	189	1.258	9	2.571	0.0332
17.	GO:9615: response to virus	2	0.0133	1	0.286	0.0461

The GO's containing significantly up-regulated HR-related genes were further investigated, by the ''gene list inspector'' function of the ''GeneSpring GX'' software.

5.5.1. Response to pathogen (GO: 42828)

The GO: 42828 annotated for ''response to pathogen'' included four genes (Appendix 16). Among these four pathogen-responding genes, the PGSC transcripts PGSC0003DMT400071827 and PGSC0003DMT400013860 had the highest fold-change expression of 76.2 and 26.1, respectively, in the spraing vs. spraing-free volcano plot (Fig. 5.10). Both of these genes were annotated as unknown protein product [Arabidopsis thaliana]. The other two genes, PGSC0003DMT400039281 and PGSC0003DMT400046161 were annotated as 4-coumarate-CoA ligase/ fatty-acyl-CoA synthase [Arabidopsis thaliana] and SAR8.2 protein precursor [*Capsicum annuum*] with fold-change of expression in the spraing vs. spraing-free volcano plot of 17.1 and 12.2, respectively. None of these genes showed any differential expression in the spraing-free vs. healthy volcano plot, except for the SAR8.2 protein precursor that had a 2.7 fold-change.

5.5.2. Response to reactive oxygen species (GO: 302)

The GO: 302 annotated for ''response to reactive oxygen species'', comprised five probes representing four PGSC transcripts (Appendix 17). The microarray probes MICRO.3508.C3_976 and MICRO.3508.C1_978, in the spraing vs. spraing-free volcano plot, had the highest fold-change expression of 48.7 and 36.1, respectively (Fig. 5.11). Both these probes detected the same PGSC transcript (PGSC0003DMT400057521) and so had the same annotation of Suberization-associated anionic peroxidase 2 precursor (TMP2). The gene PGSC0003DMT400057522, annotated as Suberization-associated anionic peroxidase precursor (POPA) had a 9.6 fold-change of expression. The probes

MICRO.14166.C1_ 1246 and MICRO.14166.C2_1271, with a fold-change expression of 4.8 and 4.4, respectively, in the spraing vs. spraing-free volcano plot, were from the same PGSC transcript (PGSC0003DMT400001375) and had the same annotation of peroxidase [*Arabidopsis thaliana*]. None of these genes was differentially expressed in the spraing-free vs. healthy volcano plot.

5.5.3. Defence response (GO: 6952)

A total of twenty-six genes included in the ‘‘defence response’’ -related gene ontology (GO: 6952) are given in appendix 18. Among these genes the Pathogenesis-related protein STH-21 (PGSC0003DMT400011604) was highly over-expressed with a 256.5 fold-change of expression in the spraing vs. spraing-free volcano plot (Fig. 5.12, a, and b), followed by the genes annotated as ‘‘unnamed protein product’’ and ‘‘similar to pathogenesis-related protein STH-2 [*Solanum lycopersicum*]’’ with 76.2 and 69.3 fold-change of expression. The NBS-LRR protein [*Solanum acaule*] was up-regulated 2.7 and 2.0-fold in the spraing vs. spraing-free and spraing-free vs. healthy volcano plots, respectively. It should be remembered that TRV is present in all of the S and SF samples of the spraing vs. spraing-free volcano plot, whereas, in the spraing-free vs. healthy volcano plot TRV is present only in the SF samples.

5.5.4. Cell-death (GO: 8219)

The ‘‘cell-death’’ related gene ontology (GO: 8219) includes 13 genes (Appendix 19). Among these genes the most highly expressed was annotated as ‘‘unnamed protein product’’ with a 76.2 fold-change of expression in the spraing vs. spraing-free volcano (Fig. 5.13). The next most highly expressed genes in this ontology encoded the ‘‘Putative disease resistance protein, identical [*Solanum tuberosum*]’’ and ‘‘RGC1 [*Solanum tuberosum*]’’ with 5.1 and 3.9 fold-change of expression, respectively. Except for the gene coding for ‘‘NBS-LRR protein [*Solanum acaule*]’’ with 2.7 and 2.0 fold-change of expressions in the spraing-free vs. healthy and

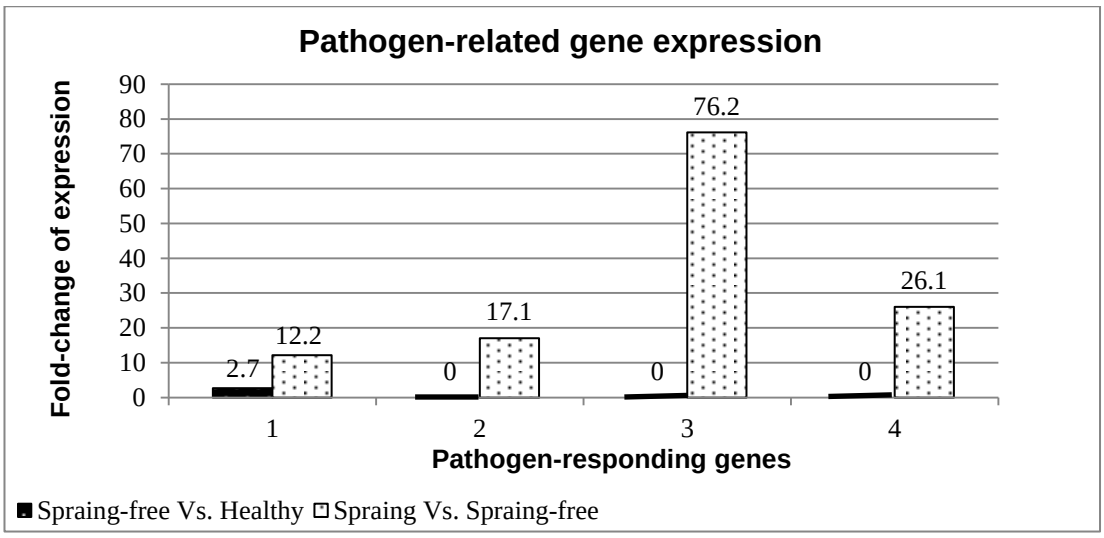

Figure 5.10. Pathogen-related gene expression in spraing tuber. (1) SAR8.2 protein precursor [*Capsicum annuum*]. **(2)** 4-coumarate-CoA ligase/ fatty-acyl-CoA synthase [*Arabidopsis thaliana*]. **(3)** Unnamed protein product [*Arabidopsis thaliana*]. **(4)** Unknown protein [*Arabidopsis thaliana*]. The fold-change expression value of each gene is given in data labels, above each gene bar.

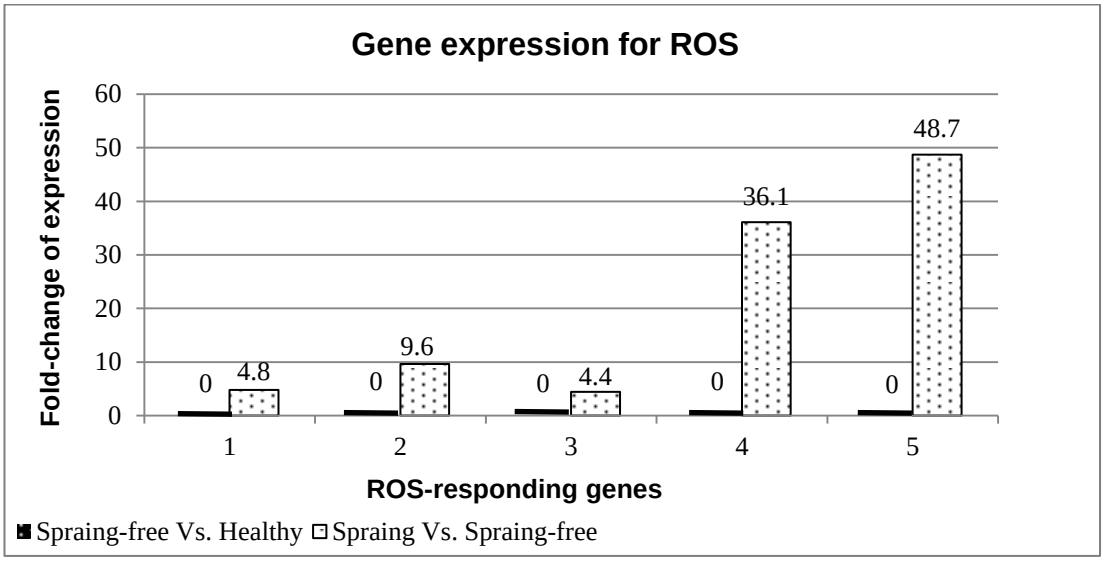

Figure 5.11. Up-regulation of Reactive Oxygen Species (ROS)-associated genes in the spraing-affected tuber. (1, 3) Peroxidase [*Arabidopsis thaliana*]. **(2)** Suberization-associated anionic peroxidase precursor (POPA). **(4, 5)** Suberization-associated anionic peroxidase 2 precursor (TMP2)].

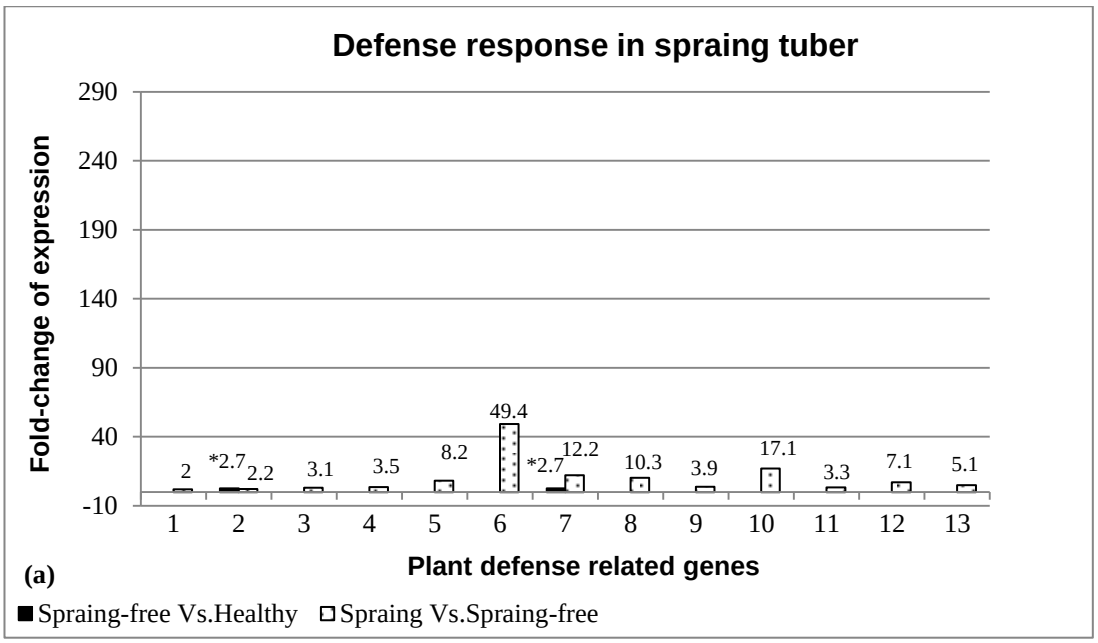

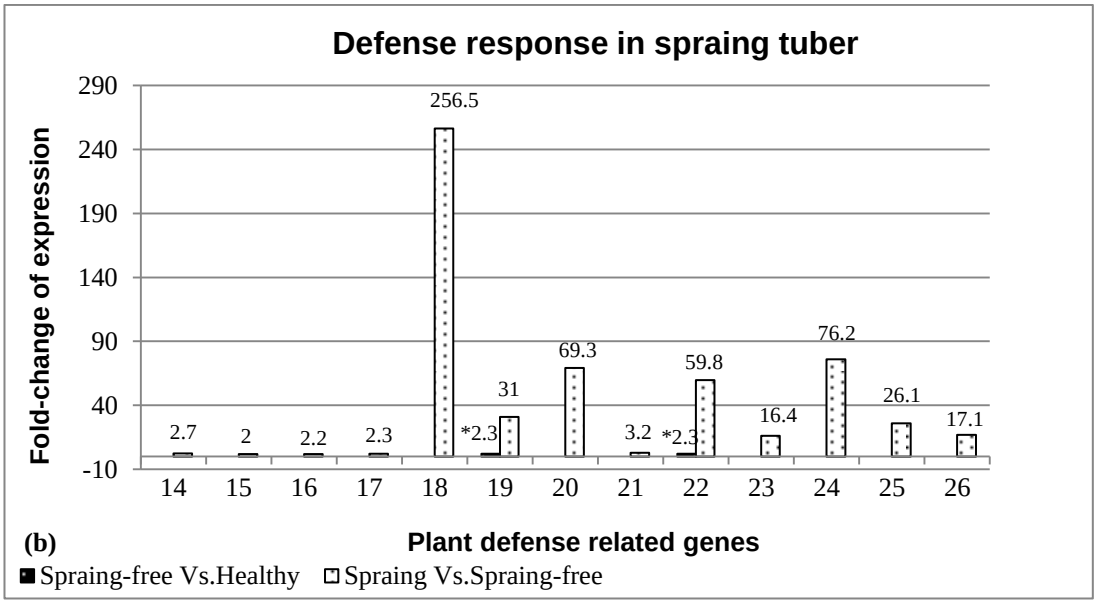

Figure 5.12. Differential expression of plant defense response-inducing genes in spraing tuber. The microarray probe IDs and annotations of the genes **1-13 (a)** and **14-26 (b)** are sequentially enlisted in the appendix 18, respectively. The fold-change expression value of each gene is given in data labels, above each gene bar. Genes 2, 7, 19, and 22 each have two data bars, with left one (indicated by *) relating to SF vs. H and the right one relating to S vs. SF.

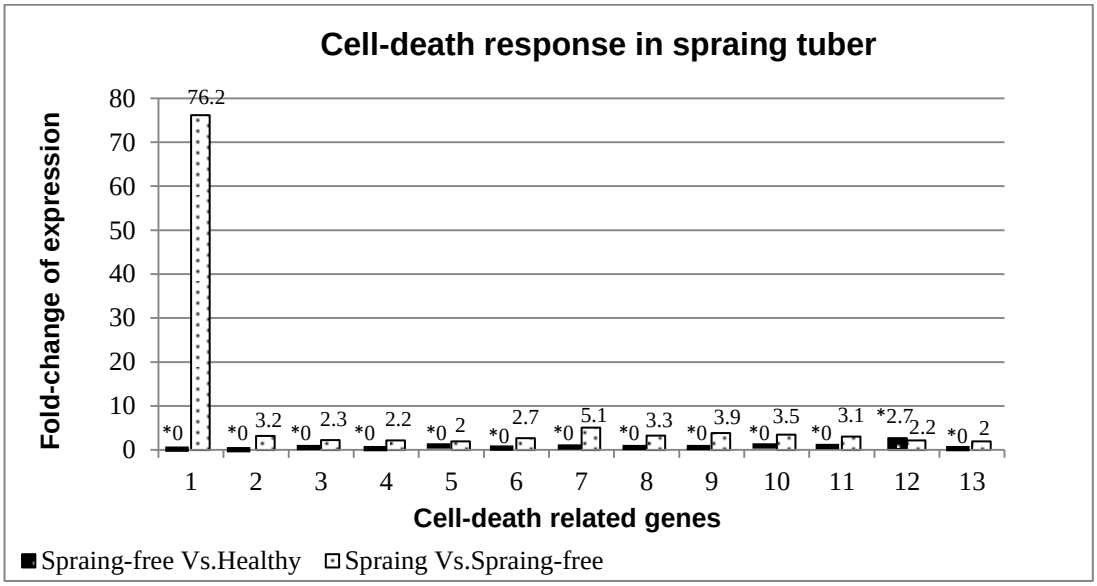

Figure 5.13. Differential expression of cell-death-related genes in spraing tuber. (1) Unnamed protein product [*Arabidopsis thaliana*]. **(2)** NB-ARC domain containing protein [*Solanum demissum*]. **(3)** Disease resistance protein BS2 [Capsicum chacoense]. **(4, 8)** TMV resistance protein N, putative [*Solanum demissum*]. **(5)** Disease resistance protein N. **(6)** Hero resistance protein 2 homologue [*Solanum lycopersicum*]. **(7)** Putative disease resistance protein, identical [*Solanum tuberosum*]. **(9)** RGC1 [*Solanum tuberosum*]. **(10, 11, 13)** Bacterial spot disease resistance protein 4 [*Lycopersicon esculentum*]. **(12)** NBS-LRR protein [*Solanum acaule*]. The fold-change expression value of each gene is given in the data labels, above each gene annotation. Each lane has two data bars, with left one (indicated by *) relating to SF vs. H and the right one relating to S vs. SF. The microarray probe IDs are orderly enlisted in the appendix 19, respectively.

spraing vs. spraing-free volcanoes, respectively; none of the genes included in the GO for cell-death were differentially-expressed in the spraing-free vs. healthy volcano plots at the imposed 2 fold-change and p-value restrictions.

5.5.5. Pathogenesis-related protein 1-c (PAR-1c) gene expression

Investigation of pathogenesis-related protein 1-c (PAR-1c), revealed three probes on the microarrays with a PAR1-c annotation (Appendix 20). Each of these PAR-1c probes represented a different PGSC transcript. The highest fold-change of expression (393.5, Fig. 5.14) was for PGSC0003DMT400037209 (MICRO. 1833.C1_689), followed by the PGSC transcript PGSC0003DMT400037234 (POAD763TV_514) with a 171.5 fold-change of expression in the spraing vs. spraing-free volcano plot. None of the three probes of the PAR-1c were found to be differentially expressed in the spraing-free vs. healthy volcano plot.

5.5.6. SAR associated gene expression

Among the genes associated with systemic acquired resistance (SAR), four probes were with the SAR related annotations (Appendix 21). Among these probes the SDBN002J05u.scf_220 probe representing PGSC transcript PGSC0003DMT400046161 had the highest fold-change expression of 12.2 in the spraing vs. spraing-free volcano plot (Fig. 5.15). Two of these probes viz; STMJH65 TV_362 and MICRO.9261.C1_716, representing the same PGSC transcript (PGSC0 003DMT400032096) annotated commonly as 1-aminocyclopropane-1-carboxylate synthase [*Lycopersicon esculentum*], had 9.5 and 7.6 fold-change of expression, respectively. Probe BPLI16E1TH_626 (PGSC0003DMT400036081) annotated as ‘‘1-aminocyclopropane-1-carboxylate oxidase 2 (ACC oxidase 2) (Ethylene-forming enzyme) (EFE) (Protein GTOMA)’’ had a 8.3 fold-change of expression. None of these genes was found to be differentially expressed in the spraing-free vs. spraing volcano, except probe SDBN002J05u.scf_220, with a 2.7 fold-change of expression.

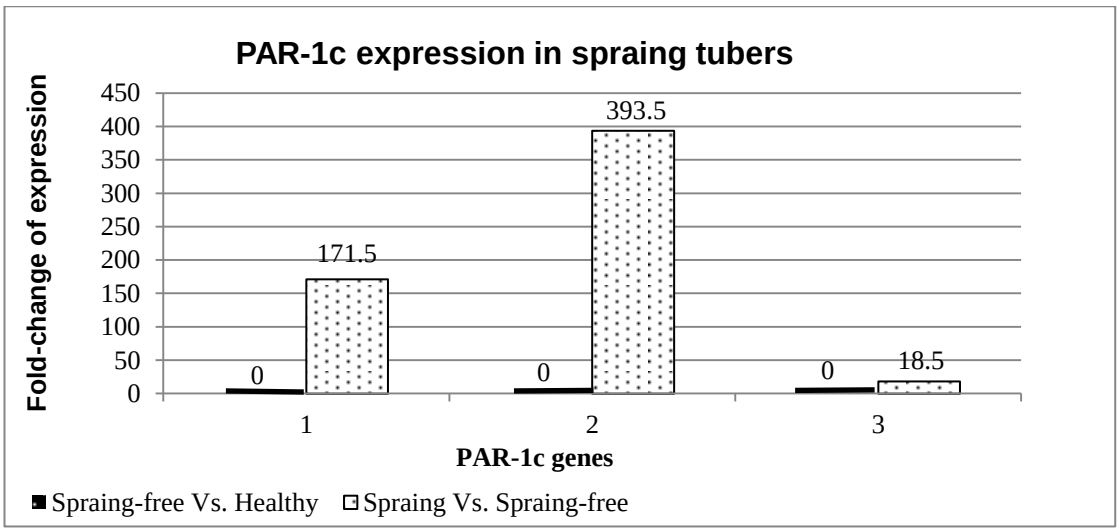

Figure 5.14. Up-regulation of PAR-1c genes in spraing tubers. (1-3) PAR-1c [*Nicotiana tabacum*]. The fold-change expression value of each gene is given in the data labels, above each data bar.

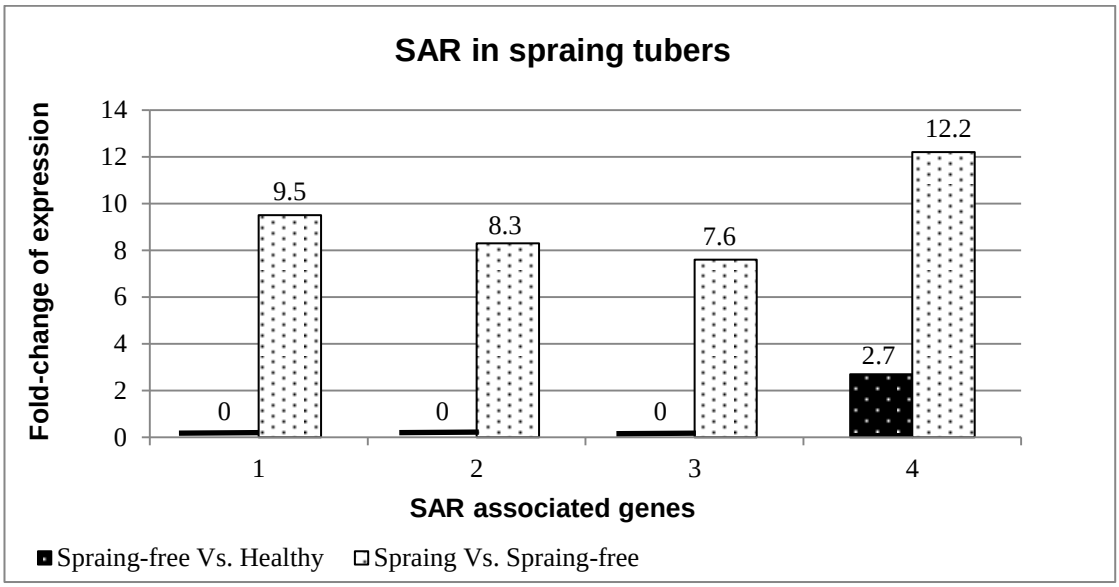

Figure 5.15. Up-regulation of Systemic Acquired Resistance (SAR)-related genes in spraing tubers. (1, 3) 1-aminocyclopropane-1-carboxylate synthase [*Lycopersicon esculentum*]. **(2)** 1-aminocyclopropane-1-carboxylate oxidase 2 (ACC oxidase 2) (Ethylene-forming enzyme) (EFE) (Protein GTOMA). **(4)** SAR8.2 protein precursor [*Capsicum annuum*]. The fold-change expression value of each gene is given in the data labels, above each data bar.

5.6. Quantitative RT-PCR of tuber samples

The quantitative (q) RT-PCR assay is a robust and highly sensitive technique for gene expression studies. The authenticity of the microarray data was evaluated by the qRT-PCR testing of a sub-set of five genes (Table No. 5.4) selected from the HR-related GOs described in section 5.5. The ‘‘PGSC transcript IDs’’ of these significantly up-regulated HR-related genes were acquired from the microarray data and the transcript sequence was extracted from the database curated at the website (http://potato.plantbiology.msu.edu/index.shtml) of ‘‘Potato Genomics Resource’’ maintained at Michigan State University. The potato genome was searched, using the ‘‘PGSC transcript ID’’, in the *S. tuberosum* group ‘‘Phureja DM1-3’’ data-base at this website.

Table 5.4. HR-related genes selected for qRT-PCR validation of the microarray data

S.No.	Microarray probe ID	PGSC transcript ID	PGSC gene annotation and ID*	Gene Abbr.	Fold-change of expression from microarray	
					SF vs. H	S vs.SF
1.	MICRO.149.C1_1078	PGSC0003DMT400036487	Peroxidase (PGSC0003DMG400014055)	PER	-----	649.5
2.	MICRO.1833.C1_689	PGSC0003DMT400037209	PAR-1c protein (PGSC0003DMG400014347)	PAR	-----	393.5
3.	MICRO.3508.C3_976	PGSC0003DMT400057521	Suberization associated anionic peroxidase 2 (PGSC0003DMG400022341)	SP	-----	48.7
4.	MICRO.592.C19_586	PGSC0003DMT400005549	Glutathione-S-transferase (PGSC0003DMG400002170)	GST	-----	45.8
5.	MICRO.17075.C1_576	PGSC0003DMT400063688	Respiratory burst oxidase homolog protein B (PGSC0003 DMG400024754)	RBO	2.8	-----
6.		PGSC0003DMT400088259	Elongation factor 1-alpha (PGSC0003DM G400037830)	Ef-1 α	Ref	Ref

*The gene annotations are as retrieved, on 17-06-14, from the website of ‘‘Potato Genomics Resource’’ (http://potato.plantbiology.msu.edu); **EnsemblP: EnsemblPlants search engine; PGSC: Potato Gene Sequencing Consortium; TIGR: The Institute for Genomic Research; Gene Abbr.: Gene abbreviation; S: Spraing; SF: Spraing-free; H: Healthy; (----): no significant difference in expression; Ref: Reference gene

Before proceeding to the qRT-PCR of the microarray samples, the specificity and accuracy of the qRT-PCR primer sets (Appendix. 22) was tested by conventional RT-PCR. The amplified fragments were cloned into the pGEMT-Easy vector and sequenced to confirm their identity. After confirming the specificity of these primer sets, the optimal concentration for their use in the quantitative assay was determined.

5.6.1. Optimization of primer(s) concentrations, for qRT-PCR of the HR-related genes in tuber samples

The qRT-PCR reagents and thermal cycling protocol is given in section 2.4.8 cDNA aliquots (1/ 25 dilution) from all the twelve RNA samples used in the microarray experiment were pooled together to make a bulked sample representative of all the sample types. For amplification of the target genes, 5 µl of the pooled cDNA sample was used as a template in a 25 µl qRT-PCR reaction. Each primer-pair was combined in a range of concentrations (from 50 nM to 900 nM) and the combination that resulted in productive amplification at the lowest number of cycles (C_T mean) and with an acceptably low variation in the C_T number (C_T standard deviation, C_T S.D) was selected to be used for primer validation and further qRT-PCR assays. The optimal concentrations (Opt. Conc.) of the tested primer-pairs with the lowest C_T means and acceptable C_T S.Ds (< 0.167) are given in Table No. 5.5.

Table 5.5. Optimal concentration of the primer-pair(s) for the qRT-PCR of HR-related genes in tuber samples

S.No.	Targeted gene	Primer name	Primer number	Opt.Conc. (nM)	C_T mean	C_T S.D
1.	PER	qPER_fwd	2329	300	24.119	0.047
		qPER_rev	2330	300		
2.	PAR	qPAR_fwd	2331	300	20.851	0.018
		qPAR_rev	2332	900		
3.	SP	qSP_fwd	2335	300	23.662	0.085
		qSP_rev	2336	900		
4.	GST	qGST_fwd	2343	900	21.638	0.037
		qGST_rev	2344	300		
5.	RBO	qRBO_fwd	2345	900	27.456	0.120
		qRBO_rev	2346	900		
6.	TRV1	qTRV1_fwd	2353	300	16.324	0.008
		qTRV1_rev	2354	300		
7.	Ef-1α	qEf-1_fwd	2323	300	28.298	0.079
		qEf-1_rev	2324	900		

Opt. Conc. Optimal concentration; nM: Nano-Molar; C_T mean: Cyclic threshold; C_T S.D: C_T Standard Deviation; PER: Peroxidase; PAR: Pathogenesis-related-protein1-c; SP: Suberization anionic peroxidase; GST: Glutathione-S-Transferase; RBO: Respiratory Burst Oxidase; TRV1: TRV1 Replicase; Ef-1α: Elongation factor-1 alpha.

5.6.2. Validation of the primer-set(s) for qRT-PCR of the HR-related genes

A dilution series of cDNA standards was prepared as discussed in section 2.4.7. PCR amplification efficiency of the primer-set (s) was evaluated by standard-curve quantitation and analysis (Appendix 23).

The melt-curve analysis (Appendix 23, a) of the different amplicons produced single Tm peaks that indicated no significant amplification of non-specific products by these primer-sets. The standard-curve analysis for the PER, PAR-1c, SP, GST, RBO, and the TRV1 genes provided regression-line slopes of -3.206, -3.224, -2.96, -3.296, -3.286, and -3.308 with an EFF % of 105.081, 104.251, 117.69, 101.081, 101.534, and 100.563, respectively. The regression co-efficient (R^2) between the standard curve regression-line and C_T data points of the amplification-plots were 0.994, 0.998, 0.995, 0.997, 0.986, and 0.997, respectively, indicative of a very close match between the regression-line and the C_T data points. The primers for the Ef-1 α gene,

used as the internal control for normalization of the amplification of the other genes, resulted in a regression-line slope of -2.979 with an EFF % of 116.595 and a R^2 value of 0.982.

The results of the primer validations for all the selected genes were within the acceptable range that confirmed the suitability of these primers for qRT-PCR validation of the microarray data.

Initially, all the twelve tuber samples (S1-H4) including all four TRV-infected spraing-symptomatic (S1-S4), all four TRV-infected spraing-free (SF1-SF4), and all four healthy tuber (H1-H4) samples were investigated by qRT-PCR to determine the relative amount of TRV present in each sample. Two samples each of the spraing (S1 and S4) and spraing-free (SF3 and SF4) samples, were found with the highest TRV-levels. All the four samples from the healthy tubers (H1-H4) were confirmed to be TRV-free.

5.7. Validation of the microarray data

The tuber samples with the highest levels of TRV infection (S1, S4, SF3 and SF4) and the healthy (TRV-free) tuber samples (H1 and H2) were selected for qRT-PCR validation of the microarray data that was done by the comparative C_T ($\Delta\Delta C_T$) method of quantification. New RNA samples extracted from the original freeze-dried tuber samples were prepared, as discussed before, and aliquots were stored in a freezer at -80 $^{\circ}$C. All the RNA samples were assayed in triplicate. The cDNA of healthy tuber (H2) was used as a calibrator or reference sample for calculation of the relative quantitation of the other tuber cDNAs. The fluorescence signals of the target genes were normalized either with the endogenous control gene Ef-1 α (Nicot *et al.*, 2005; Campbell *et al.*, 2010; Ross *et al.*, 2011) or the cyclophilin gene (as described by Hunter, 2013) or both (multiple endogenous controls). Use of these three approaches for normalization of the gene expression data gave different actual

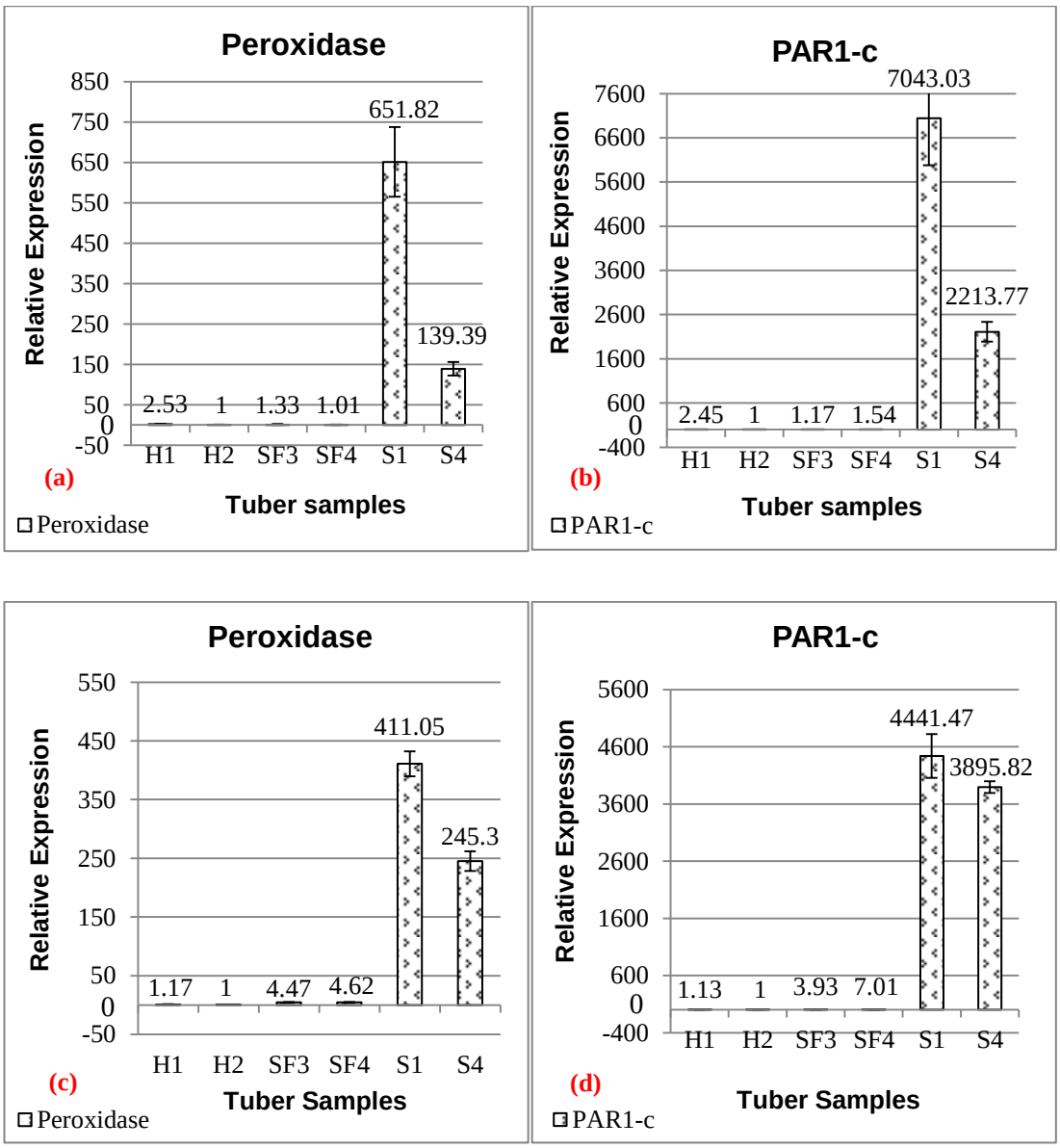

Figure 5.16. Gene expression of peroxidase and PAR1-c genes (normalized with Ef-1 α or cyclophilin gene). Relative expression of peroxidase (**a** and **c**) and PAR1-c (**b** and **d**) genes in the samples of healthy (H1 and H2), spraing-free (SF3 and SF4), and spraing-affected tubers (S1and S4) was normalized with the expression of EF-1α (**a** and **b**) and cyclophilin (**c** and **d**) genes. H2 was the calibrator for relative quantitation; "ɪ" is the error-bar representing the standard error of ΔΔCT measurements; value above the bar is fold-change of expression.

Table 5.6. Relative gene expression levels of peroxidase and PAR-1c genes, using three approaches of normalizing the data

S.No.	HR-related gene	Tuber sample	Gene expression normalized with		
			Ef-1 α	**Cyclophilin**	**MC**
1.	PER	S1	651.82	411.05	517.62
		S4	139.39	245.3	184.92
		Mean	**395.60**	**328.17**	**351.27**
		St. Dev.	**362.34**	**117.20**	**235.25**
		SF3	1.33	4.47	2.44
		SF4	1.01	4.62	2.16
		Mean	**1.17**	**4.54**	**2.3**
		St. Dev.	**0.23**	**0.11**	**0.2**
		H1	2.53	1.17	1.72
		H2	1	1	1
		Mean	**1.76**	**1.08**	**1.36**
		St. Dev.	**1.08**	**0.12**	**0.51**
2.	PAR-1c	S1	7043.03	4441.47	5592.98
		S4	2213.77	3895.82	2936.74
		Mean	**4628.4**	**4168.64**	**4264.86**
		St. Dev.	**3414.80**	**385.83**	**1878.24**
		SF3	1.17	3.98	2.14
		SF4	1.54	7.01	3.28
		Mean	**1.35**	**5.49**	**2.71**
		St. Dev.	**0.26**	**2.14**	**0.81**
		H1	2.45	1.13	1.67
		H2	1	1	1
		Mean	**1.72**	**1.06**	**1.33**
		St. Dev.	**1.02**	**0.09**	**0.47**

PER: Peroxidase; PAR1-c: Pathogenesis-related protein-1-c; H1 and H2: Healthy tubers; SF3 and SF4 Spraing-free tubers; S1and S4: Spraing tubers; Endogenous internal controls (EF-1α: Elongation Factor-1 alpha, and Cyclophilin); MC: Multiple endogenous controls (both EF-1α and Cyclophilin)

calculated relative quantities (RQs) for each gene. However, the general trend of significant up-regulation of all the genes assayed in the spraing samples was maintained (see Table No. 5.6), regardless of whether Ef-1 α or cyclophilin was used as the comparator, however, the cyclophilin gene was shown to be a more sensitive comparator and was used for most of the qRT-PCR experimentation in this study.

The $\Delta\Delta C_T$ quantitation of the peroxidase (PER) and pathogenesis-related protein1-c (PAR1-c) genes (Fig. 5.16), confirmed the significant up-regulation of their expression in the spraing-samples relative to the spraing-free samples. The highest RQ of peroxidase when normalized with Ef-1 α was found in the tuber sample S1,

followed by sample S4 with RQ expression of 651.82 and 139.39, respectively. For the samples SF3, SF4, and H1 the RQ expression was 1.33, 1.01 and 2.53, respectively (Fig. 5.16, a). Likewise, following Ef-1 α normalization and calibration, the expression of the PAR1-c gene was the highest in sample S1, followed by the S4 sample, with RQs of 7,043.03 and 2,213.77, respectively. The RQ of the PAR-1c gene in the samples SF3, SF4, and H1 was 1.17, 1.54 and 2.45, respectively (Fig. 5.16, b).

Normalization of the peroxidase gene with expression of the cyclophilin gene also revealed higher expression in the spraing samples as compared to the spraing-free samples. The cyclophilin-normalized peroxidase gene was highly expressed in spraing sample S1, followed by the sample S4 with RQs of 411.05 and 245.3, respectively (Fig. 5.16, c). For the cyclophilin-normalized samples SF3, SF4, and H1 the RQ of expression was 4.47, 4.62 and 1.17, respectively. The cyclophilin-normalized PAR1-c gene was also found to be very highly expressed in the spraing sample S1, followed by sample S4 with an RQ of 4,441.47 and 3,895.82, respectively (Fig. 5.16, d). The RQ of PAR1-c gene expression for the cyclophilin-normalized samples SF3, SF4, and H1 was 3.98, 7.01 and 1.13, respectively.

Similarly, normalization with multiple endogenous controls (both Ef1-alpha and the cyclophilin genes combined) also resulted in significantly higher gene expression of the PER and PAR-1c genes in the spraing samples. The multiple-gene-normalized peroxidase gene had RQs of 517.62 and 184.92 for the spraing sample S1 and S4, respectively (Fig. 5.18, a) that was higher than the samples SF3, SF4, and H1 with a RQ of 2.44, 2.16, and 1.72, respectively. Likewise the multiple-gene-normalized PAR1-c also had a significantly higher RQ of 5,592.98 and 2,936.74 for the spraing samples S1 and S4, respectively. The RQ of multiple-gene-normalized PAR1-c gene in the samples SF3, SF4, and H1 was 2.14, 3.28 and 1.67, respectively (Fig. 5.18, b).

Following all three discussed schemes of expression normalization, the relative expression of the peroxidase and PAR1-c genes was found to be much higher in the spraing samples than the other samples. For the spraing samples the mean RQ of the cyclophilin-normalized PER and PAR1-c genes (328.17 and 4168.64) and the mean RQ of the multiple-gene-normalized PER and PAR1-c genes (351.27 and 4264.86) was lower than the mean RQ of the Ef-1 α-normalized PER and PAR1-c genes (395.60 and 4628.4) for the same samples (Table No. 5.6). Further, analysis of the gene expression results revealed that the cyclophilin derived C_T means of 18.715 to 21.310 (for the samples S1 to H4) were lower than the Ef1-alpha-derived C_T means (30.911 to 31.135) from the same samples. Therefore, the cyclophilin gene was shown to be a more sensitive comparator and was used for all further qRT-PCR experimentation in this study.

The $\Delta\Delta C_T$ quantitation of the Suberization associated anionic peroxidase 2 **(**SP) and the Glutathione-S-transferase (GST) genes showed that the spraing samples (S1 and S4) had significantly increased expression of both genes, compared to the spraing-free (SF3 and SF4) and healthy tuber samples (H1 and H2). The SP gene was found to be highly expressed in the spraing samples S1 and S4, with RQs of 53.88 and 31.23, respectively (Figure 5.17, a), compared to the spraing-free (SF3 and SF4) and healthy (H1) samples with RQs of 0.34, 0.61, and 0.68, respectively. The expression of the GST gene was also found to be highly up-regulated in the spraing samples (S1 and S4) with RQs of 92.36 and 60.40, respectively compared to RQs of 3.65, 6.01, and 1.05, for the SF3, SF4 and H1 samples, respectively (Fig. 5.17, b).

The $\Delta\Delta C_T$ quantitation of the Respiratory burst oxidase homolog (RBO) revealed up-regulation of the RBO gene in one of the spraing sample (S4) with an RQ of 28.14, figure 5.17, c. Whereas, in the second spraing sample (S1) the RBO gene was less expressed (RQ of 2.85) than one of the Spraing-free (SF3, RQ of 6. 7) sample.

The SP, GST and RBO genes were expressed to higher levels (RQs 42.55, 76.38, and

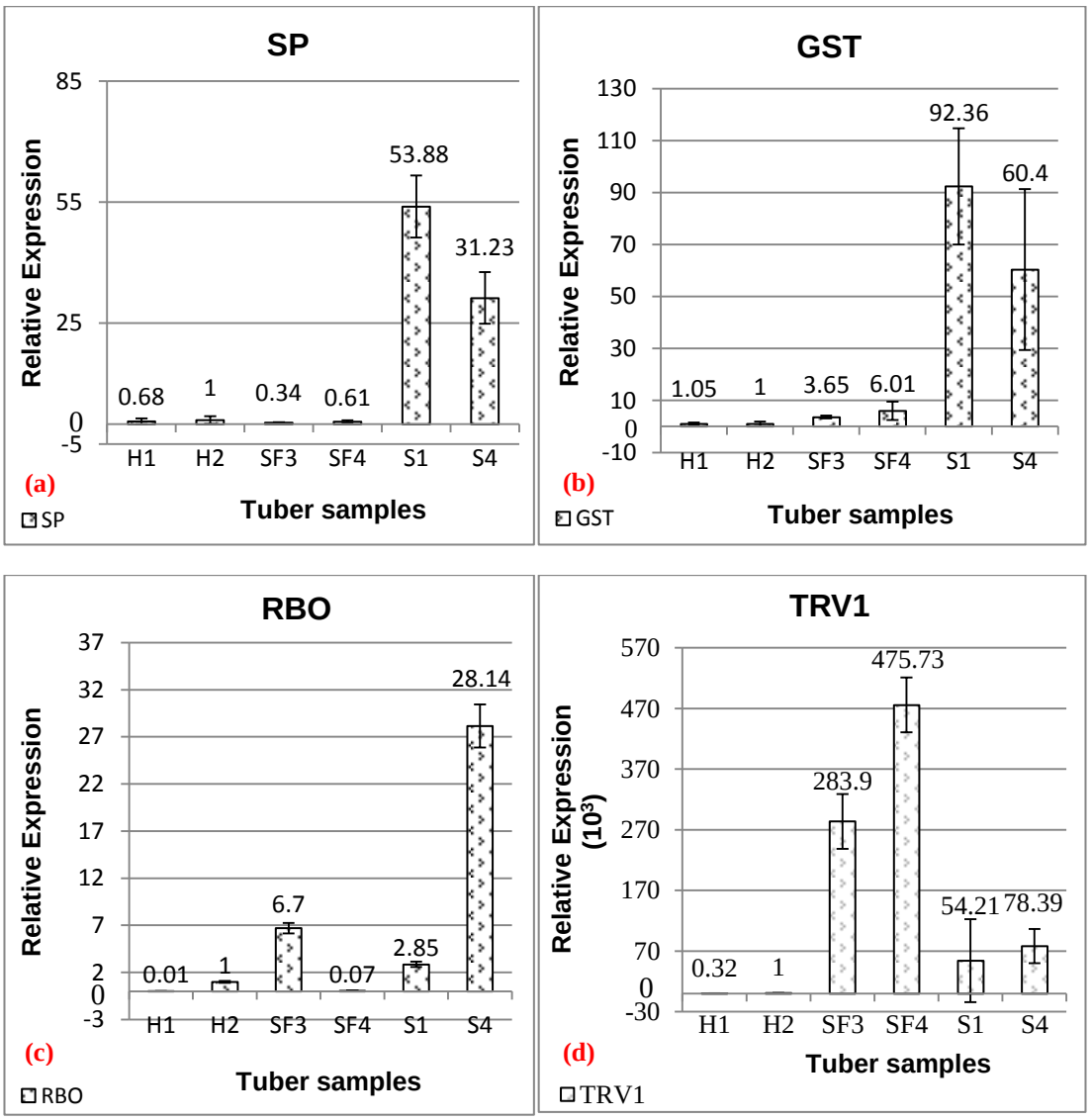

Figure 5.17. Gene expression of SP, GST, RBO, and TRV1 genes in tuber samples. Relative expression of **(a)** SP, **(b)** GST, **(c)** RBO, and **(d)**TRV-replicase genes in the samples of healthy (H1 and H2), spraing-free (SF3 and SF4), and spraing-affected tubers (S1and S4) was normalized with the expression of cyclophilin. H2 was the calibrator for relative quantitation; "ɪ" is the error-bar representing standard error of ΔΔCT measurements; value above bar is fold-change of expression.

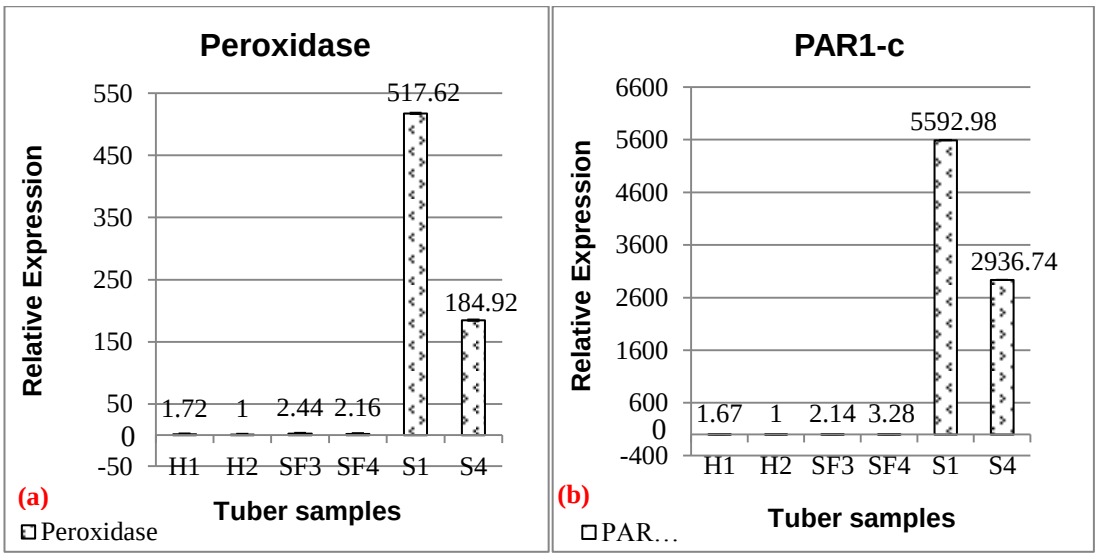

Figure 5.18. Gene expression of peroxidase and PAR1-c genes normalized with multiple endogenous control genes. Relative expression of peroxidase (**a**) and PAR1-c (**b**) genes was normalized with the expression of multiple control (both EF-1α and cyclophilin) genes. H2 was the calibrator for relative quantitation; "ɪ" is the error-bar representing standard error of ΔΔCT measurements; value above bar is fold-change of expression.

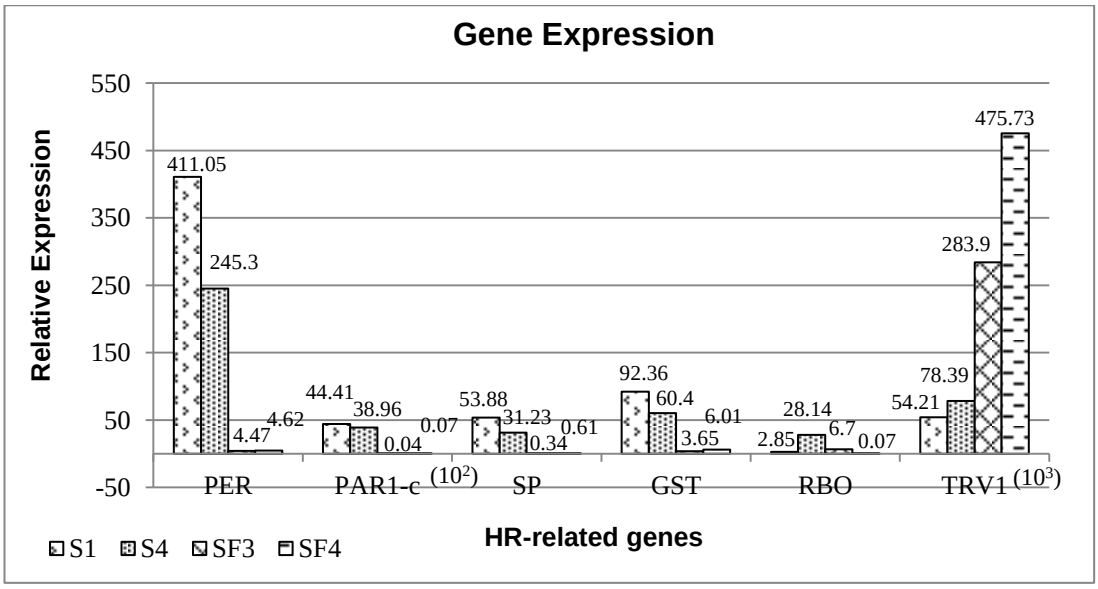

Figure 5.19. Expression of tuber genes compared to TRV-infection. RQ of PAR1-c and TRV1 is given in hundreds (x10^2) and thousands (x10^3) fold-change, respectively.

Table 5.7. Gene expression of SP, GST, RBO and TRV1 genes in tuber samples

S.No.	HR-related gene	Tuber sample	Normalized Expression	Mean Expression	St. Dev.
1.	SP	S1	53.88	42.55	16.02
		S4	31.23		
		SF3	0.34	0.47	0.19
		SF4	0.61		
		H1	0.68	0.84	0.23
		H2	1		
2.	GST	S1	92.36	76.38	22.60
		S4	60.4		
		SF3	3.65	4.83	1.67
		SF4	6.01		
		H1	1.05	1.025	0.03
		H2	1		
3.	RBO	S1	2.85	15.495	17.88
		S4	28.14		
		SF3	6.7	3.385	4.69
		SF4	0.07		
		H1	0.01	0.505	0.70
		H2	1		
4.	TRV1	S1	54.21	66.3	17.10
		S4	78.39		
		SF3	283.9	379.815	135.64
		SF4	475.73		
		H1	0.32	0.66	0.48
		H2	1		

The target gene expression was normalized with Cyclophilin used as the endogenous / internal control; Sample H2 was the calibrator for RQ of expression. RQ of TRV1 is given in thousands ($x10^3$) fold-change of expression.

15.49, respectively) in the spraing samples than the spraing-free and healthy samples (Table No. 5.7). Contrary to the up-regulation of all five HR-related genes (PER, PAR1-c, SP, GST and RBO genes) in the spraing samples, the TRV1 was found at lower levels in the spraing samples with a RQ of 54.21 $x10^3$ and 78.39 $x10^3$ for S1 and S4 samples as compared to an RQ of 283.9 $x10^3$ and 475.73 $x10^3$ for the spraing-free SF3 and SF4 samples, respectively (Fig. 5.17, d). The mean RQ of TRV1 in the spraing samples (66.3 $x10^3$) was much less than the mean RQ of TRV1 in the spraing-free samples (379.815 $x10^3$, Table No. 5.7) suggesting a suppressive role of spraing symptoms in virus accumulation.

5.8. Suppression of TRV infection by spraing associated gene-expression

The current studies revealed that the expression of four of the five selected tuber-genes (except the RBO) was higher in the spraing sample with the lowest amount of TRV (S4) than in the sample with the relatively higher level of TRV (S1) infection (Fig. 5.19). This observation indicates that for four of HR-related genes (PER, PAR1-c, SP and GST), their up-regulation is associated with the suppression of TRV infection. TRV in the spraing sample S1 (RQ of 54.21 x 10^3) and S4 (RQ of 78.39 x 10^3) had a mean RQ of 66.3 x 10^3 that was less than a quarter of the mean RQ of TRV (379.81x10^3) found in the spraing-free samples SF3 (RQ of 283.9x 10^3) and SF4 (RQ of 475.37 x 10^3, Table No. 5.7). Thus, the spraing sample with the lowest amount of TRV (S1) had the highest expression of HR-related genes and vice versa. In contrast, the RBO gene was less expressed (RQ of 2.85) in the spraing sample (S1) with comparatively lower TRV infection (RQ of 54.21 x 10^3), and it was more highly expressed (RQ of 28.14) in the spraing sample (S4) with the higher infection of TRV (RQ of 78.39 x 10^3). Thus, RBO expression appears to be stimulated either by TRV infection or by production of spraing symptoms. This mirrors the microarray results for this gene (Table No. 5.7) where only modest differential expression was found when comparing spraing-free versus healthy samples and no differential expression was found when comparing spraing versus spraing-free samples.

5.9. Histochemical staining for HR reactions in tubers

To complement the gene expression studies, for confirming the involvement of HR processes in spraing production, some tissue staining approaches were used to further examine the biochemical basis of spraing. The results presented in Fig. 5.20 are representative of the results obtained from each experiment done in triplicate.

5.9.1. Cell-death in spraing tissue

Cell-death in spraing symptomatic tissue was assayed by the trypan-blue staining protocol given in section 2.4.9 (1). The images (Fig. 5.20, group T) of tuber-sections (a, b) and (c, d) are from a healthy and spraing-affected tuber, respectively. Images of the same tuber sections captured before and after staining with the trypan-blue lactophenol solution, are given in (a, c) and (b, d), respectively. Both types of tuber sections (a, c) were treated with an equal amount of stain solution for the same time and were then destained (b, d) for an equal time. Intense staining, due to trypan-blue uptake, of dead cells (blue-colour) in and around the spraing-affected tissue was evident. This proved the occurrence of cell-death, in and around the spraing tissue. Some background staining of the tissue-sections was also visible. This was due to trypan-blue uptake by the cells that had died during the preparation of the tuber cross-sections, due to the infliction of mechanical injury (d).

5.9.2. ROS activity in spraing tissue

The 3, 3′-Diaminobenzidine (DAB) stain is used for the visualization of hydrogen peroxide (H_2O_2) production and accumulation. The DAB stain is preferred for use in immunohistological preparations as it produces an intense brown-black precipitate in response to the peroxidase activity and is insoluble in alcohol. DAB staining (section 2.4.9, 3) of the tuber slices from a healthy (a, b) and spraing-affected (c, d) tuber is presented in Fig. 5.20, group D. The images of the same tuber slices captured before and after the DAB staining are given in panels (a, c) and (b, d), respectively. The intense deposition of dark-brown coloured precipitates in and around the vicinity of the spraing-affected tissue (d) suggests an enriched production of peroxides, such as H_2O_2, in this diseased area of the tuber. Whereas, the background staining of DAB in the spraing tuber slice (d) and the healthy tuber slice (b) is due to the endogenous generation of the peroxides as a by-product of normal metabolic process.

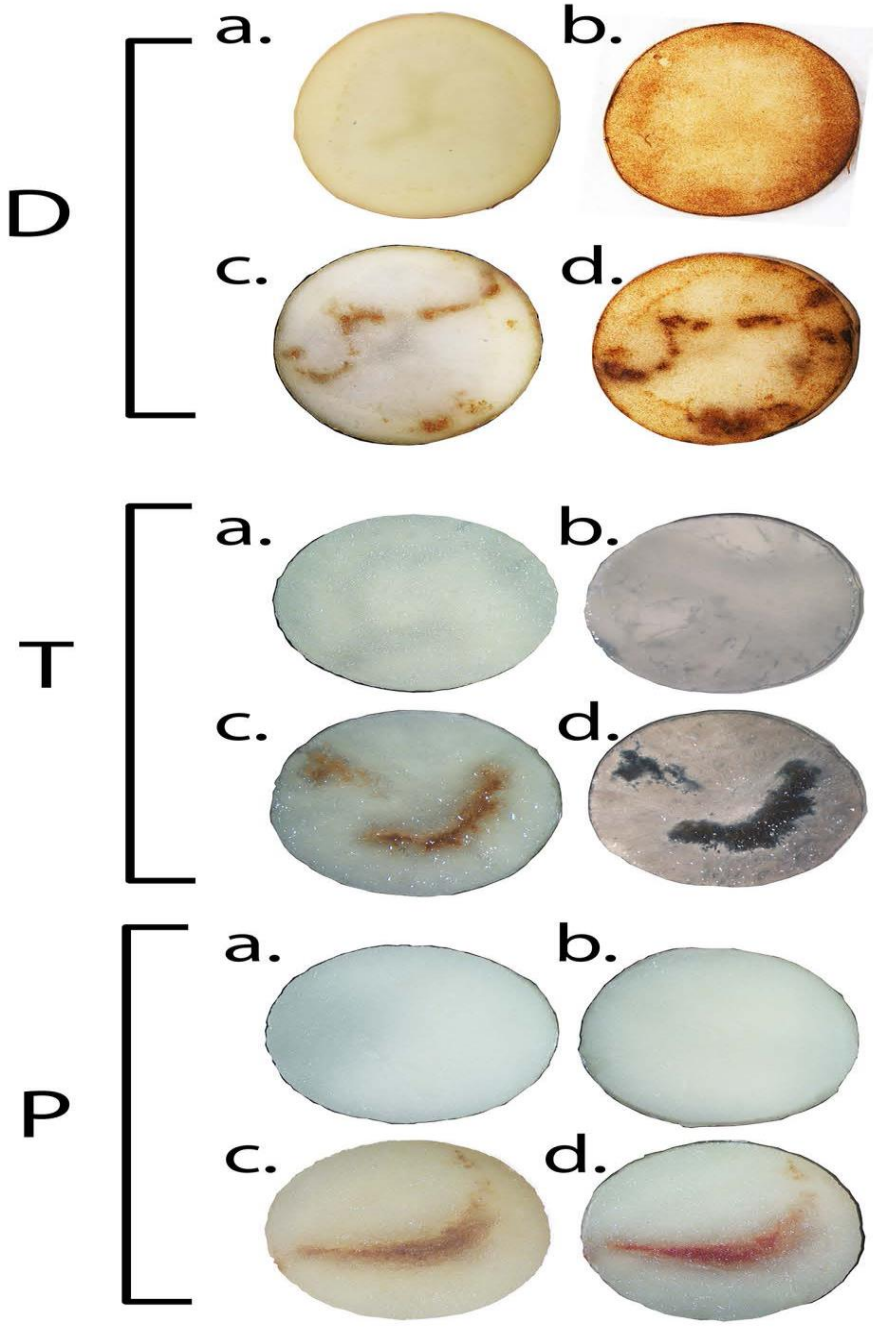

Figure 5.20. Histochemical staining of spraing tissue. Tuber group **D**, stained with DAB; group **T**, stained with trypan blue; group **P**, stained with phloroglucinol. Healthy tuber **(a**, **b**) and spraing-affected tuber **(c**, **d**) slices. Tuber slices before **(a**, **c**) and after staining **(b**, **d**) with histochemical-stains.

5.9.3. Lignin deposition in spraing tissue

Spraing disease is also known in some countries as corky ring spot disease, with researchers suggesting that the dark inclusions have a corky nature. Cork is a complex tissue enriched in suberin that forms the structural part of the cell wall and is augmented by additional binding compounds such as lignin and non-lignin organic (aromatic) compounds (Pereira, 2007). Biochemical reaction of the coniferyl and sinapyl aldehyde chains of lignin with phloroglucinol, produces a reddish-pink coloured product.

Lignin deposition in the spraing tissue was tested by the protocol given in section 2.4.9 (2) and the results are presented in Fig. 5.20, group P. The images (a, b) and (c, d) were captured from a healthy and spraing-affected tuber, respectively. Whereas, the images of the same tuber sections before and after the phloroglucinol staining are given in (a, c) and (b, d), respectively. The spraing-affected tissue (d) was stained reddish-pink by the phloroglucinol that confirmed the deposition of lignin in the spraing tissue.

5.10. Examination of HR-related genes in spraing-affected tubers with different genetic make-up

The microarray and subsequent qRT-PCR experiments found up-regulation of a number of HR-related genes in spraing-affected tubers of c.v. Pentland Dell. We decided to examine the genetic expression of these genes from potato tubers that were genetically different to Pentland Dell; to be sure that gene expression associated with the spraing disease of potato is independent of variety. Since spraing symptoms in potato tubers are associated with infection by TRV or PMTV, we sourced more spraing-affected potato tubers that had been assessed in other laboratories as being infected with PMTV. We subsequently examined HR-related gene expression in a selection of these newly obtained tubers. For this purpose the potato tubers from two

different sources viz.; a JHI PMTV field-trial (varieties not known) and SASA (varieties Burren and Electra) examined germplasm were acquired (section 2.1.4). Before proceeding to the qRT-PCR verification for up-regulation of the selected HR-related genes, we confirmed the status (presence or absence) of each of the spraing-inducing viruses (TRV and PMTV) in the germplasm either by Enzyme Linked Immunosorbent Assay (ELISA, PMTV) or RT-PCR (both PMTV and TRV) testing.

The ELISA-based screening against PMTV, showed 9 out of 11 tubers to be PMTV-positive from the PMTV field-trial of Louise Sullivan (Table No. 5.8). Leaf-sap from PMTV-infected *N. benthamiana* plants, extracted at 6 dpi, and a mock-inoculated (1X PBS) *N. benthamiana* plant were the positive and negative controls in the assay, respectively. The tuber samples that producd a ELISA value of twice the absorbance value of the negative control, measured at A° 405 nm, were considered to be positive for PMTV. ELISA readings recorded after one hour of incubation with the detection reagent, resulted in 8 out of 11 tubers identified as PMTV-positive. But with an

Table 5.8. ELISA-based screening of potato tubers from a PMTV field-trial

S.No.	Spraing Sample	A°405nm (1 hour)	A°405nm (Overnight)	PMTV status (-ve or +ve)
1.	Non-Infected *N. benth*	0.066	0.089	-ve
2.	PMTV-infected *N. benth*	0.456	2.575	+ve
3.	LS1	0.070	0.088	-ve
4.	LS2	0.088	0.247	**+ve**
5.	LS3	0.068	0.094	-ve
6.	LS4	0.384	2.233	**+ve**
7.	LS5	0.192	1.022	**+ve**
8.	LS6	0.154	0.762	**+ve**
9.	LS7	0.257	1.385	**+ve**
10.	LS8	0.267	1.394	**+ve**
11.	LS9	0.210	1.121	**+ve**
12.	LS10	0.210	1.088	**+ve**
13.	LS11	0.153	0.715	**+ve**

-ve: PMTV-free; +ve: PMTV positive; LS: Spraing-affected sample from tubers of Louise Sullivan field-trial.

overnight incubation one more sample (LS2) was recorded as PMTV-positive. The potato tubers L1 and L3 proved to be PMTV-free in these ELISA tests.

Although, the ELISA results suggested tuber L3 (sample LS3) to be PMTV-free, this tuber was found to be affected with spraing symptoms. Therefore, it was decided to re-confirm the results of ELISA by RT-PCR testing of selected samples. Five tuber samples (LS2, LS3, LS4, LS9 and LS11) were selected for detection of PMTV and TRV by RT-PCR.

5.10.1. RT-PCR testing of potato tubers acquired from PMTV field-trial and SASA.

In addition to the five field-trial acquired tubers described above, I also examined a further five spraing-affected tubers supplied by Dr. Christophe Lacomme (SASA, Edinburgh). The total RNA isolation, RNA clean up, DNase digestion and cDNA synthesis from these tubers was done as already explained (section 2.4.1-5). The PCR reagents and the thermal cycling protocol were the same as used before (section 2.4.5). The primer-set for PMTV detection and reference (Ef-1 α) gene amplification is given in section 2.4.5 and appendix 1, respectively. The detection of TRV was performed by using three TRV1-based primer-sets. One of these was the 16K-based primer-set (DJR Primer-set; for 463 bp amplicon), another primer-set was the MP gene-specific (MP, Primer No. 2467 and 2370; for 568 bp amplicon) and the third primer-set for a portion of the replicase gene (R, Primer No. 2367 and 2368; for 474 bp amplicon). Five spraing-affected tuber samples each from the SASA (BTS, ETS, EPS1, EPS2 and EPS3) and PMTV field-trial (LS2, LS3, LS4, LS9 and LS11) sources were tested. So, in total, 10 tuber-samples and one sample each of a positive control (*N. benthamiana* plant, known to be infected with the test-virus) and a negative control (PEBH, potato tuber-sample known to be virus-free) were tested by RT-PCR.

A. Detection of TRV

The 16K-based primer-set detected TRV1 (463 bp amplicon) in three (BTS, ETS and LS4) out of the ten tuber-samples. However, amplification from sample EPS2 gave a smeared band with these primers (Fig. 5.21, I, a). The MP-based primer-set detected TRV1 (568 bp amplicon) from two (BTS and EPS2) out of ten samples. But this primer-set failed to detect TRV1 from the samples ETS and LS4, which were found positive for TRV by using the 16K-based primer-set. However, the MP-based primer-set was able to detect TRV1 from the sample EPS2, for which the 16K-based primer-set had failed to detect the TRV (Fig. 5.21, II, a). The TRV-R, replicase gene-based primer-set, detected TRV1 (474 bp amplicon) from seven of ten samples (BTS, ETS, EPS1, EPS2, LS2, LS3 and LS9). Whereas, three tuber (EPS3, LS4 and LS11) were found to be TRV-free when tested by the replicase-based primer-set (Fig. 5.21, III, a). Thus, as a result of using a series of different TRV-specific primer pairs, only two tubers (EPS3 and LS11) among all the ten tubers were found to be TRV-free.

B. Detection of PMTV

PMTV was detected in nine out of the eleven tubers. Two samples (BTS and PEBH) did not produce a PMTV-specific (356 bp) amplicon (Fig. 5.21, IV, a), confirming the PMTV-free status of these tubers.

The amplification of the Ef-1α gene from all the tuber-samples (255 bp, Fig. 5.21, IV, b) and the positive control sample of *N. benthamiana* (150 bp; Fig. 5.30, IV, c) confirmed the integrity of the total RNA and cDNA of these samples. The non-template control (NTC) and the mixed sample from uninfected potato tubers (PEBH), used as the negative control did not show amplification of TRV or PMTV confirming the virus- and contamination-free status of these samples. The TRV-related PCR products from most of the samples except tuber-sample BTS were amplified to lower levels than the PMTV-related PCR products from the same

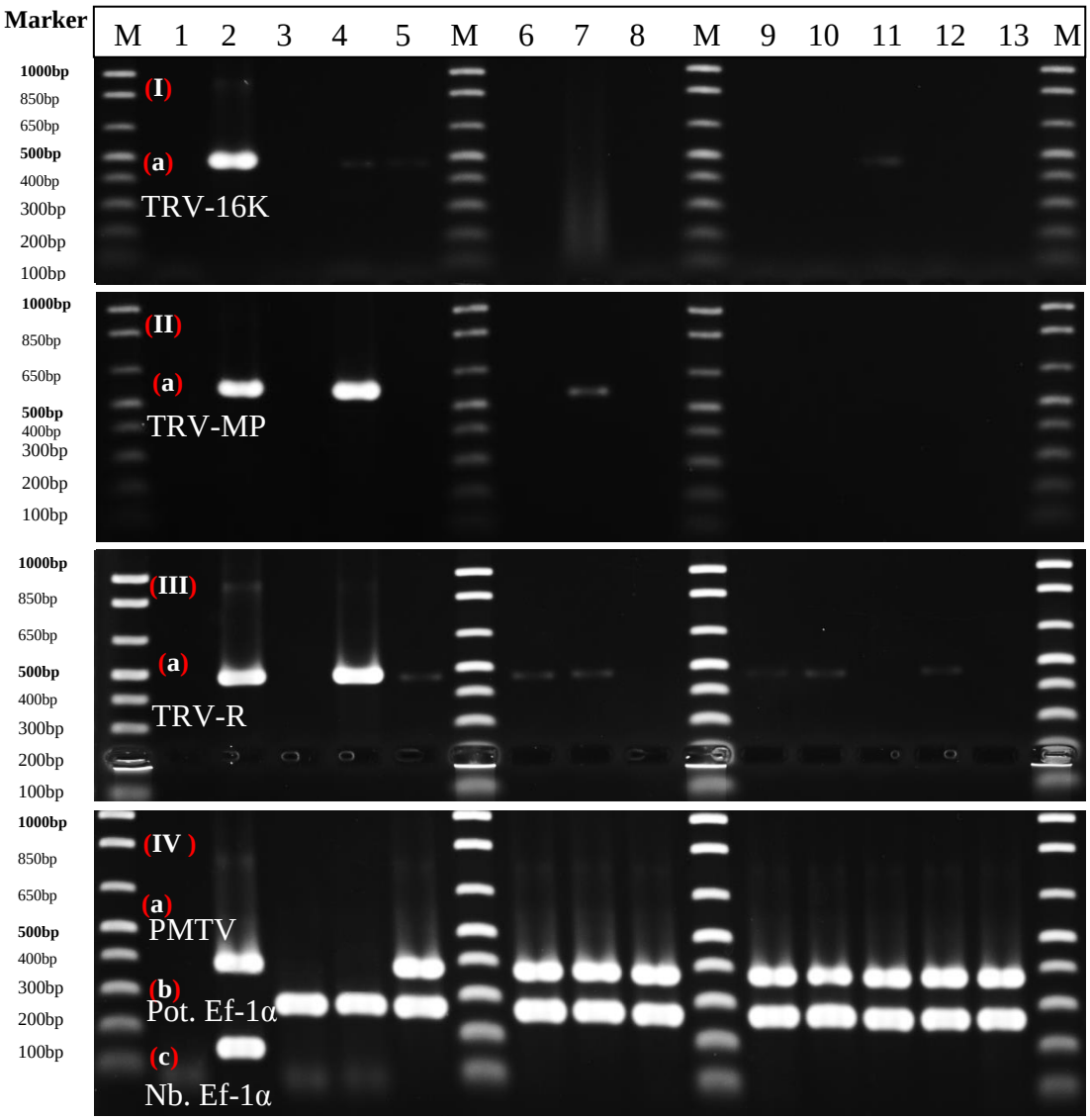

Figure 5.21. RT-PCR detection of TRV and PMTV in spraing-affected samples from genetically different tubers. Lane M: 1 Kb Plus DNA Marker. **Lane 1**: Non-Template Control (NTC). **Lane 2**: Positive control (amplicon from virus-infected *N.benthamiana*). **Lane 3**: Negative control (PEBH, Pooled healthy tuber-sample). **Lane 4**: Burren spraing-affected sample (BTS). **Lane 5, 6, 7** and **8**: Electra spraing-affected sample ETS, EPS1, EPS2 and EPS3, respectively. **Lane 9,10,11,12** and **13**: Louise spraing-affected sample LS2, LS3, LS4, LS9 and LS11, respectively. **(I, a)** TRV-16K primer-set based amplicon (462bp). **(II, a)** TRV Movement Protein (MP) based amplicon (568 bp). **(III, a)** TRV-Replicase (R) based amplicon (474 bp). **(IV, a)** PMTV TGB2 based amplicon (356 bp). **(IV, b** and **c)** Amplicon of house-keeping (Ef-1 α) gene from potato-tuber (255 bp, Pot.Ef-1 α) and virus-infected *N. benthamiana* (150 bp, Nb. Ef-1 α), respectively.

samples. This might suggest a relatively lower amount of TRV than PMTV in these tubers. However, both PMTV and TRV were not quantified in these samples.

The virus-status of all the ten tubers is summarised in Table No. 5.9. The tubers, based on the type of viral-infection, were categorized into four classes, viz: only TRV-infected tubers (BTS), only PMTV-infected tubers (EPS3, LS4, and LS11), tubers with mixed infection of both TRV and PMTV (ETS, EPS1, EPS2, LS2, LS3 and LS9) and the tubers that were both TRV- and PMTV-free (apparently healthy tubers).

Table 5.9. Virus-status of the potato tubers chosen from the PMTV field-trial and the SASA examined potatoes

S.No.	Tuber	Sample	TRV	PMTV	Mixed infection	Virus status
1.	BT	BTS	√	NIL	NIL	+ve
2.	ET	ETS	√	√	√	+ve
3.	EP1	EPS1	√	√	√	+ve
4.	EP2	EPS2	√	√	√	+ve
5.	EP3	EPS3	NIL	√	NIL	+ve
6.	L2	LS2	√	√	√	+ve
7.	L3	LS3	√	√	√	+ve
8.	L4	LS4	NIL	√	NIL	+ve
9.	L9	LS9	√	√	√	+ve
10.	L11	LS11	NIL	√	NIL	+ve
11.	Pooled	EBPH	NIL	NIL	NIL	-ve

NIL: Not detected; √: Virus-detected; -ve: Virus-free; +ve: Virus-positive; SASA examined potatoes (Burren and Electra); Burren spraing-affected tuber-sample, BTS; Electra spraing-affected tuber-sample, ETS, EPS1-3; Spraing-affected tuber samples collected from Louise Sullivan / PMTV field-trial : LS2, 3, 4, 9, and 11; PEBH: mixed sample from uninfected tuber.

5.10.2. Quantitation of HR-related gene expression in the tubers with different genetic make-up and virus-infections

Seven of these tubers were selected for qRT-PCR analysis. In order to represent all viral infection-types under study, at least one tuber was chosen from each of the 4 above given classes. The selected tubers were BT (TRV only); EP3, L11 (PMTV only); ETS, EPS1, EPS2 and LS2 (Mixed viral infection); and PEBH (PMTV and

TRV-free, apparently healthy). The spraing-affected (S) and spraing-free (SF) tissue was excised from each tuber as discussed before (section 2.1.1). The total RNA extraction, DNase treatment, and cDNA synthesis protocols were the same as discussed before.

Two of the HR-related genes (PAR-1c and the SP gene) were again examined for their differential expression in S vs. SF samples. The expression of both of the selected genes was quantitated and analysed by the $\Delta\Delta C_T$ quantitation method. Each sample was assayed in triplicate and the expression of the cyclophilin gene was used for normalization of the target gene-expression. The qRT-PCR protocol was the same as explained before except that, in this analysis, a mixed sample from uninfected tubers (PEBH) served as a calibrator sample to determine the relative quantity of target gene expression. A summary of the RQ's of both of the assayed genes and the types of viral-infections in the evaluated samples is given in Table No.5.10.

The RQ plot for the PAR1-c gene showed (Fig. 5.22, a) significantly increased expression in the spraing tissue samples of all the seven tubers. The highest RQ of the PAR1-c gene (2533.31) was found in the spraing-affected sample LS11. The SF-sample (LSF11) from the same tuber L11 had a RQ of 13.93. The PAR1-c had the second highest expression level (RQ of 1007.86) in the spraing-affected sample (EPS1) from the tuber EP1, while the SF-sample (EPSF1) from the same tuber had a RQ of 4.06. The lowest level of PAR1-c gene expression (RQ of 58.1) was in the spraing-affected sample (EPS2) from the tuber EP2 and was significantly higher in expression than the SF-sample (EPSF2) of the same tuber, with a RQ of 7.06.

Similarly, the SP gene was also highly expressed in the spraing-samples as compared to the spraing-free samples from the same tubers (Fig. 5.22, b). The SP gene was most highly expressed (RQ of 46.68) in the spraing-affected sample (EPS2) of the tuber EP2 and the spraing-free sample (EPSF2) of the same tuber had

a RQ of 1.56. The next highest expression of the SP gene (RQ of 29.78) was in the spraing-affected sample (BTS3) of the tuber BT3 and the SF-sample of the same tuber (BTSF3) had a RQ of 1.98. Among all the spraing-affected samples, the lowest RQ of SP (7.32) was found in the sample LS11 of the tuber L11 and the spraing-free sample (LSF11) of the same tuber had a RQ of 0.1.

Table 5.10. RQs of expression of the PAR1-c and the SP genes in different tuber samples, with different types of viral-infections

S.No.	HR-related gene	Variety	Tuber sample	Viral-infection	Normalized RQ
1.	PAR1-c	Burren	BTS	TRV only	466.73
			BTSF	//	6.15
		Electra	EPS3	PMTV only	110.65
			EPSF3	//	4.44
		Unknown	LS11	//	2533.31
			LSF11	//	13.93
		Electra	ETS	TRV+PMTV	110.92
			EPS1	//	1007.86
			EPS2		58.1
			ETSF	//	42.69
			EPSF1	//	4.06
			EPSF2	//	7.06
		Unknown	LS2	//	745.25
			LSF2	//	9.27
		Pooled	PEBH	NIL	1
2.	SP	Burren	BTS	TRV only	29.78
			BTSF	//	1.98
		Electra	EPS3	PMTV only	8.42
			EPSF3	//	1.48
		Unknown	LS11	//	7.32
			LSF11	//	0.1
		Electra	ETS	TRV+PMTV	10.562
			EPS1	//	8.96
			EPS2	//	46.68
			ETSF	//	4.38
			EPSF1	//	1.16
			EPSF2	//	1.56
		Unknown	LS2	//	25.55
			LSF2	//	0.28
		Pooled	PEBH	NIL	1

BTS: Burren spraing-affected sample; ETS, EPS1, EPS2, EPS3: Electra spraing-affected samples; LS2, LS11: spraing-affected samples from tubers with unknown genetic background (PMTV–field trial); BTSF: Burren spraing free-sample; ETSF, EPSF1, EPSF2, EPSF3: Electra spraing free-samples; LSF2, LSF11: spraing free-samples from tubers with unknown genetic background (PMTV–field trial); PEBH: Mixed sample from uninfected tubers, was the calibrator.

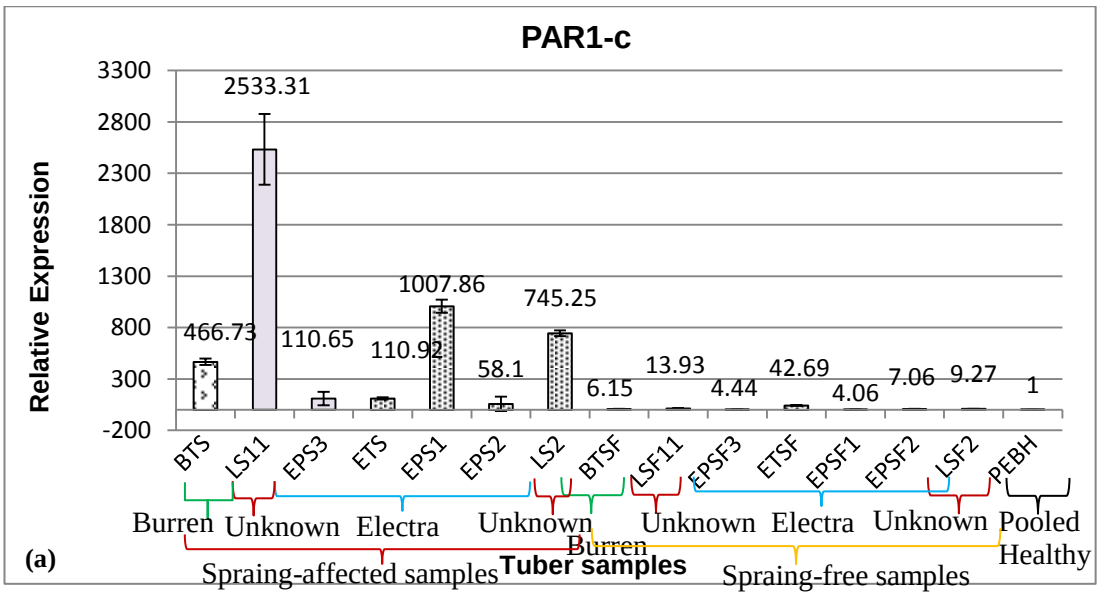

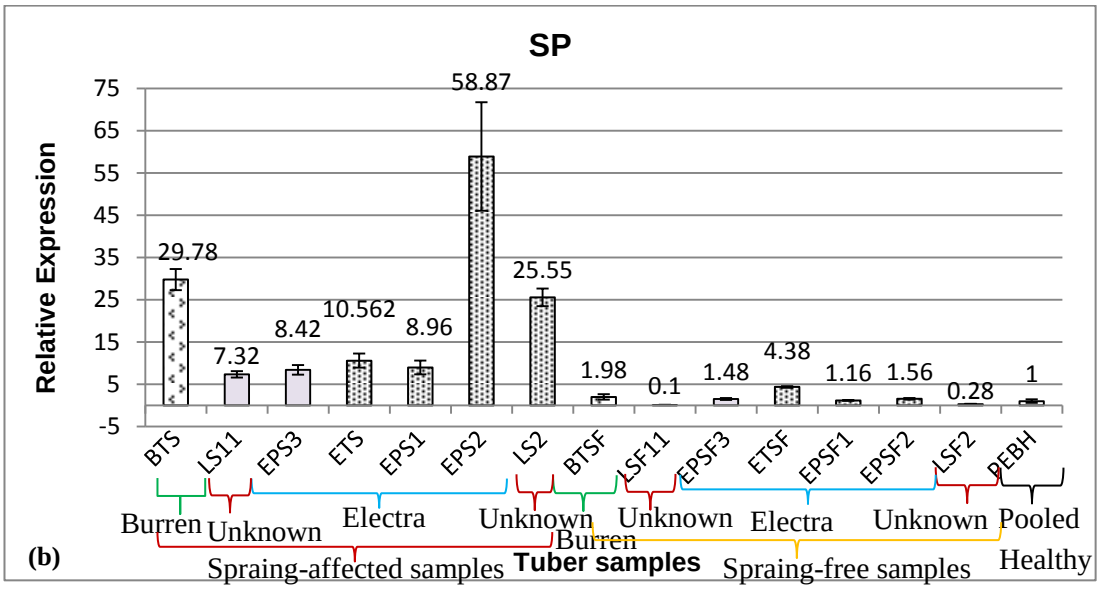

.

Figure 5.22. Expression of the HR-related genes in the tubers with different genetic make-up and virus infections. Relative expression of SP **(a)** and PAR1-c **(b)** genes in the tuber samples of Burren (BTS, BTSF), Electra (ETS, EPS1, EPS2, EPS3, ETSF, EPSF1, EPSF2, and EPSF3) and the tubers with unknown genetic make-up, PMTV–field trial (LS2, LS11, LSF2, LSF11). PEBH: Mixed sample from uninfected tubers, was the calibrator. ''ɪ'' is the error-bar representing standard error of ΔΔCT measurements; value above bar is fold-change of expression.

The mean RQs of both of the assayed genes for the investigated varieties and the types of viral infections are given in Table No.5.11. Since, in this assay, only a single sample of TRV-infected tuber (variety Burren) was included, the reported RQ for this sample is not a mean value.

The mean RQ of PAR1-c (719.84) for all the seven spraing-affected samples (BTS3, LS11, EPS3, ETS, EPS1, EPS2, and LS2) was significantly higher than the respective spraing-free samples (BTSF3, LSF11, EPSF3, ETSF, EPSF1, EPSF2, and LSF2) with a mean RQ of 12.51. Similarly, the mean RQ of the SP gene (19.61) for all the seven spraing-affected samples was significantly higher than all the seven respective spraing-free samples (mean RQ of 1.56). Both of the HR-related genes were significantly up-regulated in the spraing-affected tissue of these different potato varieties, following the pattern previously found for Pentland Dell. The up-regulation and association of HR-related genes with spraing-affected tissue supports the notion of spraing as a HR-reaction.

Table 5.11. Mean RQs of the PAR1-c and the SP genes in the tuber samples with different genetic make-up and types of viral infections

S.No.	HR-related gene	Mean RQ	Mean RQ of samples infected with				Mean RQ of variety		
			TRV*	PMTV	Both Viruses	No virus (PEBH)	Burren	Electra	Unknown (LS)
Spraing-affected samples									
1.	PAR1-c	719.84	466.7	1321.98	482.05	1	466.73	323.4	1639.28
2.	SP	19.61	29.78	7.87	22.94	1	29.78	18.65	16.43
Spraing-free samples									
3.	PAR1-c	12.51	6.15	9.18	15.77	1	6.15	14.56	11.60
4.	SP	1.56	1.98	0.79	1.84	1	1.98	2.14	0.19

*The RQ for TRV-infected sample (Burren) is not a mean RQ

Fig. 5.23 shows the up-regulation of PAR1-c and SP genes in relation to virus-status of the different spraing symptomatic tuber samples. The results show that these genes were up-regulated by both viruses and there does not appear to be any additive effect when the tuber is infected simultaneously by both viruses. Virus levels were not

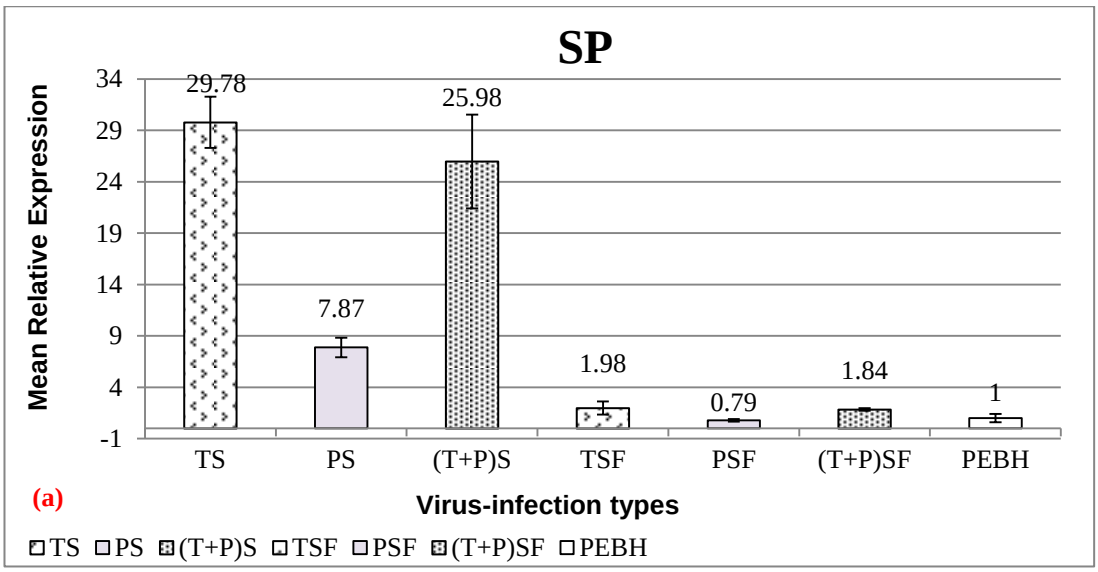

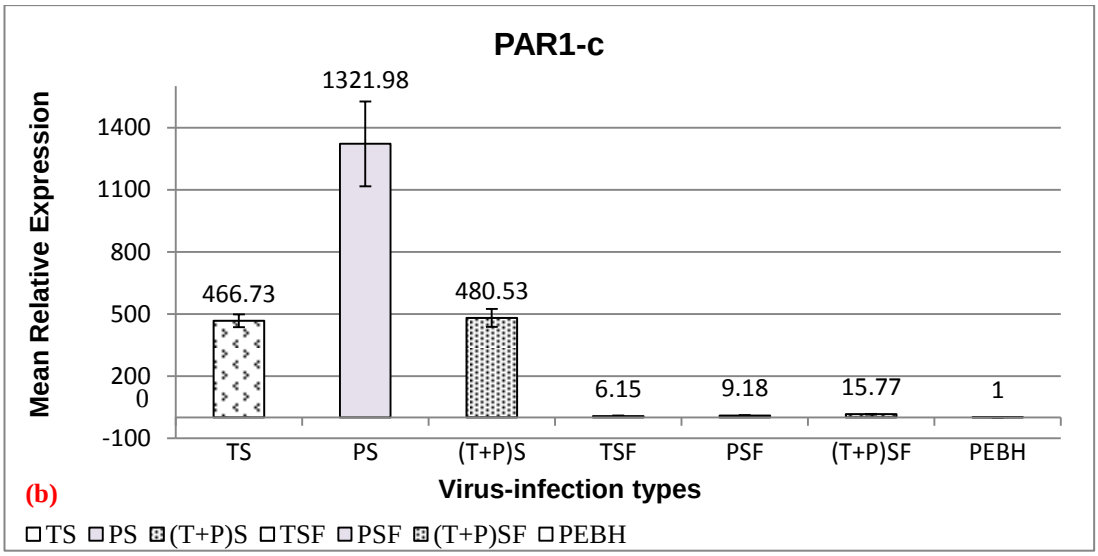

Figure 5.23. Effect of type of viral infection on the expression of the HR-related genes in spraing-affected tubers. Relative expression of SP **(a)** and PAR1-c **(b)** genes in the tubers infected by TRV (T), PMTV (P), and TRV plus PMTV (T+P).S denotes samples showing spraing symptoms, SF are samples without spraing symptoms. PEBH: Mixed sample from uninfected tubers, was the calibrator. "I" is the error-bar representing standard error of ΔΔCT measurements; value above bar is fold-change of expression.

quantified in these samples and so no comment can be made about possible synergism between TRV and PMTV in potato tuber.

5.11. Distribution of TRV in a spraing-affected tuber

TRV is unevenly distributed within a spraing-affected tuber. The spraing-affected tissue is always associated with the TRV infection whereas, the occurrence of TRV in spraing-free tissue is erratic (Crosslin and Thomas, 1995; Xenophontos *et al*., 1998). A large-sized spraing-affected Pentland Dell tuber (>33.6 cm^2 diameter) was washed with tap-water, dried on filter-paper, and sliced in cross-section with a sharp knife. 11 samples (20-35 mm^2 of the tuber), comprising either of spraing-affected or spraing-free tissue, were excised from the tuber-slice (Fig. 5.24, a). Eight out of these 11 samples were collected from visibly spraing-free areas (i.e.; SF1-SF8), two samples (S10, S11) from areas that had strong spraing symptoms and one sample (S9) was gathered from a small area of faint spraing. RT-PCR was done to detect TRV (section 2.2.16) in RNA extracted (section 2.4.2-3) from these 11 samples. The TRV RNA1 was detected in the positive control sample (S2, spraing sample known for TRV-infection in the microarray experiment), in all the three spraing-symptomatic samples (S9, S10, and S11) and in five out of the eight spraing-free samples (SF3, SF5, SF6, SF7, and SF8, Table No. 5.12). Virus was not detected in the healthy (negative) control (H) sample and in three spraing-free samples (SF1, SF2, and SF4). The house keeping gene (Ef-1 α) was successfully amplified (255 bp; Fig. 5.24, b) from all of the tuber RNA samples confirming their integrity.

Interestingly, TRV was strongly amplified from five of the eight spraing-free areas and weakly amplified from a sixth (SF1). All the three spraing-affected areas (S9, S10, and S11) amplified a TRV signal that was noticeably weaker than the majority of the spraing-free areas, suggesting a relatively-reduced load of TRV at these sites. Possibly, formation of the spraing had a suppressive effect on the accumulation of TRV so that the virus infection was reduced in the areas of tuber bearing spraing

symptoms. These results were supportive of the previous TRV quantitation results derived from the microarray-analysed samples (Fig.5.17, d; Table No. 5.7), where,

Table 5.12. Prevalence-profile of TRV1 and GST in a spraing-affected tuber, determined in some selected-sites

S.No.	Sampling site / Sample No.	Spraing status (SF / S)	TRV-status (P /A)	Nor. Mean RQ of TRV1	Nor. Mean RQ of GST
1.	SF1	SF	P	1.156	1.376
2.	SF2	SF	A	N / A	N / A
3.	SF3	SF	P	N / A	N / A
4.	SF4	SF	A	N / A	N / A
5.	SF5	SF	P	N / A	N / A
6.	SF6	SF	P	1046240.619	1.188
7.	SF7	SF	P	113348.411	2.332
8.	SF8	SF	P	N / A	N / A
9.	S9	S	P	N / A	N / A
10.	S10	S	P	74470.342	8.921
11.	S11	S	P	87773.433	20.738
12.	H1	H	H	Calibrator for RQ	Calibrator for RQ

S: Spraing-affected; SF: Spraing-free; H1: Healthy, TRV-free; P: Present; A: Absent; Nor. Mean RQ: Gene-expression of the target, normalized with the gene expression of the reference gene (Ef-1α); TRV: Tobacco rattle virus-replicase; N / A: Not analysed.

TRV was found in reduced amounts in the spraing samples as compared to the spraing-free samples.

5.12. Quantitation of TRV across a spraing-affected tuber slice

TRV quantification in a diseased tuber had not been reported by earlier researchers. To further study the association between the relative level of virus and appearance of spraing symptoms in tuber tissue, we quantified the amount of TRV in different areas of a single spraing-affected tuber. The accumulation of TRV and one of the HR-related genes (GST) was determined by qRT-PCR quantification (ΔΔCT quantitation) in five of the samples (SF1, SF6, SF7, S10, and S11, section 5.11), selected as having different spraing or spraing-free appearances in the diseased tuber.

A TRV-free (healthy) tuber-sample (H1) from Pentland Dell was used as a calibrator for the relative gene-quantitation and the qRT-PCR protocol was the same as described before. Each sample was assayed in triplicate and the Ef-1 α reference gene was used for expression normalization.

This analysis showed the highest amount of TRV in two of the three spraing-free samples, with one of them (SF6, RQ of $1046.24x10^3$) containing 9 times more TRV than the second highest sample (SF7, RQ of $113.35x10^3$), and nearly 12 times more TRV than either of the two spraing-samples (S11, RQ of $87.78x10^3$; S10, RQ of $74.47x10^3$). Virus was found in the least amount at the site SF1 with a RQ of 1.16 (Fig. 5.24, c; Table No. 5.12). These results revealed that TRV was more abundantly present in the vicinity of the spraing-affected tissue but its amount was reduced within the spraing-tissue itself and also at the far-distant spraing-free sites.

Contrary to the TRV1 quantification, the results of GST quantification (Fig. 5.24, d) showed a higher expression of GST in the spraing-affected than the spraing-free tissue. The GST gene expression was nearly nine times higher in both of the spraing samples (S10, RQ of 8.92 and S11, RQ of 20.74) than either of the three spraing-free samples (SF1, SF6 and SF7) with a RQ of 1.38, 1.19 and 2.33, respectively. As before, the results revealed that production of spraing symptoms is associated with up-regulation of the GST gene.

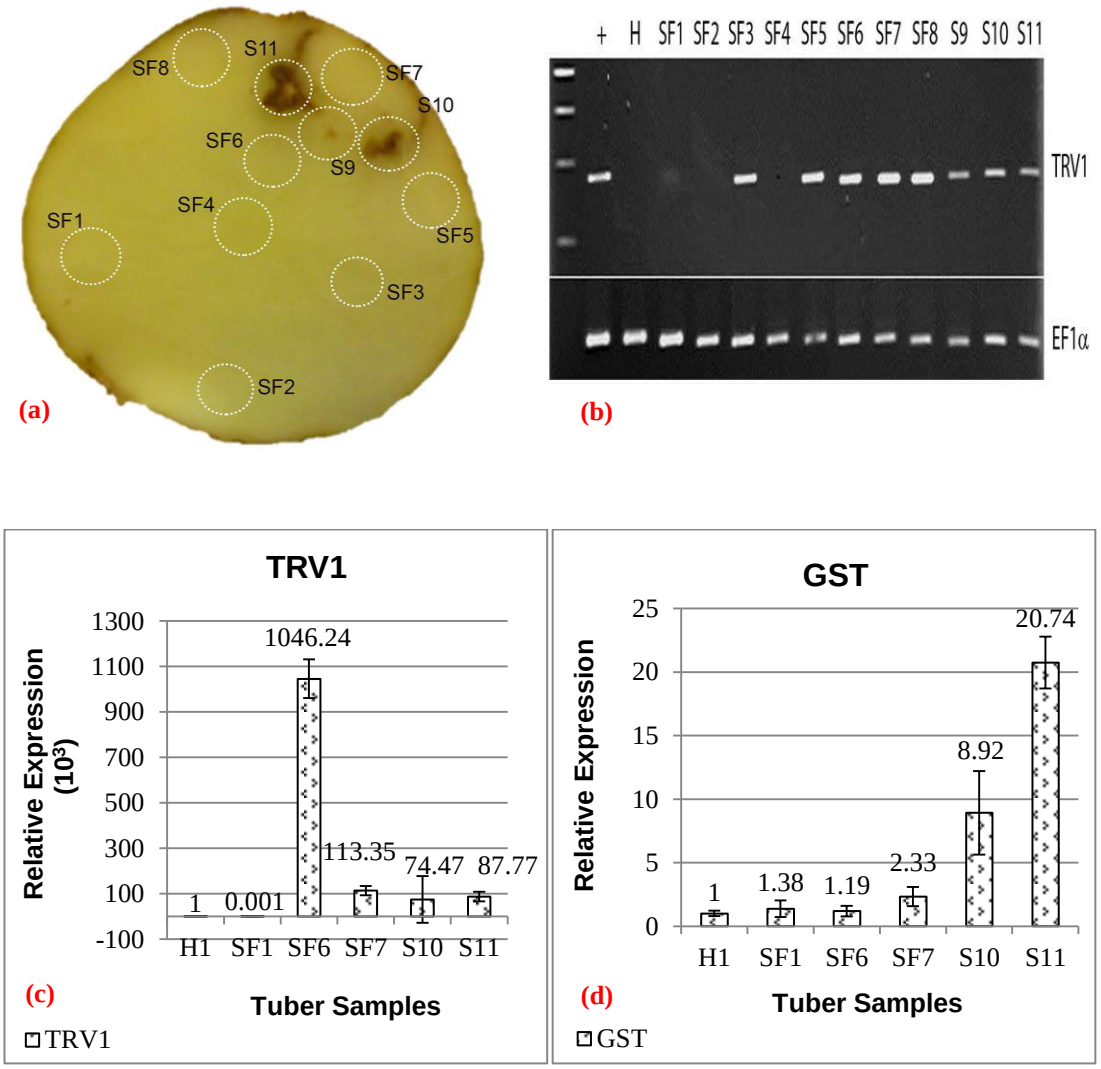

Figure 5.24. Distribution of TRV across a potato tuber section. (a) shows a potato tuber section with areas of visible spraing production in the tuber. Named sampled areas are indicated by white dotted circles. **(b)** RT-PCR of the different sampled areas. SF denotes visibly spraing-free, S denotes visible spraing formation. Samples were tested by amplification for TRV RNA1 and potato Ef-1α, + denotes a known TRV-infected potato sample, H is a known uninfected potato sample. DNA ladder appears at the left of the figure. **(c)** qRT-PCR of TRV1 and **(d)** GST in the selected spraing-symptomatic and spraing-free areas.

5.13. Discussion

The sequencing of the potato genome has made it possible to gain further insight into the genetic details of potato. The potato genome comprises of twelve chromosomes. More than 85% of the 844 Mb (megabase) of the potato genome has been sequenced identifying more than 39,000 translatable genes of which there are more than 800 disease-resistance genes (Xu, *et al*., 2011). Spraing disease of potato (see section 1.4.2) has been described as a hypersensitive response to viral infection (Engsbro, 1973). We in the current studies have investigated the molecular details of spraing disease and have used microarray analysis to explore the gene expression in spraing-affected tissue. In this microarray analysis, expression of 27,895 probes was detected from the Potato genome 4x44K array that comprised a total of 42,034 potato unigenes. Only 15, 019 (53.84%) probes out of the total of 27,895 expressed probes were annotated in the potato genome database. The pair-wise comparison, performed at a high stringency level with imposed restriction of two-fold change in expression, identified 844 differentially expressed probes for the spraing vs. spraing-free comparison (S/SF) and 1,024 probes for the spraing-free vs. healthy comparison (SF/H).

The gene enrichment analysis of this expression data identified several GOs that were associated to the defence responses. The gene ontologies comprising the HR-related annotations were selected (see section 5.6.5) and qRT-PCR of HR-related genes (Peroxidase, Pathogenesis-related protein, Suberin peroxidase, Glutathione-S-Transferase, and Respiratory burst oxidase) as well as TRV1-replicase and the endogenous Elongation-factor-1 alpha gene was done.

The HR is associated with production of short-lived reactive oxygen species (ROS), commonly known as the ‘‘oxidative burst’’, that produces reactive oxygen intermediates (ROI) consisting of superoxide (O^{-2}) and hydrogen peroxide (H_2O_2) that are involved in the host defence mechanism (Wojtaszek, 1997; Grant and Loake, 2000). Constitutively production of ROS, in lower amounts, is involved in cell

signalling but when produced in higher amounts, such as under stress, is toxic to the cell. The cell producing ROS above the normal cellular level is said to be in a condition of ‘‘oxidative stress’’. The increased production of ROS can cause degradation of lipids, denaturation of proteins, damage to nucleic acids, affects the enzymatic activities, stimulates programmed cell death (PCD) and finally leads to death of the affected cell. Among the ROS, hydrogen peroxide (H_2O_2) is relatively more stable and is the only species that can diffuse through the plasma membrane. It affects the permeability and integrity of the cellular membranes. H_2O_2 is used as a substrate for lignin and suberin biosynthesis that are the constituents of the cork-tissue. Excessive production of H_2O_2 is lethal for cellular homeostasis and can cause cell-death. However, for induction of cell-death excessive H_2O_2, above a certain threshold, is required (Sharma *et al.*, 2012). The abnormal amounts of H_2O_2 are scavenged by cellular protectant enzymes such as catalases (Scandalios, 1997). Glutathione-S-transferase (GST) is involved in the degradation of products of lipid membranes (Tenhaken *et al*., 1995). However, the concept of ‘‘Oxidative Burst’’ is being replaced with the ‘‘ROS wave’’ in which ROS spreads through different tissues to distant areas of the plant (Mittler, *et al.*, 2011).

The differential up-regulation of HR-related genes in the spraing-affected tissue was revealed by the analysis of microarray data and was validated for five of the HR-related genes (Peroxidase, Pathogenesis-related protein (PAR-1c), Suberin peroxidase, Glutathione-S transferase and Respiratory burst oxidase) by qRT-PCR. In the current studies, the differential up-regulation of the PAR-1c and the Suberin-peroxidase gene was also verified in some additional spraing-affected tubers that were of different varieties and had different combinations of viral infections.

The histological occurrence of the HR in the spraing-affected tubers was further confirmed by the trypan-blue staining of the spraing-affected tissue and the occurrence of cell-death was confirmed. The accumulation of H_2O_2 in the spraing-

affected tubers was confirmed by DAB staining of the spraing-affected tuber-slice and the deposition of lignin was confirmed by Phloroglucinol staining.

The distribution of TRV in a spraing-affected tuber was reported to be of non-uniform occurrence (Xenophontos *et al.,* 1998). I obtained similar results from the tuber slice sampled from a spraing-affected tuber. The qRT-PCR quantitation of TRV-1 and the GST gene showed that TRV-1 was suppressed in the spraing-affected samples but the expression of GST was found to be highly increased in the spraing-affected samples as compared to the spraing-free samples.

The results in the current studies are supportive of the notion that induction of spraing-symptoms in a diseased potato is a hypersensitive response which may inhibit further ingress and spread of the virus.

Several studies have reported the analysis of host plant gene expression following virus infection, however, the majority of these have not involved TRV. Rodrigo *et al*. (2012) compared the results of different microarray experiments that examined infection of *Arabidopsis thaliana* by seven RNA plant viruses, including TRV, and one DNA plant virus. The individual studies used a variety of *Arabidopsis* genotypes which were sampled at different time points, nevertheless, statistically robust comparative data could be derived from these combined studies. The analysis showed that when all eight viruses were considered together, 5,296 of the >22, 000 genes on the arrays were over-expressed and 2,650 genes were under-expressed. However, the number of these genes affected by more than one virus declined exponentially as the list of viruses increased, so that only seven plant genes were upregulated in common by six viruses. So, it appears that alteration of host gene expression is virus-specific at the individual gene level. From this work, alteration of some metabolic pathway components, including cellulose biosynthesis and nitrogen fixation were seen as a "common" response to infection by at least five of the eight viruses. Interestingly, the four viruses that were classified as a natural brassica-

infecting group, and so were considered to be better adapted to *Arabidopsis*, induced a distinctive set of changes to host pathways affecting growth and development, carbohydrate metabolism and tolerance to biotic stress. TRV was not one of the brassica-infecting viruses.

A second study of TRV infection in *Arabidopsis* (Fernandez-Calvino *et al.*, 2014), highlighted changes in photosynthesis components, responses to abiotic stress (salt, drought and cold), redox regulation, sugar metabolism, protein synthesis and lipid metabolism. In contrast to our potato tuber study, only one *Arabidopsis* gene involved in lignin biosynthesis (a putative cinnamyl-alcohol dehydrogenase), four categorised as defense-related and two listed as hydrogen peroxide metabolism-related were upregulated following TRV infection. Some microarray analysis of virus infection of potato has been done (Pompe-Novak *et al.*, 2006; Baebler *et al.*, 2009; Kogovšek *et al.*, 2010), however, these studies have involved PVY rather than TRV and gene expression was examined in potato leaves rather than tubers.

The best understood virus diseases of potato (Potato virus X, Potato leaf roll virus) involve transmission of the virus by aphids into the leaves (Solomon-Blackburn and Barker, 2001). Here the virus passes directly into the phloem and uses the vascular system to then move into the potato tuber. In contrast, TRV, in most instances, is introduced into potato plants by transmission from feeding nematodes, although the actual plant growth stage at which this transmission most often occurs is not known. Potato tubers are formed from swellings that develop at the end of stolons, which are outgrowths of the stem that are located underground. It would seem possible that infection of the developing stolon tip by TRV might result in a widespread later infection of the tuber where the virus and associated spraing are located throughout the tuber. If the virus is introduced into the epidermal cells of a more mature tuber then it might be expected that the virus and spraing would be located at one side of the tuber, near to the site of introduction. Both of these patterns of spraing are seen in field-grown potatoes.

Interestingly, our results show that high levels of TRV can occur across a wide area of the tuber that does not show spraing symptoms. Whether the virus reaches these areas passively as the tuber expands and matures, or if it actively moves through the tuber is not known. In stem and leaf tissue the virus moves initially over long distances via the vascular system and then between adjacent cells in the leaf via plasmodesmata. In tubers, the vascular system is present as a ring located at a distance below the surface layer of the tuber. Limited observational studies in plants other than potato found that the trichodorid nematodes that transmit TRV feed on epidermal cells at the root tip and penetrate the cell to a depth of only 2-3 µm with their spear-shaped stylet (onchiostyle) (Taylor and Brown, 1997). Access of TRV to the tuber vasculature could occur only after initial cell-to-cell movement of the virus from the epidermal cells of the stolon or developing tuber.

Previously, studies using RT-PCR to detect TRV in potato tubers found that the virus was unevenly distributed (Crosslin and Thomas (1995); Xenophontos *et al*, 1998; Crosslin *et al.*, 1999). TRV was more reliably detected in areas containing spraing tissue or located just inside a necrotic arc rather than outside of or distant from such an arc. However, no attempt was made to quantify the virus in different parts of the tuber. Using qRT-PCR we have shown that higher levels of TRV can exist in symptom-free areas of the tuber that are located some distance away from the arc of spraing tissue. An important practical consequence from this work is that there can be high levels of TRV in tubers of spraing-reactive potato cultivars (e.g. Pentland Dell) that do not at the time of sampling show visible signs of spraing. This is particularly important if these tubers are selected as seed for subsequent potato cultivation, and indicate the need to apply molecular testing rather than simple phenotypic observations for seed potato production.

Spraing development can be affected by environmental factors, so that in field trials of selected varieties the incidence and severity of TRV spraing symptoms has been shown to be different between locations (Robinson *et al.*, 2004). This could be due to

differences in the numbers and activity of nematodes at the different sites. In addition, larger tubers displayed more spraing symptoms, and tubers harvested at later dates had more spraing than tubers harvested at earlier dates. Rydén *et al.* (1994) found that non-symptomatic tubers infected with TRV developed spraing when they had been cut and stored at cool temperature for several weeks. This phenomenon had been noted previously with PMTV-infected tubers (Harrison and Jones, 1971a). However, storage of uncut TRV-infected tubers did not lead to spraing development (Rydén *et al.*, 1994; Robinson *et al.*, 2004), whereas, similar storage of PMTV-infected tubers did lead to the development of spraing (Harrison and Jones, 1971b).

Previous work described several potato cultivars (e.g. King Edward, Santé and Wilja) where systemic TRV infection was detected but which did not exhibit classical spraing symptoms, although a few scattered brown flecks were noticed in some Wilja and Santé tubers (Xenophontos *et al.*, 1998; Dale and Neilson, 2006). Further work showed that repeated propagation of TRV-infected Wilja plants leads to the production of more tubers that are smaller, malformed, and have altered metabolic profiles compared to uninfected tubers (Dale *et al.*, 2000). One of these cultivars, King Edward, was examined during a survey of potato tuber disease in Sweden (Beuch *et al.*, 2014). This work found that thirty four of forty six tested King Edward tubers carried TRV and also exhibited spraing symptoms. By contrast, no spraing was seen in any of twelve tubers that were shown to contain PMTV. Thus, it seems that the reaction of specific cultivars to virus infection is highly dependent on field conditions. Nevertheless, a quantitative trait locus for "resistance" to spraing disease has been identified and mapped onto the potato genome (Khu *et al.*, 2008).

The quantitative analysis described in this chapter showed that TRV levels are highest in regions of the tuber that do not exhibit spraing symptoms. I interpret this to suggest that the formation of spraing is a host reaction to virus infection and multiplication that leads to a reduction in virus levels where spraing develops. It is

also apparent from this work that defence gene expression in Pentland Dell potato, exemplified by PAR1-c and SP in this study, responds similarly to TRV and PMTV. As these viruses are not related in their genome sequences or encoded proteins, these parts of the host defence pathway must be reacting to a generic signal such as metabolic stress or perhaps double-stranded RNA accumulation, which is formed as a replication intermediate of many RNA plant viruses. It will be interesting to do further quantitative studies to discover whether cultivars that react most strongly with spraing production initially maintain higher levels of virus than do cultivars in which spraing is either never or only sporadically formed.

6. General Discussion and Future Work

6.1. General discussion

In my studies the KK20 recombinant isolate of TRV was identified as a virulent isolate in *N. benthamiana* plants and accumulated at higher levels in the systemically-infected leaves than did the the two other K20 RNA-2-containing isolates (i.e.; the SK20 and OK20 isolates). However, K20 RNA-2 based isolates did not cause an enhanced systemic infection in the potato plants as compared to the other isolates used in this study. The severity of disease symptoms is not necessarily associated with higher virus-load in the infected plant but is rather the out-come of a precise interaction between a host and infecting pathogen (Whitham and Wang, 2004). Among the 15 TRV recombinant isolates examined in this work the PaY4 RNA-2- containing isolates accumulated to the highest levels (at 8 dpi) in infected *N. benthamiana* plants. The viral load itself is not a true indicator of host susceptibility as highly susceptible plants can have a lower viral load (Baebler *et al*., 2011; Dobnik *et al*., 2016).

The pseudo recombinant isolate I6K2 (containing I6 RNA-2 and PpK-20 RNA-1) infected all the 6 tetraploid potato species. The commercially grown cultivar Bintje, known as a TRV resistant-cultivar, was revealed to be susceptible to the TRV (I6K2) and this finding was in general agreement with the results reported by Robinson (2004) and Beuch *et al*., (2014). More than one-fourth of the tobravirus isolations, from the bulb-crop growing coastal areas of the Netherlands, were natural recombinants between TRV and PEBV (Ploeg *et al*., 1991). Such interspecies recombination is a common characteristic within tobraviruses (MacFarlane, 1997; Batista *et al*., 2014) that enables them to face climatic challenges. I6 RNA-2 is a natural recombinant between TRV and PEBV with its coat protein being derived from the PEBV. It is that possible that capture of the PEBV CP gene helps it to evade

the surveillance of potato defence genes. Although, the presence of the CP encoded by RNA-2 is not an absolute requirement for the systemic infection of TRV that can take place with RNA-1 on its own (Swanson *et al.*, 2002). Nevertheless, RNA-2 has a coordinated function that is supportive to the systemic infection of TRV. Deng *et al*. (2013) used the wild type TRV-1 (wt.RNA-1) and the mutant clones having either most of their 16K gene deleted or prevented from translation. They found that inoculation of these viruses alongwith RNA-2 on *N. benthamiana* plants resulted in higher accumulation of TRV.

Due to the possible deletion around the genomic-sequence of the TRV 16K-gene, the primer-set flanking this gene was found incapable of amplifying TRV in the systemically infected leaves of tetraploid potatoes. In the current studies, a replicase gene based primer-set was designed and shown to be much better for diagnosing TRV in various types of plant tissues, including different potato tissues.

Among the various diploid potatoes that were screened in order to identify TRV-susceptible potato genotypes, *Solanum jamesii* (CPC Accession No. JAM 7653) was discovered to be an ideal as a model species for conducting TRV infection studies in potato. The VIGS experiments using *S. jamesii* as a host plant, have given some promising results. VIGS is generally known as a short-lived phenomenon (Liu *et al*., 2002b; Lu *et al*., 2003) that can mostly continue for three weeks and in some cases up to three months. Senthil-Kumar and Mysore (2011b) demonstrated that VIGS could continue for more than a couple of years and potentially persist up to the physiological senescence of the plant. However, the authors have suggested that in order to prove the persistence of VIGS for years and its transmission to several generations, further experiments using a range of viral-vectors in different plant species are required. VIGS is also transmissible to the seed-derived progeny of *N. benthamiana* and tomato plants. TRV transmission of less than 50% has been reported in the seed tubers of cultivar Saturna (Hoek *et al*., 2006). The current studies, include the first experimental demonstration of the transmission of TRV-

induced silencing (PDS-VIGS) to the potato tubers and the subsequent emerging plantlets. Other researchers have shown that the prevalence and continuity of VIGS is affected by the age of plant, virus-load, and the environmental conditions such as humidity and temperature (Fu *et al*., 2006; Tuttle *et al*., 2008; Senthil-Kumar and Mysore, 2011a, b). With some further optimization in the cultural and virus inoculation practices, *S. jamesii* could be harnessed as a good potato resource for TRV-infection and VIGS studies. The current studies have revealed that if the plantlets (apical stem-cuttings) inoculated with the PDS-construct were raised from more succulent shoots, the produced photo-bleaching symptoms were more severe and widespread than those occurring in the cuttings raised from more woody tissue.

The symptomless infection and uneven distribution of TRV in spraing-affected tubers (Xenophontous *et al*., 1998; Crosslin *et al*., 1999; Brown *et al*., 2009) could lead to erroneous diagnosis that poses serious challenges to the seed-certification services and ultimately to potato production. The symptomless but infected tubers can be responsible for introducing TRV into the previous declared virus- and disease-free areas. In the current studies, the erratic distribution of TRV within a spraing-affected tuber, with the relatively lower amounts of TRV in spraing-tissue as compared to spraing-free tissue of the same TRV-infected tuber, reflected the activity of the HR to limit TRV-infection in the diseased tuber. Thus, the induction of spraing coincided with a suppressive effect on the TRV infection.

The qRT-PCR validation of the HR-related genes that were found to be differentially up-regulated in the microarray analysis of the spraing-affected tissue provided experimental evidence to confirm the induction of spraing as an hypersensitive response to TRV infection. TRV infection alters the sugar-metabolism that is an active player of inducing the programed cell-death in HR (Dale *et al*., 2000; Fernández-Calvino *et al*., 2014). The trypan-blue uptake by the dead-cells in and around the vicinity of the spraing-affected tissue provided evidence of cell-death related to hypersensitive response.

When a plant-cell encounters an aggressive pathogen, it immediately produces reactive oxygen species (ROS) such as superoxide ($.O_2^-$) or hydrogen peroxide (H_2O_2) for fortification of the cell wall (Grant and Loake, 2000). Cellular protectants like glutathione S-transferase (GST) are also up-regulated (Tenhaken *et al*., 1995). The DAB staining of the spraing-affected tissue caused the differential staining of the tuber-tissue that confirmed the production of H_2O_2 in the spraing-affected tuber tissue. Thus taken together this suggests that spraing is a defence response incited in the potato tubers to halt the further ingress and spread of TRV-infection.

6.2. Future work

In the current studies, the replicase gene-based primer-set was demonstrated to work effectively for TRV detection. In future, it would be tested on some more genotypes and types of tissues. If the findings of TRV detection are the same as reported here, then recommendations would be made for use of this primer-set in place of the widely used 16K flanking primer-set.

The suggested ability of the pseudorecombinant isolate KI6 to cause enhanced systemic infection should be evaluated on more genotypes of potato under varied environmental conditions. The pTRV-vector commonly used for the VIGS-related studies has a backbone from the PpK-20 isolate (RNA-2). This vector could be replaced with the I6 RNA-2 based vector and should be tested on some more tetraploid potato genotypes to assess whether it can initiate VIGS in these plants. Comparative studies would be carried out for the PpK-20 and I6 RNA-2 based VIGS vectors and the efficacy of VIGS would be evaluated to recommend the most efficient vector for future VIGS-related studies.

An interesting observation in these studies was the production of characteristic necrotic-rings on the leaves of *S. jamesii* when mechanically-inoculated with the PpK-20 RNA-1 inoculum, whereas, these symptoms were masked when the plants were inoculated with the M-type virus. Ghazala and Varrelmann (2007) had reported

the involvement of the 29K (MP) in production of TRV-induced foliar (necrotic) symptoms in potato. Deng *et al*. (2013) have recently reported that there is a coordination of expression of MP and 16K proteins in the suppression of necrosis in the TRV RNA-1 inoculated *N. benthamiana* plants. In their studies the 16K gene was shown to influence the differential accumulation levels of various TRV-mutants and the M-type virus produced milder symptoms as compared to the RNA-1-only infections. The current findings on *S. jamesii* show that the foliar symptoms were masked by M-type virus. Previously, the 16K protein had been reported as a ‘‘silencing suppressor’’ (Reavy *et al*., 2004; Martin-Hernández and Baulcombe, 2008; Ghazala *et al*., 2008). Now, the 29K protein has also been shown to play an interactive role with the 194K protein for the suppression of RNA silencing and emphasis has been laid on the well-adjusted production of 29K and 16K proteins for the progression of TRV infection (Deng *et al*., 2013). The role of 13K open reading frame within the 16K gene (MacFarlane, 2010) would be investigated for effects on TRV pathogenicity.

Mechanical inoculation of the CP-frameshift (KCPfs) mutant on *S. jamesii* plants produced shoestring-like (filiformic) leaves. Gene expression in plants is regulated by endogenous small RNAs called ‘‘microRNAs’’ (miRNAs) that can be affected by the viral infection resulting in the expression of various symptoms and sometimes leading to a change in plant shape and structure such as the shoestring-like leaves (Andrade *et al*., 1981; Bazzini *et al*., 2007; Cillo *et al*., 2002, 2009; Mach, 2012). The filiformic leaves are mostly produced by compromised regulation of the organ polarity genes (Husbands *et al*., 2009) that are regulated by small RNAs (Yifhar *et al*., 2012). Wang *et al*. (2015) using VIGS of tomato *argonaute*1 (*Sl*AGO1) and the subsequent microarray analysis of the infected plants have reported that the suppression of *Sl*AGO1 results in the abnormal development of tomato leaves. Microarray analysis and *in-situ* localization of the KCPfs mutant in the infected *S. jamesii* plants could be done at various time points of the infection to reveal the

differentially up-regulated genes and to get an insight into the molecular details of this shoestring phenomenon.

Viral-suppressors of RNA silencing can also impede the regulation of miRNAs resulting in abnormal plant growth and development (Li and Ding, 2006; Ding and Voinnet, 2007; Ye *et al*., 2008). The 16K proteins from various TRV RNA-1 isolates vary in the carboxy part of the protein. Various frameshift and deletion mutant clones of the 16K protein of the three different RNA-1 isolates (viz.,SYM, PpO-85 and PpK-20) could be created and the differential RNA suppression activity of these mutants investigated by inoculation onto the *N. benthamiana* and *S. jamesii* plants. Structural motifs responsible for the suppression activity of 16K protein could also be investigated in future studies.

The results of these future experiments could shed new light on understanding the molecular details of the TRV disease cycle and will provide more in depth details about the virulence pattern of TRV infection.

7. References

Adams, M.J., Heinze, C., Jackson, A.O., Kreuze, J.F., Macfarlane, S.A. and Torrance, L. (2012)**.** Family Virgaviridae. In: Virus Taxonomy: Classification and Nomenclature of Viruses - Ninth Report of the International Committee on Taxonomy of Viruses. King, A.M.Q., Adams, M.J., Carstens, E.B, Lefkowitz, E.J. (eds.), Elsevier Academic Press, USA. pp. 1139-1162.

Alonso, A.B., **and Preece, T.F.** (1970). Assessment of spraing caused by Tobacco Rattle Virus in potato tubers. *Plant Pathology* **19,** 25-28.

Anandalakshmi, R., **Pruss, G.J., Ge, X., Marathe, R., Mallory, A.C., Smith, T.H., and Vance, V.B.** (1998). A viral suppressor of gene silencing in plants. *Proceedings of the National Academy of Sciences of the United States of America* **95,** 13079-13084.

Andrade, O., **Latorre, B.A., and Escaffi, O.** (1981). Tomato mosaic virus associated with shoestring symptoms in Chilean tomatoes. *Plant Disease* **65,** 761-762.

Andrey G. S., Natalia O. K., and Sergey, Y. M. (2012). Recent advances in research of plant virus movement mediated by triple gene block. *Frontiers in Microbiology* **3** (276), 1-8.

Angenent, G.C., Linthorst, H.J.M., Van Belkum, A.F., Cornelisen, B.J.C., and Bol, J.F. (1986). RNA-2 of tobacco rattle virus strain TCM encodes an unexpected gene. *Nucleic Acids Research* **14** (11), 4673- 4682.

Angenent, G.C., Posthumus, E., Brederode, F.Th., and Bol, J.F. (1989). Genome structure of tobacco rattle virus strain PLB: Further evidence on the occurrence of RNA recombination among tobraviruses. *Virology* **171** (1), 271- 274.

Anonymous. (2009). Manual 1907M Revision F. TURBO DNA-free™ Kit. AB Applied Biosystem. pp. 1-12.

Anonymous. (2011). Stability of the amylopectin trait in tubers of amlfora starch potatoes grown in 2010. Post-Market monitoring Report 2010. BASF Plant Science Company GmbH. pp. 240-254.

Ashfaq, M., McGavin, W., and MacFarlane, S.A. (2011). RNA2 of TRV SYM breaks the rules for tobravirus genome structure. *Virus Research* **160** (1-2), 435- 438. DOI: 10.1016/j.virusres.2011.07.007.

Askew, M.F. (2001). The economic importance of the potato. In: Virus and virus-like diseases of potatoes and production of seed potatoes. Loebenstein, G. *et al.* (eds.). Kluwer Academic Publishers, London pp.1-18.

Axtel, M.J. (2008). Evolution of microRNAs and their targets: Are all microRNAs biologically relevant. *Biochimica et Biophysica Acta* **1779,** 725-734.

Bawden, F.C. (1936). Plant viruses and virus diseases. (Leiden, The Netherlands: Chronica Botanica Company).

Baebler, S., Krečič-Stres, H., Rotter, A., Kogovšek, P., Cankar, K., Kok, E.J., Gruden, K., Kovač, M., Žel, J., Pompe-Novak, M. and Ravnikar, M. (2009). PVYNTN elicits a diverse gene expression response in different potato genotypes in the first 12 h after inoculation. *Molecular Plant Pathology* **10**: 263-275.

Baebler, Š., Stare, K., Kovač, M., Blejec, A., Prezelj, N., Stare, T., Kogovšek, P., Maruša, P-N., Rosahl, S., Ravnikar, M., Gruden, K. (2011). Dynamics of responses in compatible potato-potato virus Y interaction are modulated by salicyclic acid. PLoS ONE. 2011; 6:e29009. DOI: 10.1371/journal. pone. 0029009.

Banttari, E.E., Ellis, P.J., and Khurana, S.M.P. (1993). Management of diseases caused by viruses and virus like pathogens. In: Potato Health Management. Row, R.C. (ed.). *The American Phytopathological Society* p.130.

Barker, H., and Dale, M.F.B. (2006). Resistance to viruses in potato. In: Natural resistance mechanism of plants to viruses. Loebenstein, G., and Carr, J.P. (eds.). Spinger, Dordrecht, Netherlands. pp. 341-366.

Batista, A.R.S., Nicolini, C., Rodrigues, K.B., Melo, F.L., Vasques, R.M., de Macêdo, M.A., Inoue-Nagata, A.K., and Nagata, T. (2014). Unique RNA2 sequences of two Brazilian isolates of *Pepper ringspot virus*, a tobravirus. *Virus Genes* **49**, 169-173.

Baulcombe, D. (2004). RNA silencing in plants. *Nature* **431**, 356-363.

Bazzini, A.A., Hopp, H.E., Beachy, R.N., and Asurmendi, S. (2007). Infection and coaccumulation of tobacco mosaic virus proteins alter microRNA levels, correlating with symptom and plant development. *PNAS* **104** (29), 12157-12162.

Benedito, V.A., Visser, P.B., Angenent, G.C., and Krens, F.A. (2004). The potential of virus-induced gene silencing for speeding up functional characterization of plant genes. Genetics and Molecular Research **3**(3), 323-341.

Bergh, S.T., Koziel, M.G., Huang, S.C., Thomas, R.A., Gilley, D.P., and Siegel, A. (1985). The nucleotide sequence of tobacco rattle virus RNA-2 (CAM strain). *Nucleic Acids Research* **13**, 8507-8519.

Bernacki, S., Karimi, M., Hilson, P., and Robertson, N. (2010). Virus induced gene silencing as a reverse genetics tool to study gene function. In: Plant Development Biology, Methods in Molecular Biology 655, Hennig, L. and Köhler, C. (eds.). Springer Protocols. Humana Press. Totowa, New Jersey. pp. 27-45.

Beuch, U., Persson, P., Edin, E. and Kvarnheden, A. (2014). Necrotic diseases caused by viruses in Swedish potato tubers. *Plant Pathology* **63**, 667-674.

Blackburn, R.M.S., and Barker, H. (2001). Breeding virus resistant potatoes (*Solanum tuberosum*): a review of traditional and molecular approaches. *Heredity* **86**, 17-35.

Boccara, M., Hamilton, W.D.O., and Baulcome, D.C. (1986). The organization and interviral homologies of genes at the 3′ end of tobacco rattle virus RNA1. *EMBO Journal* **5**, 223-229.

Bol, J.F., and Linthorst, H.J.M. (1990). Plant pathogenesis-related proteins induced by virus infection. *Annual Review of Phytopathology* **28**, 113-138.

Brigneti, G., Voinnet, O., Li, W.X., Ji, L.H., Ding, S.W., and Baulcombe, D.C. (1998). Viral pathogenicity determinants are suppressors of transgene silencing in *Nicotiana benthamiana*. *The EMBO Journal* **17** (22), 6739-6746.

Brigneti, G., Martin-Hernandez, A.M., Jin, H., Chen, J., Baulcombe, D.C., Baker, B., and Jones, J.D.G. (2004). Virus-induced gene silencing in *Solanum* species. *The Plant Journal* **39**, 264-272.

Brodersen, P., and Voinnet, O. (2006). The diversity of RNA silencing pathways in plants. *Trends in Genetics* **22**(5), 268-280.

Brown, D.J.F., and Boag, B. (1987). Transmission of virus by trichodorid nematodes. Scottish Crop Research Institute Report for 1986, 126-127.

Brown, D.J.F., and Boag, B. (1988). An examination of methods used to extract virus-vector nematodes (Nematoda: Longidoridae and Trichodoridae) from soil samples. *Nematologia Mediterranea* **16**, 93-99.

Brown, D.J.F., Ploeg, A. T. and Robinson, D. J. (1989). A review of reported associations between *Trichodorus* and *Paratrichodorus* species (Nematoda: Trichodoridae) and tobraviruses with a description of laboratory methods for examining virus transmission by trichodorids. *Revue Nèmatol* **12** (3), 235-241.

Brown, C.R., Mojtahedi, H., Crosslin, J.M., James, S., Charlton, B., Novy, R.G., Love, S.L., Wales, M.I., and Hamm, P. (2009). Characterization of resistance to corky ringspot disease in potato: A case for resistance to infection by Tobacco rattle virus. *American Journal of Potato Research* **86**, 49-55.

Brown, C.R., Mojtahedi, H., Santo, G.S., and Hamm, P. (2000). Potato germplasm resistant to corky ringspot disease. *American Journal of Potato Research* **77**, 23-27.

Brown, E.B., and Skyes, G.B. (1973). Control of tobacco rattle virus (spraing) in potatoes. *Annals of Applied Biology* **75**, 462-464.

Brunt, A.A. (2001). The main viruses infecting potato crops. In: Virus and virus-like diseases of potatoes and production of seed potatoes. Loebenstein, G. *et al.* (eds.). Kluwer Academic Publishers, London. pp.65-68.

Brunt, A.A., Crabtree, K., Dallwitz, M.J., Gibbs, A.J., and Watson, L. (eds.). (1996). Viruses of plants. Description and lists from the VIDE database. Wallingford, UK: CAB International. pp.1484.

Burch-Smith, T.M., Schiff, M., Liu, Y., and Dinesh-Kumar, S.P. (2006). Efficient virus-induced gene silencing in Arabidopsis. *Plant Physiology* **142**, 21-27.

Burgyan, J. (2006). Virus induced RNA silencing and suppression: defence and counter defence. *Journal of Plant Pathology* **88** (3), 233-244.

Bustin, T. A., Benes, V., Garson, J. A., Hellemans, J., Huggett, J.,Kubista, M., Mueller, R., Nolan, T., Pfaffl, M.W., Shipley, G. L,.Vandesompele, J., and

Wittwer, C.T. (2009). The MIQE Guidelines: Minimum Information for Publication of Quantitative Real-Time PCR Experiments. *Clinical Chemistry* **55**(4), 611-622. DOI: 10.1373/clinchem.2008.112797.

Cadman, C.H. (1959). Potato stem mottle disease in Scotland. *European Potato Journal* **2,** 165-175.

Cadman, C.H., and Harrison, B.D. (1959). Studies on the properties of soil borne viruses of the tobacco rattle type occurring in Scotland. *Annals of Applied Biology* **47**(3), 542-556.

Camire, M.E., Kubow, S., and Donnelly, D.J. (2009). Potatoes and human health. *Critical Reviews in Food Science and Nutrition* **49** (10), 823-840.

Campbell, R., Ducreux, L.J.M., Morris, W. L., Morris, J.A., Suttle, J. C., Ramsay, G., Bryan, G. J., Hedley, P. E., and Taylor, M.A. (2010). The Metabolic and Developmental Roles of Carotenoid Cleavage Dioxygenase from Potato. *Plant Physiology*, **154,** 656–664.

Carrington, J. C., Kasschau, K.D., Mahajan, S. K., and Schaad, M.C. (1996). Cell-to-cell and long-distance transport of viruses in plants. *The Plant Cell*, 8, 1669–1681.

Chen, T.A., Hirumi, H., and Maramorosch, K. (1969). Tobacco rattle virus in roots of mechanically inoculated plants. *Journal of Phytopathology*, **65** (1)**,** 15–20.

Chen, J.C., Jiang, C.Z., Gookin, T.E., Hunter, D.A., Clark, D.G., and Reid, M.S. (2004). Chalcone synthase as a reporter in virus-induced gene silencing studies of flower senescence. *Plant Molecular Biology* **55,** 521–530.

Chung, E., Seong, E., Kim, Y.C., Chung, E.J., Oh, S.K., Lee, S., Park, J.M., Joung, Y.H., and Choi, D. (2004). A method of high frequency virus-induced gene silencing in chili pepper (*Capsicum annum* L. cv. Bukang). *Molecules and Cells* **17** (2)**,** 377–380.

Cillo, F., Roberts, I.M., and Palukaitis, P. (2002). In situ localization and tissue distribution of the replication associated proteins of Cucumber mosaic virus in tobacco and cucumber. *Journal of Virology* **76** (21), 10654-10664.

Cillo, F., Mascia, T., Pasciuto, M.M., and Gallitelli, D. (2009). Differential effects of mild and severe Cucumber mosaic virus strains in the perturbation of microRNA-regulated gene expression in tomato map to the 3′ sequence of RNA2. *Molecular Plant–Microbe Interactions* **22** (10), 1239-1249.

CIP. (2014). Potato. International Potato Centre (Centro Internacional De La Pappa). Retrieved 25 April, 2014, from http://cip.wpengine.com

Collier, G.F., Wurr, D.C.E., and Huntington, V.C. (1978). The effect of calcium nutrition on the incidence of internal rust spot in the potato. *Journal of Agricultural Sciences* **91**, 241-243.

Cornelissen, B.J.C., Linthorst, H.J.M., Brederode, F.T., and Bol, J.F. (1986). Analysis of the genome structure of tobacco rattle virus strain PSG. *Nucleic Acids Research* **14** (5), 2157-2169.

Crosslin, J.M., and Thomas, P.E. (1995). Detection of tobacco rattle virus in tubers exhibiting symptoms of corky ringspot by polymerase chain reaction. *American Potato Journal* **72**, 605-609.

Crosslin, J.M., Hamm, P.B., Kirk, W.W., and Hammond, R.W. (2010). Complete genomic sequence of a Tobacco rattle virus isolate from Michigan-grown potatoes. *Archives of Virology* **155**, 621-625.

Crosslin, J.M., Thomas, P.E., and Brown, C.R. (1999). Distribution of tobacco rattle virus in tubers of resistant and susceptible potatoes and systemic movement of virus into daughter tubers. *American Journal of Potato Research* **76**, 191-197.

Crosslin, J.M., Thomas, P.E., and Hammond, R.W. (2003). Genetic variability of genomic RNA 2 of four tobacco rattle tobravirus isolates from potato fields in the Northwestern United states *Virus Research* **96**, 99-105.

Cruz, S.S., Roberts, A. G., Prior, D.A.M., Chapman, S., and Oparka, K.J. (1998). Cell-to-cell and phloem-mediated transport of Potato Virus X: The role of virions. *The Plant Cell* **10**, 495-510.

Cruz, S.S. (1999). Perspective: phloem transport of viruses and macromolecules-what goes in must come out. *Trends in Microbiology* **7** (6), 237-241.

Dale, M.F.B. (2009). Tobacco rattle virus in potatoes. *Aspects of Applied Biology* **94**, 41-47.

Dale, M.F.B., and Neilson, R. (2006). Free living nematodes and spraing. British Potato Council Research Review, Oxford, U.K. pp.62.

Dale, M.F.B., and Barker, H. (2007). Diagnostic procedures to assess the distribution of Tobacco rattle virus in the UK. In: Abstracts of papers presented at the 90th Annual Meeting of the Potato Association of America, Madison, Wisconsin. *American Journal of Potato Research* **84**, 73-123. DOI: 10. 1007/ BF02986299.

Dale, M.F.B., and Solomon, R.M. (1988). A glass house test to assess the sensitivity of potato cultivars to tobacco rattle virus. *Annals of Applied Biology* **112**, 225-229.

Dale, M.F.B., Robinson, D.J., Griffiths, D.W., and Todd, D. (2004). Effects of systemic infections with tobacco rattle virus on agronomic and quality traits of a range of potato cultivars. *Plant Pathology* **53**, 788-793.

Dale, M.F.B., Robinson, D.J., Griffiths, D.W., Todd, D., and Bain, H. (2000). Effects of tuber borne M type strain of tobacco rattle virus on the yield and quality attributes of potato tubers of the cultivar Wilja. *European Journal of Plant Pathology* **106**, 275-282.

Daudi, A., Cheng, Z., O'Brien, J. A., Mammarella, N., Khan, S., Ausubel, F. M., and Bolwell, G. P. (2012). The apoplastic oxidative burst peroxidase in *Arabidopsis* is a major component of pattern-triggered immunity. *Plant Cell* **24** (1), 275-287.

Deng, X., Kelloniemi, J., Haikonen, T., Vuorinen, A.L., Elomaa, P., Teeri, T. H., and Valkonen, J.P.T. (2013). Modification of *Tobacco rattle virus* RNA1 to

serve as a VIGS vector reveals that the 29K movement protein is an RNA silencing suppressor of the virus. *Molecular Plant–Microbe Interactions* **26** (5), 503-514.

Ding, S.W., and Voinnet, O. (2007). Antiviral immunity directed by small RNAs. *Cell* **130**, 413-426.

Di Stilio, V.S., Kumar, R.A., Oddone, A. M., Tolkin, T.R., Salles, P., and McCarty, K. (2010). Virus-induced gene silencing as a tool for comparative functional studies in *Thalictrum*. *PLoS ONE* **5** (8), e 12064.

Dobnik, D., Lazar, A., Stare, T., Gruden, K., Vleeshouwers, V. G. A. A., and Žel, J. (2016). *Solanum venturii*, a suitable model system for virus-induced gene silencing studies in potato reveals St*MKK6* as an important player in plant immunity. *Plant Methods* 12:29. DOI: 10.1186/s13007-016-0129-3.

Duan, C.G., Wang C.H., and Guo, H. S. (2012). Application of RNA silencing to plant disease resistance. *Science* 3:5. DOI: 10.1186/1758-907X-3-5

Ducreux, L.J.M., Morris, W.L., Prosser, I.M., Morris, J.A., Beale, M.H., Wright, F., Shepherd, T., Bryan, G.J., Hedley, P.E., and Taylor, M.A. (2008). Expression profiling of potato germplasm differentiated in quality traits leads to the identification of candidate flavour and texture genes. *Journal of Experimental Botany* ***59****, 4219-4231*.

Edreva, A. (2005). Pathogenesis-related proteins: research progress in the last 15 years. *Genetics of Applied Plant Physiology* **31**(1-2), 105-124.

Eibner, R. (1959). Untersuchungen über die ‘‘Eisenfleckigkeit’’ der Kartoffel. Doctoral Dissertation, Justus-Liebig-Universität, Giessen, Germany.

Ekengren, S.K., Liu, Y., Schiff, M., Dinesh-Kumar, S.P., and Martin, G.B. (2003). Two MAPK cascades, NPRI, and TGA transcription factors play a role in Pto-mediated disease resistance in tomato. *Plant Journal* **36**, 905-917.

Engsbro, B. (1973). Undersøgelser og forsøg vedrørende jordbårne vira.I. Rattlevirus, fortsatte undersøgelser i kartofler. Soil-borne viruses. I. Rattle-virus (continued investigations). *Tidsskrift for Planteavl* **77**, 103-117.

Faivre-Rampant, O., Gilroy, E., Hrubikova, K., Hein, I., Millam, S., Loake, G.J., Birch, P., Taylor, M., and Lacomme, C. (2004). Potato virus X-induced gene silencing in leaves and tubers of potato. *Plant Physiology* **134**, 1308-1316.

FAO. (2008). Potatoes, nutrition and diet. International Year of the Potato Secretariate. Food and Agriculture Organization (FAO). Retrieved 14 August, 2015, from http://www.fao.org/potato-2008/en/potato/tuber.html

FAO Stats, (2014). Statistical Database. Food and Agriculture Organization (FAO). Retrieved 25 April, 2014, from http://faostat3.fao.org

Fernández-Calvino, F., Osorio, S., Hernández, M. L., Hamada, I. B., del Toro, F.J., Donaire, L., Yu, A., Bustos, R., Fernie, A.R., Martínez-Rivas, J.M., and Llave César. (2014). Virus-Induced alterations in primary metabolism modulate susceptibility to Tobacco rattle virus in Arabidopsis. *Plant Physiology* **166**, 1821-1838. DOI: http://dx.doi.org/10.1104/pp.114.250340

Fiers, M., Edel-Hermann, V., Chatot, C., Hingrat, Y. L., Alabouvette, C., and Steinberg, C. (2012). Potato soil-borne diseases. A review. *Agronomy of Sustainable Development* **32**, 93-132.

Frost, R.R., Harrison, B.D., and Woods, R.D. (1967). Apparent symbiotic interaction between particles of tobacco rattle virus. *Journal of General Virology* **1**, 57-70.

Fu, D-Q., Zhu, B-Z., Zhu, H-L., Jiang, W-B., and Luo, Y-B. (2005). Virus-induced gene silencing in tomato fruit. *The Plant Journal* **43** (2), 299-308. DOI: 10.1111/j.1365-313X.2005.02441

Fu, D-Q., Zhu, B-Z., Zhu, H-L., Zhang, H-X., Xie, Y-H., Jiang, W-B., Zhao, X-D., and Luo, Y.B. (2006). Enhancement of virus-induced gene silencing in tomato by low temperature and low humidity. *Molecules and Cells* **21** (1), 153-160.

Gadjev, I., Stone, J.M., and Gechev, T.S. (2008). Programmed cell death in plants: new insights into redox regulation and the role of hydrogen peroxide. *International Review of Cell and Molecular Biology* **270**, 87-144.

Gassper, J.O., Vega, J., Camargo, I.J.B., and Costa, A.S. (1984). An ultra structural study of particle distribution during microsporogenesis in tomato plants infected with the Brazilian tobacco rattle virus. *Canadian Journal of Botany* **62**, 372-378.

Gebhart, C., and Valkonen, J.P.T. (2001). Organization of genes controlling disease resistance in the potato genome. *Annual Review of Phytopathology* **39**, 79-102.

Ghazala, W., and Varrelmann, M. (2007). Tobacco rattle virus 29K movement protein is the elicitor of extreme and hypersensitive-like resistance in two cultivars of *Solanum tuberosum*. *Molecular Plant–Microbe Interactions* **20** (11), 1396-1405.

Ghazala, W., Waltermann, A., Pilot, R., Winter, S., and Varrelmann, M. (2008). Functional characterization and subcellular localization of the 16K cysteine-rich suppressor of gene silencing protein of Tobacco rattle virus. *Journal of General Virology* **89**(7), 1748-1758.

Ghildiyal, M., and Zamore, P.D. (2009). Small silencing RNAs: an expanding universe. *Nature Reviews Genetics* **10,** 94-108.

Gilbertson, R.L., and Lucas, W.J. (1996). How do viruses traffic on the 'vascular highway'?. *Trends in Plant Science* **1 (**8**),** 260-266.

Goss, R.W. (1925). Two important groups of Nebraska potato diseases: I. Potato wilt and tuber rots; II. ''Run out'' potatoes caused by degeneration diseases. The University of Nebraska. Extension circular, 1256. pp14.

Gould, B., and Kramer, E.M. (2007). Virus-induced gene silencing as a tool for functional analyses in the emerging model plant Aquilegia (Columbine, Ranunculaceae). *Plant Methods* **3**, 6.

Goulden, M.G., Lomonossoff, G.P., Davies, J.W., and Wood, K.R. (1990). The complete nucleotide sequence of PEBV RNA2 reveals the presence of a novel

open reading frame and provides insights into the structure of tobraviral subgenomic promoters. *Nucleic Acids Research* **18 (**15)**,** 4507-4512.

Goulden, M.G., Lomonossoff, G.P., Wood, K.R., and Davies, J.W. (1991). A model for the generation of tobacco rattle virus (TRV) anomalous isolates: pea early browning virus RNA-2 acquires TRV sequences from both RNA-1 and RNA-2. *Journal of General Virology* **72**, 1751-1754.

Graham, T.L., and Graham, M.Y. (1999). Role of hypersensitive cell death in conditioning elicitation competency and defense potentiation. *Physiological and Molecular Plant Pathology* **55**, 13-20.

Grant, J.J., and Loake, G.J. (2000). Role of reactive oxygen intermediates and cognate redox signalling in disease resistance. *Plant Physiology* **124**:21-29.

Haase, N.U. (2008). Health aspects of potatoes as part of the human diet. *Potato Research* **51**, 239-258.

Hamilton, W.D.O., Boccara, M., Robinson, D.J., and Baulcombe, D.C. (1987). The complete nucleotide sequence of tobacco rattle virus RNA-1. *Journal of General Virology* **68**, 2563-2575.

Hartl, M., Merker, H., Schmidt, D.D., and Baldwin, I.T. (2008). Optimized virus-induced gene silencing in *Solanum nigrum* reveals the defensive function of leucine aminopeptidase against herbivores and the shortcomings of empty vector controls. *New Phytologist* **179**, 356-365.

Harrison, B.D., and Woods, R.D. (I966). Serotypes and particle dimensions of tobacco rattle viruses from Europe and America. *Virology* **28**, 610-620.

Harrison, B.D., and Jones, R.A.C. (I971a). Effects of light and temperature on symptom development and virus content of tobacco leaves inoculated with potato mop-top virus. *Annals of Applied Biology* **67**, 377-387.

Harrison, B.D., and Jones, R.A.C. (I971b). Factors affecting the development of spraing in potato tubers infected with potato mop-top virus. *Annals of Applied Biology* **68**, 281-289.

Harrison, B.D., Finch, J.T., Gibbs, A.J., Hoolings, M., Shepherd, R.J., Valenta, V., and Wetter. (1971). Sixteen groups of plant viruses. *Virology* **45**, 356-363.

Harrison, B.D., and Robinson, D.J. (1978). The tobraviruses. In : *Advances in Virus Research* **23**, 25-77.

Harrison, B.D., and Robinson, D.J. (1981). Tobraviruses. In: Handbook of Plant Virus Infection and Comparative Diagnosis. E.kurstak (ed.). Elsevier/North-Holland Biomedical Press, Amsterdam. pp. 515-540.

Harrison, B.D., and Robinson, D.J. (1982). Genome reconstitution and nucleic acid hybridization as methods of identifying particle-deficient isolates of tobacco rattle virus in potato plants with stem mottle disease. J*ournal of Virological Methods* **5**, 255-265.

Harrison, B.D., Robinson, D.J., Mowat, W.P., and Duncan, G.H. (1983). Comparison of nucleic acid hybridization and other tests for detecting tobacco

rattle virus in narcissus plants and potato tubers. *Annals of Applied Biology* **102**, 331-338.

Harrison, B.D., and Robinson, D.J. (1986). Tobraviruses. In: The Plant Viruses, Vol.2 (van Regenmortel, M.H.V. and Fraenkel-Conrat, H., eds.). Plenum Press, New York. pp. 339-369.

Harris, M.A., Clark, J.I., Ireland, A, et al. (2006). The Gene Ontology (GO) project in 2006. *Nucleic Acids Research* 34, D322-D326. Database issue. Retrieved 11 June, 2014 from http://nar.oxfordjournals.org/cgi/screenpdf/34/suppl_1/D322.pdf

Hawkes, J.G. (1990). The potato: evolution, biodiversity and genetic resources. Belhaven Press, Oxford, UK. pp.259.

Hawkes, J.G. (1991a). History of the potato. In: The potato crop, the scientific basis for improvement. Harris, P.M. (ed.). Chapman and Hall, London. pp. 01-11.

Hawkes, J.G. (1991b). Biosystematics of the potato. In: The potato crop, the scientific basis for improvement. Harris, P.M. (ed.). Chapman and Hall, London. pp. 13-60.

Heinze, C., von Bargen, S., Sadowska-Rybak, M., Willingmann, P., and Adam, G. (2000). Sequences of tobacco rattle viruses from potato. *Journal of Phytopathology* **148**, 547-554.

Hernandez, C., Mathis, A., Brown, D.J.F., and Bol, J.F. (1995). Sequence of RNA-2 of a nematode transmissible isolate of tobacco rattle virus. *Journal of General Virology* **76**, 2847-2851.

Hernandez, C., Carette, J.E., Brown, D.J.F., and Bol, J.F. (1996). Serial passage of Tobacco Rattle Virus under different selection conditions results in deletion of structural and nonstructural genes in RNA 2. *Journal of Virology* **70(**8**)**, 4933-4940.

Hernandez, C., Visser, P.B., Brown, D.J.F., and Bol, J.F. (1997). Transmission of tobacco rattle virus isolate PpK20 by its nematode vector requires one of the two non-structural genes in the viral RNA-2. *Journal of General Virology* **78**, 465-467.

Hide G.A., and Lapwood, D.H. (1992). Disease aspects of potato production. In: The potato crop: the scientific basis for improvement. Paul M. Harris (ed.). Chapman and Hall, 2-6 Boundary Row, London SE1 8HN. pp.416.

Hijmans, R.J., and Spooner, D.M. (2001). Geographic distribution of wild potato species. *American Journal of Botany* **88**(11), 2101–2112.

Hileman, L. C., Drea, S., Martino, G., Litta, A., and Irish, V. F. (2005). Virus-induced gene silencing is an effective tool for assaying gene function in the basal eudicot species *Papaver somniferum* (opium poppy). *The Plant Journal* **44**(2), 334-341. DOI: 10.1111/j.1365-313X.2005.02520

Hill, D. P., Smith, B., McAndrews-Hill, M. S., and Blake, J. A. (2008). Gene Ontology annotations: what they mean and where they come. 10th Bio-Ontologies Special Interest Group Workshop 2007. Ten years past and looking to the future**.** *BMC Bioinformatics*, 9(Suppl 5), S2. Retrieved 11 June, 2014, from http://www.biomedcentral.com/content/pdf/1471-2105-9-S5-S2.pdf

Hirschberg, J. (2001). Carotenoid biosynthesis in flowering plants. *Current Opinion in Plant Biology* **4**, 210–218.

Hoek, .J., Zoon, F.C., and Molendijk, L.P.G. (2006). Transmission of tobacco rattle virus (TRV) via seed potatoes. *Communications in Agricultural and Applied Biological Sciences*. Gent University. **71** (3), 887-896.

Hooker, W.J. (1980). Compendium of potato diseases. *American Phytopathological Society*. St. Paul, Minnesota, USA.

Hull, R. (1989). The movement of viruses in plants. *Annual Review of Plant Pathology* **27**, 213-240.

Hunter, L.J.R. (2013). The role of RNA-dependent RNA-polymerase 1 in antiviral defence. University of Cambridge, U.K. Ph.D. thesis.

Huntley, R.P., Sawford, T., Martin, M.J., and Donovan, C. O. (2014). Understanding how and why the Gene Ontology and its annotations evolve: the GO within UniProt. *GigaScience* **3**(4), 1-9.

Husbands, A.Y., Chitwood, D.H., Plavskin, Y., and Timmermans, M. C.P. (2009). Signals and prepatterns: new insights into organ polarity in plants. *Genes & Development 23* (1), 1986-1997. DOI: 10.1101/gad.1819909.

Jones, R.A.C. (1981). The ecology of viruses infecting wild and cultivated potatoes in the Andean region of South America. In: Pests, Pathogens and Vegetation. Thresh, J. M. (ed.). Pitman, London. pp. 89-107.

Jupe, F., Witek, K., Verweij, W., Sliwka, J., Pritchard, L., Etherington, G. J., Maclean, D., Cock, P. J., Leggett, R. M., Bryan, G. J., Cardle, L., Hein, I., and Jones J.D.G. (2013). Resistance gene enrichment sequencing (RenSeq) enables reannotation of the NB-LRR gene family from sequenced plant genomes and rapid mapping of resistance loci in segregating populations. *The Plant Journal* **76**, 530-544. DOI: 10.1111/tpj.12307.

Kang, B.-C., Yeam, I., Frantz, J.D., Murphy, J.F. and Jahn, M.M. (2005). The pvr1 locus in pepper encodes a translation initiation factor eIF4E that interacts with Tobacco etch virus VPg. *Plant Journal* **41**, 392-405.

Kasschau, K.D. and Carrington J.C. (1998). A counter defensive strategy of plant viruses: suppression of posttranscriptional gene silencing. *Cell* **95,** 461-470.

Kemp, G., Botha, A.M., Kloppers, F.J., and Pretorius, Z.A. (1999). Disease development and β-1, 3-glucanase expression following leaf rust infection in resistant and susceptible near isogeneic wheat seedlings. *Physiological and Molecular Plant Pathology* **55**, 45-52.

Keogh, R. C., Deverall, B. J., and Mcleod, S. (1980). Comparison of histological and physiological responses to *Phakopsora pachyrhizi* in resistant and susceptible soybean. *Transactions of the British Mycological Society* **74**, 329-333.

Khu, D. M., Lorenzen, J., Hackett, C.A., and Love, S.L. (2008). Interval mapping of quantitative trait loci for corky ringspot disease resistance in a tetraploid population of potato (*Solanum tuberosum* subsp. *tuberosum*). *American Journal of Potato Research* **85**, 129-139.

Koch, E., and Slusarenko, A. (1990). *Arabidopsis* is susceptible to infection by a Downy Mildew fungus. *Plant Cell* **2**, 437-445.

Koenig, R., Lesemann, D.-E., Pfeilstetter, E., Winter, S., and Pleij, C.W.A. (2011). Deletions and recombinations with RNA1 3′ ends of different tobraviruses have created a multitude of tobacco rattle virus TCM-related RNA2 species in *Alstroemeria* and tulip. *Journal of General Virology* **92**, 988-996.

Koenig, R., Lesemann, D.E., and Pleij, C.W.A. (2012). Tobacco rattle virus genome alterations in the *Hosta* hybrid 'Green Fountain' and other plants: reassortments, recombinations and deletions. *Archives of Virology* **157**, 2005-2008.

Kogovšek, P., Pompe-Novak, M., Baebler, S., Rotter, A., Gow, L., Gruden, K., Foster, G.D., Boonham, N. and Ravnikar, M. (2010). Aggressive and mild Potato virus Y isolates trigger different specific responses in susceptible potato plants. *Plant Pathology* **59**: 1121-1132.

Köhm, B.A., Goulden, M.G., Gilbert, J.E., Kavanagh, T.A., Baulcombe, D.C. (1993). A potato virus X resistance gene mediates an induced non-specific resistance in protoplasts. *Plant Cell* **5,** 913-920.

Kombrink, E., and Schmelzer, E. (2001). The hypersensitive response and its role in the local and systemic disease resistance. *European Journal of Plant Pathology* **107**, 69-78.

Kuipers, G. J., Jacobsen, E., and Visser, R.G.F. (1994). Formation and deposition of amylose in the potato tuber starch granule are affected by the reduction of granule-bound starch synthase gene expression. *The Plant Cell* **6**, 43-52.

Kumagai, M.H., Donson, J., Della-Cioppa, G., Harvey, D., Hanley, K., and Grill, L.K. (1995). Cytoplasmic inhibition of carotenoid biosynthesis with virus-derived RNA. *Proceedings of the National Academy of Sciences of the United States of America* **92**, 1679-1683.

Lacomme, C., Hrubikova, K., and Hein, I. (2003). Enhancement of virus-induced gene silencing through viral-based production of inverted-repeats. *The Plant Journal* **34**, 543-553.

Lakatos, L., Szittya, G., Silhavy, D., and Burgyan, J. (2004). Molecular mechanism of RNA silencing suppression mediated by p19 protein of tombusviruses. *EMBO Journal* **23,** 876-884.

Lamb, C., and Dixon, R.A. (1997). The oxidative burst in plant disease resistance. *Annual Review of Plant Physiology and Plant Molecular Biology* **48**, 251-275.

Legorburu, F.J., Robinson, D.J., Torrance, L., and Duncan, G. H. (1995). Antigenic analysis of nematode-transmissible and non-transmissible isolates of tobacco rattle tobravirus using monoclonal antibodies. *Journal of General Virology* **76**, 1497-1501.

Legorburu, F.J., Robinson, D.J., and Torrance, L. (1996). Features on the surface of tobacco rattle tobravirus particle that are antigenic and sensitive to proteolytic digestion. *Journal of General Virology* **77**, 855-859.

Li, F. and Ding, S.W. (2006). Virus counterdefense: diverse strategies for evading the RNA-silencing immunity. *Annual Review of Microbiology* **60**, 503-531.

Lihnell, D. (1958). Investigations on spraing. Proceedings of the third conference on potato virus diseases. Lisse-Wageningen, 24-28, Wageningen. pp. 184-188.

Liljegren, S. (2010). Phloroglucinol stain for lignin. Cold Spring Harbor Protocols. DOI:10.1101/pdb.prot4954.

Lin, J. (2013). Non host resistance to bean pod mottle virus in *Nicotiana benthamiana*. The Ohio State University, USA. Ph.D thesis.

Lister, C.E. (2013). The composition and health benefits of potatoes-an update (2009-2013). A report prepared for Potatoes New Zealand Inc. Plant & Food Research data: Milestone No. 54498. Contract No. 30063. *The New Zealand Institute for Plant & Food Research Ltd*, Private Bag 92169,Victoria Street West, Auckland 1142, New Zealand. pp 01-34. Retrieved 31 May, 2016, from http://www.potatoesnz.co.nz/assets/Uploads/Education-/Nutrition/9215-The-composition-and-health-benefits-of-potatoes.pdf

Lister, R.M. (1966). Possible relationships of virus-specific products of tobacco rattle virus infections. *Virology* **28** (2), 350-353.

Lister, R.M. (1968). Functional relationships between virus specific products of infection by viruses of the tobacco rattle type. *Journal of General Virology* **2**, 43-58.

Lister, R.M., and Bracker, C.E. (1969). Defectiveness and dependence in three related strains of tobacco rattle virus. *Virology* **37**, 262-275.

Liu, H., Reavy, B., Swanson, M., and MacFarlane, S.A. (2002). Functional replacement of the Tobacco rattle virus cysteine-rich protein by pathogenicity proteins from unrelated plant viruses. *Virology* **298**, 231-239.

Liu, Y., Shiff, M., Marathe, R., and Dinesh-Kumar, S.P. (2002a). Tobacco Rar1, EDS1 and NPR1/NIM1 like genes are required for N-mediated resistance to tobacco mosaic virus. *The Plant Journal* **30**(4), 415-429.

Liu, Y., Shiff, M., and Dinesh-Kumar, S.P. (2002b). Virus-induced gene silencing in tomato. *The Plant Journal* **31**(6), 777-786.

Love, A.J., Laird, J., Holt, J., Hamilton, A.J., Sadanandom, A, and Milner, J.J. (2007). Cauliflower mosaic virus protein P6 is a suppressor of RNA silencing. *Journal of General Virology* **88,** 3439-3444.

Lu, R., Martin-Hernandez, A.M., Peart, J.R., Malcuit, I., and Baulcombe, D.C. (2003). Virus-induced gene silencing in plants. *Methods* **30,** 296-303.

Lucas, W. J. (2006). Plant viral movement proteins: agents for cell-to-cell trafficking of viral genomes. *Virology* 344, 169-184.

Mach, J. (2012). Why wiry, Tomato mutants reveal connections among small RNAs, auxin response factors, virus infection, and leaf morphology. *The Plant Cell* **24**, 3486.

Machida-Hirano, R. (2015). Diversity of potato genetic resources. *Breeding Science* **65**, 26-40.

MacFarlane, S.A., and Brown, D.J.F. (1995). Sequence comparison of RNA2 of nematode transmissible and nematode non transmissible isolates of pea early browning virus suggests that the gene encoding the 29kDa protein may be involved in nematode transmission. *Journal of General Virology* **76**, 1299-1304.

MacFarlane, S.A., Wallis, C.V., and Brown, D.J.F. (1996). Multiple virus genes involved in the nematode transmission of pea early browning virus. *Virology* **219**, 417-422.

MacFarlane, S.A. (1997). Natural recombination among plant virus genomes: evidence from tobraviruses. *Seminars in Virology* **8**, 25-31.

MacFarlane, S.A., Vassilakos, N., and Brown, D.J.F. (1999). Similarities in the genome organization of tobacco rattle virus and pea early browning virus isolates that are transmitted by the same vector nematode. *Journal of General Virology* **80**, 273-276.

MacFarlane, S.A. (1999). Molecular biology of the tobraviruses. *Journal of General Virology* **80**, 2799-2807.

MacFarlane, S.A. (2003). Molecular determinants of the transmission of plant viruses by nematodes. *Molecular Plant Pathology* **4**(3), 211-215.

MacFarlane, S.A. (2010). Tobraviruses plant pathogens and tools for biotechnology. *Molecular Plant Pathology* **11** (4), 577-583.

Mandahar, C.L. (2006). Subgenomic RNAs. In: Multiplication of Plant Viruses. Springer, The Netherlands. pp. 195-222.

Martin-Hernandez, A. M., and Baulcombe, D.C. (2008). Tobacco rattle virus 16-kilodalton protein encodes a suppressor of RNA silencing that allows transient viral entry in meristems. *Journal of Virology* **82**(8), 4064-4071.

Más, P., and Pallás, V. (1996). Long-distance movement of cherry leaf roll virus in infected tobacco plants. *Journal of General Virology* **77**, 531-540.

May, M. J., Hammond-Kosack, K.E., and Jones, J.D.G. (1996). Involvement of reactive oxygen species, glutathione metabolism, and lipid peroxidation in the Cf-gene-dependent defense response of tomato cotyledons induced by race-specific elicitors of *Cladosporium fulvum*. *Plant Physiology* **110**, 1376-1379.

Mayo, M.A., Robertson, W.M., Legorburu, F.J., and Brierley, K.M. (1994). Molecular approaches to an understanding of the transmission of plant viruses by nematodes. In: Advances in molecular nematology. Lamberti, F., De Giorgi, C. and Bird, D.M. (eds.). Plenum Press, New York. pp. 277-293.

Mclean, B.G., Waigmann, E., Citovsky, V., and Zambryski, P. (1993). Cell-to-Cell movement of plant viruses. *Trends in Microbiology*. **1**, (3), 105-109

Miles, G.P., Samuel, M.A., Chen, J., Civerolo, E.L., and Munyaneza, J.E. (2010). Evidence that cell death is associated with Zebra Chip disease in potato tubers. *American Journal of Potato Research* **87**, 337-349.

Mittler, R., Vanderauwera, S., Suzuki, N., Miller, G., Tognetti, V.B., Vandepoele, K., Gollery, M., Shulaev, V., and van Breusegem, F. (2011).

ROS signaling: the new wave? *Trends in Plant Science* **16** (6), 300-309. DOI: 10.1016/j.tplants.2011.03.007.

Mlotshwa, S., Voinnet, O., Mette, M.F., Matzke, M., Vaucheret, H., Ding, S.W., Pruss, G., and Vance, V.B. (2002). RNA silencing and the mobile silencing signal. *The Plant Cell* **14**, S289-S301.

Mojtahedi, H., Santo, G.S., Crosslin, J.M., Brown, C.R., and Thomas, P.E. (2000). Corky ringspot: review of current situation. *Proceedings of the 39th Washington State Potato Conference Trade Fair*. Moses Lake, WA. pp 9–13.

Mysore, K.S., and Ryu, C.M. (2004). Nonhost resistance: how much do we know? *Trends in Plant Science* **9**(2), 97-104.

Nicolaisen, M., Bosze, Z., and Nielsen S.L. (1999). Detection of tobacco rattle virus in potato tubers using a simple RT-PCR procedure. *Potato Research* **42**, 173-179.

Nicot, N., Hausman, J.F., Hoffmann, L., and Evers, D. (2005). Housekeeping gene selection for real-time RT-PCR normalization in potato during biotic and abiotic stress. *Journal of Experimental Botany* **56**, 2907–2914.

Padmanabhan M., Dinesh-Kumar, S.P. (2009). Virus-induced gene silencing as a tool for delivery of dsRNA into plants. *Cold Spring Harbor Protocols* **4** (2), 1-4. DOI:10.1101/pdb.prot5139

Palukaitis, P., and Carr, J.P. (2008). Plant resistance responses to viruses. *Journal of Plant Pathology* **90** (2), 153-171.

Palukaitis, P. (2012). Resistances to viruses of potato and their vectors. *Plant Pathology Journal* **28** (3), 248-258.

Pelham, H.R.B. (1979). Translation of tobacco rattle virus RNAs in vitro: four proteins from three RNAs. *Virology* **997**, 256-265.

Pereira, H. (2007). Cork biology. In: Cork, biology, production and uses. Elsevier, The Netherlands. p.55.

Ploeg, A.T., Asjes, C.J. and Brown, D.J.F. (1991). Tobacco rattle virus serotypes and associated nematode vector species of Trichodoridae in the bulb-growing areas in the Netherlands. *Netherlands Journal of Plant Pathology* **97**(5), 311-319. DOI: 10.1007/BF01974226

Ploeg, A.T., Brown, D.J.F. and Robinson, D.J. (1992a). Acquisition and subsequent transmission of tobacco rattle virus isolates by *Paratrichodorus* and *Trichodorus* nematode species. *Netherlands Journal of Plant Pathology* **98**, 291-300.

Ploeg, A.T., Brown, D.J.F., and Robinson, D.J. (1992b). The association between species of *Trichodorus* and *Paratrichodorus* vector nematodes and serotypes of tobacco rattle tobravirus. *Annals of Applied Biology* **121**, 619-630.

Ploeg, A.T., Mathis, A., Brown, D.J.F., and Robinson, D.J. (1993a). Susceptibility of transgenic tobacco plants expressing tobacco rattle virus coat protein to nematode-transmitted and mechanically inoculated tobacco rattle virus. *Journal of General Virology* **74**, 2709-2715. DOI:10.1099/0022-1317-74-12-2709

Ploeg, A.T., Robinson, D.J., and Brown, D.J.F. (1993b). RNA-2 of tobacco rattle virus encodes the determinants of transmissibility by trichodorid vector nematodes. *Journal of General Virology* **74**, 1463-1466. DOI:10.1099/0022-1317-74-7-1463

Pompe-Novak, M., Gruden, K., Baebler, S., Krečič-Stres, H., Kovač, M., Jongsma, M. and Ravnikar, M. (2006). Potato virus Y induced changes in the gene expression of potato (*Solanum tuberosum* L.). *Physiological and Molecular Plant Pathology* **67**: 237-247.

Purkayastha, A., and Dasgupta, I. (2009). Virus-induced gene silencing: A versatile tool for discovery of gene functions in plants. *Plant Physiology and Biochemistry* **47,** 967-976.

Quanjer, H.M. (1943). Bijdrage tot de kennis van de in Nederland voorkomende ziekten van Tabak en van de Tabaksteelt op kleigrond. (Contribution to the knowledge of the Tobacco diseases occurring in Holland and of Tobacco cultivation on clay soil. Netherland Journal of Plant Pathology). *Tijdschrift over Plantenziekten* **49** (2), 37-51.

Ramachandran, S., and Sundaresan, V. (2001).Transposons as tools for functional genomics. *Plant Physiology and Biochemistry* **39,** 243−252.

Ramegowda, V., Senthil-Kumar, M., Udayakumar, M., and Mysore, K.S. (2013). A high-throughput virus-induced gene silencing protocol identifies genes involved in multi-stress tolerance. *BMC Plant Biology* **13**: 193.

Ramegowda, V., Mysore, K.S., and Senthil-Kumar, M. (2014).Virus-induced gene silencing is a versatile tool for unravelling the functional relevance of multiple abiotic-stress-responsive genes in crop plants. *Frontiers in Plant Science* **5,** Article 323.

Ratcliff, F., Harrison, B. D., and Baulcombe, D.C. (1997). A similarity between viral defence and gene silencing in plants. *Science* **276**, 1558-1560.

Ratcliff, F., Martin-Hernandez, A. M., and Baulcombe, D.C. (2001). Technical advance: Tobacco rattle virus as a vector for analysis of gene function by silencing. *The Plant Journal* **25**, 237-245. DOI: 10.1046/j.0960-7412.2000.00942.

Reavy, B., Dawson, S., Canto, T., and MacFarlane, S.A. (2004). Heterologous expression of plant virus genes that suppress post-transcriptional gene silencing results in suppression of RNA interference in *Drosophila* cells. *BMC Biotechnology* **4**: 18.

Rich, A.E. (1983). Diseases caused by viruses, viroids and mycoplasmas. In: Potato diseases. Academic Press, New York. pp. 92-136.

Robertson, D. (2004). VIGS vectors for gene silencing: many targets, many tools. *Annual Review of Plant Biology* **55,** 495-519.

Robinson, D.J. (1977). A variant of tobacco rattle virus: evidence for a second gene in RNA-2. *Journal of General Virology* **35**, 37-43.

Robinson, D.J. (1992). Detection of tobacco rattle virus by reverse transcription and polymerase chain reaction. *Journal of Virological Methods* **40**, 57-66.

Robinson, D.J. (1994). Sequences at the ends of RNA-2 of I6, a recombinant tobravirus. *Archives of Virology* [Supplementum] **9**:245-251.

Robinson, D.J. (2004). Identification and nucleotide sequence of a *Tobacco rattle virus* RNA-1 variant that causes spraing disease in potato cv. Bintje. *Journal of Phytopathology* **152**, 286-290.

Robinson, D.J., Mayo, M.A., Fritsch, C.A., Jones, A.T., and Raschke´, J.H. (1983). Origin and messenger activity of two small RNA species found in particles of tobacco rattle virus strain SYM. *Journal of General Virology* **64**, 1591-1599.

Robinson, D.J., and Harrison, B.D. (1985a). Unequal variation in the two genome parts of tobraviruses and evidence for the existence of three separate viruses. *Journal of General Virology* **66**, 171-176.

Robinson, D.J., and Harrison, B.D. (1985b). Evidence that broad bean yellow band virus is a new serotype of pea early-browning virus. *Journal of General Virology* **66**, 2003-2009.

Robinson, D.J., Hamilton, W.D.O., Harrison, B.D., and Baulcombe, D.C. (1987). Two anomalous tobravirus isolates: evidence for RNA recombination in nature. *Journal of General Virology* **68**, 2551-2561.

Robinson, D.J., and Harrison, B.D. (1989). Tobacco rattle virus. In: *AAB Descriptions of Plant Viruses No. 346* (No.12 revised). *Association of Applied Biologists*. p. 6.

Robinson, D.J., Dale, M.F.B., and Todd, D. (2004). Factors affecting the development of disease symptoms in potatoes infected by tobacco rattle virus. *European Journal of Plant Pathology* **110**, 921-928.

Robinson, D.J., and Dale, M.F.B. (1994). Susceptibility, resistance and tolerance of potato cultivars to tobacco rattle virus infection and spraing disease. *Aspects of Applied Biology* **39**, 61-66.

Rodrigo, G., Carrera, J., Ruiz-Ferrer, V., Toro, F.J., Llave, C., Voinnet, O. and Elena, S.F. (2012). A meta-analysis reveals the commonalities and differences in Arabidopsis thaliana in response to different viral pathogens. PLoS ONE 7: e40526

Ross, H.A., Wright, K.M., McDougall, G. J., Roberts, A. G., Chapman, S. N., Morris, W. L., Hancock, R. D., Stewart, D., Tucker, G. A., James, E. K.,and Taylor, M. A. (2011). Potato tuber pectin structure is influenced by pectin methyl esterase activity and impacts on cooked potato texture. *Journal of Experimental Botany* **62** (1), 371–381.

Roth, B.M., Pruss, G.J., and Vance, V.B., (2004). Plant viral suppressors of RNA silencing. *Virus Research* **102,** 97-108.

Rowe, R.C. (1993). Potato health management: A holistic approach. In: Potato Health Management. The American Phytopatological Society. pp. 03-10.

Ruiz de Galerreta, J.I., Carrasco, A., Salazar, A., Barrena, I., Iturritxa, E., Marquinez, R., Legorburu, F.J., and Ritter, E. (1998). Wild Solanum

species as resistance sources against different pathogens of potato. *Potato Research* **41**, 57-68.

Ruiz, M.T., Voinnet, O., and Baulcombe, D.C. (1998). Initiation and maintenance of virus-induced gene silencing. *The Plant Cell* **10**, 937-946.

Ryden, K., Sandgren, M., and Hurlado, S. (1994). Development during storage of spraing symptoms in potato tubers infected with tobacco rattle virus. *Potato Research* **37**, 99-102.

Salaman, R.N. (1921). Degeneration of potatoes. In: Report on the International Potato Conference. Royal Horticultural Society, London. pp. 79-91.

Sänger, H.L. (1968). Characteristics of tobacco rattle virus. I. Evidence that its two particles are functionally defective and mutually complementing. *Molecular and General Genetics* **101**, 346-367.

Sambrooke, J., Fritsch, E.F., and Maniatis, T.A. (1989). Molecular Cloning: A Laboratory Manual. 2nd ed. Cold Spring Harbour Laboratory, New York.

Santala, J., Samuilova, O., Hannukkala, A., Latvala, S., Kortemaa, H., Beuch, U., Kvarnheden, A., Persson, P., Topp, K., Orstad, K., Spetz, C., Nielsen, S.L., Kirk, H.G., et al. (2010). Detection, distribution and control of Potato mop-top virus, a soil-borne virus, in northern Europe. *Annals of Applied Biology* **157**, 163-178.

Scandalios, J. G. (1997). Molecular Genetics of Superoxide Dismutases in Plants. In: Oxidative stress and the molecular biology of antioxidant defenses. Scandalios, J.G. (eds.) Cold Spring Harbor. **1** (1), 527-568. DOI: 10.1101/087969502.34.527

Scherer, N.M., Thompson, C.E., Freitas, L.B., Bonatto, S.L., and Salzano, F.M. (2005). Patterns of molecular evolution in pathogenesis-related proteins. *Genetics and Molecular Biology* **28** (4), 645-653.

Scott, K. P., Kashiwazaki, S., Reavy, B., and Harrison, B. D. (1994). The nucleotide sequence of potato mop-top virus RNA 2: a novel type of genome organization for a furovirus. *Journal of General Virology*. **75** (12), 3561-3568.

Sels, J., Mathys, J., De Coninck, B.M.A., Cammue, B.P.A., and De Bolle, M.F.C. (2008). Plant pathogenesis-related (PR) proteins: A focus on PR peptides. *Plant Physiology and Biochemistry* **46**, 941–950.

Senthil-Kumar, M., and Mysore, K.S. (2011a). New dimensions for VIGS in plant functional genomics. *Trends in Plant Science* **16** (12), 656-665.

Senthil-Kumar, M., and Mysore, K.S. (2011b). Virus-induced gene silencing can persist for more than 2 years and also be transmitted to progeny seedlings in *Nicotiana benthamiana* and tomato. *Plant Biotechnology Journal* **9**, 797-806.

Sharma, P., Jha, A.B., Dubey, R.S., and Pessarakli, M. (2012). Reactive oxygen species, oxidative damage, and antioxidative defense mechanism in plants under stressful conditions. *Journal of Botany*. 1-26.

Sherwood, J.L. (1988). In: Plant Resistance to Viruses. Evered, D., and Harnett, S. (eds.), Wiley, Chichester, UK. pp. 136-150.

Shewry, P.R. (2003). Tuber storage proteins. *Annals of Botany* **91,** 755-769.

Singh, R.P., Nie, X., and Tai, G.C.C. (2000). A novel hypersensitive resistance response against potato virus A in cultivar 'Shepody'. *Theoretical Applied Genetics* **100**, 401-408.

Singh, A., Kumar, P., Jiang, C-Z., and Reid, M.S. (2013). TRV Based Virus Induced Gene Silencing in Gladiolus (*Gladiolus grandiflorus* L.), A Monocotyledonous Ornamental Plant. *VEGETOS* **26** (Special), 170-174. DOI:10.5958/j.2229-4473.26.2s.137

Smith, A.M., Denyer, K., and Martin, C. (1997). The synthesis of the starch granule. *Annual Reviews in Plant Physiology and Plant Molecular Biology* **48**, 67-87.

Smith, A.M., Zeeman, S.C., and Denyer, K. (2001). The synthesis of amylose. In: Starch: Advances in structure and function. Barsby, T. L., Donald, T. M., and Frazier, P.J. (eds.). The Royal Society of Chemistry. Cambridge, U.K. pp. 150-163.

Solomon-Blackburn, R.M., and Barker, H. (2001). Breeding virus resistant potatoes (*Solanum tuberosum*): a review of traditional and molecular approaches. *Heredity* **86**, 17-35. DOI:10.1046/j.1365-2540.2001.00799

Soosaar, J.L.M., Burch-Smith, T.M., and Dinesh-Kumar, S.P. (2005). Mechanisms of plant resistance to viruses. *Nature Reviews Microbiology* **3**, 789-798.

Sokmen, M.A., Barker, H., and Torrance, L. (1998). Factors affecting the detection of potato mop-top virus in potato tubers and improvement of test procedures for more reliable assays. *Annals of Applied Biology* **133**, 55-63.

Stevenson, W.R., Loria, R., Franc, G.D., and Weingartner, D.P. (eds.). (2001). Compendium of potato diseases, Second edition. The American Phytopathological Society. pp.144. ISBN 978-0-89054-275-0.

Stewart, D., and McDougall, G. (2012). Potato; A nutritious, tasty but often maligned staple food. Food and Health Innovation Service Report. Retrieved 25 December, 2013 from http://www.hutton.ac.uk/webfm_send/743 (All data extracted from FINELI database- http://www.fineli.fi)

Storey, M. (2007). The Harvested Crop. In: Potato biology and biotechnology: Advances and perspectives. Vreugdenhil, D. (ed.). Elsevier Ltd., London. pp. 441-470.

Sudarshana, M.R., and Berger, P.H. (1998). Nucleotide sequence of both genomic RNAs of a North American tobacco rattle virus isolate. *Archives of Virology* **143**, 1535-1544.

Swanson, M., Barker, H., and MacFarlane, S.A. (2002). Rapid vascular movement of tobraviruses does not require coat protein: evidence from mutated and wild type viruses. *Annals of Applied Biology* **141**, 259-266.

Tamura, K., Stecher, G., Peterson, D., Filipski, A. and Kumar, S. (2013). MEGA6: Molecular Evolutionary Genetics Analysis version 6.0. *Molecular Biology and Evolution* **30**, 2725-2729.

Taylor, C.E., and Brown, D.J.F. (1997). Nematode vectors of plant viruses.CAB International. Wallingford, U.K. pp. 286.

Tenhaken, R., Levine, A., Brisson, L.F., Dixon, R.A. and Lamb, C. (1995). Function of oxidative burst in hypersensitive disease resistance. *Proceedings of the National Academy of Sciences of the United States of America* **92**, 4158-4163.

Thordal-Christensen, H., Zhang, Z., Wei, Y., and Collinge, D. B. (1997). Subcellular localization of H_2O_2 in plants. H_2O_2 accumulation in papillae and hypersensitive response during the barley-powdery mildew interaction. *The Plant Journal* **11**(6), 1187-1194.

Tuttle, J.R., Idris, A.M., Brown, J.K., Haigler, C.H., and Robertson, D. (2008). Geminivirus-mediated gene silencing from *Cotton leaf crumple virus* is enhanced by low temperature in cotton . *Plant Physiology* **148,** 41-50.

Valentine, T.A., Shaw, J., Blok, V.C., Phillips, M.S., Oparka, K.J., and Lacomme C. (2004). Efficient virus-induced gene silencing in roots using a modified tobacco rattle virus vector. *Plant Physiology* **136**, 3999-4009.

Valkonen, J.P.T., Jones, R.A.C., Slack, S.A., and Watanabe, K.N. (1996). Resistance specificities to viruses in potato: standardization of nomenclature. *Plant Breeding* **115**, 433-438.

van Hoof, H.A. (1964a). Het tijdsstip van infectie en veranderingen in de concentratie van ratel virus (Kringerigheid) in de aardappelknol (Summary: The time of infection and change in concentration of rattle virus (spraing) in potato tubers. *Mededelingen van de Lanbouhogeschool in de Opzoekingsstations van de Staat te Gent* **29**, 944-955.

van Hoof, H.A. (1964b). Trichodorus teres a vector of rattle virus. *Netherlands Journal of Plant Pathology* **70**(6), p187.

van Hoof, H.A. (1968). Transmission of tobacco rattle virus by *Trichodorus* species. *Nematologica* **14** (1), 20-24.

van Hoof, H.A.; Maat, D.Z.; and Seinhorst, J.W. (1966). Viruses of the tobacco rattle virus group in northern Italy: their vectors and serological relationships. *Netherlands Journal of Plant Pathology* **72**, 253-258.

Vance, V., and Vaucheret, H. (2001). RNA silencing in plants-defence and counterdefence. *Science* **292,** 2277-2280.

Vassilakos, N., Vellios, E. K., Brown, E. C., Brown, D.J.F. and MacFarlane, S.A. (2001). Tobravirus 2b protein acts *in trans* to facilitate transmission by Nematodes. *Virology* **279** (2), 478-487.

Vaucheret, H., Becllin, C., and Fagard, M. (2001). Post-transcriptional gene silencing in plants. *Journal of Cell Science* **114**(17), 3083-3091.

Velasquez, A. C., Chakravarthy, S., and Martin, G.B. (2009). Virus-induced gene silencing (VIGS) in *Nicotiana benthamiana* and Tomato. *Journal of Visualized Experiments* **28**, 1-4.

Verwoerd, T.C., Dekker, B.M.M., and Hoekema, A. (1989). A small scale procedure for the rapid isolation of plant RNAs. *Nucleic Acids Research* **17** (6), 2362.

Visser, R.G.F., Stoite, A., and Jacobsen, E. (1991). Expression of a chimeric granule-bound starch synthase-GUS gene in transgenic potato plants. *Plant Molecular Biology* **17**, 691-699.

Visser, P.B., and Bol, J.F. (1999). Non-structural proteins of tobacco rattle virus which have a role in nematode transmission: expression pattern and interaction with viral coat protein. *Journal of General Virology* **80**, 3273-3280.

Visser, P.B., Brown, D.J.F., Brederode, F.T., and Bol, J.F. (1999). Nematode transmission of tobacco rattle virus serves as a bottleneck to clear the virus population from Defective Interfering RNAs. *Virology* **263**: 155-165.

Vleeshouwers, V.G.A.A, Finkers, R., Budding, D., Visser, M., Jacobs, M.M.J., Berloo, R.V., Pel, M., Champouret, N., Bakker, E., Krenek, P., Rietman, H., Huigen, D., Hoekstra, R., Goverse, A., Vosman, B., Jacobsen, E., and Visser, R.G.F. (2011). SolRgene: an online database to explore disease resistance genes in tuber-bearing *Solanum* species. *BMC Plant Biology* **11**, 116.

Voinnet, O. (2005a). Non-cell autonomous RNA silencing. *FEBS Letters* **579**, 5858-5871.

Voinnet, O. (2005b). Induction and suppression of RNA silencing: Insights from viral infections. *Nature* **6**, 206-221.

Wang, D., MacFarlane, S.A., and Maule, A.J. (1997). Viral determinants of pea early browning virus seed transmission in pea. *Virology* **234**, 112-117.

Wang, X., Hadrami, A.E., Adam, L.R., and Daayf, F. (2005). Genes encoding pathogenesis-related proteins PR-2, PR-3 and PR-9, are differentially regulated in potato leaves inoculated with isolates from US-1 and US-8 genotypes of *Phytophthora infestans* (Mont.) de Bary. *Physiological and Molecular Plant Pathology* **67**, 49-56.

Wang, T., Li, R., Wen, L., Fu, D., Zhu, B., Luo, Y., and Zhu, H. (2015). Functional analysis and RNA sequencing indicate the regulatory role of *Argonaute* 1 in tomato compound leaf development. *PLoS ONE* **10** (10)**:** e0140756. Doi:10.1371/journal.pone.0140756.

Weingartner, D.P. (2001). Potato viruses with soil-borne vectors. In: Virus and Virus-like Diseases of Potatoes and Production of Seed-Potatoes. Loebenstein, G. *et al.* (eds.). Kluwer Academic Publishers, London. pp.177-194.

Whithamn, S.A., and Wang, Y. (2004). Roles for host factors in plant viral pathogenicity. *Current Opinion in Plant Biology* **7**, 365-371.

Wintermantel, W.M., and Schoelz, J.E. (1996). Isolation of recombinant viruses between cauliflower mosaic virus and a viral gene in transgenic plants under conditions of moderate selection pressure. *Virology* **223**, 156-164.

Wojtaszek, P. (1997). Oxidative burst: an early plant response to pathogen infection. *Journal of Biochemistry* **322**, 681-692.

Wright, K.M., Duncan, G.H., Pradel, K.S., Carr, F., Wood, S., Oparka, K.J., and Cruz, S.S. (2000). Analysis of the N gene hypersensitive response induced by a fluorescently tagged tobacco mosaic virus. *Plant Physiology* **123**, 1375-1385.

Wu, C., Jia, L., and Goggin, F. (2011). The reliability of virus-induced gene silencing experiments using tobacco rattle virus in tomato is influenced by the size of the vector control. *Molecular Plant Pathology* **12** (3), 299-305. DOI: 10.1111/j.1364-3703.2010.00669.

Xenophontos, S., Robinson, D.J., Dale, M.F.B., and Brown D.J.F. (1998). Evidence for persistent, symptomless infection of some potato cultivars with tobacco rattle virus. *Potato Research* **41**, 255-265.

Xin, H.W., and Ding S.W. (2003). Identification and molecular characterization of a naturally occurring RNA virus mutant defective in the initiation of host recovery. *Virology* **317**, 253-262.

Xu, X., Pan, S., Cheng, S., Zhang, B., Mu, D., Ni, P., Zhang, G., Yang, S., Li, R. and Wang, J. (2011). Genome sequence and analysis of the tuber crop potato. *Nature* **475**, 189-197. DOI:10.1038/nature10158.

Ye, J., Qu, J., Zhang, J-F., Geng, Y-F., and Fang, R-X. (2008). A critical domain of the *Cucumber mosaic virus* 2b protein for RNA silencing suppressor activity. *FEBS Letters* **583**, 101-106.

Yifhar, T., Pekker, I., Peled, D., Friedlander, G., Pistunov, A., Sabban, M., Wachsman, G., Alvarez, J.P., Amsellem, Z., and Eshed, Y. (2012). Failure of the tomato *Trans*-acting short interfering RNA program to regulate AUXIN RESPONSE FACTOR3 and ARF4 underlies the wiry leaf syndrome. *The Plant Cell* **24**(9), 3575-3589. DOI: 10.1105/tpc.112.100222.

Yin, Z., Pawelkowicz, M., Michalak, K., Chrzanowska, M., and Zimnoch-Guzowska, E. (2014a). The genomic RNA1 and RNA2 sequences of the tobacco rattle virus isolates found in Polish potato fields. *Virus Research* **185**, 110-113.

Yin, Z., Pawelkowicz, M., Michalak, K., Chrzanowska, M., and Zimnoch-Guzowska, E. (2014b). Single-nucleotide polymorphisms and reading frame shifts in RNA2 recombinant regions of tobacco rattle virus isolates Slu24 and Deb57. *Archives of Virology* **159**, 3119-3123.

Zamore, P.D. (2004). Plant RNAi: How a viral silencing suppressor inactivates siRNA. *Current Biology* **14**, R198-R200.

Zhang, X., Yuan, Y.-R., Pei, Y., Lin, S.-S., Tuschl, T., Patel, D. J., and Chua, N.-H. (2006). Cucumber mosaic virus-encoded 2b suppressor inhibits Arabidopsis Argonaute1 cleavage activity to counter plant defense. *Genes & Development* **20**, 3255-3268.

Zhixin, X., and Qi, X. (2008). Diverse small RNA-directed silencing pathways in plants. *Biochimica et Biophysica Acta* **1779,** 720-724.

Internet resources:-

http://www.dpvweb.net/dpv/showdpv.php?dpvno=398

http://www.dpvweb.net/notes/showgenus.php?genus=Tobravirus

http://faostat.fao.org/site/339/default.aspx

http://www.fao.org/potato-2008/en/potato/tuber.html

http://potato.plantbiology.msu.edu

http://www.hutton.ac.uk/webfm_send/743

http://cip.wpengine.com

http://www.fineli.fi

http://nar.oxfordjournals.org/cgi/screenpdf/34/suppl_1/D322.pdf

8. Appendices

Appendix 1. Primers for studies on TRV-isolates

S. No.	Oligo name & number	Gene annotation & Oligo Sequence (5' - 3')	Position on transcript sequence (nts)	Exon Boundary or target	Primer length	Tm (C°)	GC %	Amplicon size (bp)
1.	DJR 16K+ (1761) or (2350)	16K GACGTGTGTACTCAAGGGTT	6113--6132	Flanking 16 K gene	21	56.0	50.0	463 bp
2.	DJR 16K- (1760) or (2349)	16K CAGTCTATACACAGAAACAGA	6555--6575		20	50.0	38.0	
3.	TRV1H_ fwd (2365)	ACTTGATGCTGACTAAACCTG	282—-302	Helicase gene	21	54.0	43.0	351 bp
4.	TRV1H_ rev (2366)	GATTTGGACAACAGGAATGAAT	611—-632		22	53.0	36.0	
5.	TRV1R_ fwd (2367)	AGTGGAGATGCTGATACTTA	4742--4761	Replicase gene	20	53.8	40.0	474 bp
6.	TRV1R_ rev (2368)	ACTCTTAATATGCTTCCATAGCG	5193--5215		23	54.0	39.0	
7.	TRV1MP_ fwd (2369)	GACTATTCAGAGATTCAAAGC	5669--5689	MP gene	21	50.0	38.0	318 bp
8.	TRV1MP_ rev (2370)	GCCTCAATCGTCTTCATCTC	5967--5986		20	54.0	50.0	
9.	TRV1K1_ fwd (2371)	GAATGAAGTCACTGTTCTTG	6137--6156	Within 16K	20	52.1	40.0	190 bp
10.	TRV1K1_ rev (2372)	TTCAAGGTGACTACGGC	6310--6326		17	53.5	52.9	
11.	TRV1MK_ fwd (2373)	GAGATGAAGACGATTGAGGC	5967--5986	MK spanning	20	54.0	50.0	271bp
12.	TRV1MK_ rev (2374)	CACACCTACGTGTGACACC	6219--6237		19	56.0	58.0	
13.	TRV 3′ end Primer(1759	CCCCGGGCGTAATAACGCTTACGTAGGC	Tobravirus 3′ UTR	Tobravirus 3′ end	28	68.0	61.0	
	Tobravirus 3′ end Universal; Primer No. 2371 and 1759 produce an amplicon (KU) of 655 bp.							
14.	qTRV2f (2357)	CAGTGCTCTTGGTGTGAT	249-----267 CP gene	PpK20 CP gene	18	53.0	50.0	114 bp
15.	qTRV2r (2358)	GTCGTAACCGTTGTGTTTG	344-----362 CP gene		19	53.0	47.0	
16.	PpK-20 (199-F)	CCAACTTCGCCGATTGGTCG	3014--3033		20	60.0	60.0	540 bp
17.	PpK-20 (300-R)	CGAGAATGTCAATCTCGTAGG	3534--3554		21	54.0	48.0	
18.	PKCPFwd (2381)	TCCTGCTGACTTGATGG	42-------58 598-----614	PpK20 CP gene	17	52.8	52.9	574 bp
19.	PKCPrev (2382)	CTAGGGATTAGGACGTATCG	596-----615 1152---1171		20	57.3	50.0	
20.	PpK-CPF	ACGATTCTTGGGTG	615----634	PpK20 CP	20	55.0	45.0	358 bp

	(2432)	GAATCA		gene				
21.	PpK-CPR (2433)	TCTTCCAAAGTCGAGCCAGT	953----972		20	57.0	50.0	
22.	PpK-CPF (2468)	GTTACTAGCGGCACTGAATA	156----175	PpK20 CP gene	20	53.0	45.0	373 bp
23.	PpK-CPR (2469)	TTTCTCAAAGTTCCTTCGGT	509----528		20	53.0	40.0	
24.	K20 CP fwd (2486)	ACTCACGGGCTAACAGTGCT	nt 792		20	60.0	55.0	
25.	PEBV CP (130)	CTCGGTTTGCTGACCTA	460----476	TpA56 CP + 112bp	17	52.0	53.0	751 bp
26.	PEBV CP (1962)	GCCACTCCACTCTCCAT	1194---1210		17	54..0	59.0	
27.	I-6 (130-F)	CTCGGTTTGCTGACCTA	460----476		17	52.0	53.0	450 bp
28.	I-6 (105-R)	GACTCTCTGGGCGGT	896----910		15	53.0	67.0	
29.	I6CP_fwd (2422)	ATGGTGAAAGGAAAGTATGAAG	552----573	I6 CP gene	22.0	52.0	36.0	627 bp
30.	I6CP_rev (2423)	GGGCCTAGTGTGACATGA	1161---1178		18	55.0	56.0	
31.	PaY-4 (238-F)	GGTTAGACCCGTTACCGGTA	1084--1103		20	57.0	55.0	503 bp
32.	PaY-4 (240-R)	AATGAGTGATGCGAACCAC	1569--1587		19	54.0	47.0	
33.	PYCPfwd (2383)	TTGGAGCGATGTCCTTA	78------94	PaY4 CP gene	17	50. 4	47.1	509 bp
34.	PYCPrev (2384)	CTACCGCATTAACACCTG	569----586		18	53.7	50.0	
35.	TpO-1 (398-F)	GGAATATGGACTGAAGTGGG	993---1012		20	53.0	50.0	708 bp
36.	TpO-1 (399-R)	ACAAAGTGAGCGTCCTGAGG	1682--1701		20	58.0	55.0	
37.	TpO-1 CP (1958)	ATGGGTTCGTACGGTGATTC	475---494	Tpo-1 CP	20	56	50	591 bp
38.	TpO-1CP (1959)	TCACACGACCGGTCCCTTA	1047--1065		19.0	59.0	58.0	
39.	SYM (1066-F)	ACGGCTAGTGTTGCTGCTCT	1173-1192		20	60.0	55.0	559 bp
40.	SYM (1065-R)	CACGATATGTTCAGCCACGA	1713-1732		20	56.0	50.0	
41.	SYM CP (1960)	ATGTCTGATGAAATGTACGACG	2232--2253	SYM CP	22	54.0	41.0	650 bp
42.	SYM CP (1961)	AATTACTGTTTGTTAGGCACTGG	2859---2881		23	55.0	39.0	
43.	Sq_RT_Pot.Ef-1 alpha_fwd (2304)	CCACTTCCCACATTGCTGTA	53---72	EF-1α 1Exon	20	56.0	50.0	255 bp
44.	Sq_RT_Pot.Ef-1 alpha _rev (2305)	CTTGTTTATTGGCACCAGTTG	287---307	PGSC0003DMT400008259	21	54.0	43.0	

Appendix 2. Protein extraction buffer for fluorometry and western blotting

S.No.	Buffer	Buffer Conc.
1.	HEPES, pH 7.5 adjusted with KOH	20mM
2.	Sucrose	13%
3.	EDTA	1mM
	Filter sterilize the mixture	
4.	DTT	1mM
5.	Sigma*Fast*™ Proteinase Inhibitor cocktail tablet	1 tablet per 10ml buffer
Total volume		

HEPES: 4-(2-hydroxyethyl)-1-piperazineethanesulfonic acid) is an organic buffer agent with neutral charge and is widely used in the biological studies for maintaining the physiological pH; EDTA: Ethylenediaminetetraacetate is a water-dissolvable colourless powder reagent that has the ability to withdraw the metal ions such as the Ca+2, Mg+2 and the Fe+3 ions from the solutions. Thus suppresses the catalytic activity of the metal ions in the solutions; DTT: Dithiothreitol also known as the Cleland's reagent is a special powerful reducing agent that is mostly used for the reduction of disulphide bonds formed in the proteins.

Appendix 3. Primers for full-length sequencing of I6 RNA-2 (p215)

S. No.	Oligo name & number	Gene annotation & oligo Sequence (5' to 3')	Position on transcript sequence (nts)	Exon Boundary or target	Primer length	Tm (C°)	GC %
1.	M13 F	GTAAAACGACGGCCAGTG	N/A	N/A	18	54.0	56.0
2.	M13 R	GGAAACAGCTATGACCATG	N/A	N/A	19	51.0	47.0
3.	107	GGTTATATTGCAATT	PEBV RNA2 , +ve sense., 2384-2399	To sequence 23K	15	27	36
4.	109	GGTCTGCGATCCACG	PEBV RNA2, +ve sense, 2675-2690	To sequence 23K	15	52	67
5.	110	AAGATATTAGTATGA	PEBV RNA2, +ve sense, 1593-1608.	To sequence 29K	15	31	20
6.	111	ATGATCAAGTTCTAC	PEBV RNA2, +ve sense, 1745-1760	To sequence 29K	15	37	33
7.	112	GAGAATGATTTGTTA	PEBV RNA2, +ve sense, 1895-1910.	To sequence 29K	15	35	27
8.	113	ACTTGTCGGTCAAAG	PEBV RNA2, +ve sense, 2043-2058.	To sequence 29K	15	45	47
9.	114	AGTAAGTTGGCACGTCCT	PEBV RNA2, +ve sense, 2538-2556.	To sequence 23K (replaces oligo 108)	18	54	50
10.	122	GAGAGTGGAGTGGCTACC	PEBV RNA2, 1197-1214. 5' oligo for PCR amplification of (3'RACE)	9K gene from tissue derived RNA	18	54	61
11.	132	CGCAATTGCACAAATTC	SP5 CP, +ve sense, 758-774.	To sequence SP5 CP gene	17	48	41
12.	134	AAGAGACTCCCC	SP5 CP, +ve sense,	To sequence	17	54	59

		AGCAG	1060-1076.	SP5 CP gene			
13.	145	TAGGAGGTGCCC TTTAT	PEBV RNA2, 1393-1409 , +ve sense sequencing primer	To sequence TPA56	17	50	47
14.	150	CAGCGTTGGTAG GTTGG	PEBV RNA2, 2336-2352, +ve sense sequencing primer	To sequence TPA56	17	53	59
15.	228	GCTACTGTGGTT AGACCGCCC	PEBV RNA2, 882-902, +ve sense primer	To sequence TPA56	21	62	61
16.	427	ACATTGTGGCCT AATGATCGGC	PEBV RNA2, 1484-1505, +ve sense primer	To sequence TPA56	22	59	50
17.	648	GAGCATAATTAT ACTGATTT	PEBV RNA2, 393-412 +ve sense sequencing	To sequence TPA56	20	44	25

Appendix 4. Spectrophotometric quantification of total RNA-isolation by large-scale extraction protocol

Sr.No.	TRV NM – type isolate	O.D 260nm	O.D 280nm	R value (O.D 260 nm / O.D 280 nm)	Concentration (µg / µl)	Storage 100 µg / tube
1.	SYM	0.105	0.043	2.442	0.105x40x1000= 4.20 µg / µl	23.80 µl / tube (04 tubes)
2.	PpO-85	0.733	0.712	1.029	0.733x40x1000= 29.0 µg / µl	03.44 µl / tube (13 tubes)
3.	PpK-20	0.199	0.091	2.137	0.199x40x1000= 7.96 µg / µl	12.50 µl / tube (08 tubes)

SYM: Spinach Yellow Mottle; PpO-85: *Paratrichodorus pachydermus* Overloon-85; PpK-20: *Paratrichodorus pachydermus* Kinshalday-20; O.D: Optical density.

Appendix 5. Fluorometric assay of the GFP expressing samples

Sr.No	Well	Sample	AFU	Mean AFU	St. Dev.	Nor. Mean AFU
1.	A1	CB28,1	929.945	928.434	52.771	652.314
2.	B1	CB28,1	926.630			
3.	C1	CB28,2	1010.223			
4.	D1	CB28,2	952.326			
5.	E1	CB28,3	852.234			
6.	F1	CB28,3	899.249			
7.	G1	*N.benth* Mock,1	239.078	276.119	30.570	276.12
8.	H1	*N.benth* Mock,1	253.324			
9.	A2	*N.benth* Mock,2	271.847			
10.	B2	*N.benth* Mock,2	327.876			
11.	C2	*N.benth* Mock,3	284.262			
12.	D2	*N.benth* Mock,3	280.326			

13.	E2	Ext. Buffer,1	110.498	112.434	8.177	112.434
14.	F2	Ext. Buffer,1	118.934			
15.	G2	Ext. Buffer,2	123.743			
16.	H2	Ext. Buffer,2	106.104			
17.	A3	Ext. Buffer,3	101.546			
18.	B3	Ext. Buffer,3	113.779			
19.	C3	S49, 4dpi, 1	1393.714	1362.473	37.942	1086.353
20.	D3	S49, 4dpi, 1	1400.540			
21.	E3	S49, 4dpi, 2	1386.600			
22.	F3	S49, 4dpi, 2	1311.517			
23.	G3	S49, 4dpi, 3	1322.630			
24.	H3	S49, 4dpi, 3	1359.835			
25.	A4	O49, 4dpi, 1	820.127	797.598	21.216	521.478
26.	B4	O49, 4dpi, 1	800.864			
27.	C4	O49, 4dpi, 2	806.160			
28.	D4	O49, 4dpi, 2	815.123			
29.	E4	O49, 4dpi, 3	773.414			
30.	F4	O49, 4dpi, 3	769.900			
31.	G4	K49, 4dpi, 1	1704.784	1741.098	20.029	1464.978
32.	H4	K49, 4dpi, 1	1759.596			
33.	A5	K49, 4dpi, 2	1823.989			
34.	B5	K49, 4dpi, 2	1683.189			
35.	C5	K49, 4dpi, 3	1745.251			
36.	D5	K49, 4dpi, 3	1729.778			
37.	E5	BLANK	48.759	50.027 *	2.097	50.027
38.	F5	BLANK	49.650			
39.	G5	BLANK	48.603			
40.	H5	BLANK	53.095			
41.	A6	S49, 8dpi, 1	966.372	966.124	10.693	690.001
42.	B6	S49, 8dpi, 1	949.05			
43.	C6	S49, 8dpi, 2	969.289			
44.	D6	S49, 8dpi, 2	961.308			
45.	E6	S49, 8dpi, 3	969.185			
46.	F6	S49, 8dpi, 3	981.538			
47.	G6	O49, 8dpi, 1	537.348	523.638	13.104	247.518
48.	H6	O49, 8dpi, 1	502.933			
49.	A7	O49, 8dpi, 2	532.021			
50.	B7	O49, 8dpi, 2	531.721			
51.	C7	O49, 8dpi, 3	524.449			
52.	D7	O49, 8dpi, 3	513.357			

53.	E7	K49, 8dpi, 1	488.706	502.668	24.593	226.548
54.	F7	K49, 8dpi, 1	547.715			
55.	G7	K49, 8dpi, 2	484.734			
56.	H7	K49, 8dpi, 2	482.371			
57.	A8	K49, 8dpi,3	510.762			
58.	B8	K49, 8dpi, 3	501.718			

CB28: Transgenic *N. benthamiana* expressing GFP; AFU: Arbitrary Fluorescence Unit; Nor. Mean AFU: Mean AFU of the test samples normalized with the mean AFU of the mock inoculated *N. benthamiana*; St. Dev.: Standard deviation of means; *N.benth* Mock: Mock inoculated *N.benth*; Ext. Buffer: Extraction Buffer; BLANK: empty well; S49: Inoculated with SYM RNA-1 and capped transcript of GFP engineered RNA-2 of TRV (Cap49T); O49: Inoculated with O-85 RNA-1 and Cap49T; K49: Inoculated with PpK-20 RNA-1 and Cap49T; dpi: days post inoculation; 1, 2, 3: represents the no. of biological replicate from which sample was collected.

Appendix 6. Normalized mean absorbance of the BSA standards

Sr. No.	**Conc. Of BSA STD.** (mg/ml)	**Absorbance (A°) measured at 595 nm wavelength**		**Mean A° 595**	**Nor. Mean A° 595 (Mean A° 595 - Ext. Buffer A° 595)**
		Reading-1	**Reading-2**		
1.	0.2	0.171	0.168	0.169	0.148
2.	0.4	0.328	0.342	0.335	0.314
3.	0.6	0.502	0.493	0.497	0.476
4.	0.8	0.671	0.66	0.665	0.644
5.	0.9	0.737	0.745	0.741	0.72

Conc.: Concentration; STD: Standard; Nor.: Normalized; Ext. Buffer: Extraction Buffer; Nor. Mean A° 595 of the BSA standards was calculated by subtracting the mean A° 595 of the extraction buffer (i.e.; 0.021) from the mean A° 595 of the BSA STD.

Appendix 7. Total proteins quantified in the GFP samples

Sr. No.	**Sample**	**Absorbance (A°) measured at 595 nm wavelength**		**Mean A° 595**	**Nor. Mean A° 595**	**A° 595 difference* (D)**	**Interpol. conc. of sample****	**Gel loading volume (µl)*** for 2.5µg/ well**	**Gel loading dye (µl)**
		R-1	**R-2**						
			BLOT # I						
1.	CS28	0.628	0.632	0.63	0.609	-0.035	0.765	3.27	16.73
2.	Nb.,Mock	0.747	0.735	0.741	0.72	0	0.9	2.78	17.22
3.	PpK20, Ino.	0.713	0.693	0.703	0.682	0.038	0.838	2.98	17.02
4.	S49,Ino,1	0.631	0.638	0.634	0.613	-0.031	0.769	3.25	16.75
5.	S49,Ino,2	0.659	0.652	0.655	0.634	-0.01	0.79	3.16	16.84
6.	S49,Ino,3	0.721	0.771	0.746	0.725	-0.005	0.895	2.79	17.21
7.	O49,Ino,1	0.739	0.711	0.725	0.704	-0.016	0.884	2.83	17.17

8.	O49,Ino,2	0.613	0.625	0.619	0.598	0.122	0.722	3.46	16.54
9.	O49,Ino,3	0.729	0.705	0.717	0.696	0.052	0.852	2.93	17.07
10.	K49,Ino,1	0.699	0.745	0.722	0.701	-0.019	0.881	2.84	17.16
11.	K49,Ino,2	0.737	0.749	0.743	0.722	-0.002	0.898	2.78	17.22
12.	K49,Ino,3	0.719	0.725	0.722	0.701	-0.019	0.881	2.84	17.16
13.	S49,4,1	0.681	0.666	0.673	0.652	-0.008	0.792	3.16	16.84
14.	S49,4,2	0.726	0.714	0.72	0.699	0.055	0.855	2.92	17.08
15.	S49,4,3	0.644	0.698	0.671	0.65	-0.006	0.794	3.15	16.85
16.	O49,4,1	0.532	0.418	0.475	0.454	-0.022	0.578	4.32	15.68
17.	O49,4,2	0.618	0.652	0.635	0.614	-0.03	0.77	3.25	16.75
18.	O49,4,3	0.691	0.717	0.704	0.683	0.039	0.839	2.98	17.02
19.	K49,4,1	0.709	0.683	0.696	0.675	0.031	0.831	3.01	16.99
20.	K49,4,2	0.722	0.714	0.718	0.697	0.053	0.853	2.93	17.07
21.	K49,4,3	0.693	0.721	0.707	0.686	0.042	0.842	2.97	17.03
			BLOT #II						
22.	PpK20,10	0.705	0.713	0.709	0.688	0.044	0.844	2.96	17.04
23.	CS28,	0.695	0.697	0.696	0.675	0.031	0.831	3.01	16.99
24.	S49,6,1	0.714	0.726	0.72	0.699	0.055	0.855	2.92	17.08
25.	S49,6,2	0.589	0.651	0.62	0.599	-0.045	0.755	3.31	16.69
26.	S49,6,3	0.633	0.721	0.677	0.656	0.012	0.812	3.08	16.92
27.	O49,6,1	0.648	0.666	0.657	0.636	-0.008	0.792	3.16	16.84
28.	O49,6,2	0.555	0.569	0.562	0.541	0.065	0.665	3.76	16.24
29.	O49,6,3	0.681	0.743	0.712	0.691	0.047	0.847	2.95	17.05
30.	K49,6,1	0.715	0.723	0.719	0.698	0.054	0.854	2.93	17.07
31.	K49,6,2	0.695	0.637	0.666	0.645	-0.001	0.799	3.13	16.87
32.	K49,6,3	0.489	0.513	0.501	0.48	-0.004	0.596	4.19	15.81
33.	S49,10,1	0.584	0.572	0.578	0.557	0.081	0.681	3.67	16.33
34.	S49,10,2	0.655	0.691	0.673	0.652	-0.008	0.792	3.16	16.84
35.	S49,10,3	0.611	0.637	0.624	0.596	-0.02	0.78	3.2	16.8
36.	O49,10,1	0.674	0.668	0.671	0.65	-0.006	0.794	3.15	16.85
37.	O49,10,2	0.7	0.714	0.707	0.686	0.042	0.842	2.97	17.03
38.	O49,10,3	0.706	0.698	0.702	0.681	0.037	0.837	2.99	17.01
39.	K49,10,1	0.719	0.699	0.709	0.688	0.044	0.844	2.96	17.04
40.	K49,10,2	0.689	0.697	0.693	0.672	0.028	0.828	3.02	16.98
41.	K49,10,3	0.727	0.693	0.71	0.689	0.045	0.845	2.96	17.04

CB28: Transgenic *N. benthamiana* expressing GFP; *N.benth* Mock: Mock inoculated *N.benth*; PpK20: PpK-20 infective sap inoculated plant; R: reading; dpi: days post inoculation; Ino.: represents sample collected from inoculated leaf at 4dpi; 4, 6, 10: represents sample collected from top-systemic leaf at 4, 6, and 10 dpi, respectively; 1, 2, 3: represents the no. of biological replicate from which sample was collected; S49: Inoculated with SYM RNA-1 and capped transcript of GFP engineered RNA-2 of TRV (Cap49T); O49: Inoculated with O-85 RNA-1 and Cap49T; K20: Inoculated with PpK-20 RNA-

1 and Cap49T; * A° 595 Difference (D) between the Nor. Mean A° 595 of test sample and the nearest Nor. Mean A° 595 of the BSA STD. ** Interpolated concentration was calculated by adding or subtracting D from the concentration of the nearest matching A° 595 of BSA standard. *** Gel loading volume (µl) was calculated by dividing standard loading quantity of protein (2.5 µg / ml) with the interpolated concentration of the test-sample.

Appendix 8. Primer(s) for VIGS-related studies

S. No.	Oligo name & number	Gene annotation & oligo sequence (5' to 3')	Position on transcript sequence (nts)	Exon boundary or target	Primer length	Tm (C°)	GC %	Optim. anneal. temp. (C°)	Amplicon size (bp)
	Oligos for amplification of fragment(s) for VIGS								
1.	PDS (463)	TACGCCATGGC(CTTTGATTTCTC GAAGC	51—69 1126--1155	Tomato PDS gene Potato	30	68.0	53.0	65.0	651bp
2.	PDS (464)	CGAGGGTACCT(TGTTCTTCAGTT TCTG	682—701 1747--1775	PDS gene	29	63.0	48.0		
3.	potZeaEpox VIGSF (2296)	GGTGGGATTGG AGGGTTAGT	277—-297	ZEP gene	20	57.0	55.0	62.0	408bp
4.	potZeaEpox VIGSR (2297)	CTTCTCCCCAT CATCCTCAA	664—-684		20	55.0	50.0		
5.	potGBSS VIGSL2 (2298)	CCAAGATGGCA TCCAGAACT	173----193	GBSS gene	20	56.0	50.0	61.0	444bp
6.	potGBSS VIGSR2 (2299)	CCTCTAGGGCT GCTTGACAC	596----616		20	58.0	60.0		
	Oligos for addition of Gateway recombination sequence (½ att sites) into the insert								
7.	ZEP +att (2321)	**AAAAAGCAGG CT**GGTGGGATT GGAGGGTTAGT	1/2 att site added to primer 2296 of Potato ZeaxanthinEpoxidase		32	69.0	50.0	67.0	
8.	ZEP -att (2352)	**AGAAAGCTGG GT**CTTCTCCCC ATCATCCTCAA	1/2 att site added to primer 2297 of Potato ZeaxanthinEpoxidase		32	67.0	50.0		
9.	GBSS +att (2313)	**AAAAAGCAGG CT**CCAAGATGG CATCCAGAACT	1/2 att site added to primer 2298 of Potato Granule bound starch synthase		32	67.0	47.0	67.0	
10.	GBSS -att (2351)	**AGAAAGCTGG GT**CCTCTAGGG CTGCTTGACAC	1/2 att site added to primer 2299 of Potato Granule bound starch synthase		32	69.0	56.0		
	Add 1/2 att sites (in bold letters) to the insert for cloning into the Gateway-vector								
	Oligos for addition of Gateway recombination sequence (Full att sites) into the insert								
11.	+ Full att (1992)	GGGGACAAGTT TGTACAAAAAA	Gateway attB1 full adaptor for 2nd PCR to		29	64.0	45.0	66.0	

		GCAGGCT	add complete att site to new PCR clones						
12.	-Full att (1993)	GGGGACCACTT TGTACAAGAAA GCTGGGT	Gateway attP1 full adaptor for 2nd PCR to add complete att site to new PCR clones		29	66.0	52.0		
	Amplify inserts with ½ att sites for BP cloning into DONR-vectors								
	Oligos for sequencing of pDONR 207 (p0553)								
13.	(1564)	TCGCGTTAACG CTAGCATGGAT CTC	Plus strand (upstream of 5' attP1 site)		25	62.0	52.0		
14.	(1565)	TGTAACATCAG AGATTTTGAGA CAC	Minus strand (down stream of 3' attP2 site)		25	55.0	36.0		
	Used for PCR amplification or DNA-sequencing of insert in pDONR207 (p0553)								
	Oligos for RT-PCR detection of silenced gene								
15.	PDSf(2465)	CAGAAGATTGG TTAAGGACTTG	695--716	Exon 2 to 5	22	52.0	41.0	52.0	313bp
16.	PDSr(2466)	GAATATATGCA AACCAGTCTCG	986---1007		22	53.0	41.0		
	Positioned on potato PDS, PGSC0003DMT400023666, 2,615bp.								
17.	ZEP (2294)	CTTGGGAATGC CTCTGATGT	1855--1874	Exon 9 to 12	20	56.0	50.0	55.0	177bp
18.	ZEP (2295)	CCCGCAGGTAA AAGTAACCA	2012--2031		20	56.5	50.0		
	Positioned on potato ZEP, PGSC0003DMT400010287, 2,881bp.								
19.	GBSS (2302)	GCCCAAGAACT TGTCTCTGC	1040--1059		20	57.0	55.0	55.0	344bp
20.	GBSS (2303)	TTTTTGCCAGTT CCAAGGAC	1364--1383		20	55.0	45.0		
	Positioned on potato GBSS, PGSC0003DMT400031568, 2,244bp								
21.	pTRV2 (2432)	ACGATTCTTGG GTGGAATCA	619----638	PpK20 CP	20	55.0	45.0	55.0	1180bp
22.	pTRV2 (300)	CGAGAATGTCA ATCTCGTAGG	1778--1798		21	54.0	48.0		
	pTRV2 (Liu et al;2002);VIGS TRV-destination vector								
	Oligos for qPCR								
23.	qPDSf (2459)	CAGAAGATTGG TTAAGGACTTG	695--716	Exon 2 to 3	22	52.0	41.0	59.0	80bp
24.	qPDSr (2460)	TAACTGTATTG TCTAGCTCTGG	753--774		22	53.0	41.0	59.0	
	Positioned on potato PDS, PGSC0003DMT400023666, 2,615bp.								
25.	qZEPf (2461)	CTTCTGGTTGG TGCTGAT	1127--1145	4th Exon	18	53.0	50.0	59.0	99bp
26.	qZEPr (2462)	CCAGTATAACA AGTGTAGCCA	1201--1222		21	53.0	43.0		
	Positioned on potato ZEP, PGSC0003DMT400010287, 2,881bp.								
27.	qGBSf	CATTGATGGAT	940--961	Exon	21	52.0	43.0	59.0	88bp

	(2463)	ATGAGAAGCC		8 to 9					
28.	qGBSr (2464)	CACTGTAACCA CCCTATGT	1009--1028		19	52.0	47.0	59.0	
	Positioned on Potato GBSS, PGSC0003DMT400031568, 2,244bp								

Appendix 9. Agro-infiltration buffers

S.No.	Reagents	Quantity or Volume
1.	**1M MES-buffer, 50ml, pH5**	
	2-(*N*-morpholino) ethanesulfonic acid (MES),$C_6H_{13}NO_4.S.XH_2O$	9.76g
	The MES (9.76g) was dissolved in 40ml H_2O. The pH was adjusted to 5 using the MES sodium salt or NaOH. The volume was made-up to 50ml with H_2O and the solution was filter-sterilized through 0.2µM filters.	
2.	**0.1M Acetosyringone, 10ml**	
	3,5-Dimethoxy-4-hydroxyacetophenon, 97%, $C_{10}H_{12}O_4$	196.20mg
	The Acetosyringone (196.20mg) was dissolved in 10ml H_2O and filter-sterilized through through 0.2µM filters.	
3.	**1M $MgCl_2$ Solution, 50ml**	
	The Magnesium chloride hexahydrate ($MgCl_2$.6 H_2O, Formula weight 203.3, 10.165 g) was dissolved at room temperature in distilled H_2O to make 50ml of the solution.	

Appendix 10. Melt-curve (I) and standard-curve (II) analysis of the primer-set for the (a) PDS, (b) ZEP, and (c) GBSS genes of potato.

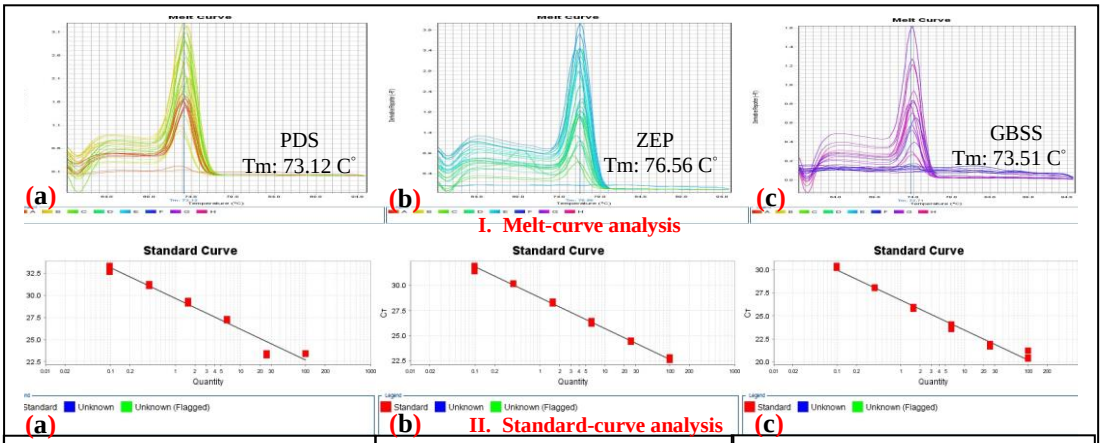

Target: PDS; Slope: -3.478 Y-inter: 29.62; R^2: 0.962 EFF % : 93.856	Target: ZEP; Slope: -3.073 Y-inter: 28.80; R^2: 0.998 EFF % : 111.566	Target: GBSS; Slope: -3.26 Y-inter: 26.71; R^2: 0.989 EFF % : 102.673

Y-inter: Y-intercept; R2: correlation coefficient or regression line coefficient; EFF %: amplification efficiency.

Appendix 11. Extraction-buffer for the total RNA isolation from potato-tubers

S.No.	Buffer	Stock Conc.	Buffer Conc.	Dilution	For 50ml	For 100ml
1.	Tris. HCL, pH 8.0	1M	0.05M	1:20	2.5 ml	5.0 ml
2.	LiCl	4M	0.05M	1:80	0.625 ml	1.25 ml
3.	EDTA	0.5M	0.005M	1:100	0.5 ml	1.0 ml
4.	SDS	20% (w/v)	0.5% (v/v)	1:40	1.25 ml	2.5 ml
5.	SDW				20.125 ml	40.25 ml
6.	**Phenol, pH 4.5**				25 ml	50 ml
Total volume					**50 ml**	**100 ml**

Appendix 12. NanoDrop quantification of column-purified total RNA extractions before DNase treatment

S.No.	RNA Sample	230 nm Absorbance	260 nm Absorbance (10 nm path)	280 nm Absorbance (10 nm path)	260/280 ratio	260/230 ratio	Concentration (ng / µl)
1.	S1	10.779	20.589	10.310	2.00	1.91	823.6
2.	SF1	8.550	16.587	8.119	2.04	1.94	663.5
3.	H1	6.800	13.464	6.633	2.03	1.98	538.6
4.	S2	10.652	22.683	10.847	2.09	2.13	907.3
5.	SF1	6.652	13.907	6.702	2.07	2.09	556.3
6.	H2	4.681	11.217	5.406	2.07	2.40	448.7
7.	S3	11.238	24.335	11.431	2.13	2.17	973.4
8.	SF3	9.967	18.848	9.079	2.08	1.89	753.9
9.	H3	7.314	16.103	7.646	2.11	2.20	644.1
10.	S4	3.889	8.400	4.077	2.07	2.17	336.8
11.	SF4	4.901	11.240	5.606	2.00	2.29	449.6
12.	H4	7.979	17.328	8.187	2.12	2.17	693.1
13.	S4 Rep.	9.290	23.617	11.179	2.11	2.54	944.7

S1-S4: Spraing affected tuber-tissue; SF1-SF4: Spraing-free tuber-tissue; H1-H4: Healthy tuber-tissue; S4 Rep.:Re-extracted total RNA from S4

Appendix 13. NanoDrop quantification of column-purified total RNA extractions after DNase treatment

S.No.	RNA Sample	230 nm Absorbance	260 nm Absorbance (10 nm path)	280 nm Absorbance (10 nm path)	260/280 ratio	260/230 ratio	Concentration (ng / µl)
1.	S1	6.915	15.454	6.990	2.21	2.23	165
2.	SF1	8.185	17.996	8.203	2.19	2.20	155
3.	H1	7.749	16.962	7.673	2.21	2.19	143
4.	S2	8.013	17.413	7.878	2.21	2.17	182
5.	SF1	6.652	13.907	6.70	2.07	2.09	150
6.	H2	8.07	18.021	8.162	2.21	2.23	187
7.	S3	9.290	23.617	11.179	2.11	2.54	174
8.	SF3	9.967	18.848	9.079	2.08	1.89	161
9.	H3	4.948	11.005	5.555	1.98	2.22	136
10.	S4	12.074	20.589	10.310	2.00	1.71	159
11.	SF4	4.901	11.240	5.606	2.00	2.29	173
12.	H4	4.681	11.217	5.406	2.07	2.40	184
13.	S4 Rep.	9.640	23.530	11.165	2.11	2.44	186

S1-S4: Spraing-affected tuber-tissue; SF1-SF4: Spraing-free tuber-tissue; H1-H4: Healthy tuber-tissue; S4 Rep.: Re-extracted total RNA from S

Appendix 14. Selected gene ontologies showing gene enrichment from spraing vs. spraing-free volcano plot.

S.No.	Category	Genes in Category	% of Genes in Category	Genes in List in Category	% of Genes in List in Category	p-Value
1.	GO:6869: lipid transport	83	0.553	14	3.333	6.57E-08
2.	GO:16998: cell wall catabolism	44	0.293	8	1.905	2.56E-05
3.	GO:6575: amino acid derivative metabolism	220	1.465	18	4.286	4.78E-05
4.	GO:50896: response to stimulus	1197	7.97	56	13.33	9.30E-05
5.	GO:19439: aromatic compound catabolism	28	0.186	6	1.429	0.000103
6.	GO:6118: electron transport	995	6.625	48	11.43	0.00015
7.	GO:9698: phenyl propanoid metabolism	143	0.952	13	3.095	0.000189
8.	GO:9808: lignin metabolism	92	0.613	10	2.381	0.000245

9.	GO:6040: amino sugar metabolism	34	0.226	6	1.429	0.000319
10.	GO:6041: glucosamine metabolism	34	0.226	6	1.429	0.000319
11.	GO:6043: glucosamine catabolism	34	0.226	6	1.429	0.000319
12.	GO:6046: N-acetyl glucosamine catabolism	34	0.226	6	1.429	0.000319
13.	GO:6032: chitin catabolism	34	0.226	6	1.429	0.000319
14.	GO:6044: N-acetyl glucosamine metabolism	34	0.226	6	1.429	0.000319
15.	GO:6030: chitin metabolism	34	0.226	6	1.429	0.000319
16.	GO:46348: amino sugar catabolism	34	0.226	6	1.429	0.000319
17.	GO:6725: aromatic compound metabolism	312	2.077	20	4.762	0.000512
18.	GO:42398: amino acid derivative biosynthesis	160	1.065	13	3.095	0.000564
19.	GO:46271: phenyl propanoid catabolism	8	0.0533	3	0.714	0.00109
20.	GO:46274: lignin catabolism	8	0.0533	3	0.714	0.00109
21.	GO:6952: defense response	488	3.249	26	6.19	0.00131
22.	GO:6468: protein amino acid phosphorylation	1192	7.937	51	12.14	0.0015
23.	GO:44247: cellular polysaccharide catabolism	47	0.313	6	1.429	0.00188
24.	GO:6979: response to oxidative stress	161	1.072	12	2.857	0.00191
25.	GO:9607: response to biotic stimulus	512	3.409	26	6.19	0.00255
26.	GO:42744: hydrogen peroxide catabolism	37	0.246	5	1.19	0.00348
27.	GO:42743: hydrogen peroxide metabolism	37	0.246	5	1.19	0.00348
28.	GO:9734: auxin mediated signalling	38	0.253	5	1.19	0.00392

	pathway					
29.	GO:19748: secondary metabolism	225	1.498	14	3.333	0.00445
30.	GO:42221: response to chemical stimulus	402	2.677	21	5	0.00465
31.	GO:6950: response to stress	482	3.209	24	5.714	0.00469
32.	GO:272: polysaccharide catabolism	58	0.386	6	1.429	0.00547
33.	GO:42219: amino acid derivative catabolism	14	0.0932	3	0.714	0.00628
34.	GO:6558: L-phenylalanine metabolism	27	0.18	4	0.952	0.00635
35.	GO:9699: phenyl propanoid biosynthesis	99	0.659	8	1.905	0.00653
36.	GO:6800: oxygen and reactive oxygen species metabolism	189	1.258	12	2.857	0.00697
37.	GO:6730: one-carbon compound metabolism	29	0.193	4	0.952	0.00823
38.	GO:9809: lignin biosynthesis	83	0.553	7	1.667	0.00852
39.	GO:9628: response to abiotic stimulus	507	3.376	24	5.714	0.00859
40.	GO:19438: aromatic compound biosynthesis	171	1.139	11	2.619	0.00872
41.	GO:16310: phosphorylation	1342	8.935	52	12.38	0.00988
42.	GO:9755: hormone-mediated signalling	86	0.573	7	1.667	0.0103
43.	GO:42542: response to hydrogen peroxide	48	0.32	5	1.19	0.0107
44.	GO:302: response to reactive oxygen species	50	0.333	5	1.19	0.0126
45.	GO:9733: response to auxin stimulus	50	0.333	5	1.19	0.0126
46.	GO:9074: aromatic amino acid family catabolism	19	0.127	3	0.714	0.0151
47.	GO:6559: L-phenylalanine	19	0.127	3	0.714	0.0151

	catabolism					
48.	GO:42446: hormone biosynthesis	35	0.233	4	0.952	0.0159
49.	GO:45449: regulation of transcription	1423	9.475	53	12.62	0.0188
50.	GO:19219: regulation of nucleobase, nucleoside, nucleotide and nucleic acid metabolism	1426	9.495	53	12.62	0.0195
51.	GO:19953: sexual reproduction	8	0.0533	2	0.476	0.0195
52.	GO:19222: regulation of metabolism	1494	9.947	55	13.1	0.0206
53.	GO:42445: hormone metabolism	40	0.266	4	0.952	0.0249
54.	GO:9664: cell wall organization and biogenesis (sensu Magnoliophyta)	23	0.153	3	0.714	0.0254
55.	GO:50791: regulation of physiological process	1577	10.5	57	13.57	0.0256
56.	GO:3: reproduction	81	0.539	6	1.429	0.0258
57.	GO:9627: systemic acquired resistance	1	0.00666	1	0.238	0.028
58.	GO:44248: cellular catabolism	540	3.595	23	5.476	0.0302
59.	GO:31323: regulation of cellular metabolism	1465	9.754	53	12.62	0.0305
60.	GO:6793: phosphorus metabolism	1436	9.561	52	12.38	0.0315
61.	GO:6796: phosphate metabolism	1436	9.561	52	12.38	0.0315
62.	GO:9693: ethylene biosynthesis	27	0.18	3	0.714	0.0387
63.	GO:9692: ethylene metabolism	27	0.18	3	0.714	0.0387
64.	GO:51244: regulation of cellular physiological process	1552	10.33	55	13.1	0.0388
65.	GO:6091: generation of precursor metabolites and energy	1427	9.501	51	12.14	0.0403
66.	GO:50794: regulation	1556	10.36	55	13.1	0.0405

	of cellular process					
67.	GO:42828: response to pathogen	47	0.313	4	0.952	0.0418
68.	GO:9072: aromatic amino acid family metabolism	91	0.606	6	1.429	0.0421

Biotic and abiotic stress-related categories are highlighted.

Appendix 15. Selected gene ontologies showing gene enrichment from spraing-free vs. healthy volcano plot.

S.No.	Category	Genes in Category	% of Genes in Category	Genes in List in Category	% of Genes in List in Category	p-Value
1.	GO:19684: photosynthesis, light reaction	83	0.553	11	3.143	3.39E-06
2.	GO:15979: photosynthesis	217	1.445	17	4.857	1.35E-05
3.	GO:9765: photosynthesis light harvesting	66	0.439	9	2.571	2.10E-05
4.	GO:7165: signal transduction	502	3.342	24	6.857	0.000726
5.	GO:19222: regulation of metabolism	1494	9.947	52	14.86	0.00211
6.	GO:50789: regulation of biological process	1715	11.42	58	16.57	0.00222
7.	GO:31323: regulation of cellular metabolism	1465	9.754	51	14.57	0.00232
8.	GO:6791: sulfur utilization	12	0.0799	3	0.857	0.00236
9.	GO:50794: regulation of cellular process	1556	10.36	53	15.14	0.00301
10.	GO:19419: sulfate reduction	4	0.0266	2	0.571	0.00315
11.	GO:19421: sulfate reduction, APS pathway	4	0.0266	2	0.571	0.00315
12.	GO:7154: cell communication	567	3.775	24	6.857	0.00364
13.	GO:19219: regulation of nucleobase, nucleoside, nucleotide and nucleic acid metabolism	1426	9.495	49	14	0.00367

14.	GO:45449: regulation of transcription	1423	9.475	48	13.71	0.00573
15.	GO:50791: regulation of physiological process	1577	10.5	52	14.86	0.00631
16.	GO:45454: cell redox homeostasis	146	0.972	9	2.571	0.00724
17.	GO:51244: regulation of cellular physiological process	1552	10.33	51	14.57	0.00729
18.	GO:6350: transcription	1524	10.15	50	14.29	0.00811
19.	GO:4: biological process unknown	1200	7.99	41	11.71	0.00855
20.	GO:42549: photosystem II stabilization	7	0.0466	2	0.571	0.0105
21.	GO:18106: peptidyl-histidine phosphorylation	39	0.26	4	1.143	0.0125
22.	GO:19725: cell homeostasis	160	1.065	9	2.571	0.0128
23.	GO:6979: response to oxidative stress	161	1.072	9	2.571	0.0132
24.	GO:9966: regulation of signal transduction	8	0.0533	2	0.571	0.0138
25.	GO:18202: peptidyl-histidine modification	41	0.273	4	1.143	0.0149
26.	GO:43467: regulation of generation of precursor metabolites and energy	9	0.0599	2	0.571	0.0175
27.	GO:42548: regulation of photosynthesis, light reaction	9	0.0599	2	0.571	0.0175
28.	GO:10109: regulation of photosynthesis	9	0.0599	2	0.571	0.0175
29.	GO:6355: regulation of transcription, DNA-dependent	934	6.219	32	9.143	0.0186
30.	GO:51052: regulation of DNA metabolism	1	0.00666	1	0.286	0.0233
31.	GO:6275: regulation of DNA replication	1	0.00666	1	0.286	0.0233
32.	GO:9627: systemic acquired resistance	1	0.00666	1	0.286	0.0233
33.	GO:42592:	179	1.192	9	2.571	0.0246

	homeostasis					
34.	GO:6351: transcription, DNA-dependent	958	6.379	32	9.143	0.0255
35.	GO:7200: G-protein signaling, coupled to IP3 second messenger (phospholipase C activating)	29	0.193	3	0.857	0.0293
36.	GO:7205: protein kinase C activation	29	0.193	3	0.857	0.0293
37.	GO:19932: second-messenger-mediated signaling	30	0.2	3	0.857	0.032
38.	GO:48015: phosphoinositide-mediated signaling	30	0.2	3	0.857	0.032
39.	GO:6800: oxygen and reactive oxygen species metabolism	189	1.258	9	2.571	0.0332
40.	GO:6108: malate metabolism	31	0.206	3	0.857	0.0348
41.	GO:30259: lipid glycosylation	13	0.0866	2	0.571	0.0357
42.	GO:30258: lipid modification	14	0.0932	2	0.571	0.041
43.	GO:6869: lipid transport	83	0.553	5	1.429	0.0444
44.	GO:18193: peptidyl-amino acid modification	58	0.386	4	1.143	0.046
45.	GO:9245: lipid A biosynthesis	2	0.0133	1	0.286	0.0461
46.	GO:46493: lipid A metabolism	2	0.0133	1	0.286	0.0461
47.	GO:9615: response to virus	2	0.0133	1	0.286	0.0461

Biotic and abiotic stress-related categories are highlighted.

Appendix 16. List of genes in GO: 42828 (Response to pathogen)

S.No.	Microarray probe ID	PGSC transcript ID	Gene annotation	Fold-change of expression from microarray	
				SF vs. H	S vs. SF
1.	MICRO.3309.C2_1096	PGSC0003DMT400071827	Unnamed protein product [*Arabidopsis thaliana*]	----	76.2
2.	MICRO.16756.C1_515	PGSC0003DMT400013860	Unknown protein [*Arabidopsis thaliana*]	----	26.1
3.	MICRO.10309.C2_1776	PGSC0003DMT400039281	4-coumarate-CoA ligase/ fatty-acyl-CoA synthase [*Arabidopsis thaliana*]	----	17.1
4.	SDBN002J05u.scf_220	PGSC0003DMT400046161	SAR8.2 protein precursor [*Capsicum annuum*]	2.7	12.2

PGSC: Potato Gene Sequencing Consortium; S: Spraing; SF: Spraing-free; H: Healthy; (----): not determined.

Appendix 17. List of genes in GO: 302 (Response to reactive oxygen species)

S.No.	Microarray probe ID	PGSC transcript ID	Gene annotation	Fold-change of expression from microarray	
				SF vs. H	S vs. SF
1.	MICRO.14166.C1_1246	PGSC0003DMT400001375	peroxidase [*Arabidopsis thaliana*]	----	4.8
2.	MICRO.3508.C7_686	PGSC0003DMT400057522	Suberization-associated anionic peroxidase precursor (POPA)	----	9.6
3.	MICRO.14166.C2_1271	PGSC0003DMT400001375	peroxidase [*Arabidopsis thaliana*]	----	4.4
4.	MICRO.3508.C1_978	PGSC0003DMT400057521	Suberization-associated anionic peroxidase 2 precursor (TMP2)	----	36.1
5.	MICRO.3508.C3_976	PGSC0003DMT400057521	Suberization-associated anionic peroxidase 2 precursor (TMP2)	----	48.7

PGSC: Potato Gene Sequencing Consortium; S: Spraing; SF: Spraing-free; H: Healthy; (----): not determined.

Appendix 18. List of genes in GO: 6952 (Defense response)

S.No.	Microarray probe ID	PGSC transcript ID	Gene annotation	Fold-change of expression from microarray	
				SF Vs. H	S Vs. SF
1.	MICRO.13961.C1_665	PGSC0003DMT400011604	Pathogenesis-related protein STH-21	0	256.5
2.	MICRO.3309.C2_1096	PGSC0003DMT400071827	Unnamed protein product [*Arabidopsis thaliana*]	0	76.2
3.	MICRO.1770.C4_547	PGSC0003DMT400073771	Similar to pathogenesis-related protein STH-2 [*Solanum lycopersicum*]	0	69.3
4.	MICRO.1770.C3_645	PGSC0003DMT400093880	TSI-1 protein [*Solanum lycopersicum*]	2.3	59.8
5.	MICRO.8733.C3_797	PGSC0003DMT400041449	Major latex-like protein [*Prunus persica*]	0	49.4
6.	bf_acdcxxxx_0042g01.t3m.scf_532	PGSC0003DMT400003936	TSI-1 protein [*Solanum lycopersicum*]	2.3	31.0
7.	MICRO.16756.C1_515	PGSC0003DMT400013860	Unknown protein [*Arabidopsis thaliana*]	0	26.1
8.	MICRO.665.C1_374	PGSC0003DMT400004791	Nonspecific lipid-transfer protein 1 precursor (LTP 1) (Pathogenesis-related protein 14) (PR-14)	0	17.1
9.	MICRO.10309.C2_1776	PGSC0003DMT400039281	4-coumarate-CoA ligase/ fatty-acyl-CoA synthase [*Arabidopsis thaliana*]	0	17.1
10.	MICRO.4230.C1_823	PGSC0003DMT400000011	Acidic 27 kDa endochitinase precursor	0	16.4
11.	SDBN002J05u.scf_220	PGSC0003DMT400046161	SAR8.2 protein precursor [*Capsicum annuum*]	2.7	12.2
12.	MICRO.592.C9_743	PGSC0003DMT400005546	Probable glutathione S-transferase (Pathogenesis-related protein 1)	0	10.3
13.	MICRO.11296.C1_1048	PGSC0003DMT400050016	Wound-induced protein WIN2 precursor	0	8.2
14.	MICRO.2909.C4_1666	PGSC0003DMT400076209	Pleiotropic drug resistance protein 1 (NpPDR1)	0	7.1
15.	MICRO.12677.C1_586	PGSC0003DMT400075885	Putative disease resistance protein, identical [*Solanum tuberosum*]	0	5.1
16.	MICRO.11103.C1_970	PGSC0003DMT400007611	RGC1 [*Solanum tuberosum*]	0	3.9
17.	SSBN002P12u.scf_502	PGSC0003DMT400083472	bacterial spot disease resistance protein 4 [*Lycopersicon esculentum*]	0	3.5
18.	SSBN003C03u.scf_372	PGSC0003DMT400024927	TMV resistance protein N, putative [*Solanum demissum*]	0	3.3
19.	STDB005N18u	PGSC0003DMT	NB-ARC domain containing protein	0	3.2

	.scf_1	400092338	[*Solanum demissum*]		
20.	STMHX57TV_614	PGSC0003DMT400083267	late blight resistance protein-like [*Solanum tuberosum*]	0	3.1
21.	bf_arrayxxx_0047d07.t7m.scf_567	PGSC0003DMT400075747	Hero resistance protein 2 homologue [*Solanum lycopersicum*]	0	2.7
22.	STMCK68TV_327	PGSC0003DMT400078333	disease resistance protein BS2 [*Capsicum chacoense*]	0	2.3
23.	bf_ivrootxx_0014f05.t3m.scf_416	PGSC0003DMT400083276	TMV resistance protein N, putative [*Solanum demissum*]	0	2.2
24.	MICRO.7950.C1_1005	PGSC0003DMT400041041	NBS-LRR protein [*Solanum acaule*]	2.7	2.2
25.	bf_mxlfxxxx_0010f06.t3m.scf_257	PGSC0003DMT400080822	bacterial spot disease resistance protein 4 [*Lycopersicon esculentum*]	0	2.0
26.	bf_suspxxxx_0008G12.t3m.scf_624	PGSC0003DMT400056338	NL27 [*Solanum tuberosum*]	0	2.0

PGSC: Potato Gene Sequencing Consortium; S: Spraing; SF: Spraing-free; H: Healthy; (----): not determined.

Appendix 19. List of genes in GO: 8219 (cell-death)

S.No.	Microarray probe ID	PGSC transcript ID	Gene annotation	Fold-change of expression from microarray	
				SF vs. H	S vs. SF
1.	MICRO.3309.C2_1096	PGSC0003DMT400071827	Unnamed protein product [*Arabidopsis thaliana*]	0	76.2
2.	STDB005N18u.scf_1	PGSC0003DMT400092338	NB-ARC domain containing protein [*Solanum demissum*]	0	3.2
3.	STMCK68TV_327	PGSC0003DMT400078333	Disease resistance protein BS2 [*Capsicum chacoense*]	0	2.3
4.	bf_ivrootxx_0014f05.t3m.scf_416	PGSC0003DMT400083276	TMV resistance protein N, putative [*Solanum demissum*]	0	2.2
5.	bf_suspxxxx_0008G12.t3m.scf_624	PGSC0003DMT400056338	Disease resistance protein N (NL27 [*Solanum tuberosum*].	0	2.0
6.	bf_arrayxxx_0047d07.t7m.scf_567	PGSC0003DMT400075747	Hero resistance protein 2 homologue [*Solanum lycopersicum*]	0	2.7
7.	MICRO.12677.C1_586	PGSC0003DMT400075885	Putative disease resistance protein, identical [*Solanum tuberosum*].	0	5.1

8.	SSBN003C03u.scf_372	PGSC0003DMT400024927	TMV resistance protein N, putative [*Solanum demissum*]	0	3.3
9.	MICRO.11103.C1_970	PGSC0003DMT400007611	RGC1 [*Solanum tuberosum*]	0	3.9
10.	SSBN002P12u.scf_502	PGSC0003DMT400083472	Bacterial spot disease resistance protein 4 [*Lycopersicon esculentum*]	0	3.5
11.	STMHX57TV_614	PGSC0003DMT400083267	Bacterial spot disease resistance protein 4 [*Lycopersicon esculentum*] (Late blight resistance protein-like [*Solanum tuberosum*])	0	3.1
12.	MICRO.7950.C1_1005	PGSC0003DMT400041041	NBS-LRR protein [*Solanum acaule*]	2.7	2.0
13.	bf_mxlfxxxx_0010f06.t3m.scf_257	PGSC0003DMT400080822	Bacterial spot disease resistance protein 4 [*Lycopersicon esculentum*]	0	2.0

PGSC: Potato Gene Sequencing Consortium; S: Spraing; SF: Spraing-free; H: Healthy; (----): not determined.

Appendix 20. PAR-1c gene expression in spraing-tubers

S.No.	Microarray probe ID	PGSC transcript ID	Gene annotation	Fold-change of expression from microarray	
				SF vs. H	S vs. SF
1.	POAD763TV_514	PGSC0003DMT400037234	PAR-1c [*Nicotiana tabacum*]	----	171.5
2.	MICRO.1833.C1_689	PGSC0003DMT400037209	PAR-1c [*Nicotiana tabacum*]	----	393.5
3.	POAD763TP_860	PGSC0003DMT400037234	PAR-1c [*Nicotiana tabacum*]	----	18.5

PGSC: Potato Gene Sequencing Consortium; S: Spraing; SF: Spraing-free; H: Healthy; (----): not determined.

Appendix 21. SAR associated gene expression in spraing-tubers

S.No.	Microarray probe ID	PGSC transcript ID	Gene annotation	Fold-change of expression from microarray	
				SF vs. H	S vs. SF
1.	STMJH65TV_362	PGSC0003DMT400032096	1-aminocyclopropane-1-carboxylate synthase [*Lycopersicon esculentum*]	----	9.5
2.	BPLI16E1TH_626	PGSC0003DMT400036081	1-aminocyclopropane-1-carboxylate oxidase 2 (ACC oxidase 2) (Ethylene-forming enzyme) (EFE) (Protein GTOMA)	----	8.3
3.	MICRO.9261.C1_716	PGSC0003DMT400032096	1-aminocyclopropane-1-carboxylate synthase [*Lycopersicon esculentum*]	----	7.6
4.	SDBN002J05u.scf_220	PGSC0003DMT400046161	SAR8.2 protein precursor [*Capsicum annuum*]	2.7	12.2

PGSC: Potato Gene Sequencing Consortium; S: Spraing; SF: Spraing-free; H: Healthy; (----): not determined.

Appendix 22. Primers for the qRT-PCR validation of the microarray data.

S. No.	Oligo name & number	Gene annotation & oligo sequence 5' to 3'	Position on transcript sequence (nts)	Exon boundary or target	Primer length	Tm (C°)	GC %	Optim. anneal. temp. (C°)	Amplicon size (bp)
1.	qEf-1_fwd1 (2323)	Elongation factor 1-alpha TTTGCTGTGAGAGACATGAGGA	232----253	1 exon	22	59.3	45.4	59.0	80bp
2.	qEf-1_rev1 (2324)	Elongation factor 1-alpha GTTGGCACCAGTTGTATCTTGTTTA	311---287		25	58.9	40.0		
3.	qPER_fwd (2329)	Peroxidase TGTGGTGAACTCTGCTATT	178---196	1 to 2	19	59.0	42.1	59.0	96bp
4.	qPER_rev (2330)	Peroxidase GATCCATCGCATCCATTAAC	254---273		20	59.0	45.0		
5.	qPAR_fwd (2331)	PAR-1c protein GCTTGAGTCTCGCTTTACTA	391---410	2 to 3	20	59.0	45.0	59.0	106bp
6.	qPAR_rev (2332)	PAR-1c protein ATATACACCTTCACCAGCAG	477---496		20	59.0	45.0		
7.	qSP_fwd (2335)	Suberization associated anionic	1035---1054	3rd Exon	20	59.0	55.0	59.0	95bp

		peroxidase 2 GATGGGGAACTTGCCTACCT							
8.	qSp_rev (2336)	Suberization associated anionic peroxidase 2 CCTTTCACATAGATGCCACAGA	1129---1108		22	58.1	45.4		
9.	qGST_fwd (2343)	Glutathione-S-transferase AGGAGAGGAACAAGAGAAAGCA	342------363	1 to 2	22	59.0	45.45	59.0	148bp
10.	qGST_rev (2344)	Glutathione-S-transferase AACTCCAAGCCAAATTGCCA	470-----489		20	58.5	45.00		
11.	qRBO_fwd (2345)	Respiratory burst oxidase homolog CTCTTAGTGCTTCTGCAAATAA	750-----772	4 to 5	22	59.0	36.4	57.0	116bp
12.	qRBO_rev (2346)	Respiratory burst oxidase homolog GTTGTACAGCTCAATGTATCC	845-----865		21	59.0	42.9		
13.	qTRV1_fwd (2353)	Tobacco Rattle Virus, RNA-1 TACCAAGGGAATGTGTTCTA	919---938	Replicase	20	58.0	40.0	59.0	89bp
14.	qTRV1_rev (2354)	Tobacco Rattle Virus , RNA-1 CTCGGAACTCCAGCTATC	990---1007		18	58.0	55.6		
15.	qTRV2_fwd (2357)	Tobacco Rattle Virus, RNA-2 CAGTGCTCTTGGTGTGAT	249------267	CP	18	59.0	50.0	59.0	114bp
16.	qTRV2_rev (2358)	Tobacco Rattle Virus, RNA-2 GTCGTAACCGTTGTGTTTG	344--------362		19	59.0	47.4		

Appendix 23. Melt-curve (a) and standard-curve (b) analysis of the primer-set for the PER, PAR-1c, SP, GST, RBO, TRV1 and Ef-1 α genes of potato.

(a) Melt-curve analysis

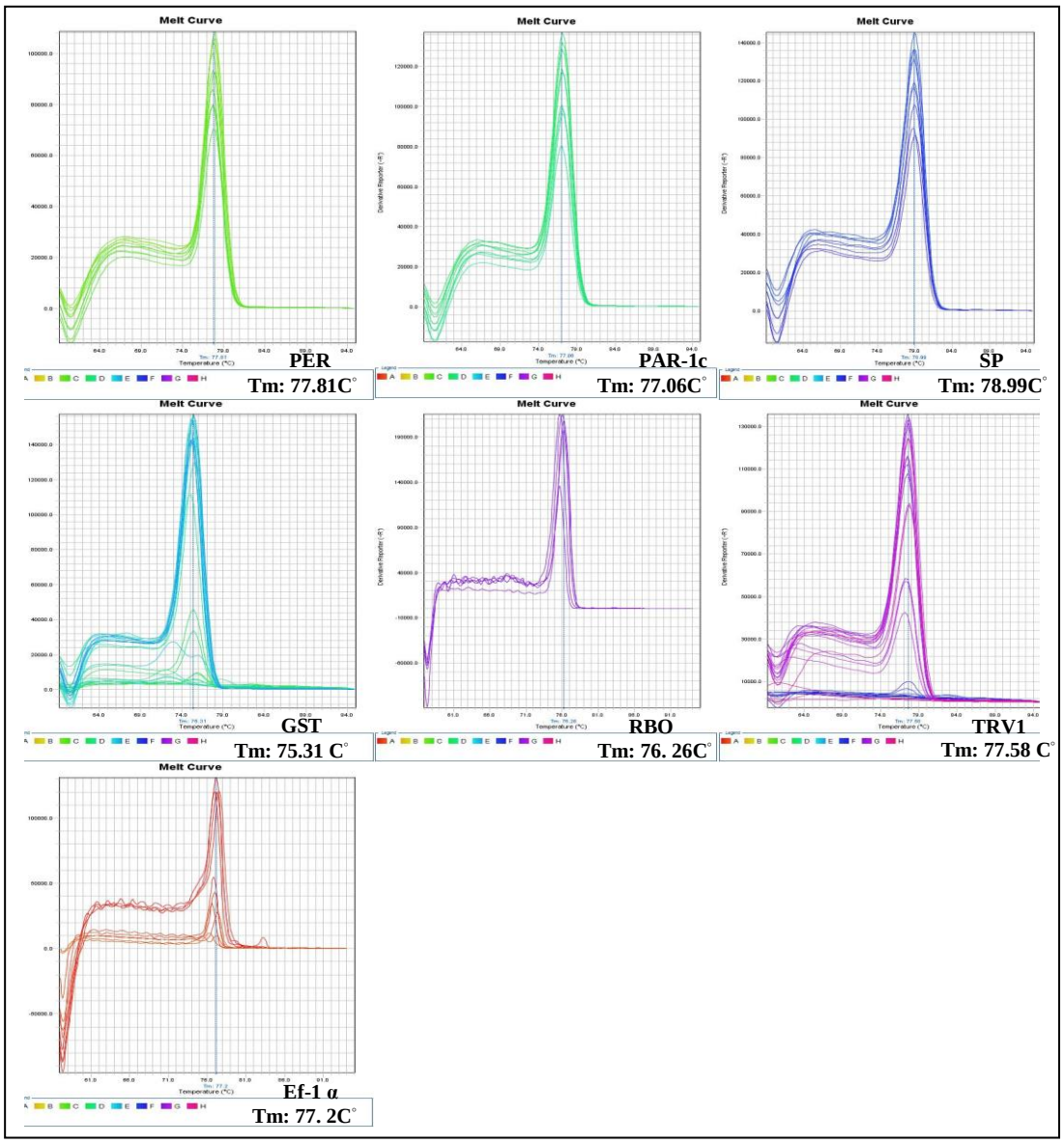

(b) Standard-curve analysis

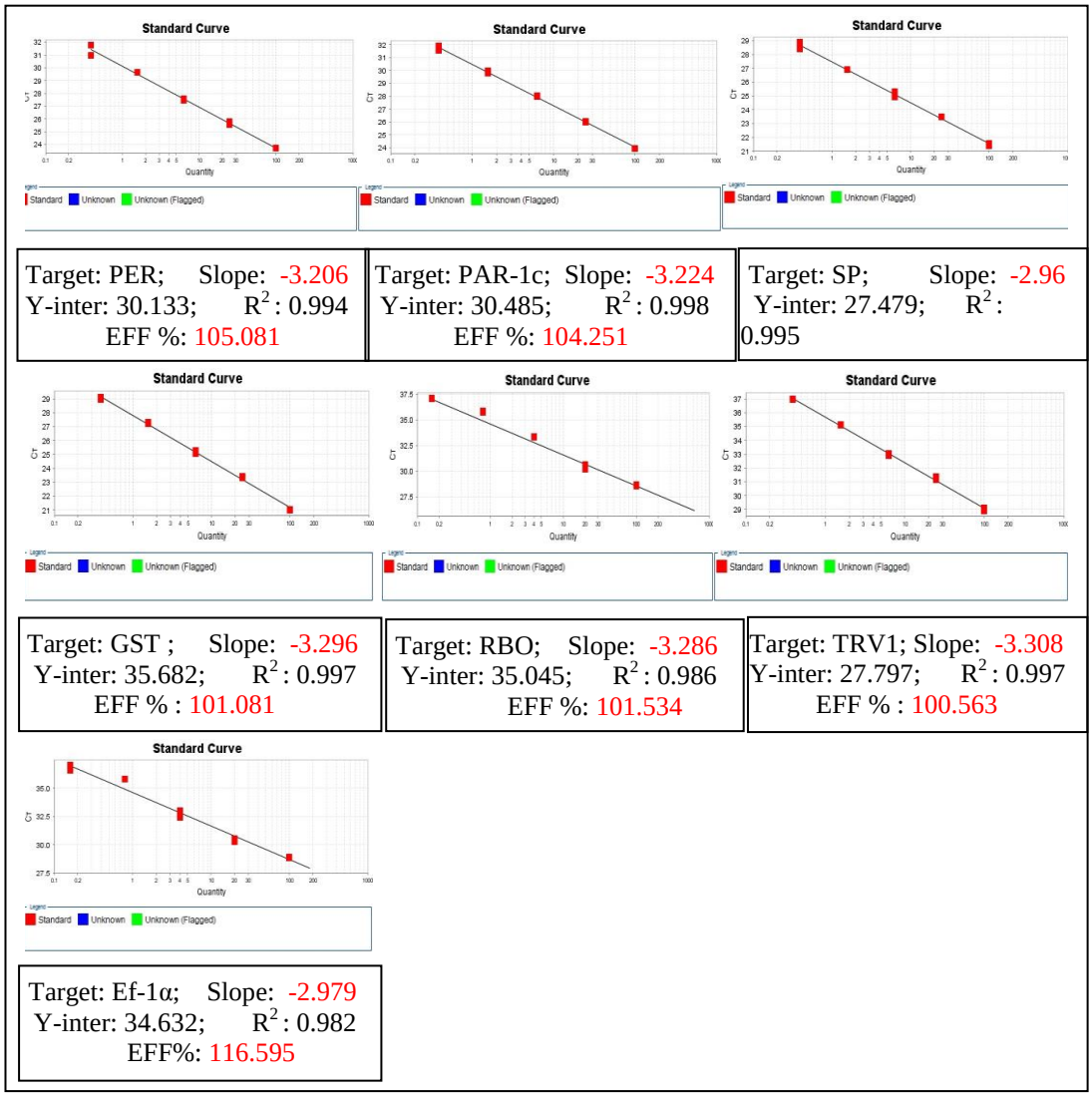

Target: PER; Slope: -3.206 Y-inter: 30.133; R^2: 0.994 EFF %: 105.081	Target: PAR-1c; Slope: -3.224 Y-inter: 30.485; R^2: 0.998 EFF %: 104.251	Target: SP; Slope: -2.96 Y-inter: 27.479; R^2: 0.995
Target: GST ; Slope: -3.296 Y-inter: 35.682; R^2: 0.997 EFF % : 101.081	Target: RBO; Slope: -3.286 Y-inter: 35.045; R^2: 0.986 EFF %: 101.534	Target: TRV1; Slope: -3.308 Y-inter: 27.797; R^2: 0.997 EFF % : 100.563
Target: Ef-1α; Slope: -2.979 Y-inter: 34.632; R^2: 0.982 EFF%: 116.595		

Y-inter: Y-intercept; R2: correlation coefficient or regression line coefficient; EFF %: amplification efficiency.